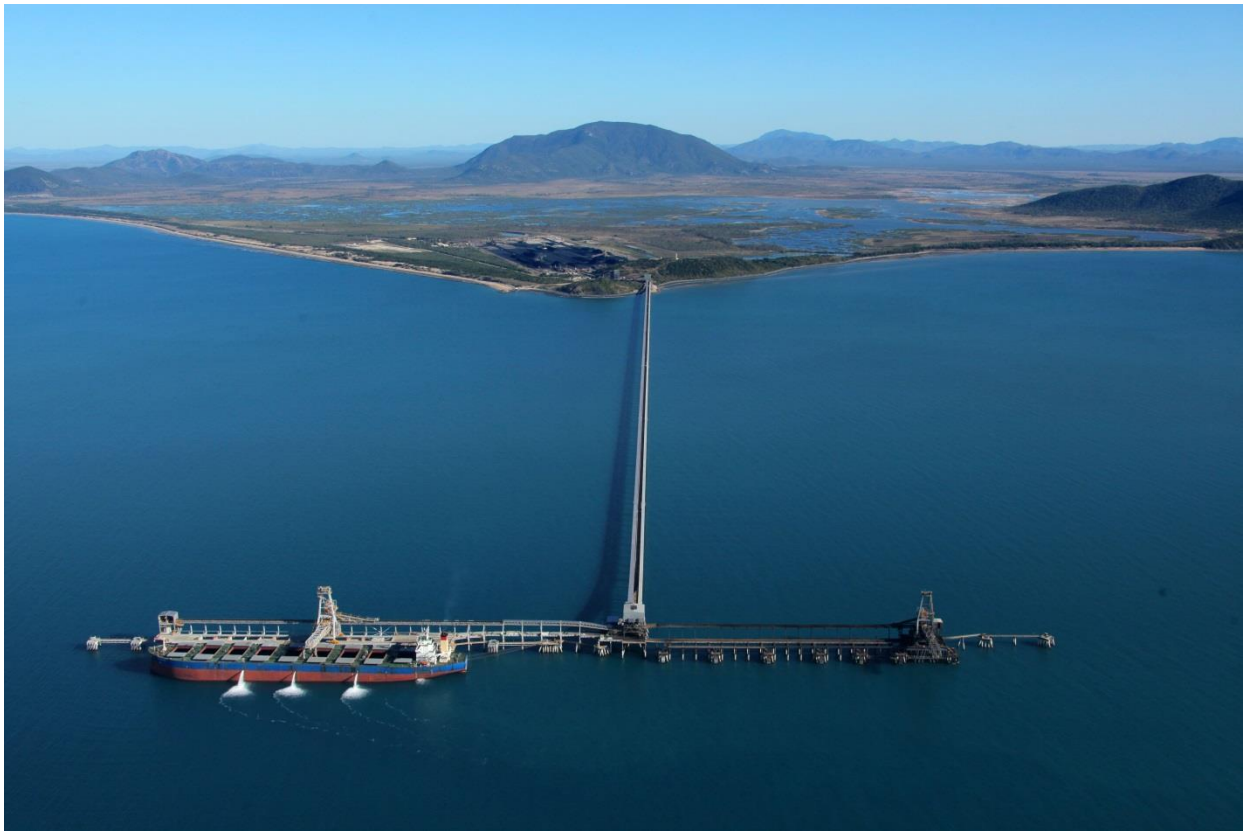

Abbot Point Growth Gateway Project
Dredging and Onshore Placement of Material
Numerical Modelling Report

WorleyParsons

3 August 2015
Final Report
8A0509

Royal HaskoningDHV
Enhancing Society Together

HASKONING AUSTRALIA
MARITIME & WATERWAYS

Unit 2
55-57 Township Drive
BURLEIGH HEADS QLD 4220
T: +61 (0) 7 5602 8540
F: +61 (0) 2 9929 0960
www.royalhaskoningdhv.com
ABN 66 153 656 252

Document title	Abbot Point Growth Gateway Project Dredging and Onshore Placement of Material Numerical Modelling Report
Document short title	Abbot Point Growth Gateway Project
Status	Final
Date	3 August 2015
Project name	Abbot Point Growth Gateway
Project number	8A0509
Client	WorleyParsons
Reference	8A0509

Issue History

Issue	Status	Drafted by	Checked by	Approved by	Date
1	Draft for Worley review	Andy Symonds	Dan Messiter	Dan Messiter	19/06/2015
2	Draft for DSD review	Andy Symonds	Dan Messiter	Dan Messiter	26/06/2015
3	Final Draft	Andy Symonds	Dan Messiter	Dan Messiter	9/07/2015
4	Final	Andy Symonds	Dan Messiter	Dan Messiter	3/08/2015

Cover image from: http://www.portstrategy.com/__data/assets/image/0019/703162/Rachel-Campbell-of-Abbot-Point.jpg

EXECUTIVE SUMMARY

Haskoning Australia Pty Ltd, a company of Royal HaskoningDHV (RHDHV), has been commissioned by WorleyParsons on behalf of the Department of State Development (DSD) to undertake numerical modelling as part of the assessment for approval of the onshore placement of material to be dredged at Abbot Point.

The Abbot Point Growth Gateway Project includes:

- dredging of approximately 1.1 million m^3 of previously undisturbed seabed for new berth pockets and ship apron areas required to support the development of Terminal 0 (T0). The dredging will be undertaken as part of a single dredging campaign in 2015 or a subsequent year;
- relocation of dredging material to dredged material containment ponds (DMCPs) within the area previously allocated for the development of Terminal 2 and the adjoining industrial land; and
- construction and use of a return/tail water pipe from the DMCPs to an offshore discharge location, or an alternate location.

The project was determined to be a controlled action for the purposes of the Environment Protection and Biodiversity Conservation Act 1999 (EPBC Act) and will be assessed by environmental impact assessment under that act. The project will also require approval under Queensland Government legislation. The Australian Government Department of Environment (DoE) statement of reasons for the decision specifies that the controlling provisions include the Commonwealth Marine Areas, the Great Barrier Reef Marine Park (GBRMP) and the Great Barrier Reef World Heritage Area and it was noted by the DoE that the dredging operations have the potential to reduce water quality. As such, this numerical modelling assessment is focused on sediment plume modelling of dredging and water discharge using a stochastic approach which incorporates deep ocean current circulation. This study also supports the marine ecology impact assessment undertaken separately by WorleyParsons.

A three dimensional (3D) hydrodynamic and sediment transport numerical model with 5 vertical layers was adopted for the assessment. A stochastic approach was applied for the modelling of sediment plumes which is considered to be leading practise. The approach takes into account the inter-annual and seasonal variability in metocean conditions for modelling the dispersion of material during the dredging and onshore placement activities, significantly increasing the confidence in the modelling and reducing risk of any sediment suspended as part of the operation behaving in an unpredicted manner. In addition, the model verification process undertaken as part of this assessment has successfully demonstrated that the model can accurately represent the regional scale Great Barrier Reef (GBR) Lagoon circulation processes. The stochastic modelling approach and the approach to represent the regional scale GBR Lagoon circulation processes were collaboratively developed with the Great Barrier Reef Marine Park Authority (GBRMPA) and the Australian Institute of Marine Science (AIMS) as part of the offshore placement assessments for the Disposal Site Analysis Plan (DSAP). The modelling has also been undertaken in accordance with the GBRMPA modelling guidelines (GBRMPA, 2012).

The modelling has been undertaken using three separate years selected from the last 20 years. To encompass the range of climatic and oceanographic variability the three years

were selected to represent a strong El Nino event, a strong La Nina event and a Neutral year. Based on the Southern Oscillation Index (SOI) over this period 1997 was selected as the El Nino, 2011 as the La Nina and 2007 as the Neutral year. This stochastic modelling approach resulted in 13 scenarios in 1997 and 2007 and 12 scenarios in 2011 (due to the occurrence of TC Anthony and TC Yasi in January and early February the first simulation was delayed and started after TC Yasi), resulting in a total of 38 scenarios.

All the results presented in this report are for the bed layer of the model, the modelling has shown that this represents the location where the total suspended solid concentration (TSS) is highest and so can be considered a worst case.

The size of the dredge vessel that will undertake the T0 dredging is not known at this stage, although it is likely that it will be either a large or medium sized dredger. As such, sensitivity testing was undertaken to determine the difference between using a large and medium sized dredge vessel. The dredging duration is considerably longer when using a medium sized vessel compared to a large vessel, with total dredging durations ranging from 13 weeks to approximately 6 weeks, respectively.

The shorter dredging duration was found to result in increased TSS concentration impacts compared to the longer dredging duration, although the impacts lasted for a shorter duration of 6 weeks compared to 13 weeks for the longer dredging duration. Both dredging durations were found to show similar impacts in terms of sedimentation rates and impacts to benthic PAR. Therefore, adopting the large dredge vessel with a shorter dredging duration of approximately 6 weeks for the stochastic modelling represents the worst case scenario in terms of the intensity and extent of potential impacts. As a result, the modelling detailed in this report has been based on the larger dredge vessel with a dredging duration of approximately 6 weeks.

Instantaneous TSS plots have been presented at weekly intervals from the simulation which was shown to result in the largest extent and highest TSS concentration in the 95th percentile TSS plots. The plots showed that over time the plume in the surface layer of the model varies spatially with TSS concentrations less than 10 mg/L except for directly adjacent to the dredging area. It is unlikely that such low surface layer TSS concentrations would result in a clearly defined visual plume.

The stochastic modelling undertaken as part of this assessment has shown the following:

- Suspended sediment released by the dredging activity is transported from the dredging area in a north-west and south-east direction due to the influence of Clark Shoal on the current directions. The residual transport is to the north-west due to the dominant south-easterly winds;
- Suspended sediment released at the discharge location is transported in both a south-westerly and south-easterly direction, with residual transport to the south-west;
- The sediment suspended at the dredging area and at the discharge location do not interact, with the areas with increased TSS due to these activities remaining in separately identifiable plumes;
- The area where the background TSS has the potential to be increased by more than 5 mg/L due to the dredging activity and return water is relatively small. Based on the scenarios tested, the area where TSS can be increased by over 5 mg/L for more

than 5 percent of the dredging duration can be up to 8.2 km in length and 1.2 km in width centred at the dredging location. The discharge location only results in a very small localised area where the TSS is greater than 5 mg/L, with the extent of this area being similar regardless of season or year;

- The modelling results show that the dredging activities and return water discharge have the potential to result in a relatively large area of influence based on the thresholds provided. However, it must be noted that the adopted thresholds of 2mg/L are low compared to the natural background TSS, as all seven of the water quality monitoring sites at Abbot Point had median TSS concentrations higher than 2 mg/L. The zone of moderate impact for TSS is restricted to the dredging area and the area immediately adjacent to the north-west up to 0.7 km from the dredging area. The return water results in a small zone of moderate impact immediately to the west of the discharge location;
- Deposition rates resulting from the dredging activities and return water discharges are relatively low, with the higher rates being limited to areas close to the dredging area and the discharge location;
- The dredging activities and return water discharge may result in localised zones of moderate impact to seagrass due to reductions in daily benthic PAR caused by suspended sediment. The largest zones of moderate impact to seagrass are indicated to occur west and south-east of the dredging and return water discharge locations during the growing season of the Neutral El Nino Southern Oscillation (ENSO) year, correlating with the largest area and highest TSS concentration shown by the 95th percentile TSS plots; and
- The TSS, deposition/resuspension and bed thickness are highest at the dredging location, with a significant reduction in all of these just 200 m away from the dredging area.

One way of quantifying the difference between the amount of material discharged to the environment from dredging of the area with a Cutter Suction Dredger as is proposed for the Project versus dredging using a Trailing Suction Hopper Dredger with offshore placement of dredging material (which has previously been proposed) is to compare the modelling results and inputs for each activity. From comparison of the results of this modelling with the dredging plume results presented in the Abbot Point Terminal 0, 2 & 3 Capital Dredging Public Environment Report (PER) it can be seen that the plume resulting from the dredging and onshore placement activities is smaller and less intense than for the dredging associated with the offshore disposal. This difference is because the mass of material released into the model as a result of the dredging activity for the onshore placement is significantly lower than in the offshore disposal modelling presented in the PER. Due to the inclusion of overspill required to fill the dredge hopper for the offshore disposal, the average mass of material released into the model during the dredging activity (excluding any disposal/placement) was approximately 17,700 tonnes/day. In contrast, for the onshore placement there was no overspill included as the material will be pumped directly to shore and so the average mass of material released into the model during the dredging activity was approximately 435 tonnes/day.

CONTENTS

LIST OF FIGURES

LIST OF TABLES

1 INTRODUCTION

1.1 Project Background

Haskoning Australia Pty Ltd, a company of Royal HaskoningDHV (RHDHV), has been commissioned by WorleyParsons on behalf of the Department of State Development (DSD) to undertake numerical modelling as part of the Abbot Point Growth Gateway Project to represent the onshore placement of material to be dredged at Abbot Point.

The Abbot Point Growth Gateway Project includes:

- dredging of approximately 1.1 million m^3 of previously undisturbed seabed for new berth pockets and ship apron areas required to support the development of Terminal 0 (T0). The dredging will be undertaken as part of a single dredging campaign in 2015 or a subsequent year;
- relocation of dredging material to dredged material containment ponds (DMCPs) within the area previously allocated for the development of Terminal 2 and the adjoining industrial land; and
- construction and use of a return/tail water pipe from the DMCPs to an offshore discharge location or an alternate location.

The project was determined to be a controlled action for the purposes of the Environment Protection and Biodiversity Conservation Act 1999 (EPBC Act) and will be assessed by environmental impact assessment under that act. The project will also require approval under Queensland Government legislation. The Australian Government Department of Environment (DoE) statement of reasons for the decision specifies that the controlling provisions include the Commonwealth Marine Areas, the Great Barrier Reef Marine Park (GBRMP) and the Great Barrier Reef World Heritage Area and it was noted by the DoE that the dredging operations have the potential to reduce water quality. As such, this numerical modelling assessment is focused on sediment plume modelling of dredging and water discharge using a stochastic approach which incorporates deep ocean current circulation. This study also supports the marine ecology impact assessment undertaken separately by WorleyParsons.

The scope of work was to undertake stochastic dredging plume modelling of the short-term response of the dredging activity and onshore placement of material at Abbot Point as part of a capital dredging program for T0. The modelling approach was developed as part of the offshore placement assessment for the Disposal Site Analysis Plan (DSAP) which was a requirement under the previous offshore disposal approval process. The approach adopted for this modelling was collaboratively developed over a 12 month period and involved extensive consultation with the Great Barrier Reef Marine Park Authority (GBRMPA) and the Australian Institute of Marine Science (AIMS), which ultimately led to their endorsement and sign off on the approach. The consultation and consensus on the modelling approach adopted was also supported by the DoE. The stochastic approach for the modelling of sediment plumes applied represents an industry first in the Great Barrier Reef and is considered to be leading practise. This approach takes into account the inter-annual variability in metocean conditions for modelling the dispersion of material during the relocation activity, significantly increasing the confidence in the use of the model as a predictive tool and reducing risk of any suspended sediment released due to the dredging and onshore placement activities behaving in an unpredicted manner.

1.2 Study Area

Abbot Point is situated approximately 25 km north-west of Bowen, located on the north-east coast of Queensland. The limits of the Port of Abbot Point extend from Abbot Bay (west) through to Gloucester Head (southeast) and are inclusive of surrounding tidal waters. The Port lies within the Great Barrier Reef World Heritage Area but is excluded from the Great Barrier Reef Marine Park (GBRMP).

The proposed areas to be dredged for T0 is located adjacent to the existing berth and jetty at Abbot Point, approximately 3 km offshore of the headland (**Figure 1**). The location of the return water discharge has been tested as part of this assessment, details of this are provided in **Section 4**.

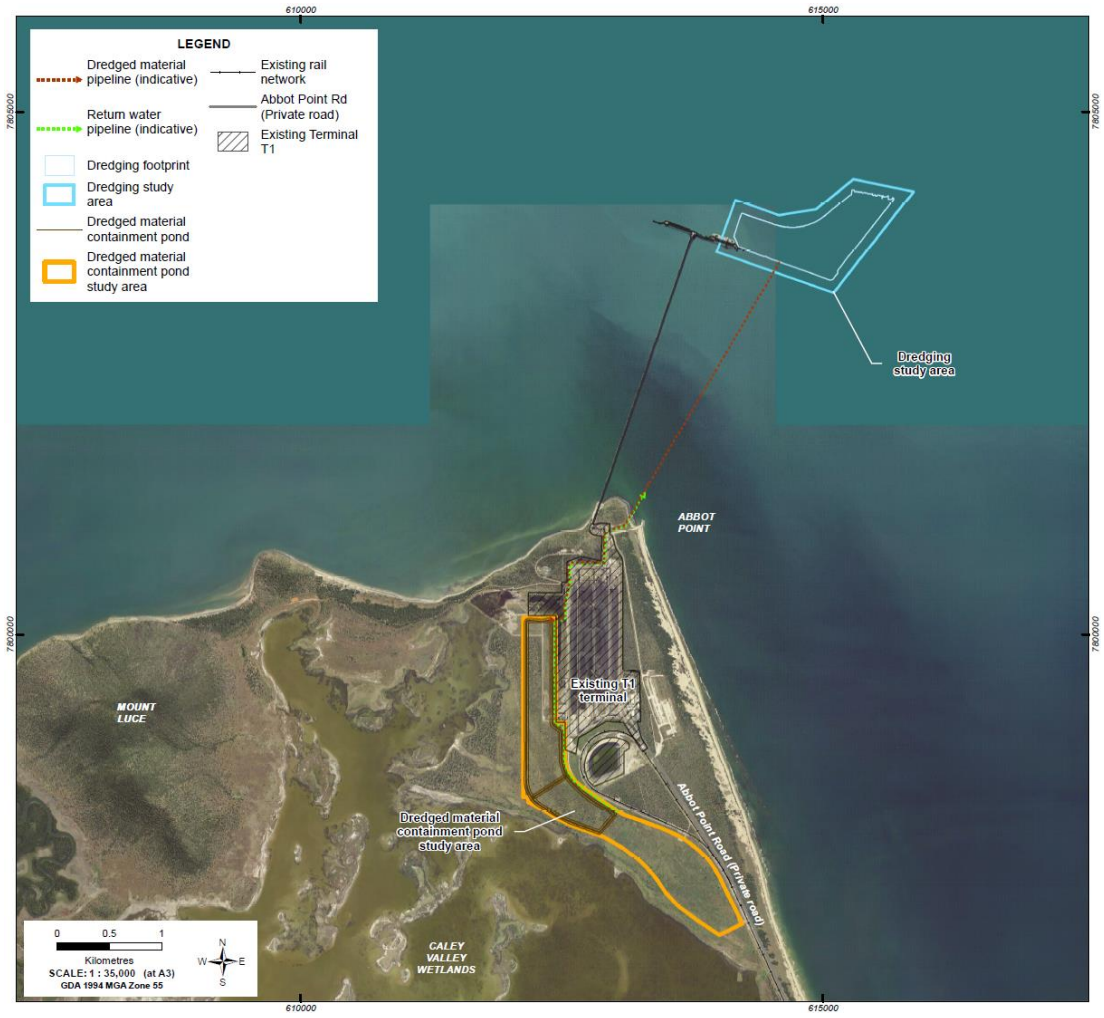

Figure 1 Location of the dredging referral area, onshore referral area and the proposed return water pipeline location (DSD, 2015).

1.3 Background to Abbot Point

The Port of Abbot Point was commissioned in 1984 and has been exporting bulk coal from the northern Bowen Basin coal reserves continuously since that time. Due to the large tracts

of land available for industrial development in the area, its remote location and access to deep water, the Port is considered a strategic asset to the State.

The existing Abbot Point Terminal 1 (T1) consists of a rail in-loading facility, coal handling terminal, and stockpile areas, as well as a wharf and ship loader located 2.8 km offshore. Adani Abbot Point Terminal Pty Ltd sought and obtained approval for the development of coal terminals T0 within the Port of Abbot Point. These approvals excluded the dredging activity required to provide sea access to these terminals.

Up to 1,100,000 m^3 of previously undisturbed seabed is proposed to be dredged and relocated as part of the proposed works for T0.

2 SITE CONDITIONS

This section provides details of available water level, current, wind, wave and dredging material particle size data. The following data has been available for the present investigation:

- Water level, current and wave data has been collected at sites approximately 8.5 km and 3 km to the west and east of the existing wharf respectively. Data was collected from July to November 2008;
- Water level, current and wave data has been collected at proposed offshore dredging material relocation sites from December 2013 to September 2014. Data has been collected simultaneously at two of the three proposed sites at any one time; and
- Wave data has been made available from a waverider buoy at a site adjacent to the existing wharf from January 2012 to the end of May 2014.

In addition to these datasets, other measured and hindcast modelled data were also obtained as part of the study. Details of the data and a description of the existing conditions are provided in the following sections.

2.1 Water Levels

Abbot Point experiences mixed semi-diurnal tides with a period of 12 hours and 25 minutes. The area has a typical maximum diurnal inequality in the order of 1.0 m at high water and 0.5 m at low water. The tidal planes for Abbot Point are shown in **Table 1**.

Table 1 Tidal levels at Abbot Point relative to AHD (MSQ, 2014).

Tidal Level	Abbot Point (19°51'S, 148°5'E) (m AHD)
HAT	1.97
MHWS	1.07
MHWN	0.44
MSL	0.06
MLWN	-0.33
MLWS	-0.96
LAT	-1.63

Example water level data from a site approximately 3km to the east of the existing wharf at Abbot Point (Site A2 in **Figure 2**) is shown in **Figure 3**. Levels fluctuate between 1.8 and -1.5 m MSL during spring tides and between 0.5 and -0.7 m MSL during neap tides. Note: mean sea level (MSL) is approximately equivalent to Australian Height Datum (AHD).

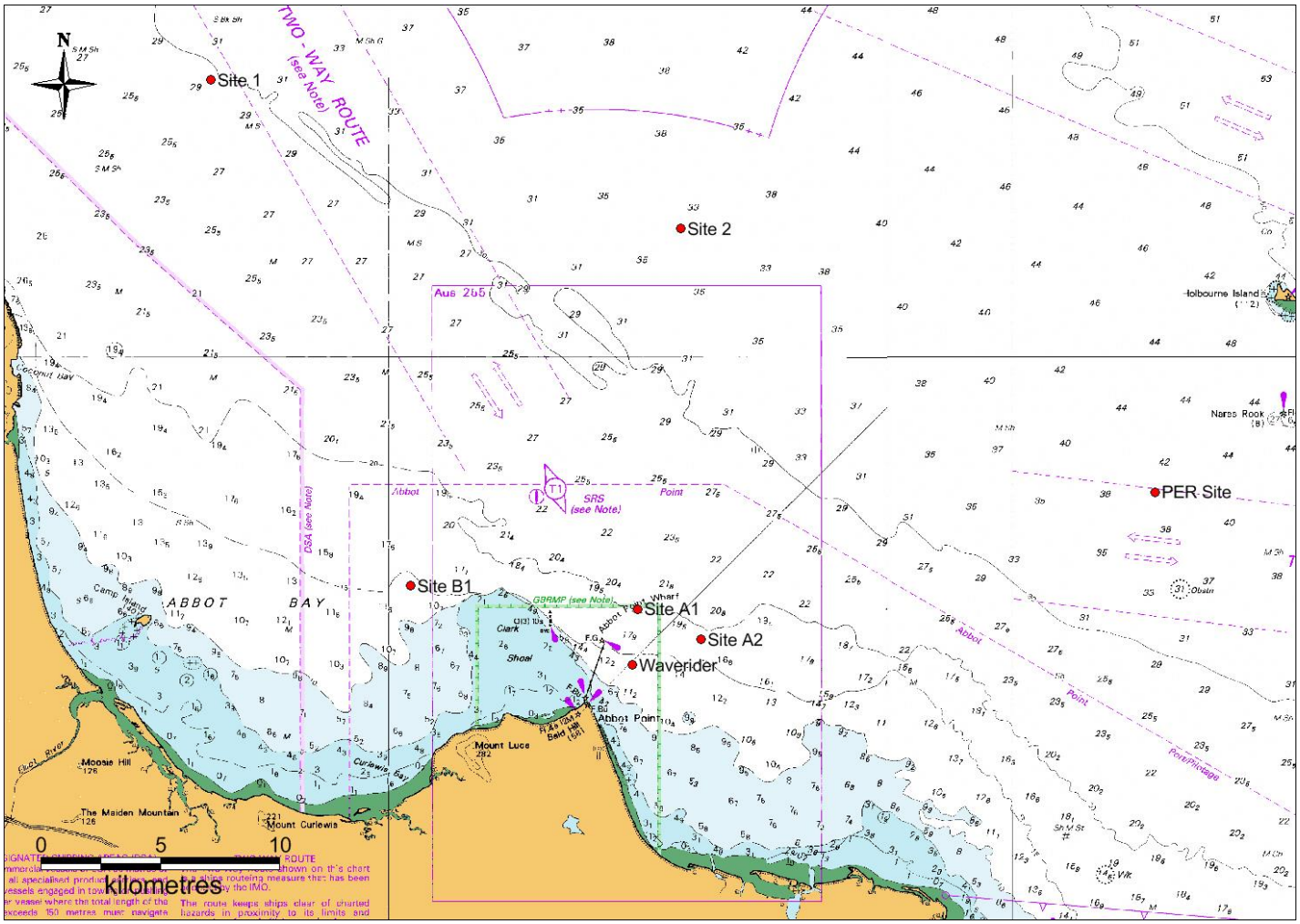

Figure 2 Locations of sites with existing measured hydrodynamic and wave data available in the region of Abbot Point.

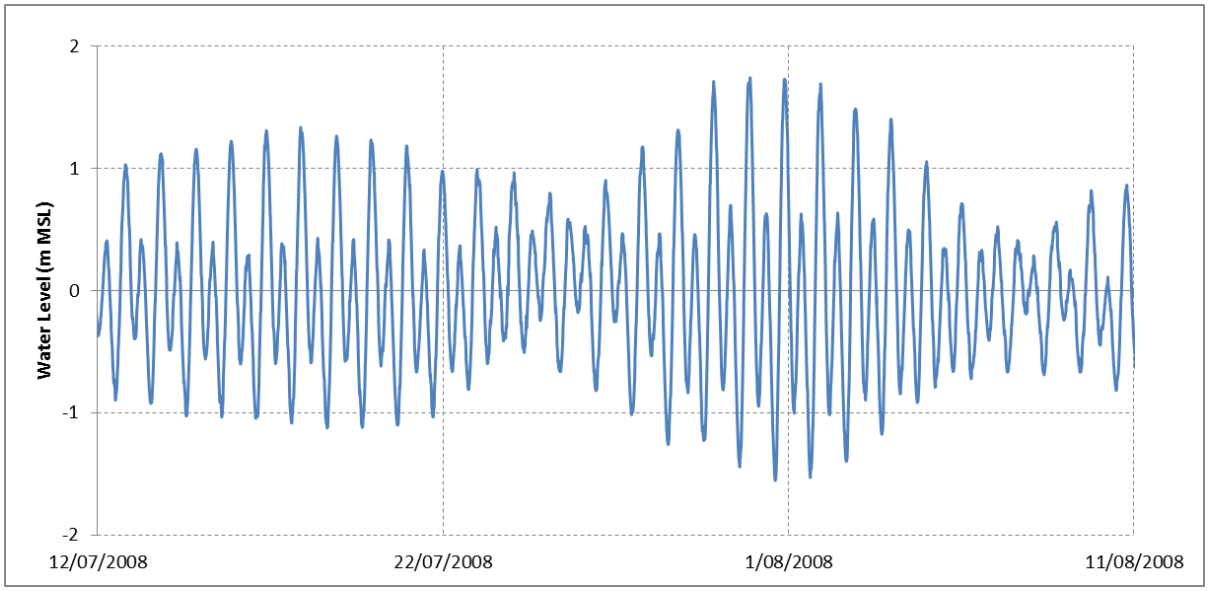

Figure 3 Measured water levels at Site A2, located approximately 3 km to the east of the existing Abbot Point Wharf.

2.2 Currents

Current speed and direction data was available at sites approximately 8.5 km and 3 km to the west and east of the existing wharf respectively (Sites B1 and A2 in **Figure 2**). Measured depth averaged current speeds and directions at these two sites are shown in **Figure 4** and **Figure 5**. The plots show that peak current speeds of approximately 0.3 m/s occur during spring tides, with higher speeds occurring at the site to the east of the existing wharf. During neap tides the peak current speeds are again higher at the site to the east of the existing wharf, with peak speeds of between 0.1 to 0.2 m/s, while at the site to the west the peak speeds are consistently less than 0.1 m/s. The peak flood currents occur just before high water and flow to the east-south-east and peak ebb currents occur just before low water and flow to the west-north-west.

In addition, current speed and direction data was also collected at proposed offshore dredging material relocation sites from December 2013 to September 2014 (Sites 1, 2 and PER in **Figure 2**). Analysis of this data was undertaken as part of the previous offshore disposal site assessment to determine the influence of different driver forces on currents in the GBR Lagoon. A summary of the findings of this assessment are provided in **Appendix A**. The analysis demonstrated that currents in the GBR Lagoon are influenced by the following:

- Astronomical tides, these provide a constant and predictable forcing;
- Local winds provide a frequent and highly variable forcing[1]. South-east trade winds blow throughout the year but tend to be more persistent during winter months while north to north-easterly winds occur predominantly in summer months but tend to be less frequent and lower in speed. Wind conditions are discussed in more detail in **Section 2.3**; and

[1] Current speeds and directions are influenced by wind and not directly by waves in this area. Waves cause an orbital current which can result in increased stresses on the bed, but do not result in a residual current.

- Regional GBR Lagoon scale circulation provides an intermittent and variable forcing.

The influence of these forcings on the currents in the local scale numerical model and the approach adopted to include the currents are further discussed in **Appendix A**. It is important to note that this approach to represent the regional scale GBR Lagoon circulation processes along with the stochastic modelling approach were collaboratively developed with the GBRMPA and AIMS as part of the offshore placement assessments for the DSAP. This consultation and consensus on the approach was also supported by the DoE (**Appendix C**).

Tropical cyclones (TCs) can result in increased current speeds and changes to current directions due to the associated strong winds. Current speeds and directions were measured during TC Dylan at Site 2 located approximately 20 km offshore of Abbot Point (**Figure 2**). **Figure 6** shows that during this event, near-bed current speeds of up to 0.9 m/s occurred at Site 2 and current directions between the west and north-west dominated.

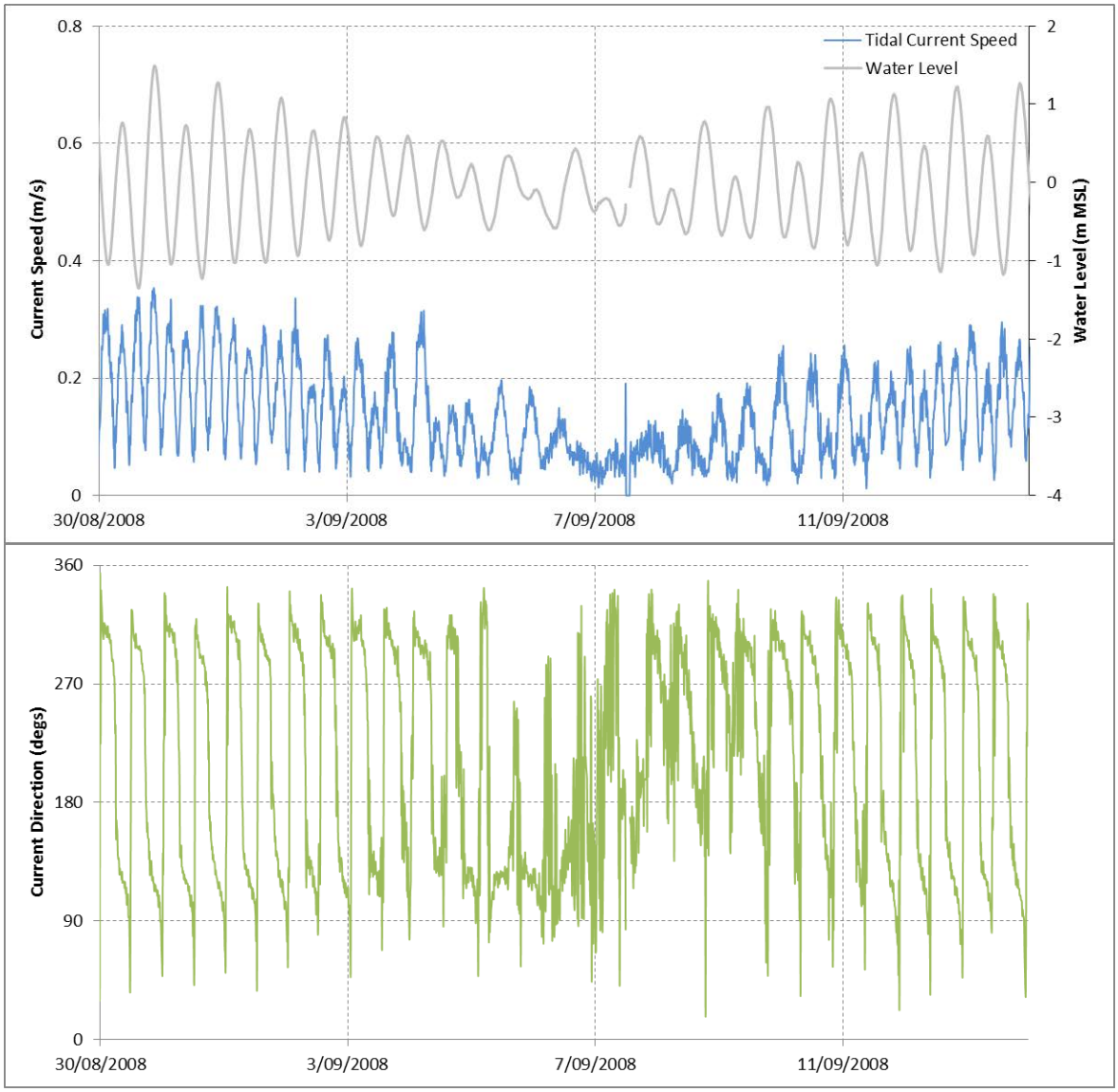

Figure 4 Measured water level and near-bed current speed and direction at Site A2, located approximately 3 km to the east of the existing wharf.

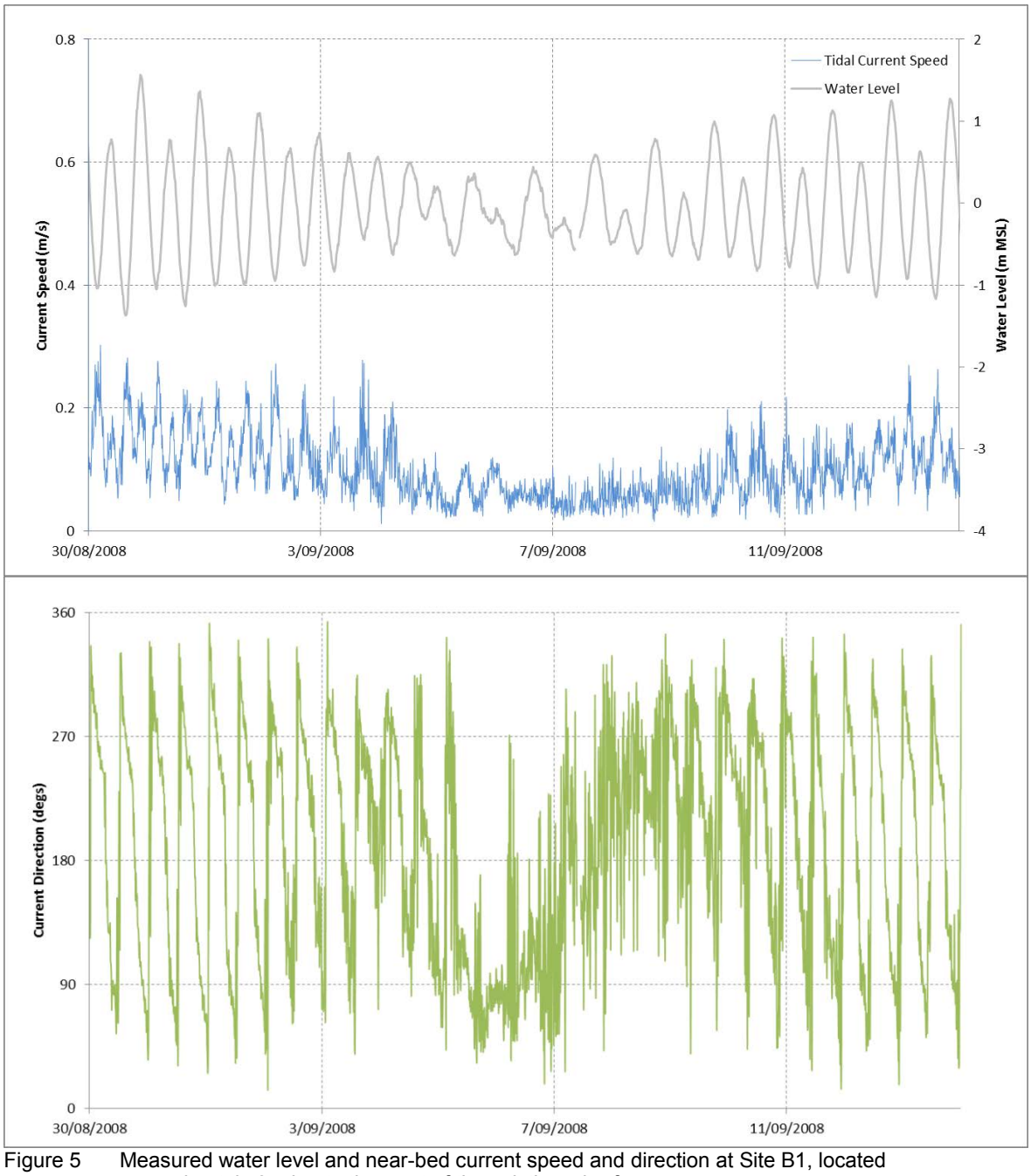

Figure 5 Measured water level and near-bed current speed and direction at Site B1, located approximately 8.5 km to the west of the existing wharf.

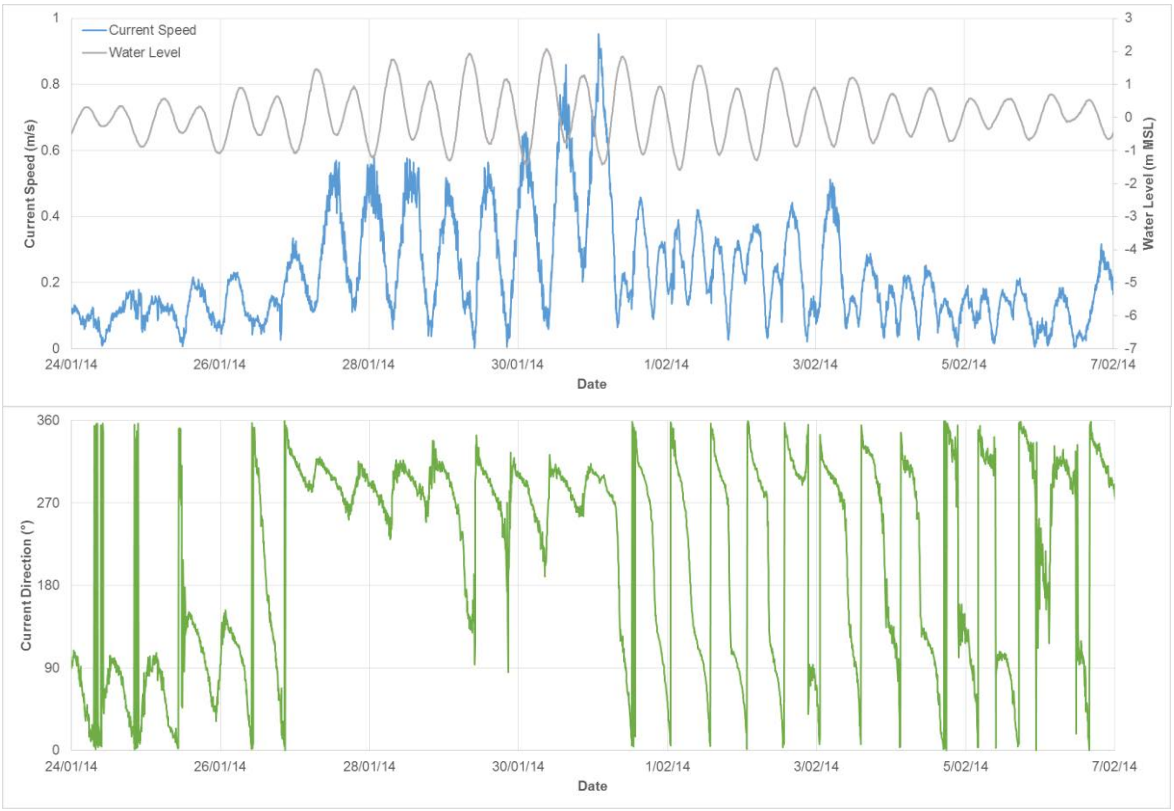

Figure 6 Measured water level and near-bed current speed and direction at Site 2, located approximately 20 km offshore of Abbot Point during TC Dylan.

2.3 Wind

Wind data was obtained from the Bureau of Meteorology (BoM) at the closest station to the site with long term wind records, Alva Beach (147.48°,-19.46°). Data was provided from 24/03/1997 to 06/02/2014, with 10 minute averaged wind speed (m/s) and direction (degrees) recorded every 30 minutes.

The dominant wind direction over the period was from the east and the east-south-east. Winds from these directions occurred for the longest duration and also tended to be of a higher speed (**Figure 7**). During the data period the wind speed for the area, defined based on the Beaufort Scale was predominately gentle to moderate (0-10 m/s) with a maximum recorded wind speed of a strong gale (21.7 m/s).

For the numerical modelling it is also important to understand the wind conditions over water as it is these offshore winds which are important driving mechanisms for the currents in the area. A wind rose using the hourly wind data from 01/01/1994 to 01/06/2014 provided from the MetOcean Solution Pty Ltd hindcast numerical model at a location approximately 20 km offshore of Abbot Point are shown in **Figure 8**. The wind conditions at this site over this 20.4 year period are predominately defined as moderate, with wind speeds generally ranging from 5 to 10 m/s from the east-south-east and south-east. The maximum hourly wind speed from the hindcast model was 30.9 m/s which is classified as a violent storm, this occurred on 02/02/11 during Tropical Cyclone (TC) Yasi.

The measured wind conditions at Alva Beach and the hindcast modelled wind conditions at the site offshore of Abbot Point show similarities in both wind speed and direction. However, the dominant direction at the offshore site is from the south-east and east-south-east while at Alva Beach it is from the east and east-south-east. There is also more directional variability in the wind at Alva Beach than at the offshore site. These directional differences are expected due to Alva Beach being located on land while the other site is offshore.

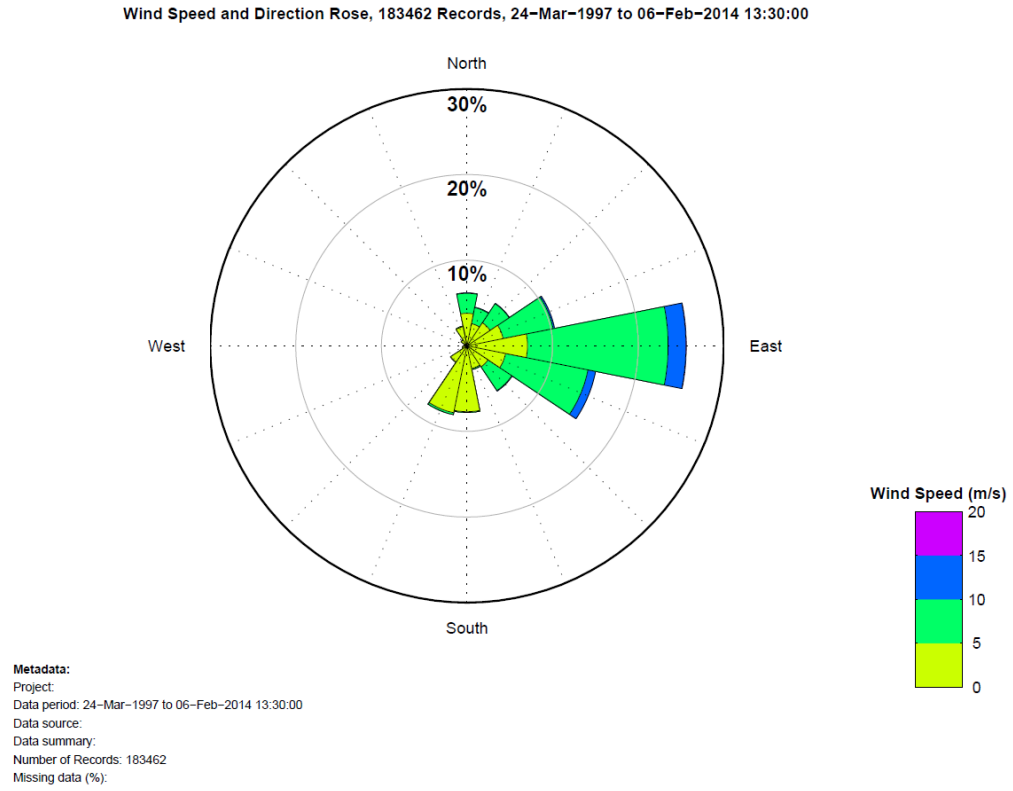

Figure 7 Wind rose at Alva Beach.

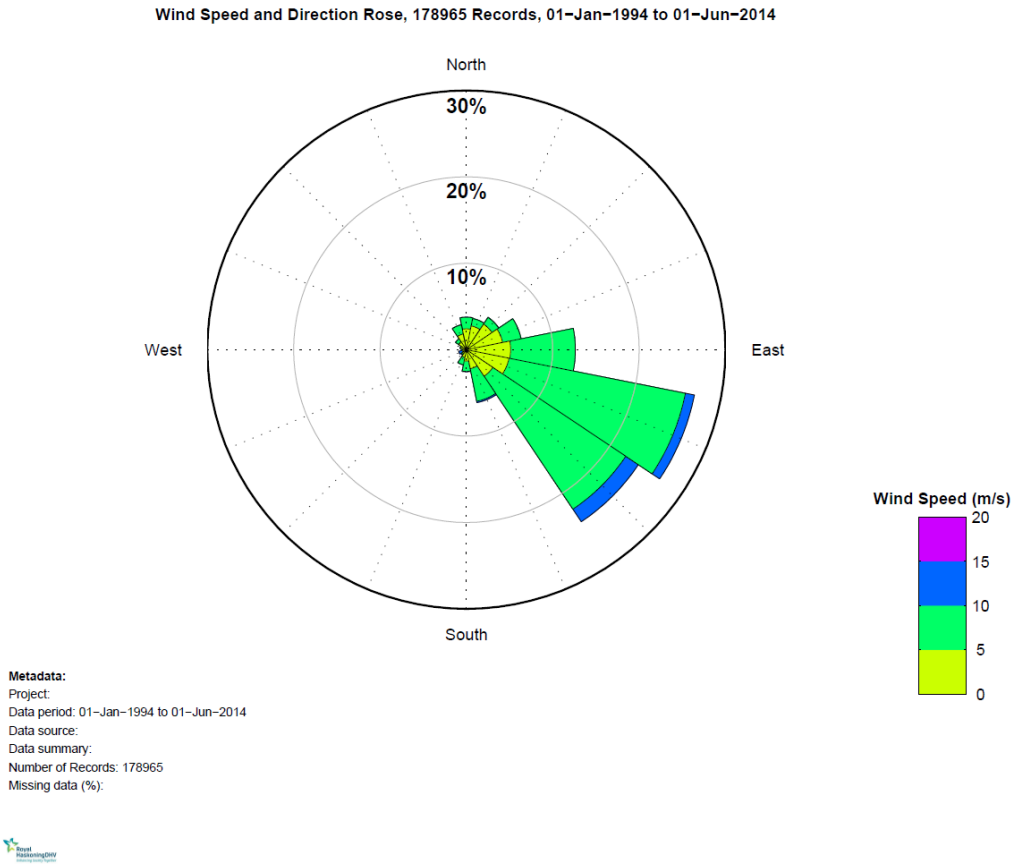

Figure 8 Wind rose at a site approximately 20 km offshore of Abbot Point.

2.4 Waves

The GBR is located offshore of Abbot Point and blocks, or significantly attenuates, the majority of long period swell wave events. However, occasional large wave events generated inshore of the reef occur due to tropical cyclones. Accordingly, the wave climate at Abbot Point is variable. As detailed by GHD (2009), the site is exposed to both sea and swell (attenuated), with spectral peak periods ranging from about 2 to 13 seconds. Locally generated sea waves dominate at a period of 3 to 5 seconds. Swell waves tend to be lower in height and vary in peak period from 7 to 13 seconds.

Wave data has been made available from a waverider buoy at a site adjacent to the existing wharf from January 2012 to the end of May 2014 (for location see **Figure 2**). **Figure 9** to **Figure 11** show time series of the measured wave conditions from February to June 2012. The plots show that over this period significant wave height (H_s) varied from 0.1 m to almost 2 m, with heights of less than 1m occurring most frequently. The peak wave period (T_p) was generally in the 2 to 6 second range, although occasional values of up to 10 seconds also occurred. Wave direction was predominantly from the east, although waves from the north-east and north also occurred.

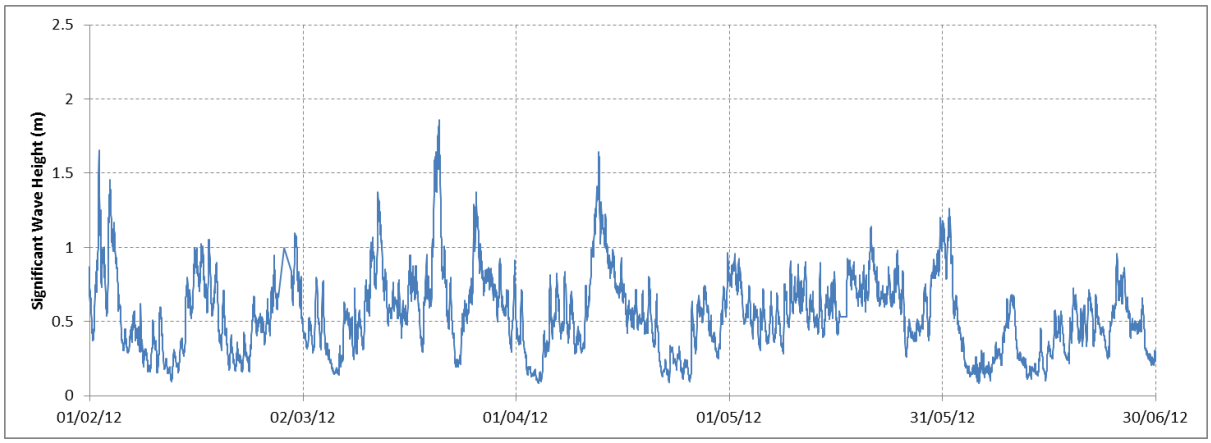

Figure 9 H_s at the Abbot Point waverider buoy.

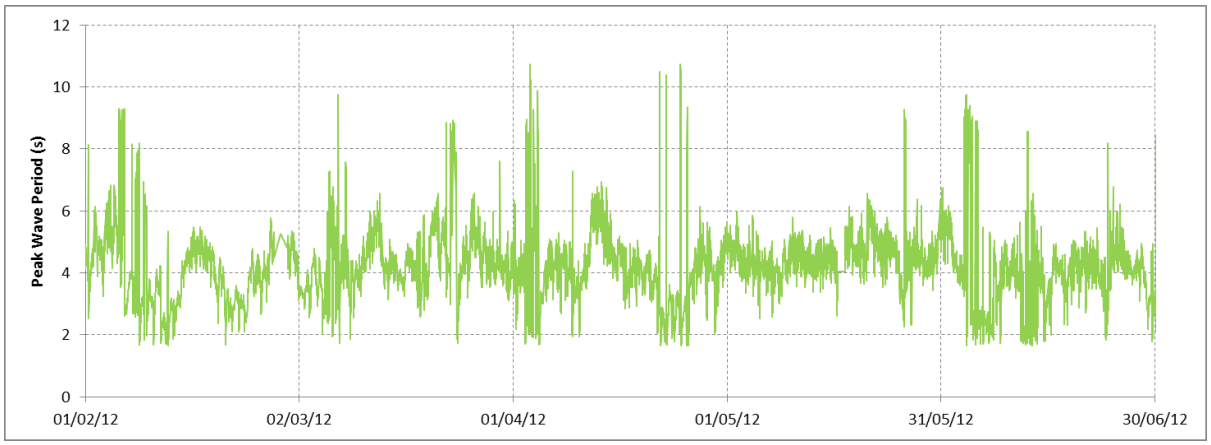

Figure 10 T_p at the Abbot Point waverider buoy.

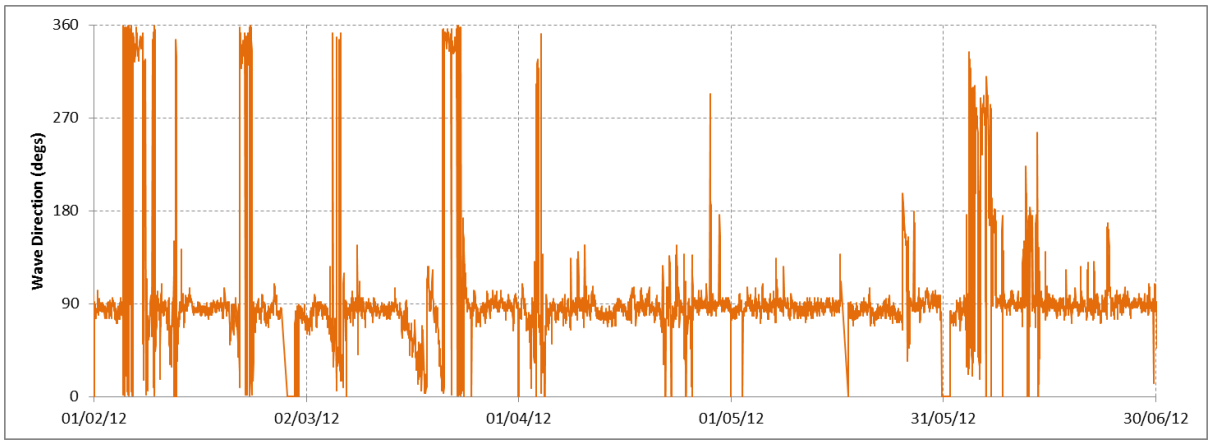

Figure 11 Mean wave direction at the Abbot Point waverider buoy.

Wave data from the Abbot Point waverider buoy is presented as a joint frequency table and a rose plot in **Table 2** and **Figure 12** respectively. The frequency table shows that for 93.5% of the time H_s was less than 1 m and that waves from the east and east-north-east were most frequent, occurring for more than 78% of the time. The maximum H_s over the 2.5 years of data was 3.81 m, which occurred on 13/03/2014 as a result of TC Ita. The peak wave period (T_p) ranged from 1.5 to 24 s with an average of approximately 4 s.

Table 2 Joint frequency table of H_s and direction at the Abbot Point waverider buoy.

Joint Frequency Table (%) Showing Hs Against Direction for the Period 17-Jan-2012 16:30:00 to 31-May-2014 23:30:00

N=40422	N	NNE	NE	ENE	E	ESE	SE	SSE	S	SSW	SW	WSW	W	WNW	NW	NNW	Total	Cumul.
0–0.25	1.31	2.29	2.46	3.49	2.22	0.37	0.36	0.19	0.17	0.03	0.02	0.03	0.19	0.10	0.23	0.96	14.44	14.44
0.25–0.5	1.90	1.35	1.87	13.23	10.22	0.48	0.23	0.25	0.12	0.02	0.01	0.01	0.11	0.03	0.38	2.66	32.89	47.32
0.5–0.75	0.56	0.23	0.60	14.52	12.85	0.21	0.01	0.02	0.01	*	*	*	–	*	0.08	0.87	29.97	77.29
0.75–1	0.11	0.03	0.20	9.01	6.70	0.05	–	*	*	–	–	–	–	–	–	0.14	16.24	93.53
1–1.25	0.12	*	0.07	3.11	1.68	–	*	–	*	–	–	–	–	–	*	0.04	5.04	98.57
1.25–1.5	0.01	*	0.02	0.78	0.27	–	–	–	–	–	–	–	–	–	–	0.05	1.14	99.72
1.5–1.75	*	0.02	0.02	0.08	0.02	–	–	–	–	–	–	–	–	–	*	*	0.17	99.89
1.75–2	*	0.02	*	*	–	–	–	–	–	–	–	–	–	–	–	*	0.04	99.93
2–2.25	–	*	*	–	–	–	–	–	–	–	–	–	–	–	–	*	0.01	99.94
2.25–2.5	*	*	*	–	–	–	–	–	–	–	–	–	–	–	–	0.01	0.03	99.97
2.5–2.75	0.01	–	–	–	–	–	–	–	–	–	–	–	–	–	–	–	0.01	99.98
2.75–3	0.01	*	–	–	–	–	–	–	–	–	–	–	–	–	–	*	0.02	100.00
Total	4.06	3.97	5.26	44.22	33.96	1.10	0.61	0.47	0.31	0.06	0.03	0.05	0.30	0.14	0.71	4.75		
Cumul.	4.06	8.03	13.28	57.50	91.46	92.56	93.17	93.65	93.96	94.02	94.05	94.10	94.40	94.54	95.25	100.00		

* denotes values less than 0.01% – denotes no records in bin

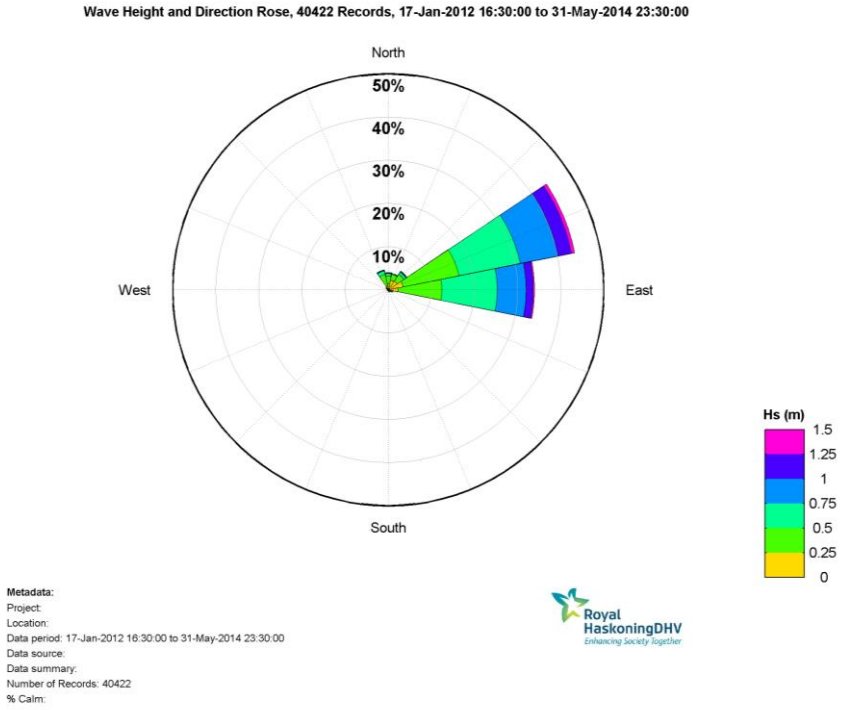

Figure 12 Wave rose of H_s at the Abbot Point waverider buoy.

2.5 Particle Size Data

Sediment samples from the berths proposed to be dredged and surrounding apron associated with the T0 and Terminal 2 (T2) and 3 (T3) developments were collected as part of the previously proposed capital dredging project using vibracoring and boreholes to characterise the sediments to be dredged (GHD, 2012). Results from sieve analysis of the coarser particles, and hydrometer analysis of the finer particles, were used to develop the percentage distribution of material types to be applied in the numerical model used in the PER for the release of material associated with the dredging. These are shown in **Table 3**. Analysis of the particle size data in the PER has shown no discernible trend in sediment distribution across the dredging area and as such the percentage distribution was determined by averaging the sediment properties over the dredging footprint. Further analysis of the geotechnical data at T0 and T3 has shown that 40% of the dredging material is made up of silts and clays (PDMC, 2014). This recent analysis did not include a detailed breakdown of the particle sizes. As such, the breakdown of the silts and clays provided in **Table 3** has been adopted to represent the particle size distribution for the 40% fines which has been assumed for the dredging plume modelling in this study.

Table 3 Distribution of sediment fractions (GHD, 2012).

Sediment Type	Av. Particle Size (µm)	% Distribution
> Very Fine Sand	>125 µm	53
Very Fine Sand	125 – 63 µm	8
Coarse Silt	63 – 31 µm	9
Medium Silt	31 - 15.6 µm	4
Fine Silt	15.6 – 3.9 µm	6
Clay	< 3.9 µm	19

2.6 Water Quality and Extreme Events

Water quality monitoring has been undertaken around Abbot Point from February 2013 to June 2014 by WorleyParsons (WorleyParsons, 2014). Seven sites have been monitored over this period, with the location of sites WQ1 to WQ7 shown in **Figure 13**. The total suspended solids (TSS) concentration at the seven sites are shown over a 12 month period in **Figure 14** and the mean, median and maximum values over the total monitoring period are detailed in **Table 4**. For reference, the visual appearance of varying TSS concentrations is shown in **Figure 16**. The measured data shows that at the seven monitoring sites around Abbot Point the TSS concentrations are generally less than 10 mg/L, except for at the shallow nearshore site WQ5 where the mean value is just over 10 mg/L. Much higher concentrations of between 150 and 950 mg/L can also occur during extreme events. During the deployment period two TCs influenced the area:

- TC Dylan was a category 2 cyclone when it crossed the coastline 35 km to the east of Bowen on 31st January 2014; and

- TC Ita was a category 1 cyclone when it tracked along the coastline from Townsville to Bowen on 13th April 2014.

Out of the seven water quality monitoring sites four recorded TSS concentrations during TC Dylan (**Figure 15**). The measurements show that over an 8 day period around the cyclone elevated TSS concentrations occurred, with concentrations generally exceeding 20 mg/L over this period and peaking above 100 mg/L. This shows that during a TC, extensive resuspension of the natural bed material occurs, with sites located in water depths in excess of 10 m LAT still exhibiting significant increases in TSS concentration. In addition, the highest TSS concentration of 948 mg/L recorded at WQ6 occurred during TC Ita.

Table 4 TSS concentration statistics for the seven water quality sites.

Site	Mean (mg/L)	Median (mg/L)	Maximum (mg/L)
WQ1	5.8	3.5	166.2
WQ2	6.1	3.1	182.8
WQ3	4.5	2.2	210.3
WQ4	6.5	3.5	320.2
WQ5	11.3	5.1	302.0
WQ6	6.9	2.8	948.3
WQ7	7.0	2.5	352.7

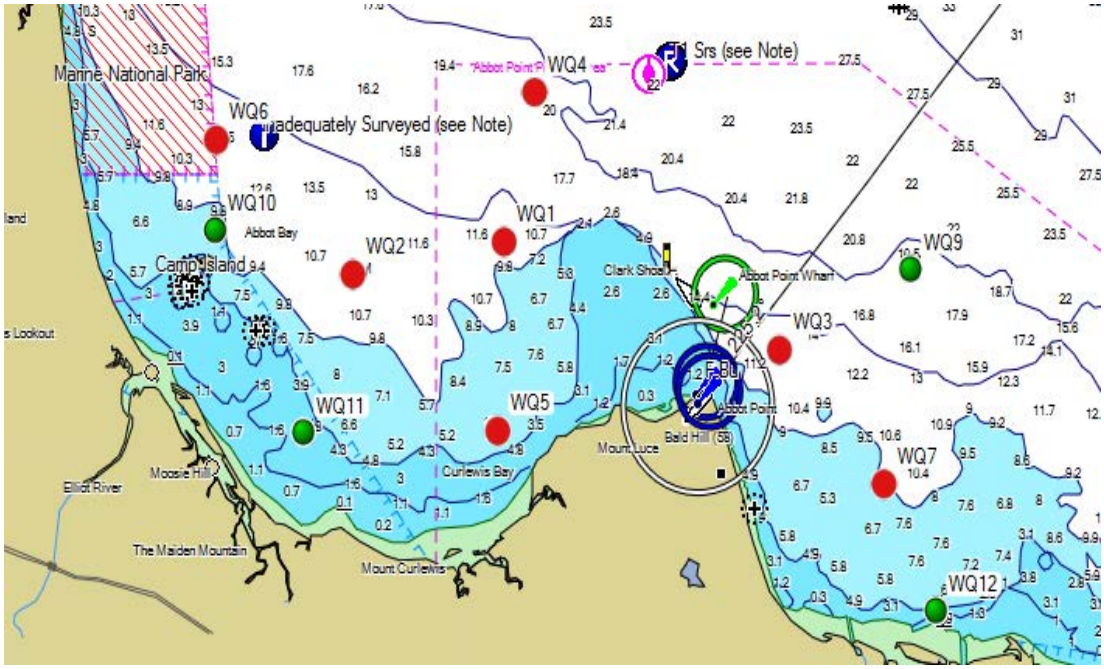

Figure 13 Location of the WorleyParsons water quality monitoring sites WQ1 to WQ7.

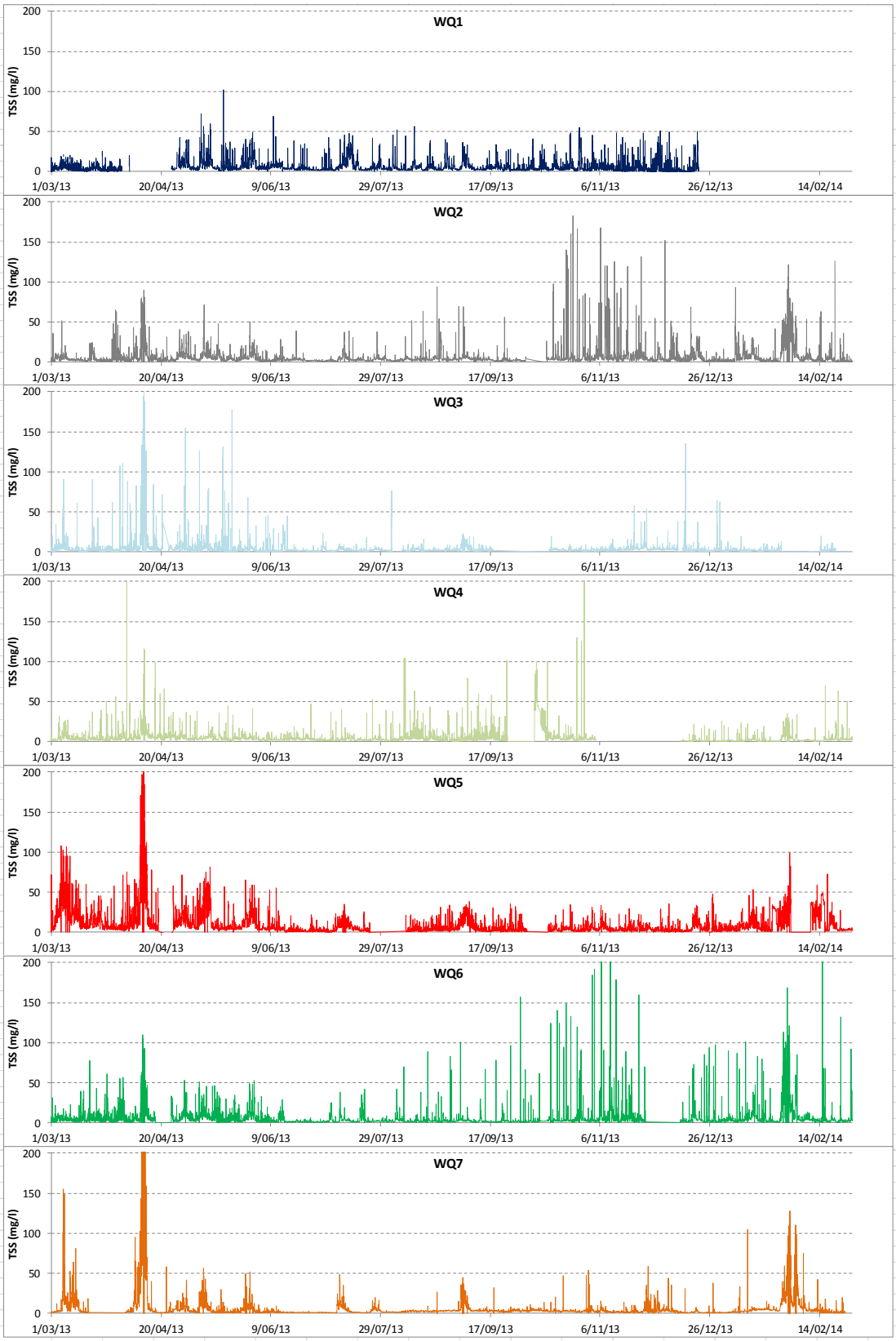

Figure 14 TSS concentrations over 12 months at the seven water quality monitoring sites. Note: the TSS scale has been fixed at 200 mg/L to show the majority of the data, as a result the maximum values may not be shown.

Figure 15 TSS concentrations during TC Dylan.

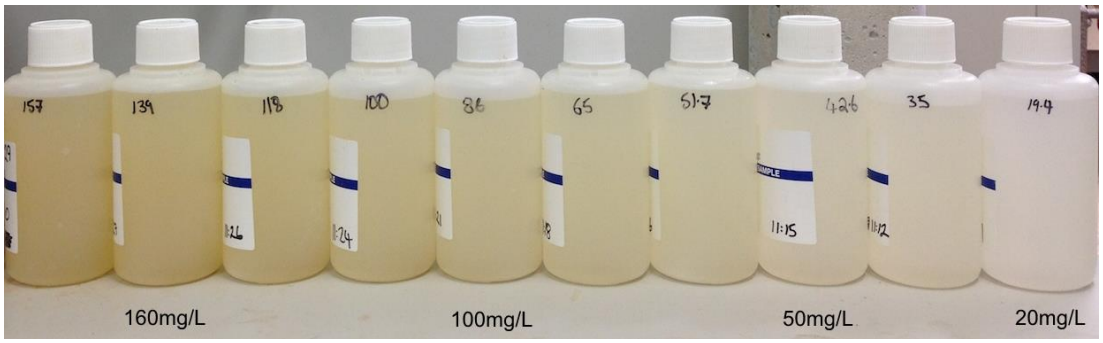

Figure 16 Water clarity for a range of TSS concentrations (NTU value is written on the bottles). Note: the sediment used is not from Abbot Point.

3 MODELLING APPROACH

The numerical modelling undertaken as part of this assessment represents a stochastic approach to determining dispersion, deposition and resuspension resulting from the proposed dredging and onshore placement activities. The stochastic modelling approach and the approach to represent the regional scale GBR Lagoon circulation processes were collaboratively developed with the Great Barrier Reef Marine Park Authority (GBRMPA) as part of the offshore placement assessments for the Disposal Site Analysis Plan (DSAP) (**Appendix C**). The DSAP was a requirement of conditions of the previous offshore placement approvals. The modelling has also been undertaken in accordance with the GBRMPA modelling guidelines (GBRMPA, 2012).

Details of the different numerical models applied, along with the methodology adopted are provided in this section. Full details on the calibration and validation of the numerical models undertaken as part of this study are provided in **Appendix B**.

3.1 Model Description

Representation of the proposed dredging and onshore placement activities of the dredging material requires the use of hydrodynamic, wave and sediment transport models. The numerical modelling for this assessment has utilised the professional engineering software package Delft3D released by Deltares (Version 4.01.00). Delft3D is a fully integrated software suite designed for multi-disciplinary use. It is able to simulate hydrodynamics, waves, sediment transport, morphological changes and ecology in marine, coastal, river and estuarine environments. The 3-Dimensional modelling system is designed in an integrated modular framework with a variety of modules, allowing the user to customise the software package to suit project requirements. In this case the Flow, Wave and Water Quality modules within the Delft3D system have been used.

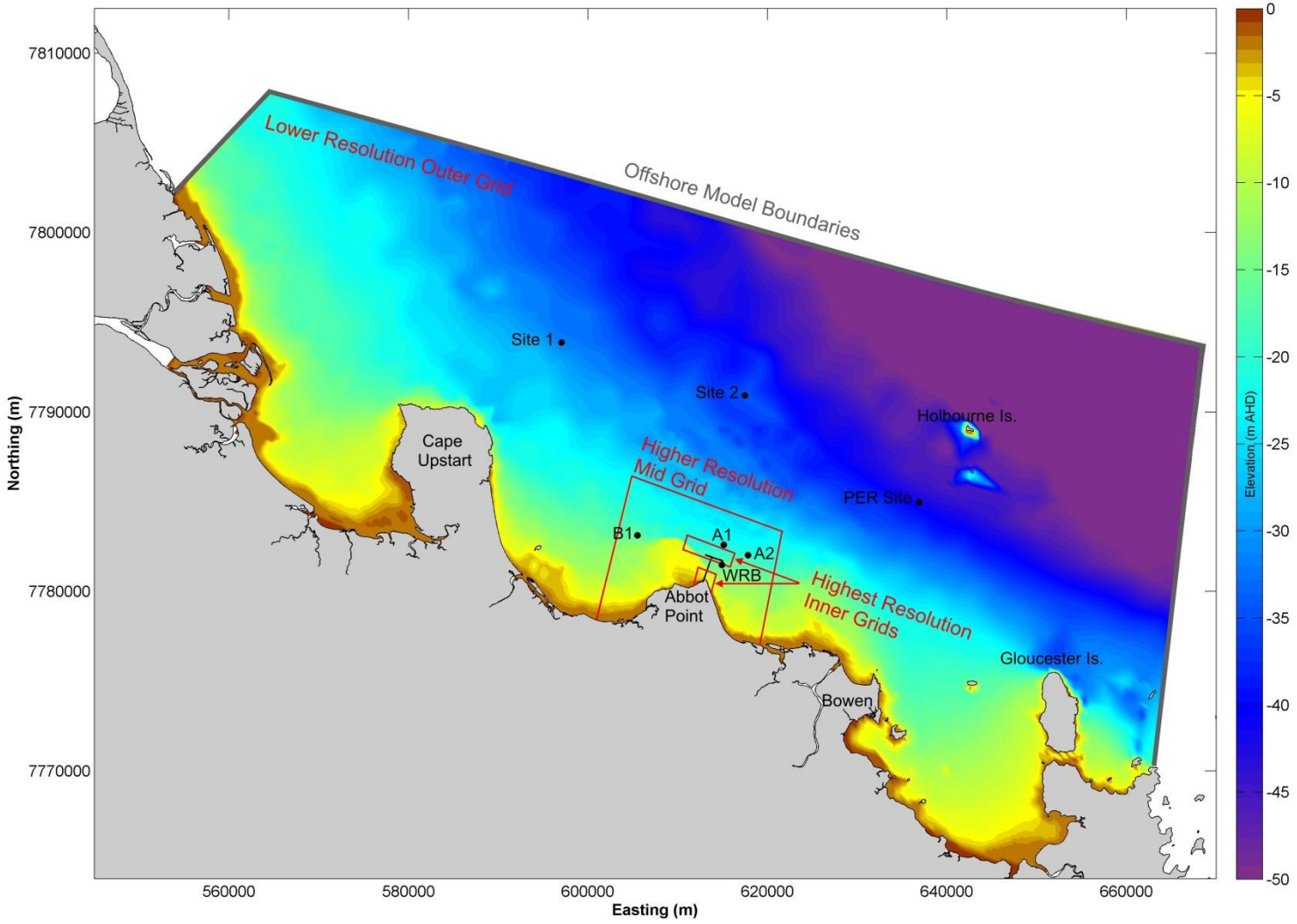

Figure 17 Model extent and bathymetry, locations of the seven calibration/verification sites.

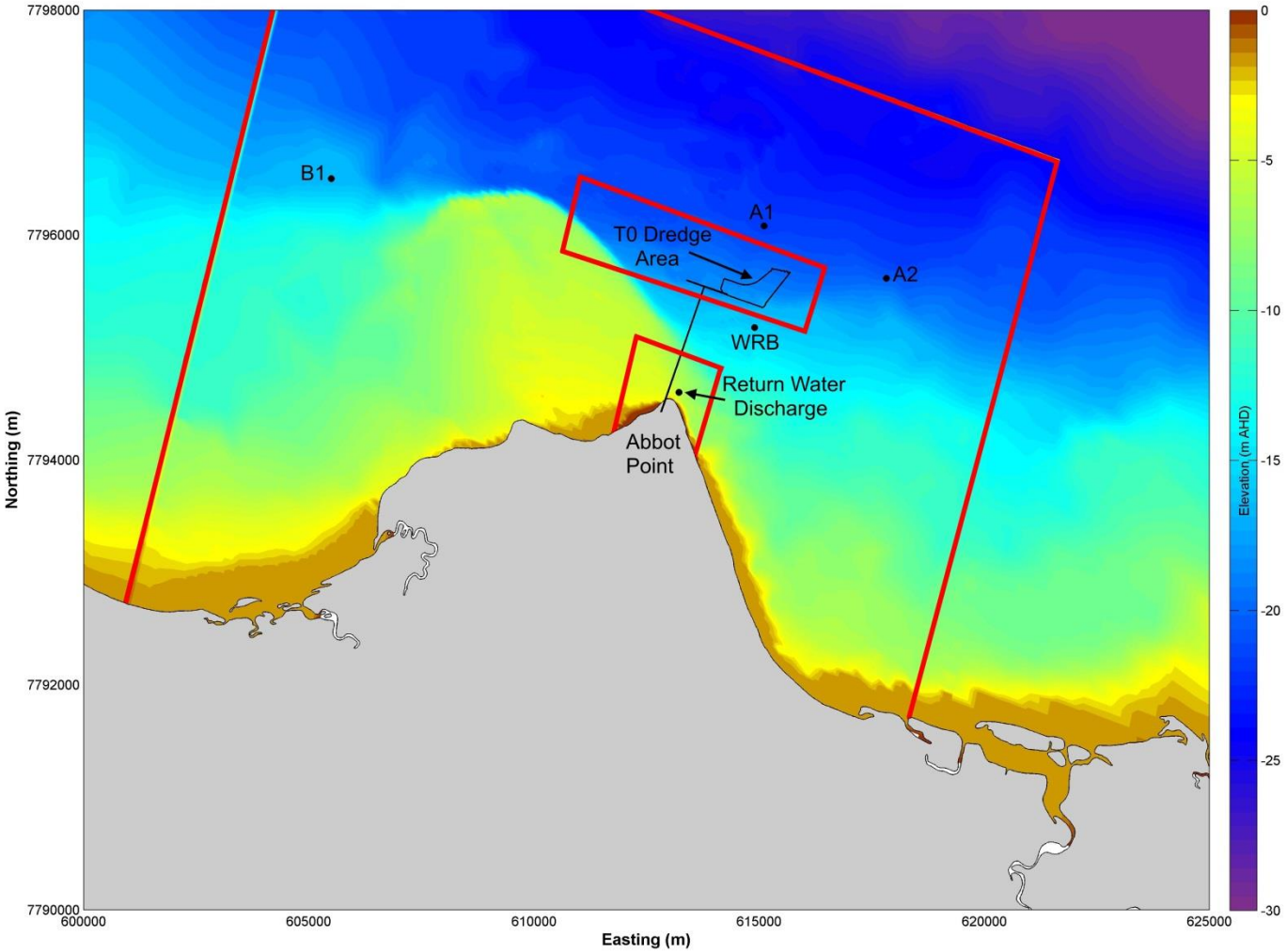

Figure 18 Close up of model extent and bathymetry showing the dredging areas, discharge location and local calibration/verification sites.

3.2 Model Setup

The extent of the model grid developed for this assessment along with the interpolated model bathymetry is shown above in **Figure 17** and **Figure 18.** The figure also shows the extent of the four different resolution grids, details of these are provided in **Table 5.**

Table 5 Model grid configuration.

Description	Extent (X by Y)	Cell Length Range (m)
Grid 1 – Outer Grid	108 km by 60 km	350 to 550 m
Grid 2 – Mid Grid	18 km by 16.5 km	110 to 180 m
Grid 3 – Inner Grid 1, Discharge Location	2 km by 2 km	30 to 60 m
Grid 4 – Inner Grid 2, Dredging Area	6 km by 2 km	30 to 60 m

This grid extent has been used as the basis for all of the numerical modelling components of the study. The higher resolution inner grids have been used in the hydrodynamic and water quality modelling for all the long-term stochastic dredging plume model runs. For the wave modelling simulations the outer grid resolution was used throughout the model domain.

3.2.1 Bathymetry

High resolution hydrographic survey data for the area surrounding the Port has been provided by North Queensland Bulk Ports Corporation (NQBP) to supplement the lower resolution bathymetric data of the remaining area obtained from digitised navigation charts provided through MIKE C-MAP. The hydrographic survey data covered an area of approximately 7 km by 7 km centred on the existing wharf at Abbot Point and was the primary dataset when interpolating onto the numerical model grid (i.e. the lower resolution bathymetric data was only used where there was no higher resolution data available).

The different bathymetric data utilised were corrected to Australian Height Datum (AHD) and then interpolated onto the model grid, the final model bathymetry is shown in **Figure 17** and **Figure 18**.

3.2.2 Hydrodynamic Model

The astronomical tidal boundaries for the model were derived using the DHI Global Tidal Model, KMS. The model was driven by varying water levels along the west, north and east boundaries. Testing was undertaken using other sources for the astronomical tidal boundaries including predicted water levels at secondary ports and other global tidal models, but the KMS boundaries were found to represent measured water levels and current speeds the closest.

The influence of large scale circulation processes within the GBR Lagoon on the currents at the relocation sites was represented by superimposing a water level gradient onto the astronomical tidal boundaries. This approach has been demonstrated to provide a realistic

representation of the regional GBR Lagoon scale circulation processes; further details on this are provided in **Appendix A**.

A spatially varying bed roughness was applied in the model, with a Manning's n roughness coefficient of 0.022 adopted for the nearshore regions and a coefficient of 0.03 adopted for the offshore regions with depths greater than 30 m. These values represent a medium bed roughness and were found to result in the best model calibration at the nearshore and offshore calibration and validation sites.

The currents within the GBR Lagoon and specifically in the area around Abbot Point can be significantly affected by wind forcing (SMEC, 2012). MetOcean Solutions Pty Ltd provided wind and wave data from their hindcast wave model of the area which has a spatial resolution of 0.05 degrees (approximately 5 km) and is driven by WaveWatch III. The winds extracted from the MetOcean Solutions model showed little spatial variation across the model domain. As such wind forcing was applied in this model uniformly across the domain as time series data.

The hydrodynamic model was run in 3-Dimensions, with five equally spaced σ layers each representing 20% of the depth in the model domain. Sensitivity testing has previously been undertaken to determine the optimum number of layers for the modelling. The testing showed that there was a minor difference in the plume extent between having three and five layers but there was no noticeable difference between having five and seven layers. Based on this, five layers is the optimum for this study, with there being no discernible benefit of having more than five layers in the model.

The hydrodynamic model was calibrated using water level and current data collected by two ADCP devices located relatively close to the existing wharf and jetty at Abbot Point, deployed at Sites A2 and B1 from September 2008 to October 2008 (**Figure 17** and **Figure 18**). The model was then validated for two periods using ADCP data collected at sites A1 and B1 in 2008 and sites 1 and 2 in 2014 (**Figure 17**). The calibration process demonstrated that the hydrodynamic model provides a good representation (within the bounds of the desired accuracy) of the astronomical tide, the effect of local wind on the currents and the influence of large scale circulation processes in the area offshore of Abbot Point. Further details of the calibration and validation are provided in the **Appendix B**.

For all the water quality model runs the hydrodynamic model was run fully coupled with the wave model to ensure that the effects of wave activity on the dispersion and resuspension of dredging material was included. This approach ensures that wave driven currents, enhanced turbulence and bed shear stress resulting from waves and stirring by wave breaking are all included in the numerical modelling. Further details of the wave model are provided in the following section.

3.2.3 Wave Model

As detailed in **Section 3.2** the wave model was run using the same grid as the hydrodynamic model, except that the higher resolution inner grid was not necessary to accurately represent wave conditions around Abbot Point. The model was driven using local wind and offshore wave boundary conditions. Both the wind and offshore wave boundary conditions were from MetOcean Solutions Pty Ltd hindcast wave model of the area. Offshore wave boundaries were input along the west, north and east model boundaries, and

uniform winds were applied across the entire model domain. The wave model was run in stationary mode with a JONSWAP bottom friction of 0.067 m^2/s^3. Details of the wave model calibration are provided in **Appendix B**.

For the stochastic modelling the wave model was coupled to the hydrodynamic model with the wave model running at a temporal scale of one hour.

3.2.4 Water Quality Model

Numerical models are a predictive tool which cannot replicate the natural environment exactly and approximations and assumptions have to be made to allow modelling to be undertaken. As no reliable TSS and deposition data was available from previous capital dredging campaigns at Abbot Point some approximations and assumptions had to be made in the modelling. Accordingly, some uncertainty exists in the sediment transport modelling. Although sediment transport measurements of the existing conditions can be collected (such as TSS, deposition, critical erosion and deposition thresholds and sediment consolidation and armouring), these cannot be used to provide a realistic representation of the conditions during and following dredging.

As the hydrodynamic and wave models have been demonstrated to be able to represent the driving conditions for the transport of the dredging plume well at a number of sites through the model domain, confidence can be placed in the driving forces for the sediment transport modelling. For aspects of the sediment transport modelling where there is uncertainty, conservative assumptions have been adopted to reduce the risk of any uncertainty and the risk of the model under-predicting the extent of the dredging plume. Conservative values have been selected based on sensitivity testing, information from available literature, parameters adopted for previous dredging plume modelling projects (both in Queensland and the rest of Australia) and results of subsequent monitoring activities which have consistently shown that the modelled dredging plume is overestimated due to the conservative assumptions made (Morton et al, 2014). Details of the assumptions are provided below and in **Section 3.3**.

The numerical modelling of the suspended matter in the Delft3D Water Quality (Delwaq) module is based on the method of Partheniades-Krone (Partheniades, 1962, 1965; Krone, 1962; DELWAQ Water Quality Manual, 2013). In this method, the bed shear stress plays an essential role in defining whether or not sedimentation of suspended particles or erosion of bed material occurs. Deposition can occur when the bed shear stress drops below a critical value, while erosion occurs when the bed shear stress exceeds a critical value. Suspended matter is subject to settling through the water column and sediment deposited on the bed is subject to erosion.

The critical bed shear stress for erosion depends on the resistance of the bed, which is characterised by a certain critical erosive strength. This critical stress is determined by several factors, such as the chemical composition of the bed material, particle size distribution and in the case of cohesive material the density / level of consolidation. The erosion is directly proportional to the excess of the applied shear stress over the critical erosive shear stress. The formula for erosion of homogeneous beds is based on Partheniades (1962). The erosion flux is limited by the available amount of sediment on the bed.

The sedimentation process is described with the classical formulation by Krone (1962). In this formulation, the rate of downward mass transport (deposition) is equal to the product of the near-bed velocity, the concentration and the probability that a settling particle becomes attached to the sea bed (depending on the critical shear stress of deposition). However, re-analysis of the experiments of Krone by Winterwerp and Van Kesteren (2004) revealed that the so-called critical bed shear stress for deposition does not exist. In fact, it represents the critical bed shear stress for erosion of freshly deposited sediment. Hence, the classical Krone formulation contains both a deposition and an erosion term. Therefore, Winterwerp and Van Kesteren (2004) proposed to model the sedimentation flux by applying an infinitely large critical bed shear stress for deposition. The software developers of Delft3D, Deltares, recommend the use of an infinitely high value for the critical bed shear stress for deposition for 3D-flow, sediment transport and water quality simulations. As such we have adopted the value recommended by Deltares of 1000 N/m^2 for all of our simulations.

No natural background suspended sediment is included in any of the sediment transport modelling, with all the sediment included being released as part of the material relocation activity. This is the typical approach for modelling dredging activity as it ensures that all the impacts of the dredging on the water quality can be identified and then considered relative to the natural background TSS concentrations which are determined from monitoring.

For this assessment it was necessary to represent the short-term dispersion, deposition and resuspension resulting from the placement of the dredging material onshore. A detailed description of the stochastic approach for the short-term modelling is provided in the following section.

3.3 Stochastic Modelling Approach

For the short-term modelling a stochastic, probabilistic approach was adopted which required 38 model simulations. As such, a robust and efficient approach was necessary to complete the number of simulations required. To achieve this, the Water Quality module of Delft3D, known as Delwaq, was adopted allowing multiple dredging plume dispersion simulations to be undertaken by using results from pre-run hydrodynamic and wave models. This 'offline' coupling approach provides a significant reduction in model simulation time without reducing the accuracy of the results. An outline of the stochastic dredging plume dispersion modelling is as follows:

- The modelling has been undertaken using three separate years selected from the last 20 years. To encompass the range of climatic and oceanographic variability the three years were selected to represent a strong El Nino event, a strong La Nina event and a Neutral year. Based on the Southern Oscillation Index (SOI) over this period 1997 was selected as the El Nino, 2011 as the La Nina and 2007 as the Neutral year (**Figure 19**);
- This assessment has assumed that 1.1 million m^3 of material is dredged, representing the dredging required for T0. Further details on the dredging material placement source terms applied in the modelling are provided in **Section 5**;
- A stochastic modelling approach has been used to represent the dispersion, deposition and resuspension during and immediately following material placement. Modelling of the dredging and onshore placement activities has been undertaken over a 10 month period (start of January until end of October) for each of the three

selected years. Multiple dredging relocation model simulations were undertaken during the 10 month period for each of the three years as part of the stochastic approach. A new discrete dredging relocation model simulation commenced with a start time 21 days later than the previous simulation, the first simulation commenced at the start of January and new simulations commenced every 3 weeks until the last simulation which could be completed before the end of October. Consideration of prevalent metocean conditions was included to ensure realistic representation of when dredging and placement can occur during these scenarios. Following cessation of the material placement activity each model simulation was continued for a further two weeks to ensure it provided sufficient time to determine how the dredged material advects and disperses following cessation of the material placement activity. This stochastic modelling approach resulted in 13 scenarios in 1997 and 2007 and 12 scenarios in 2011 (due to the occurrence of TC Anthony and TC Yasi in January and early February the first simulation was delayed and started after TC Yasi), resulting in a total of 38 scenarios;

- Three different sediment fractions were included in the Delwaq model to represent the fine grained material in the dredging material. Details of the fractions and the respective settling velocities which were adopted are shown in **Table 6**;
- A critical erosion threshold of 0.1 N/m^2 was adopted to represent the material released as part of the material relocation activity during the primary plume. This represents very loosely consolidated material (rheological behaviour of dilute fluid mud) which has been freshly deposited (Van Rijn, 1993; Tolhurst et al. 2009). This value is considered to provide a slightly conservative representation in terms of resuspension of the expected properties of the material released as part of these plumes;
- The dry density of any material deposited on the bed was assumed to be 150 kg/m^3. This value is only used in the model to calculate the deposition depth and as such is not critical in the numerical calculations; and
- Results from the stochastic model simulations have been combined for all simulations and for specific simulations to show how the plume extent and concentration varies depending on the SOI (El Nino, La Nina or Neutral year), season (wet, assumed to be January to April, or dry, assumed to be May to October[2]) and seagrass season (senescence, assumed to be January to June, or growing, assumed to be July to October[2]).

Table 6 Sediment fractions and settling velocities adopted in the numerical modelling.

Description	Representative Particle Size (µm)	W_s (mm/s)
Fraction 1 –Medium to Coarse Silt	45	1.82
Fraction 2 - Fine Silt	8	0.06
Fraction 3 - Clay	2	0.02[3]

[2] Dry and growing seasons continue until December, but model simulations only cover to the end of October.
[3] Note: this value incorporates an increased settling velocity associated with flocculated particles based on Winterwerp (2004) and assuming a TSS of 10 mg/L.

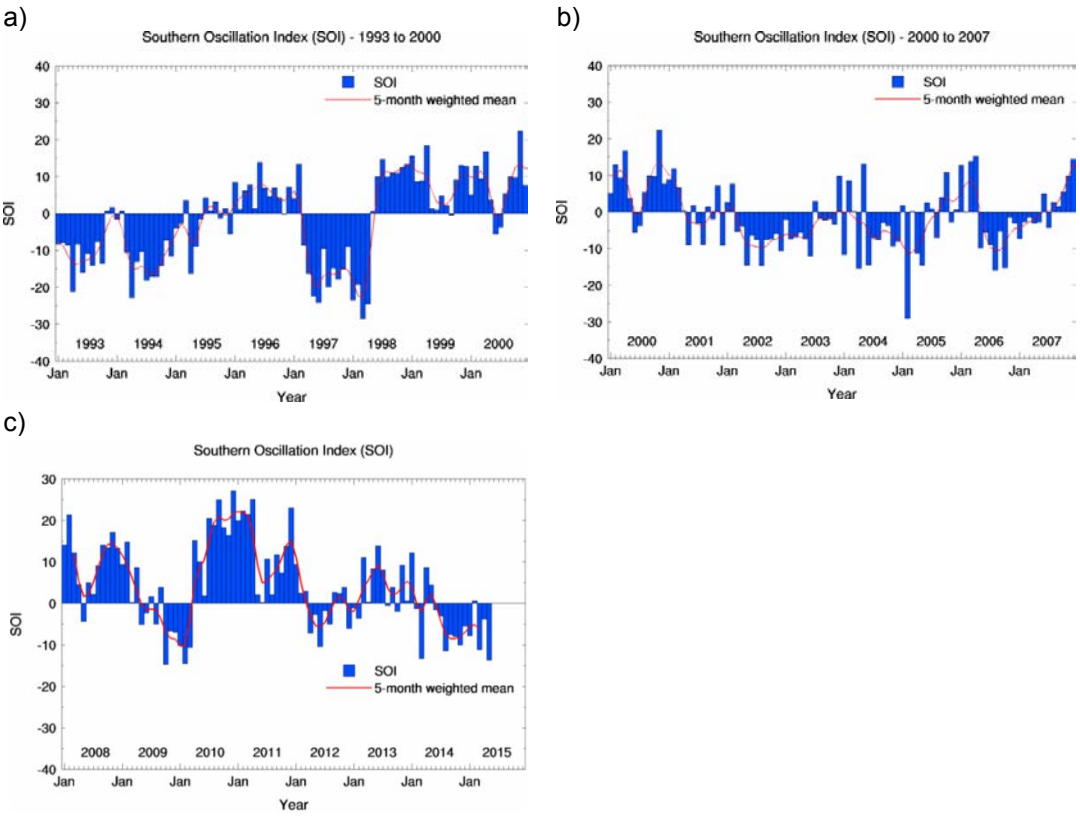

Figure 19 Southern Oscillation Index (SOI) between 1993 and 2015 (Source: www.bom.gov.au). Note: Sustained negative values of the SOI below -8 often indicate El Niño episodes, while sustained positive values of the SOI above +8 are typical of La Niña episodes.

4 SENSITIVITY TESTING

Sensitivity testing has been undertaken using the numerical model detailed in **Section 3** to help inform the model configuration and assumptions to be adopted in the stochastic model simulations. Details of the sensitivity testing which has been undertaken, along with the results and implications for the stochastic model simulations are provided in this section.

4.1 Discharge Location and TSS

Sensitivity tests have been undertaken to help inform the setup for the stochastic numerical model simulations of the onshore placement of dredged material. Sensitivity testing has been undertaken into the:

- location of the return water discharge; and
- TSS concentration in the return water discharge.

To determine how the discharge location influences the impacts resulting from the TSS discharged, dredging plume modelling has been undertaken with the discharge location at 5 different depths, 2, 3, 4, 5 and 7 m below LAT. These locations are shown in **Figure 20**. The 2, 3 and 4 m below LAT discharge locations assume the same pipeline orientation as shown in the referral (DSD, 2015), while the 5 and 7 m below LAT locations assume a different orientation to allow a shorter pipeline length due to the bathymetric variability. The dredging plume modelling has been undertaken in 3-Dimensional mode for a 1 week period of dredging which only includes the discharge location (i.e. no dredging activity) and applies a discharge TSS of 100 mg/L. This approach allows a comparative assessment of the TSS resulting from the range of discharge locations.

To determine how the impact varies depending on the TSS of the return water discharge a range of concentrations have been tested. The TSSs tested were 100, 80, 60, 50, 40 mg/L, with the discharge located at 4 m below LAT (the mid depth of the five tested). The dredging plume modelling was undertaken for a 1 week period of dredging in 2-Dimensional mode as running in 3-Dimensional model is not expected to result in any comparative differences. This approach allows a comparative assessment of the TSS resulting from the range of return water discharge concentrations.

Sensitivity testing has also been undertaken to better understand how the potential suspended sediment and deposition impacts resulting from the return water discharge vary depending on the composition of the sediment discharged. It is expected that the majority of the sediment released by the return water discharge will be fine grained silt and clay as this will be the material which has not settled in the DMCPs. However, it is difficult to determine the exact composition of the material at this stage. Accordingly, the model has been run for a complete dredge cycle of 1.1 Mm^3 with a range of fine grained sediment in the return water discharge and with just clay as detailed in Table 7.

Table 7 Sediment fraction composition and return water discharge concentrations adopted in the sensitivity testing.

Description	Test 1: Mixed Sediment		Test 2: Clay	
	Composition (%)	TSS (mg/L)	Composition (%)	TSS (mg/L)
Fraction 1 –Medium to Coarse Silt	34	34	0	0
Fraction 2 - Fine Silt	16	16	0	0
Fraction 3 - Clay	50	50	100	100

4.1.1 Findings

The TSS results from the one week long numerical model simulations have been processed to calculate the percentile TSS through the water column. The 95th percentile plots for the range of discharge locations tested are shown in **Figure 21** to **Figure 25**. The 95th percentile represents the concentration in each model grid cell for which concentrations were below for 95 percent of the simulation period. The results show that the shallower (closer to shore) discharge locations cover a greater area compared to the deeper, further offshore discharge locations. This is because higher current speeds occur closer to shore (**Figure 26** and **Figure 27**) and these are dispersing the sediment further before it settles out of suspension. It is also evident that the shallower discharges have a higher probability of reaching the shore. When the discharge location is at 4 m below LAT and deeper the peak in TSS is located away from the coastline, while when the discharge location is shallower the peak TSS is location directly adjacent to the coastline. The plots show that over the week long period tested for 95% of the time the TSS is less than 1 mg/L for all areas except directly adjacent to the discharge location. This is a very low concentration which would not be measureable above natural background concentrations.

The TSS results from the one week long numerical model simulations have been processed to calculate the percentile TSS through the water column. The 95th percentile plots for the range of return water discharge TSS tested are shown in **Figure 28** to **Figure 32**. The results show that the plume extent reduces significantly as the return water discharge TSS is reduced, with the plume extent for a discharge TSS of 100 mg/L being more than twice the extent with a discharge TSS of 60 mg/L. However, it is important to note that the plots show that over the week long period for all of the discharge location concentrations tested for 95% of the time the TSS is generally less than 1 mg/L for all areas except directly adjacent to the discharge location. As such, even though the extent of the plume shown in the plots does appear to vary significantly with the return water discharge TSS this is partially a result of a representative TSS scale being adopted to show the differences in the results. The TSS which makes up much of the plume extent (generally less than 1 mg/L) would not be directly measureable above the natural background concentrations.

The sensitivity runs with different sediment compositions in the return water show that higher TSS concentrations and sedimentation rates result due to the return water discharge including a mixed sediment composition (**Figure 33** to **Figure 36**). The areas where the TSS concentration adjacent to the return water discharge is increased by more than 1 mg/L and 2 mg/L for less than 5 percent of the dredging duration (95th percentile) are larger for the mixed composition sediment. This is a result of the finer grained clay material being more

dispersive than the silt sized material and therefore being diluted faster. Due to the relatively small amount of material being released in the return water discharge, the area where the TSS is more than 1 mg/L for less than 5 percent of the dredging duration during the dredging activity is smaller when the sediment released is just clay.

The daily deposition rate plots show that for the mixed sediment composition there is an area to the west of the return water discharge location where daily deposition rates in excess of 10 mg/cm^2 occur for less than 5 percent of the dredging duration. However, with just clay discharged this area of deposition does not occur. It is important to note that the deposition rate is a daily average rate which is exceeded for less than 5 percent of the time. This material is subsequently resuspended and so this area is not a permanent sediment sink, as discussed in more detail in **Section 6.1.2**. The sediment composition in the return water discharge does not influence any of the far field plume or sedimentation patterns. These are controlled by sediment released by the dredging activity rather than the return water discharge.

4.1.2 Summary and Recommendations

The sensitivity testing undertaken has shown the following key results about the plume resulting from suspended sediment released at the return water discharge:

- the TSS concentrations over the week long period tested are generally low, with concentrations of less than 1 mg/L for most areas except directly adjacent to the discharge location;
- when the discharge is located in deeper water the very low concentration plume extent is reduced compared to when it is in shallower water. This is a result of higher current speeds that occur closer to shore at the Abbot Point headland dispersing the sediment further;
- the very low concentration plume extent reduces significantly as the concentration in the return water discharge is reduced; and
- TSS concentration and daily deposition rate impacts with a mixed sediment composition in the discharge water are larger than with just clay sized sediment.

Based on the results it is suggested that a discharge location of 4 m below LAT is preferable as this reduces the risk of the fine grained material discharged being transported to the shore. The 4 m below LAT discharge location has been adopted for the stochastic modelling undertaken as part of this assessment.

As expected the sensitivity tests have demonstrated that the plume extent varies significantly depending on the return water discharge TSS, with a large difference in the very low concentration plume extent from return water discharge TSS of 100 and 60 mg/L. However, as the TSS is so low it is not expected to result in any significant impacts or result in a large plume extending a long way from the discharge location. As such, the highest TSS tested of 100 mg/L will be adopted for the stochastic modelling undertaken as part of this assessment. Adopting this TSS for the entire dredging period is considered highly conservative as such a concentration would only be expected to occur towards the end of the pond filling.

Based on the results of the return water discharge sediment composition sensitivity testing the mixed sediment composition has been adopted for the modelling. This is considered the

worst case as it results in larger potential impacts in terms of TSS concentration and sedimentation compared to just clay being included in the return water discharge.

4.2 Discharge Dilution

The characteristics of the return water discharge is likely to be different to the ambient characteristics of the water in the receiving environment. Compared to the receiving environmental water, the discharge waters may have different (elevated or reduced) physiochemical properties such as pH, turbidity and TSS and different chemical properties (elevated or reduced) such as particulate nutrients and dissolved nutrients. The discharge water will be subject to some initial dilution due to the effects of momentum and ambient turbulent mixing at the discharge point as these waters interact with the receiving water.

The United States Environmental Protection Agency (US EPA) dilution model Visual Plume has been used to model the expected initial dilution of dissolved substances in the return water discharge. The model has been used to determine the dilution assuming a range of ambient tidal current speeds, ranging from a speed of 0.4 m/s to no current. Current speeds in excess of 0.4 m/s occur at the return water discharge location during spring tides, while peak current speeds of between 0.1 to 0.2 m/s occur during neap tides. The results shown in Table 8 demonstrate that even with no ambient current speed at the return water discharge location a 1:40 dilution factor is reached within 60 m of the discharge location. When a current speed of 0.4 m/s occurs, as expected during peak spring currents, the 1:40 dilution factor is achieved within 15 m of the discharge location.

Table 8 Modelled horizontal distance from the return water discharge to reach a 1:40 dilution factor.

Tidal Current Speed (m/s)	Horizontal Distance (m)
0.4	15
0.2	23
0.1	33
0	58

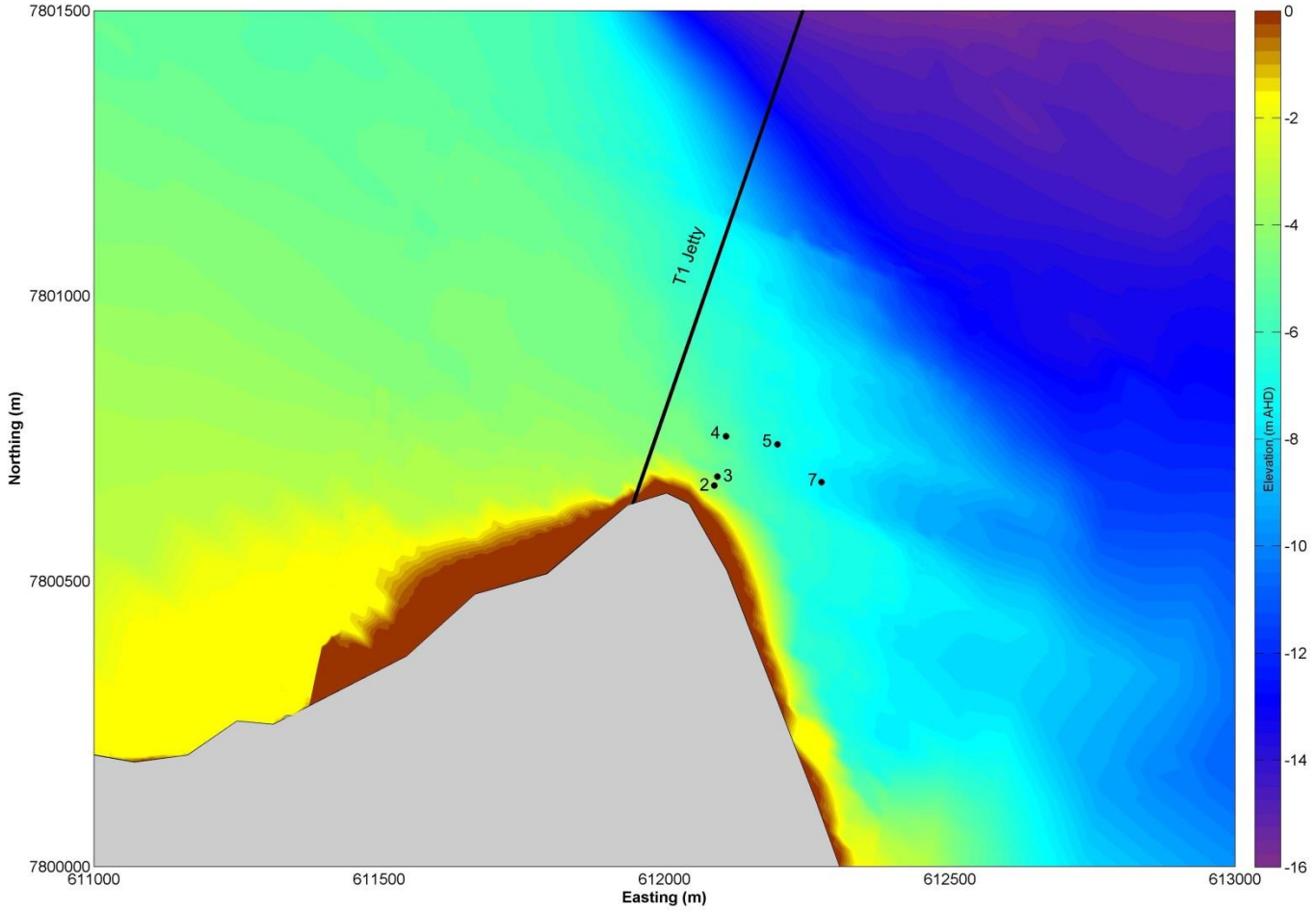

Figure 20 Model bathymetry and locations of the discharge locations tested. Note: names of discharge locations represent depth in metres below LAT.

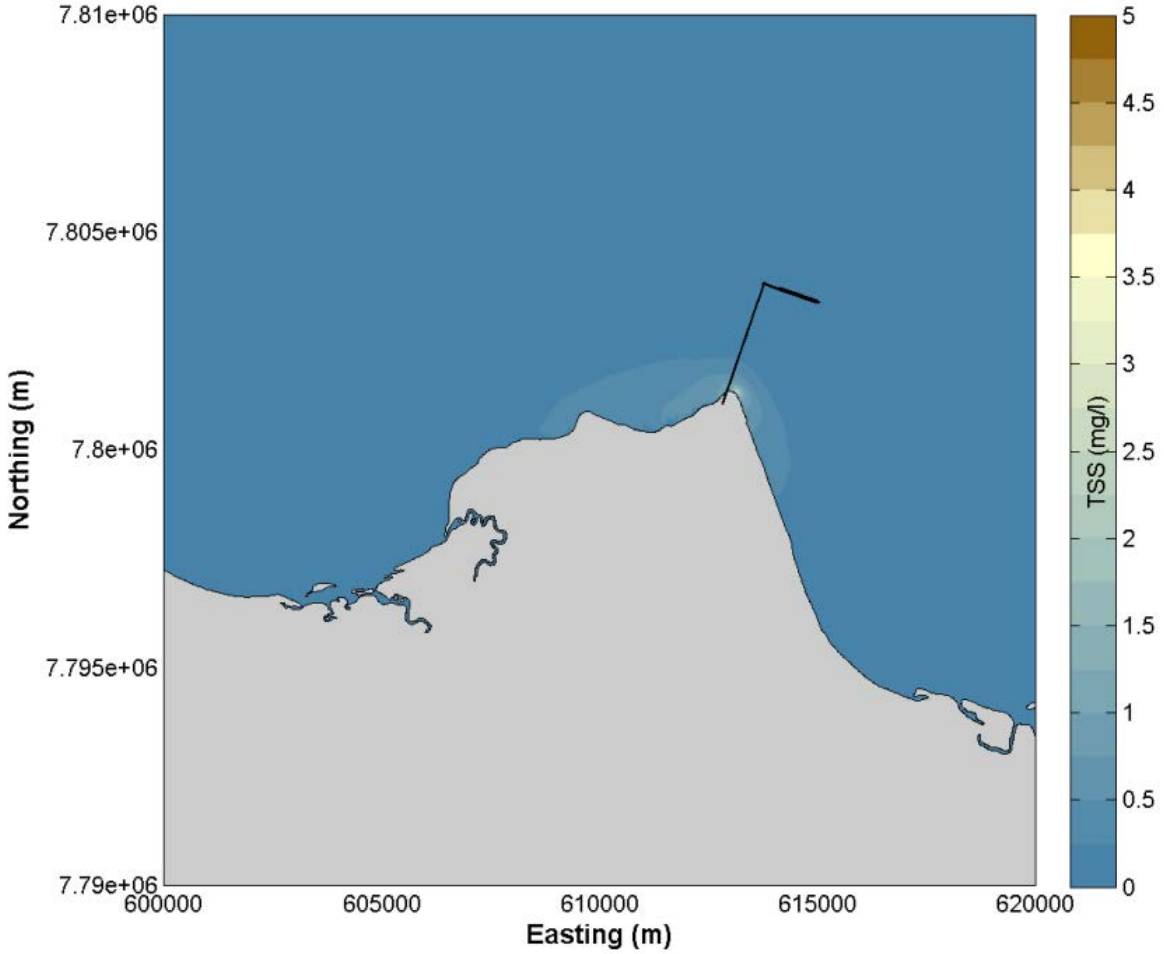

Figure 21 95th Percentile TSS with the discharge located at 2 m below LAT.

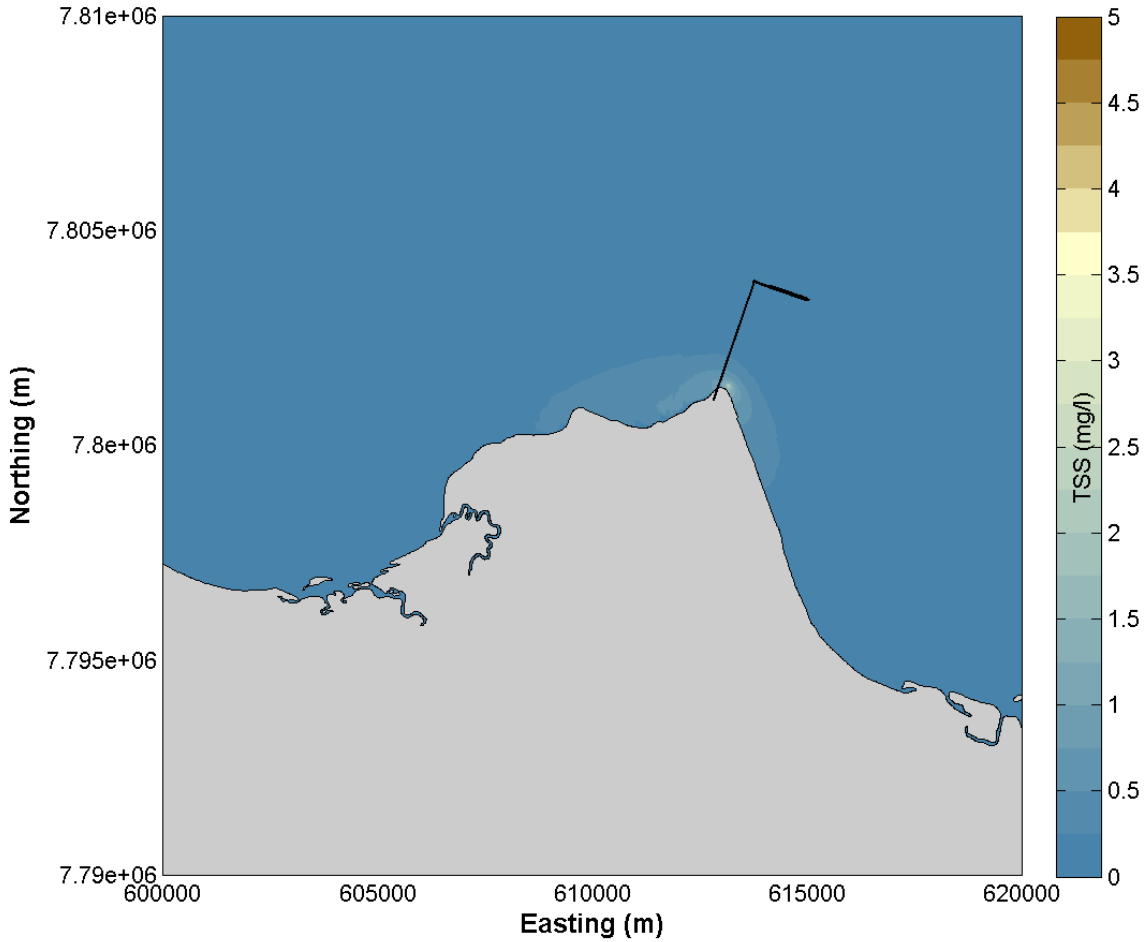

Figure 22 95th Percentile TSS with the discharge located at 3 m below LAT.

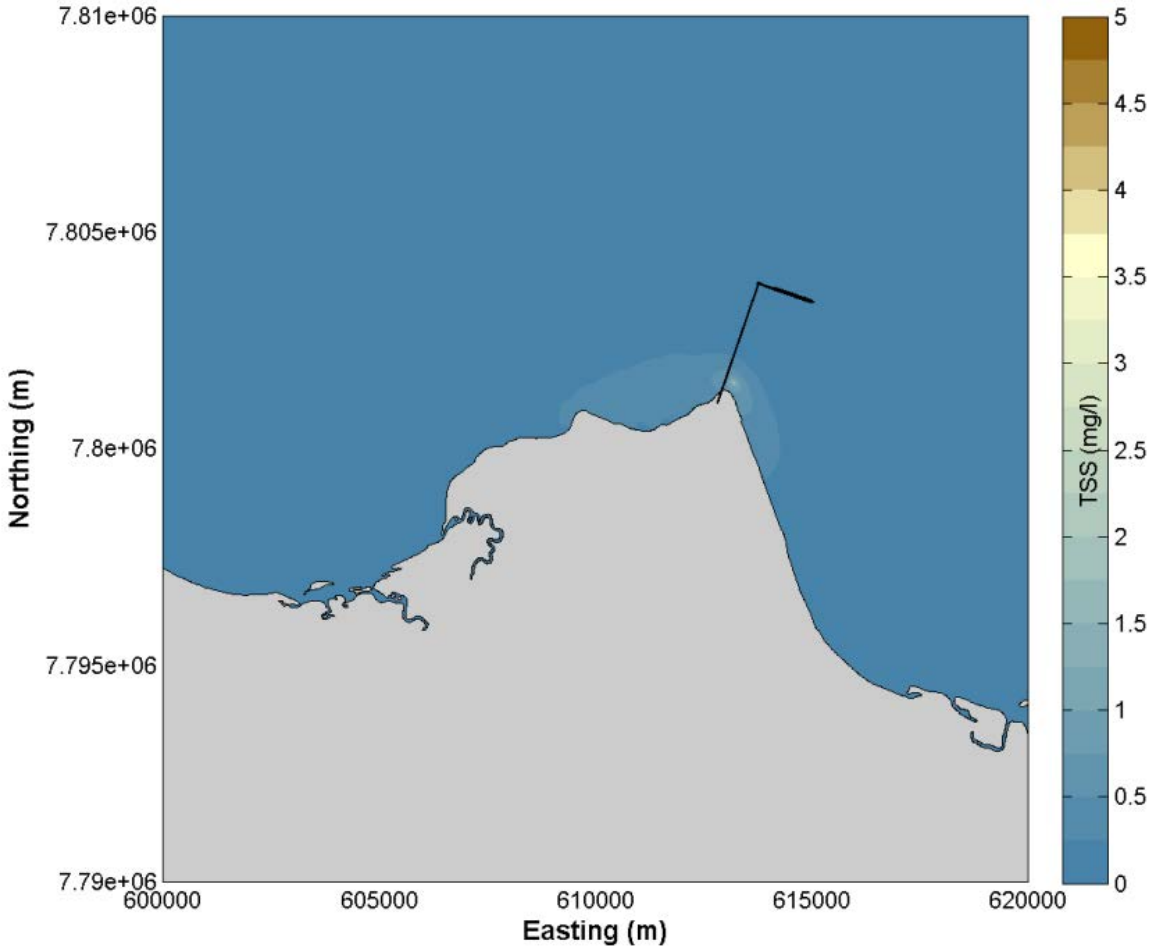

Figure 23 95th Percentile TSS with the discharge located at 4 m below LAT.

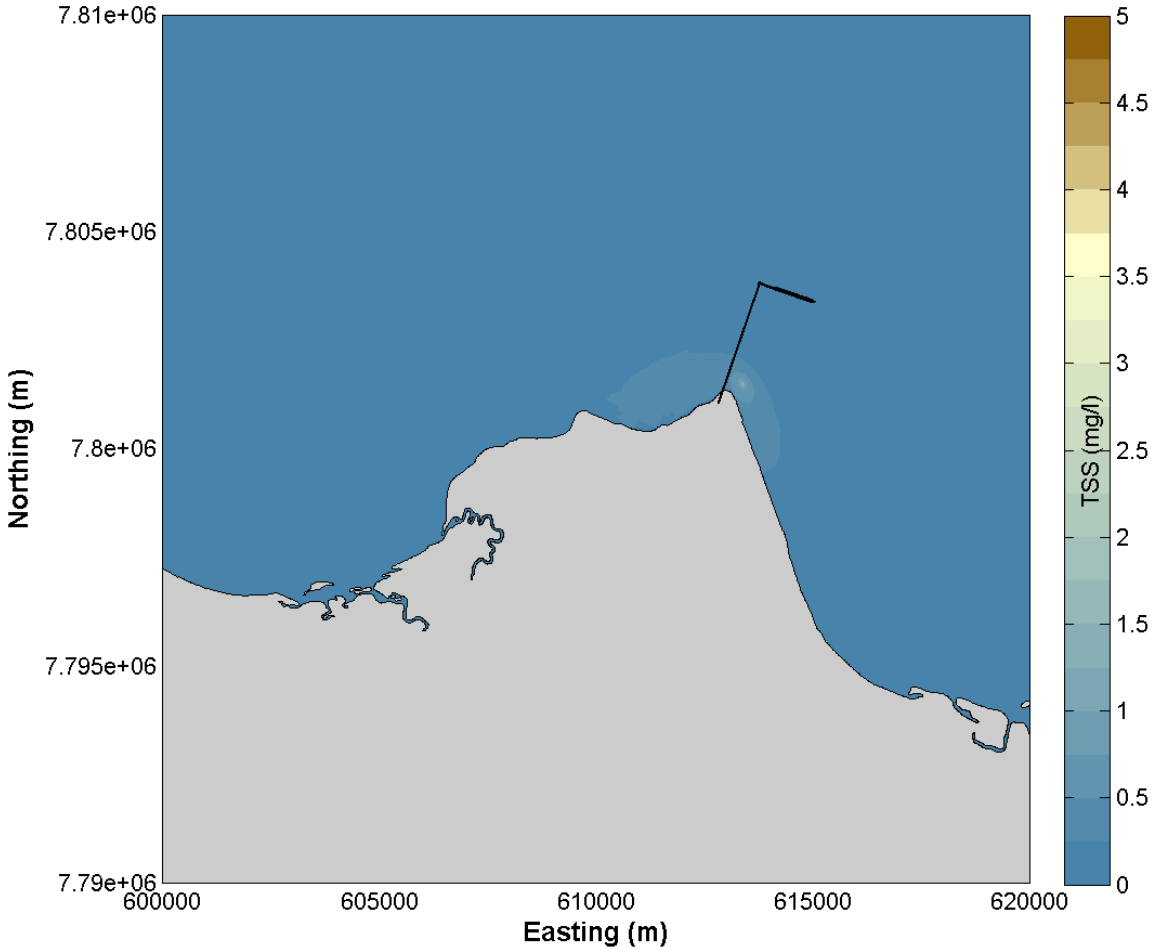

Figure 24 95th Percentile TSS with the discharge located at 5 m below LAT.

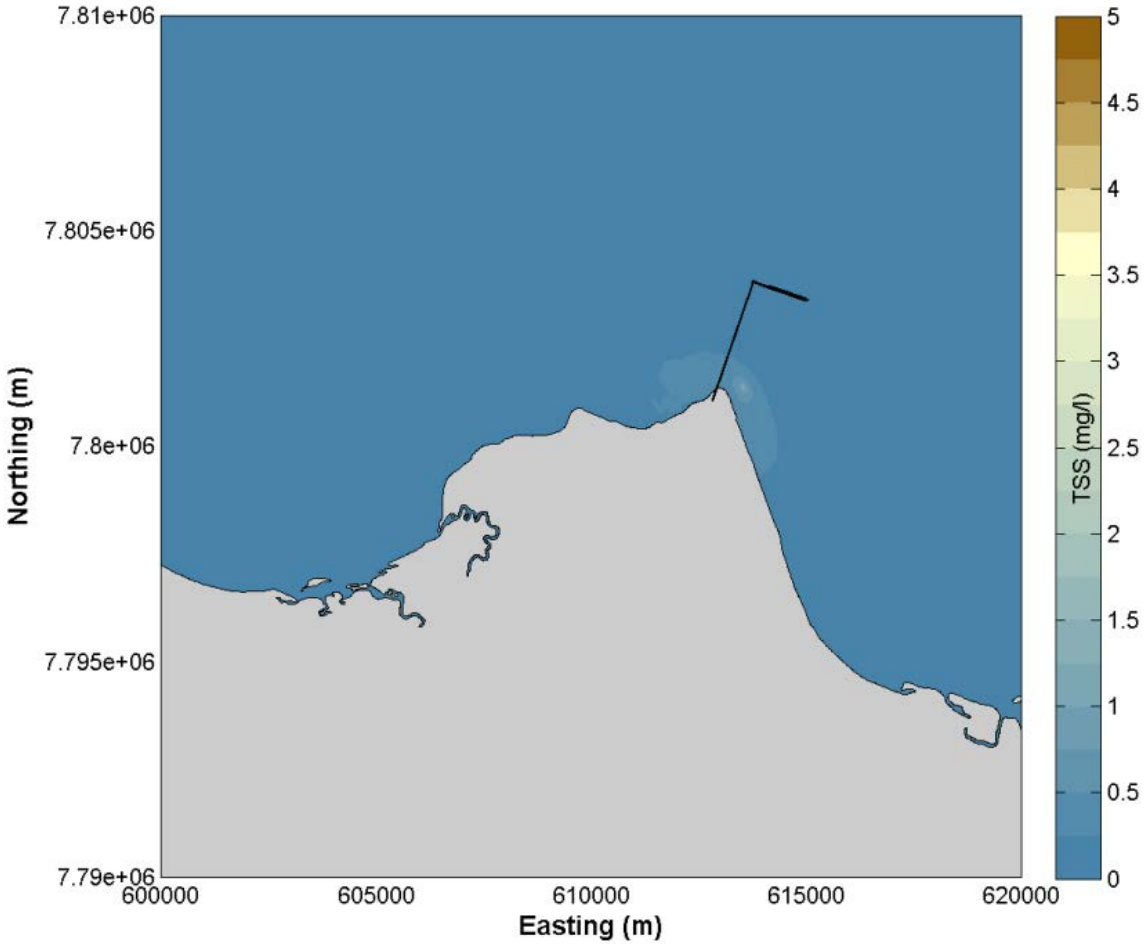

Figure 25 95th Percentile TSS with the discharge located at 7 m below LAT.

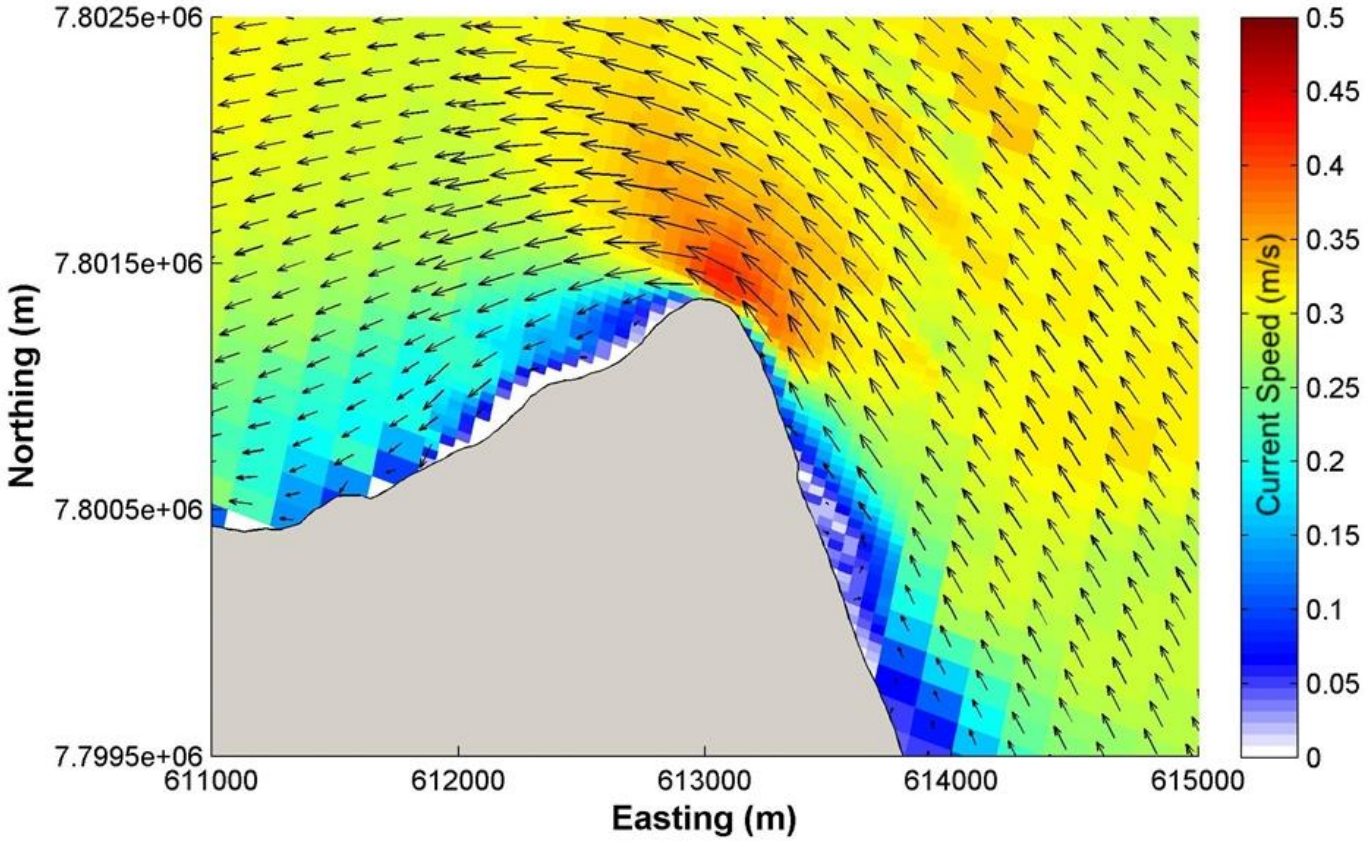

Figure 26 Tidal currents at Abbot Point during peak ebb.

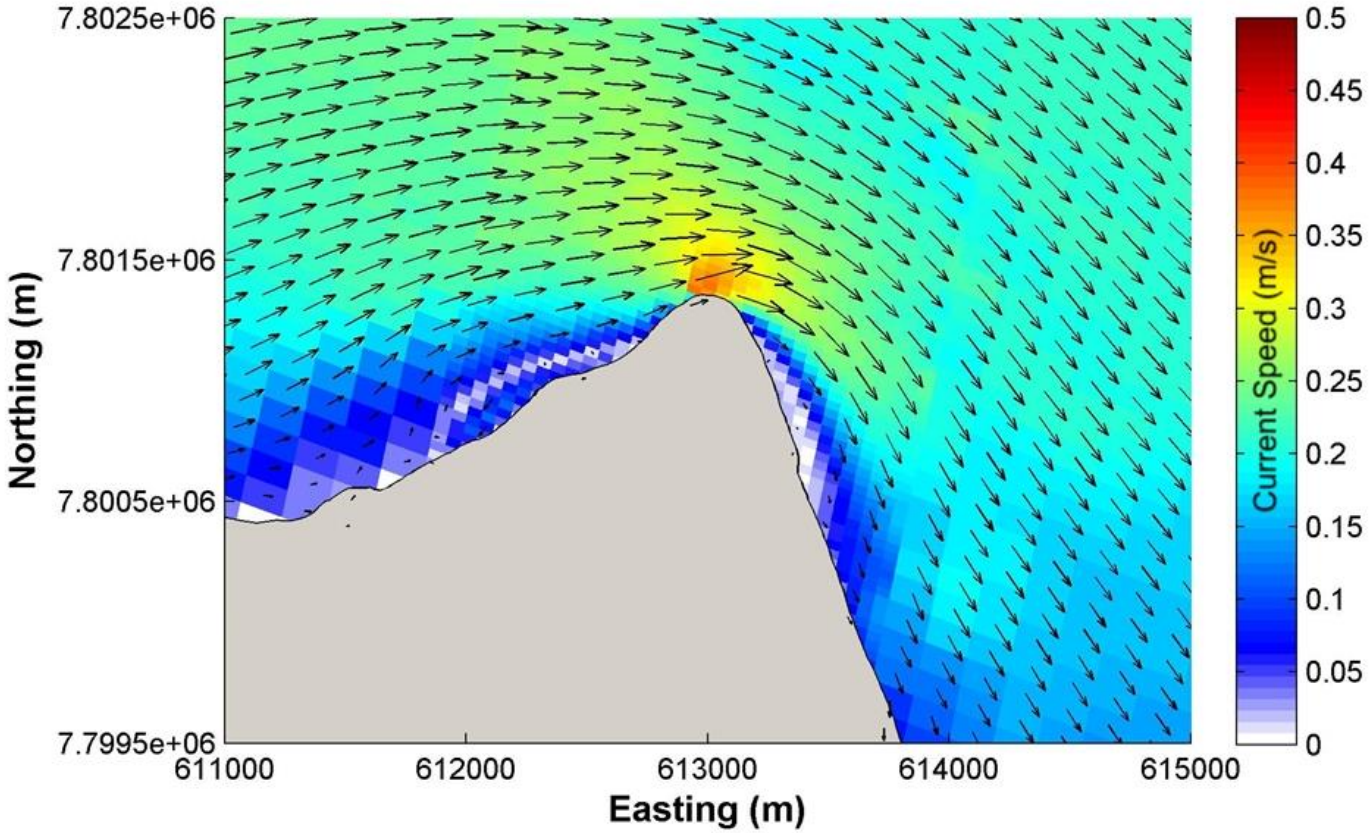

Figure 27 Tidal currents at Abbot Point during peak flood.

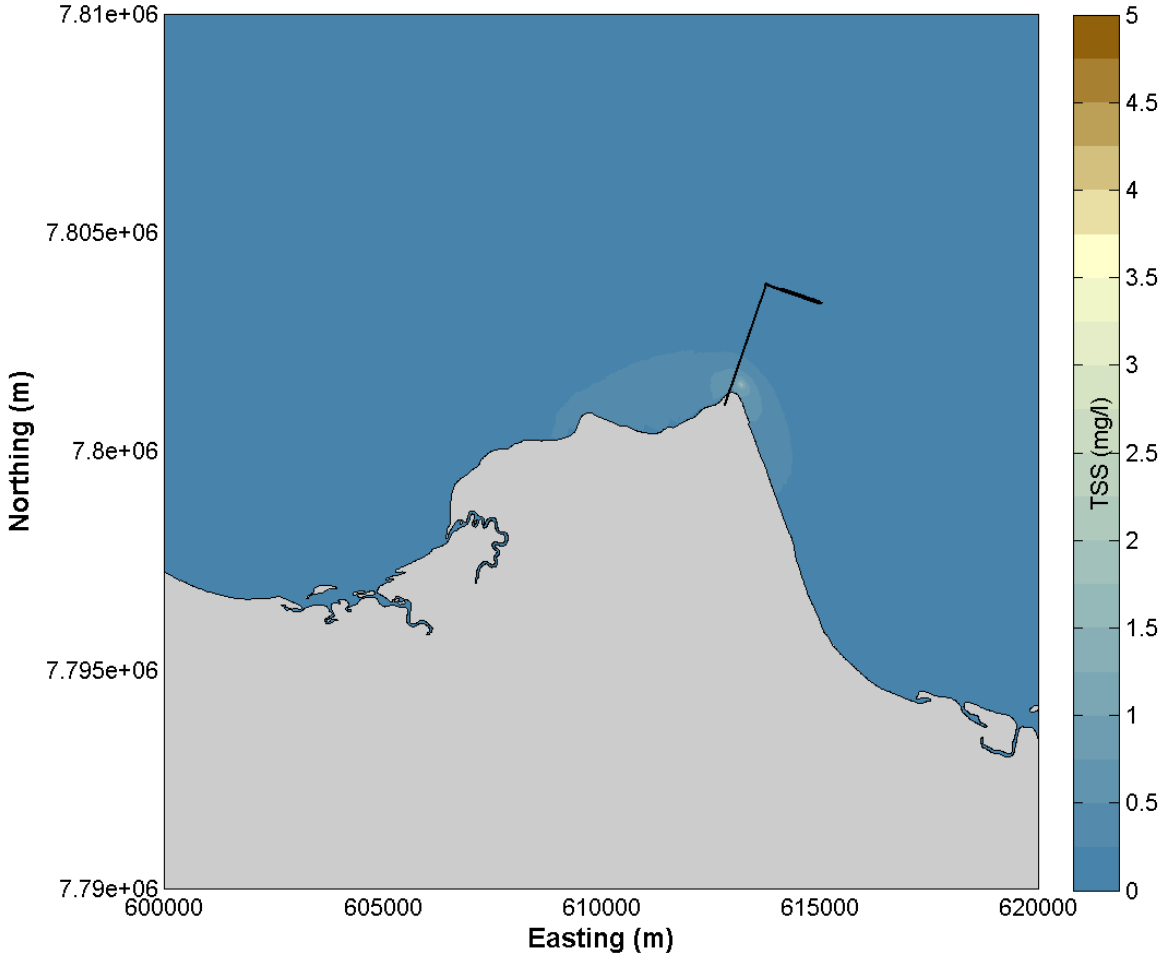

Figure 28 95th Percentile TSS with a discharge concentration of 100 mg/L.

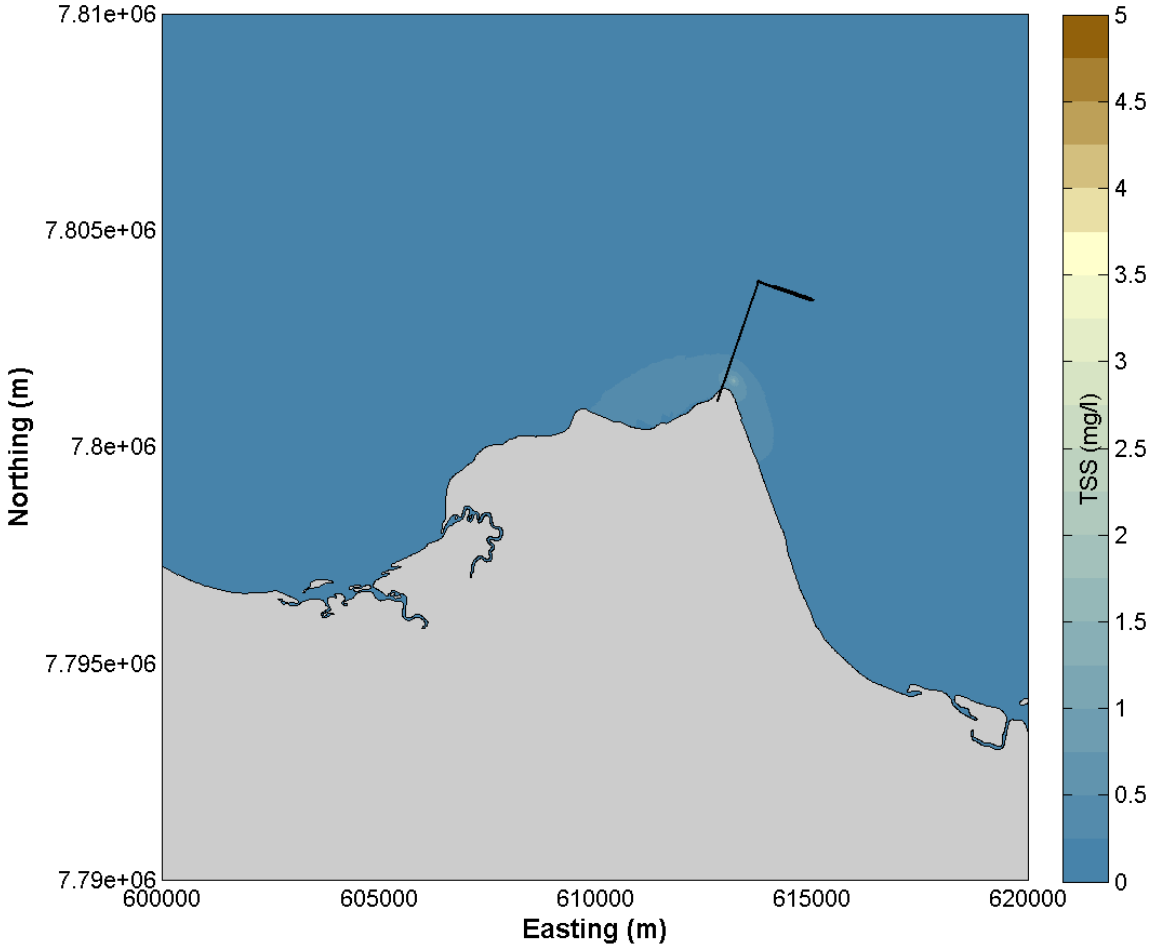

Figure 29 95th Percentile TSS with a discharge concentration of 80 mg/L.

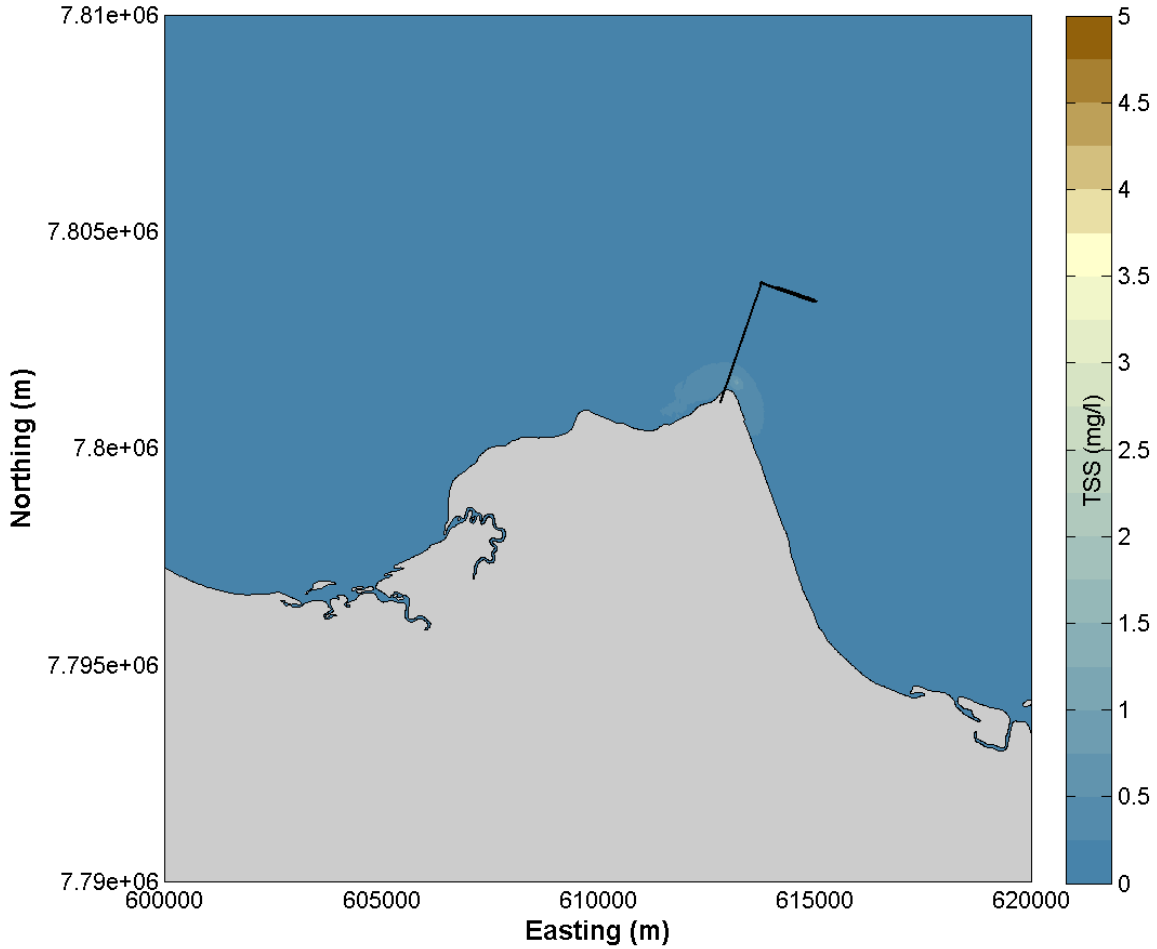

Figure 30 95th Percentile TSS with a discharge concentration of 60 mg/L.

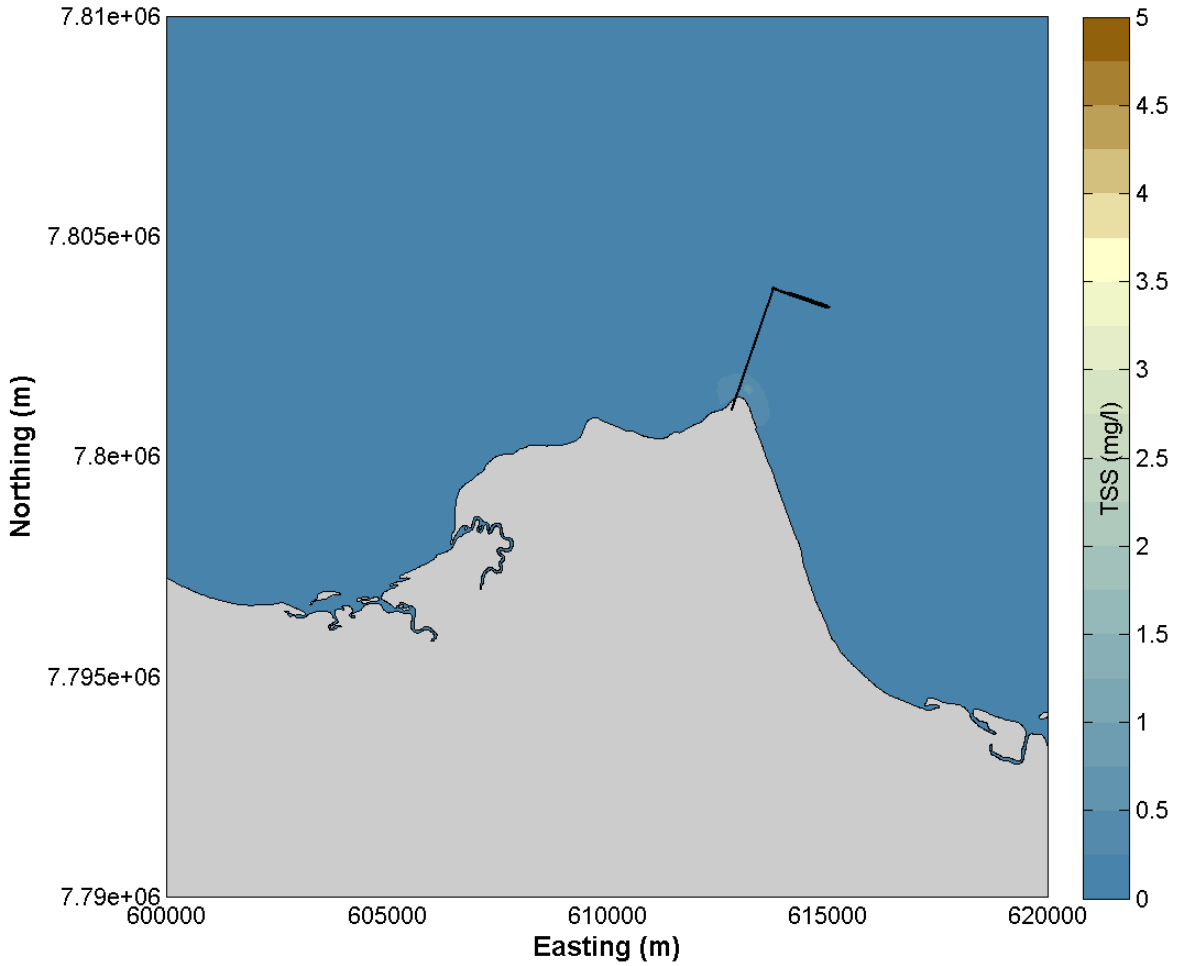

Figure 31 95th Percentile TSS with a discharge concentration of 50 mg/L.

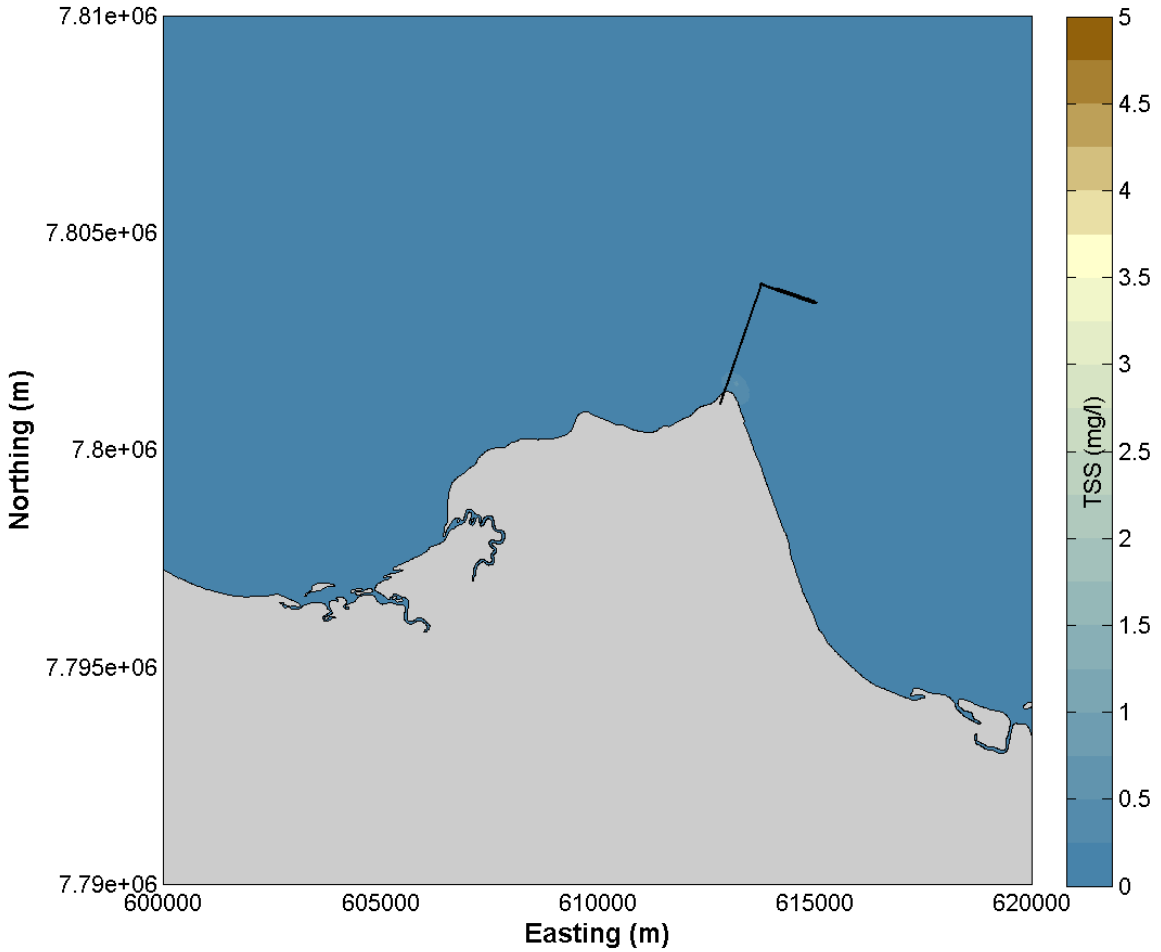

Figure 32 95th Percentile TSS with a discharge concentration of 40 mg/L.

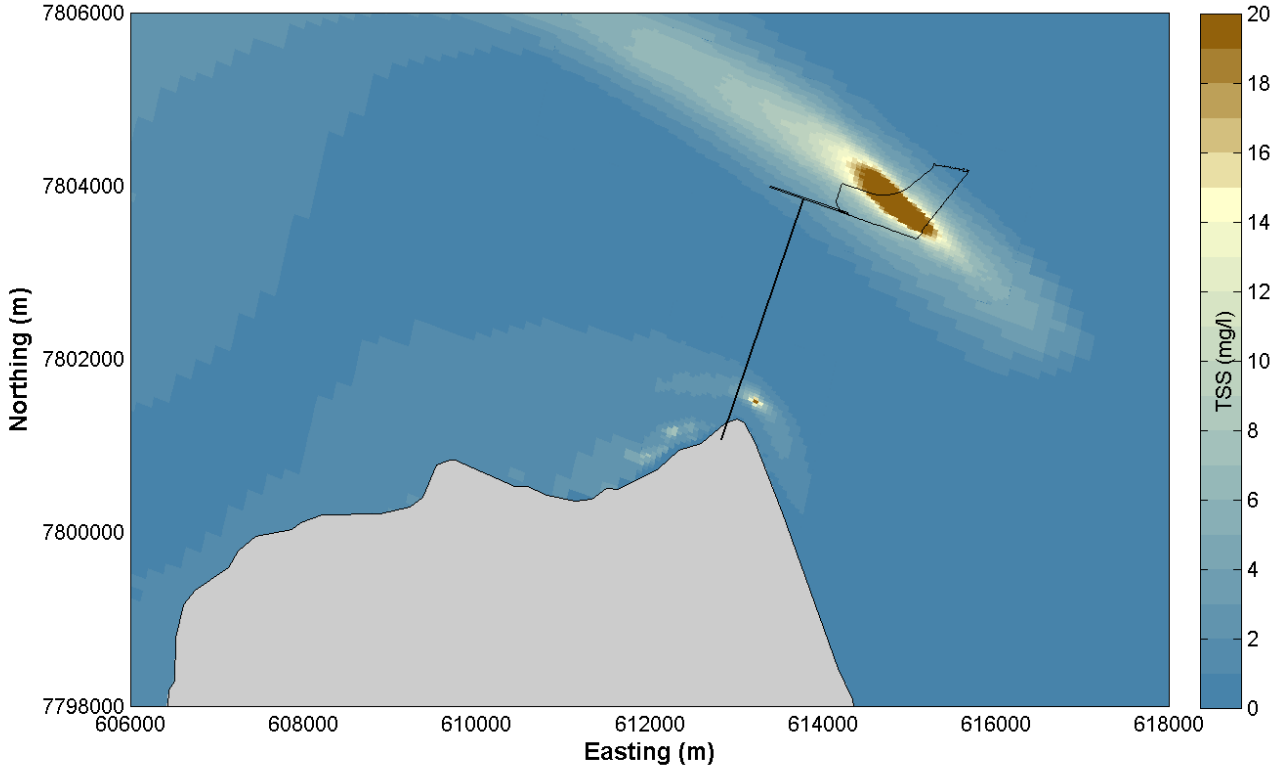

Figure 33 95th Percentile TSS with mixed sediment composition in the discharge and with the dredging activity included.

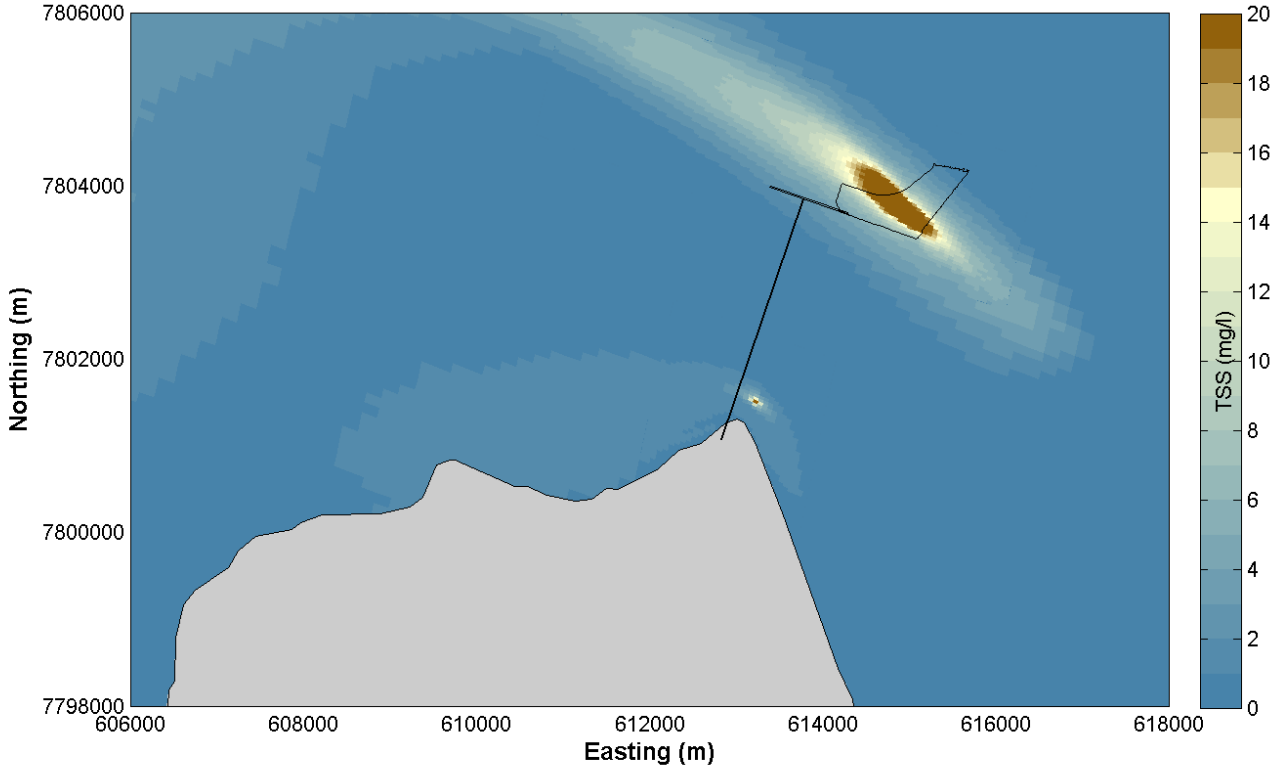

Figure 34 95th Percentile TSS with just clay in the discharge and with the dredging activity included.

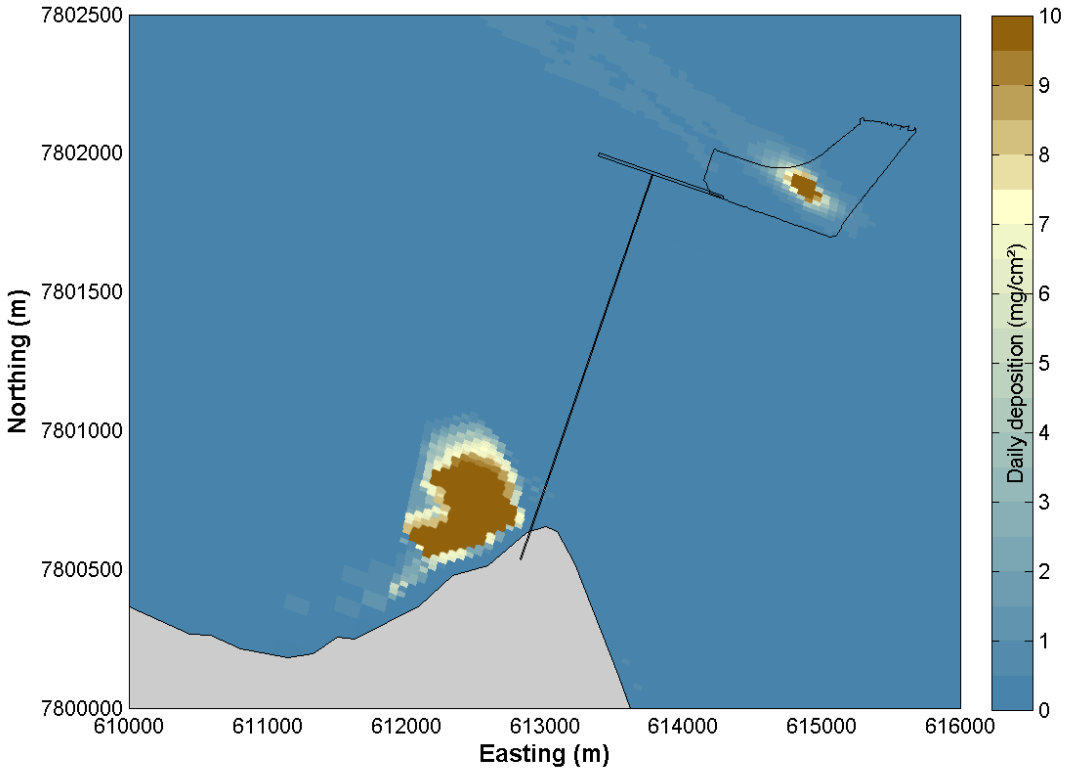

Figure 35 95th percentile sedimentation with mixed sediment composition in the discharge and with the dredging activity included.

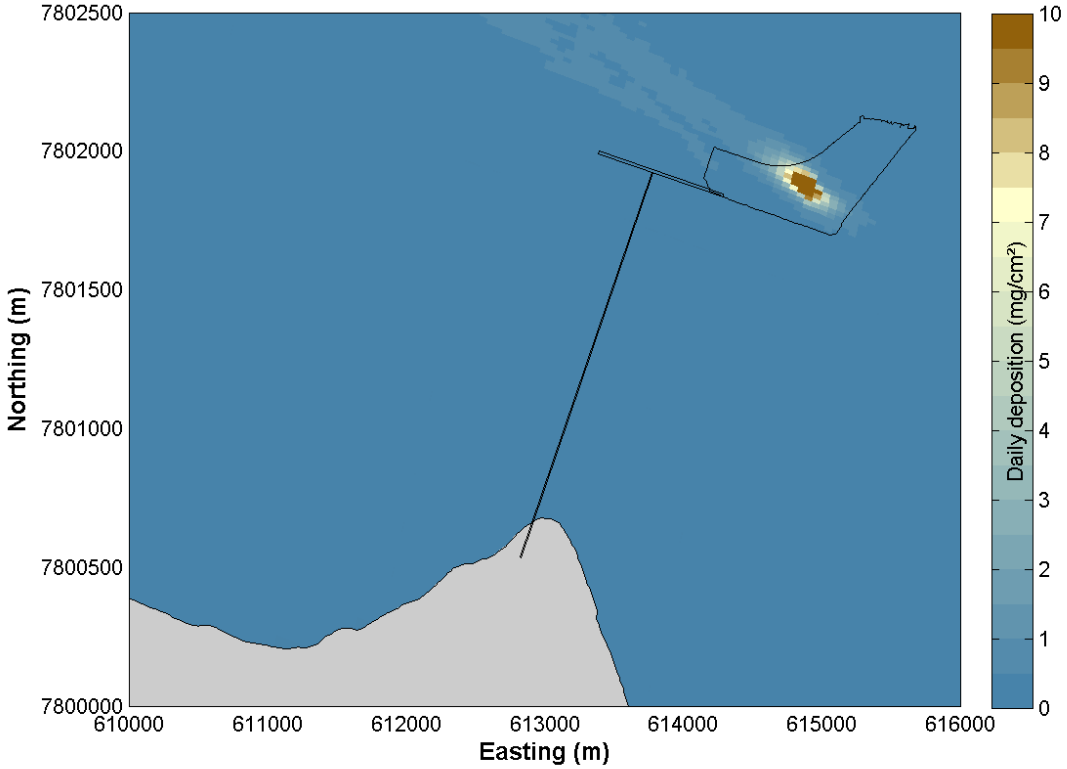

Figure 36 95th percentile sedimentation with just clay in the discharge and with the dredging activity included.

4.3 Dredging Duration

The size of the dredge vessel that will undertake the T0 dredging is not known at this stage, although it is likely that it will be either a large or medium sized dredger. The dredging rates and therefore the dredging duration will vary depending on the vessel size. For a large vessel the dredging rates are higher and the duration is expected to be approximately 6 weeks, while for a medium vessel the rates are lower and as such the duration is expected to be approximately 13 weeks. To assess the impact from the onshore placement of dredging material for dredging with a large compared to a medium sized dredge vessel, additional numerical modelling sensitivity testing simulations were undertaken. A summary of the key assumptions for the large and medium sized dredge vessels are provided below:

- model simulations have been assumed to occur during the dry (seagrass growing) season, with the dredging commencing at the start of June. Both El Nino and Neutral years have been tested;
- total in situ volume to be dredged is 1.1 million m^3 (including 0.5 m over dredge);
- dredging will be continuous for 16 hours per day, 13 days per fortnight;
- the amount of material suspended by the cutter head during the dredging activity will be 3% losses of fines. In this case fines have been assumed to represent any material of coarse silt and finer (<63 µm);
- the return pipeline outflow will be continuous for 24 hours a day throughout the duration of the dredging;
- Large dredge vessel:
    - the average dredging rate will be 1,700 m^3/hr for the apron and 2,400 m^3/hr for the berth;
    - the outflow discharge will be 8,300 m^3/hr throughout the duration of the dredging;
    - the concentration of the outflow will be 100 mg/L throughout the duration of the dredging; and
    - based on the dredging approach and associated volumes for the first dredging scenario, the apron has been calculated to take 4 weeks to dredge and the berth 1.6 weeks.
- Medium dredge vessel:
    - the average dredging rate will be 735 m^3/hr for the apron and 1,035 m^3/hr for the berth;
    - the outflow discharge will be 3,575 m^3/hr throughout the duration of the dredging;
    - the concentration of the outflow will be 100 mg/L throughout the duration of the dredging; and
    - based on the dredging approach and associated volumes for the first dredging scenario, the apron has been calculated to take 9.3 weeks to dredge and the berth 3.7 weeks.

The dredging plume modelling has been undertaken in 3-Dimensional mode for the entire dredging period for both dredge vessel sizes. The simulations include both the material suspended during the dredging activity and the material discharged from the discharge location. This approach allows a comparative assessment of the dredging plume behaviour resulting from the two different scenarios.

4.3.1 Findings

The TSS concentration results for the two different dredging duration simulations (dredging with a large vessel (approximate 6 week total dredging duration) and dredging with a medium sized vessel (approximate 13 week total dredging duration)) have been processed to show the 95th percentile over the total dredging period (**Figure 37** to **Figure 38**). The 95th percentile plots show the value which the TSS is less than for 95% of the total dredging period. The 95th percentile plots are only shown for the Neutral year as the results for the El Nino year were very similar.

The 95th percentile plots show that a much larger area experiences increased TSS concentrations when the dredging duration is approximately 6 weeks compared to 13 weeks. The area in the 95th percentile plots with increased TSS concentrations of more than 2.5 mg/L over the dredging duration extends to over 10 km for the shorter duration, while for the longer duration it is less than 5 km. The areas with higher TSS concentrations also cover a large area for the shorter duration dredging compared to the longer duration. In addition, the small localised increase in TSS concentrations resulting from the return water discharge covers a larger area and has a higher concentration for the shorter dredging duration.

The sedimentation rates results for the two different dredging durations have also been processed to show the 95th percentile over the total dredging period for both the El Nino and Neutral years (**Figure 39** to **Figure 42**). The results show that for both years the sedimentation rates at the dredging location are similar, with slightly higher rates resulting from the shorter dredging duration. The 95th percentile sedimentation patterns to the west of the Abbot Point headland resulting from the return water discharge are similar for both dredging durations for the El Nino year, while for the Neutral year the longer dredging duration results in higher sedimentation rates. The higher sedimentation rates in this area for the longer dredging duration is a result of the longer dredging duration experiencing a greater range of metocean conditions, with occasional periods of calm conditions promoting increased sedimentation rates.

Further comparison of the sedimentation rates using the 80th percentile over the total dredging period shows that the shorter dredging duration results in higher sedimentation rates, with no sedimentation occurring to the west of the return water discharge (**Figure 43** to **Figure 44**). This demonstrates that the increased sedimentation rates which the model predicted during the longer dredging duration scenario only occur for a short period of the dredging period. In addition, the metocean conditions which result in the increased sedimentation will be captured by the stochastic approach for both dredging durations. As such, the combined stochastic sedimentation results for both dredging durations would be expected to be similar, with higher sedimentation tending to occur for the shorter duration dredging.

Benthic PAR thresholds for nearshore (<6 m AHD) and offshore (>6 m AHD) seagrass sites at Abbot Point have been defined by the Centre for Tropical Water and Aquatic Ecosystem Research (TropWATER) based on recent monitoring data (McKenna et al, 2015). When the average daily benthic PAR value drops below the thresholds due to impacts from the dredging activity and return water discharge the area is considered to be a zone of moderate

impact[4] to seagrass. Further details on the thresholds and how benthic PAR has been calculated is provided in **Section 6.1.4**. The difference in the benthic PAR threshold exceedance resulting from the dredging activity and return water discharge are similar for the El Nino and Neutral years and as such only the Neutral year results have been presented. The results in **Figure 45** to **Figure 48** show that neither dredging durations result in a change to the baseline benthic PAR threshold exceedance for the nearshore thresholds. However, for the offshore thresholds both dredging durations result in changes to the benthic PAR threshold exceedance to the west and south-east of the dredging area. These changes exhibit the following difference in the zone of moderate impact resulting due to the dredging duration:

- the shorter duration dredging results in a larger zone of moderate impact to the west of the dredging area than the longer duration dredging; and
- the longer duration dredging results in a larger zone of moderate impact to the south-east of the dredging area.

This is a result of the different metocean conditions experienced during the longer dredging duration simulation relative to the shorter duration as opposed to actual differences in the potential impacts to benthic PAR. Both dredging durations have the same metocean conditions for the first 6 weeks, and then when the shorter dredging duration ends the longer dredging duration has a further 7 weeks where the dredging is exposed to new and potentially different metocean conditions. To demonstrate this, a second shorter dredging duration simulation was undertaken to start mid-way through the longer duration dredging simulation, thereby representing the same metocean conditions as the second half of the longer duration simulation.

This further simulation results in larger zones of moderate impact both to the west and south-east of the dredging area compared to the longer dredging duration (**Figure 49**). This shows that the higher TSS concentrations which occur as a result of the shorter duration dredging result in a larger potential impact to benthic PAR compared to the longer dredging duration. However, the longer duration dredging has the potential to impact different areas compared to the shorter duration as a result of the potential for additional variability in the metocean conditions resulting from the longer dredging period. It has been demonstrated that the additional metocean condition variability will be captured by the stochastic modelling approach regardless of which dredging duration is adopted. As such, the combined stochastic benthic PAR threshold exceedance results for both dredging durations would be expected to be similar, but with the shorter duration dredging resulting in larger zones of moderate impact.

The results from this assessment demonstrate that the shorter dredging duration of approximately 6 weeks, which assumes a large dredge vessel, results in increased TSS concentration impacts compared to the longer dredging duration of approximately 13 weeks, which assumes a medium sized dredge vessel. Both dredging durations show similar impacts in terms of sedimentation rates and impacts to benthic PAR, with some variability resulting due to the variable metocean conditions resulting due to the difference in dredging duration. However, this metocean variability will be captured by the stochastic modelling

[4] *Zones of moderate impact* are areas in which sustained levels of TSS, sedimentation or sediment deposition cause sub-lethal impacts to benthic organisms that inhabit the areas. Sub-lethal impacts include partial mortality and impacts to the health of the organism that may include a reduction in the ability of that organism to grow and reproduce as it normally would. The organisms in this zone are expected to recover within five years of the impact.

approach regardless of which dredging duration is adopted. Therefore, adopting the shorter dredging duration of approximately 6 weeks for the stochastic modelling represents the worst case scenario in terms of the intensity and extent of potential impacts. As a result, the modelling detailed in this report is based on the shorter dredging duration of approximately 6 weeks.

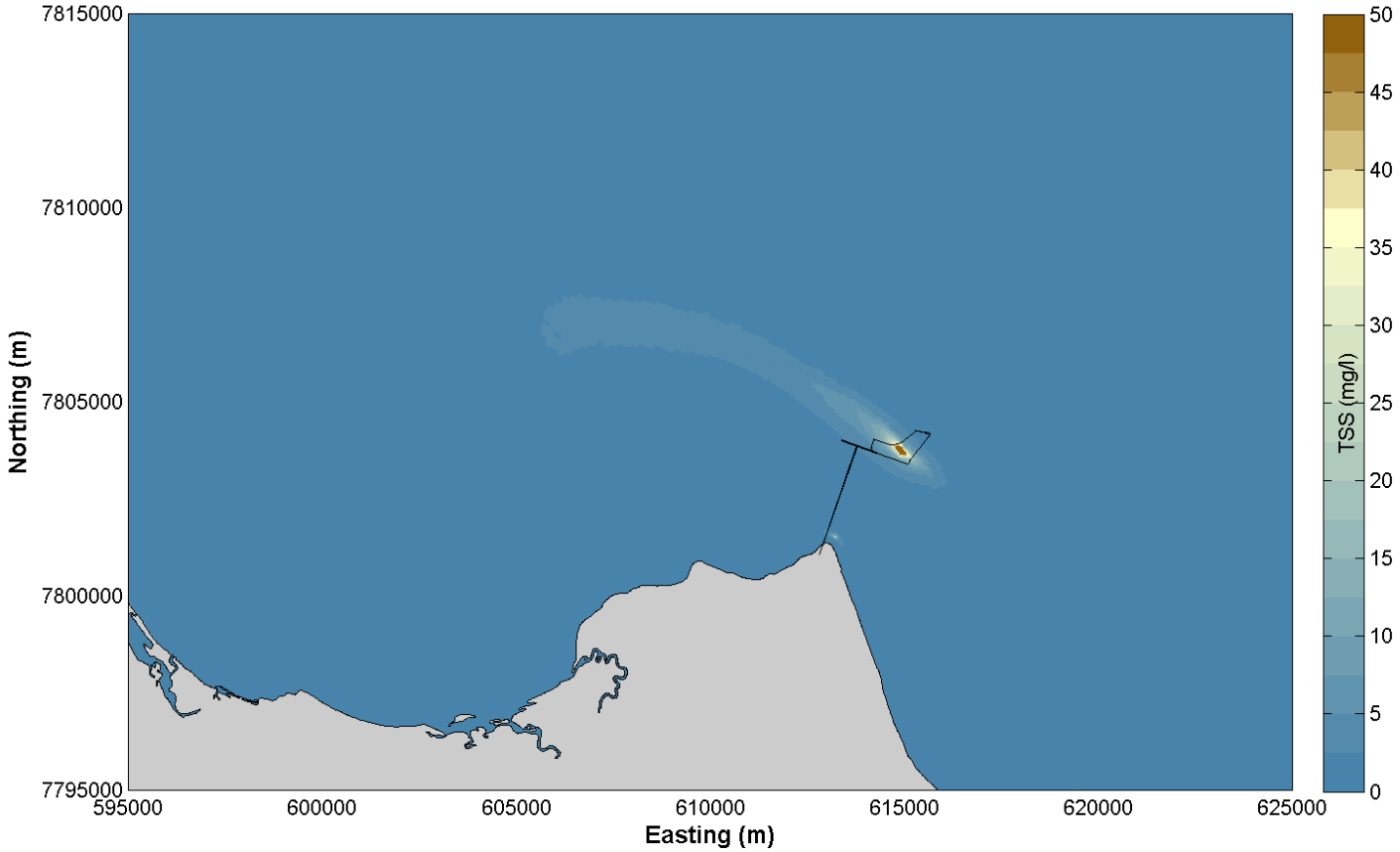

Figure 37 95th percentile TSS for dredging over a 6 week period during the growing season of a Neutral year.

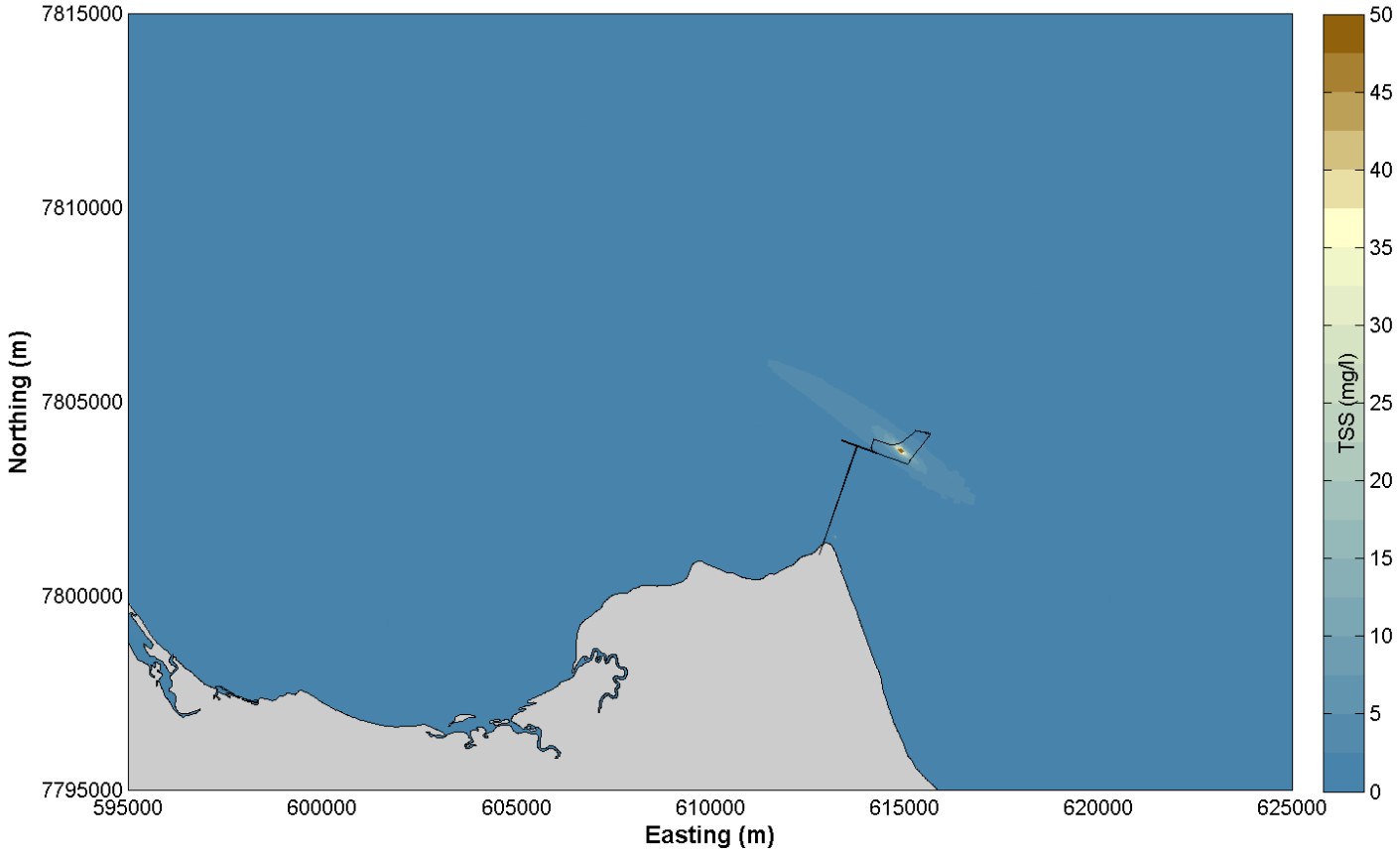

Figure 38 95th percentile TSS for dredging over a 13 week period during the growing season of a Neutral year.

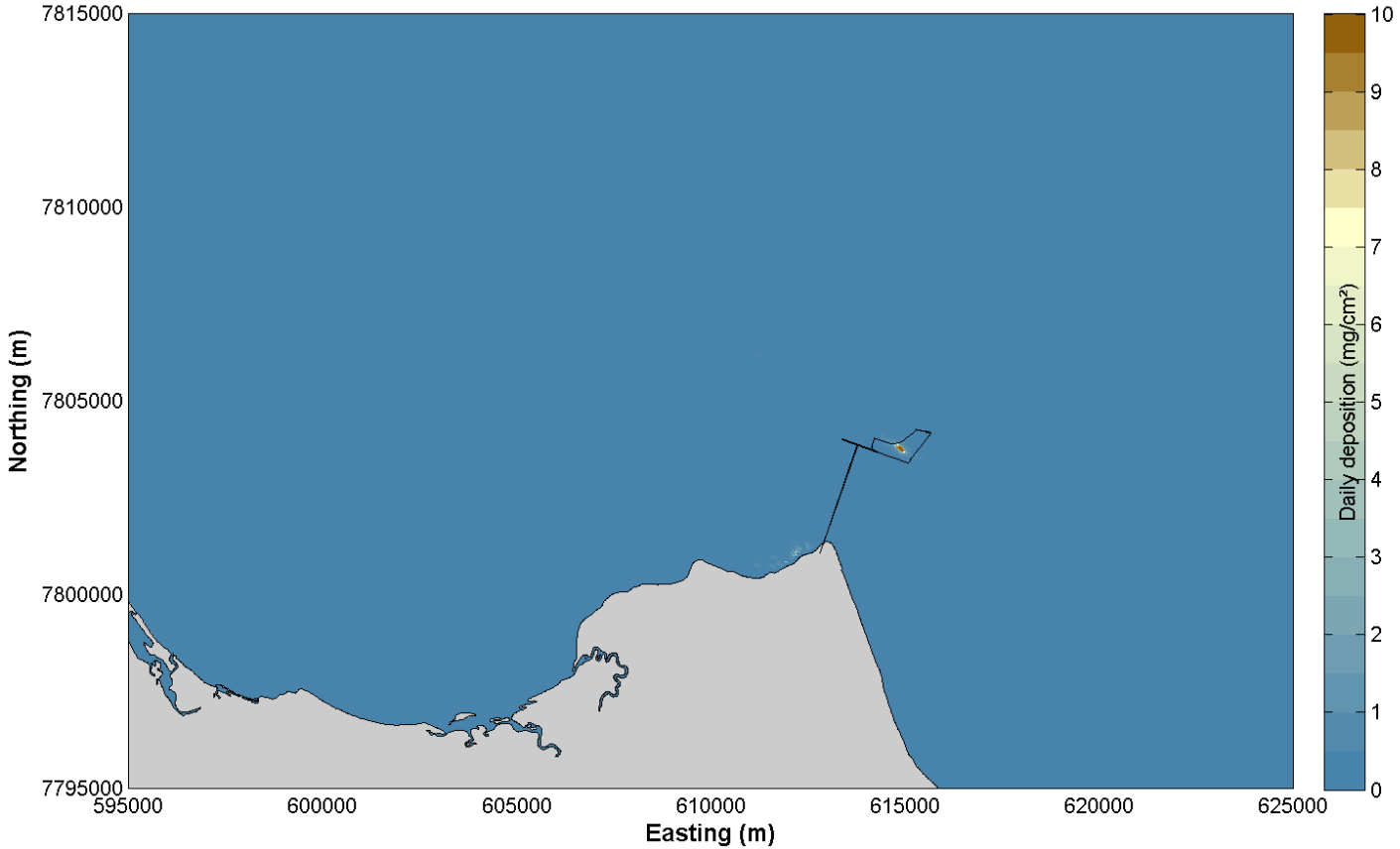

Figure 39 95th percentile sedimentation for dredging over a 6 week period during the growing season of an El Nino year.

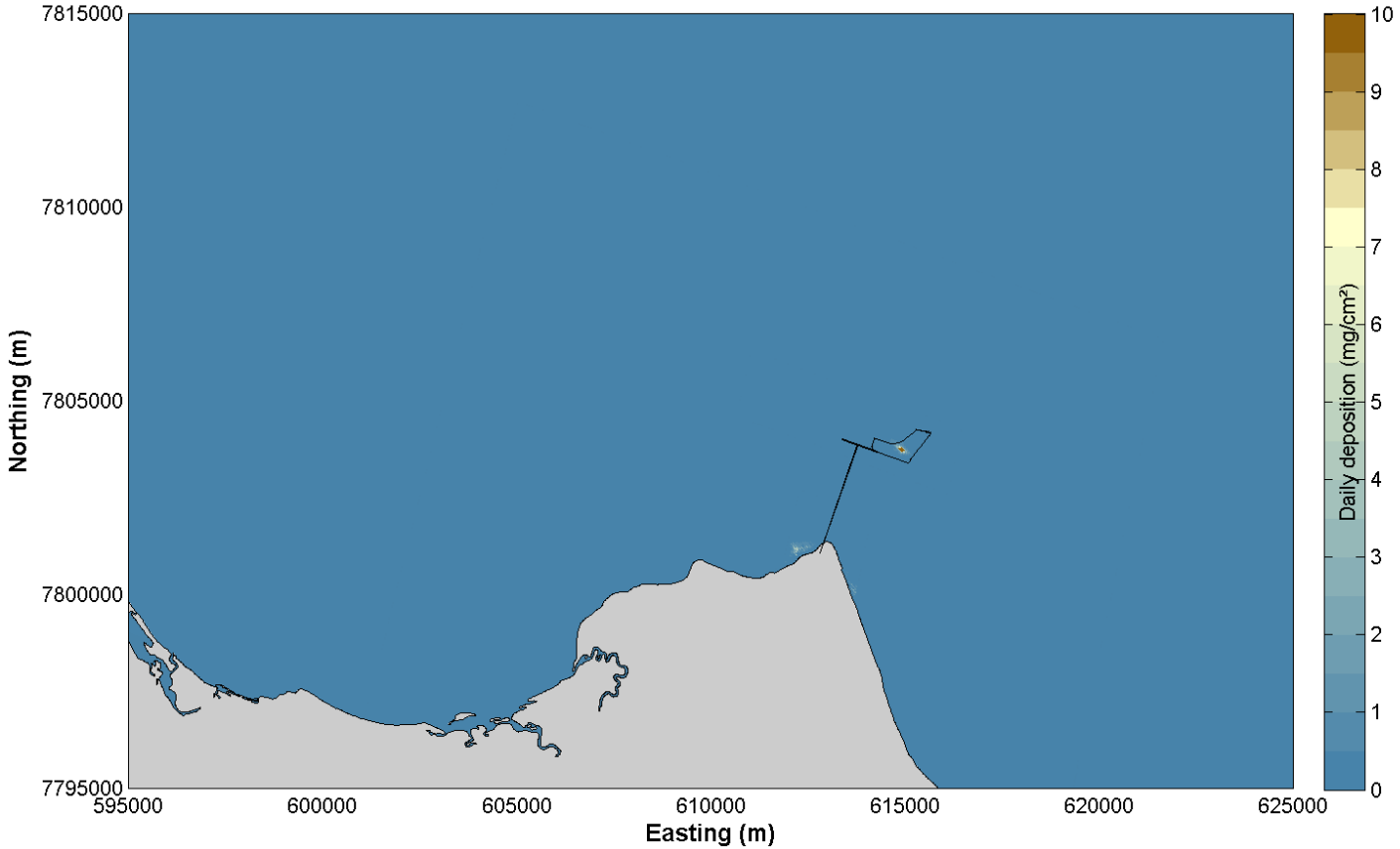

Figure 40 95th percentile sedimentation for dredging over a 13 week period during the growing season of an El Nino year.

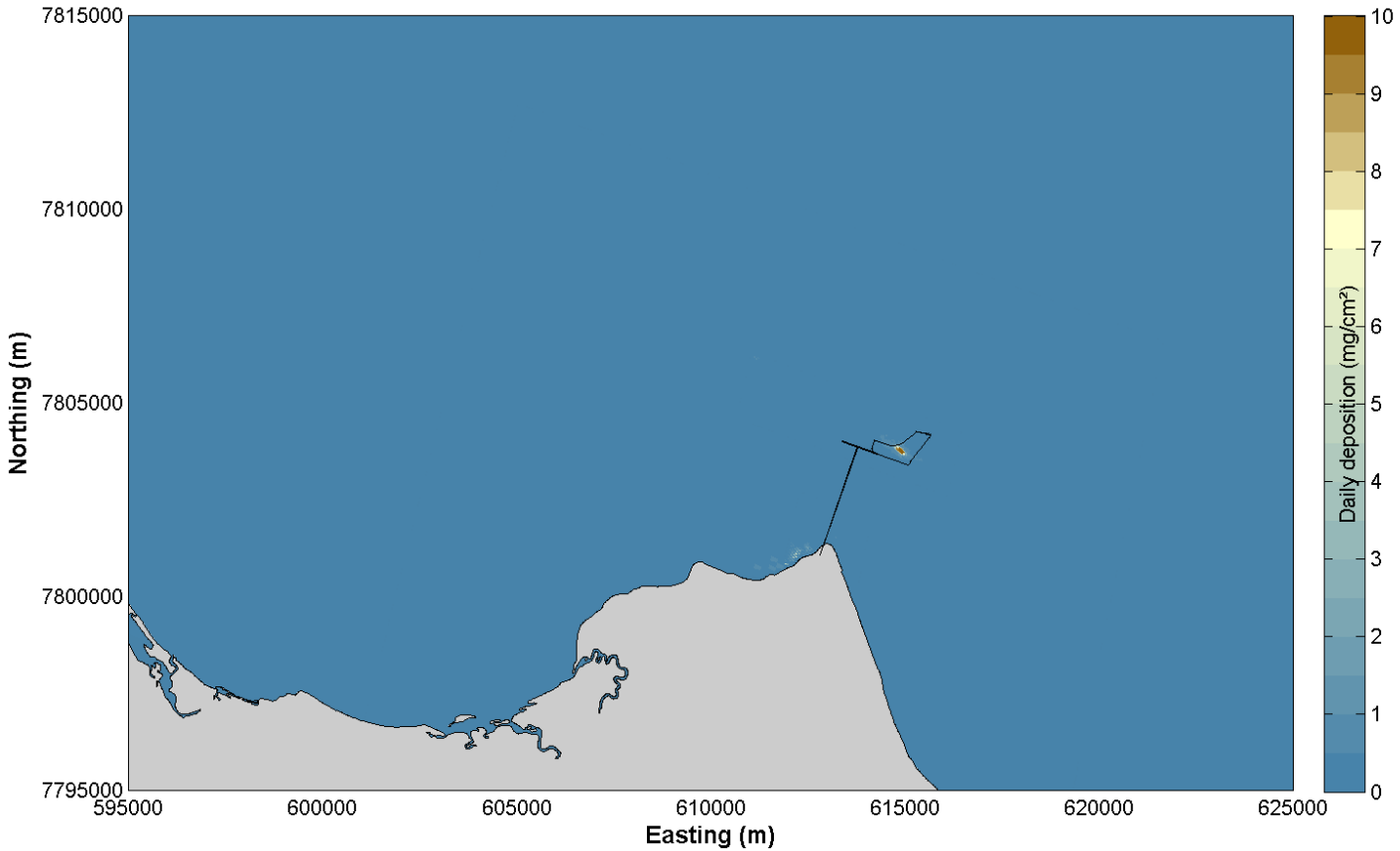

Figure 41 95th percentile sedimentation for dredging over a 6 week period during the growing season of a Neutral year.

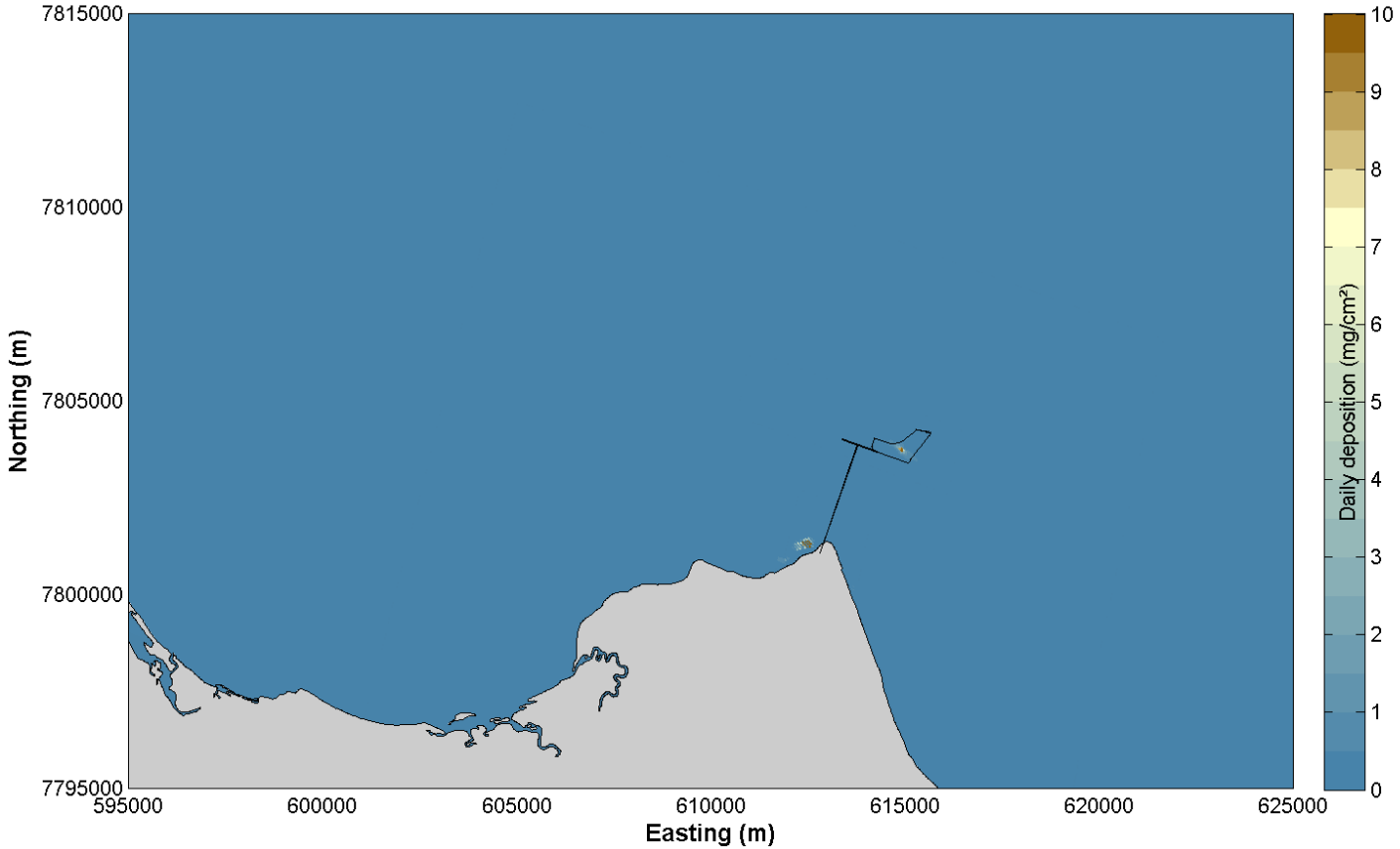

Figure 42 95th percentile sedimentation for dredging over a 13 week period during the growing season of a Neutral year.

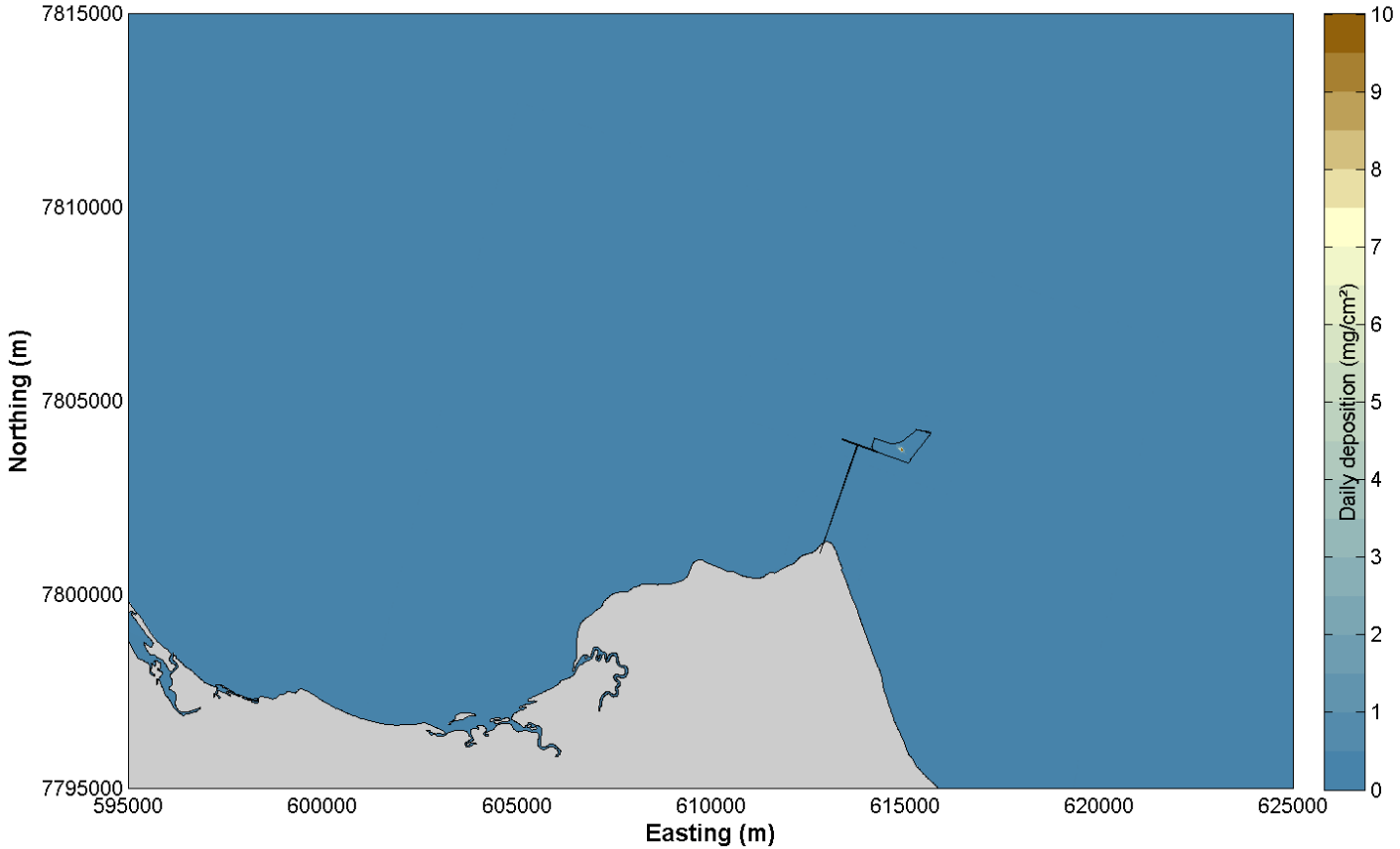

Figure 43 80th percentile sedimentation for dredging over a 6 week period during the growing season of a Neutral year.

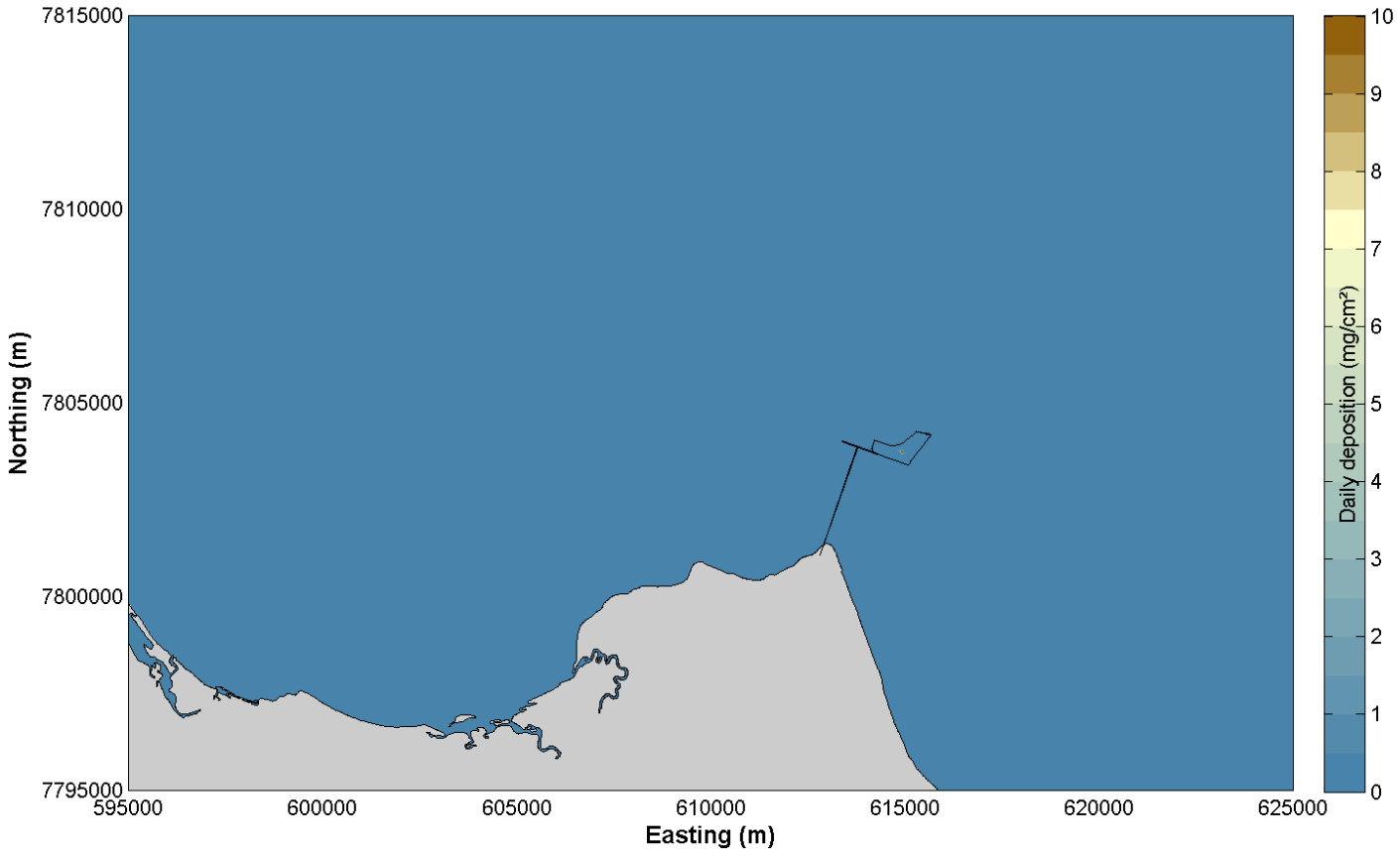

Figure 44 80th percentile sedimentation for dredging over a 13 week period during the growing season of a Neutral year.

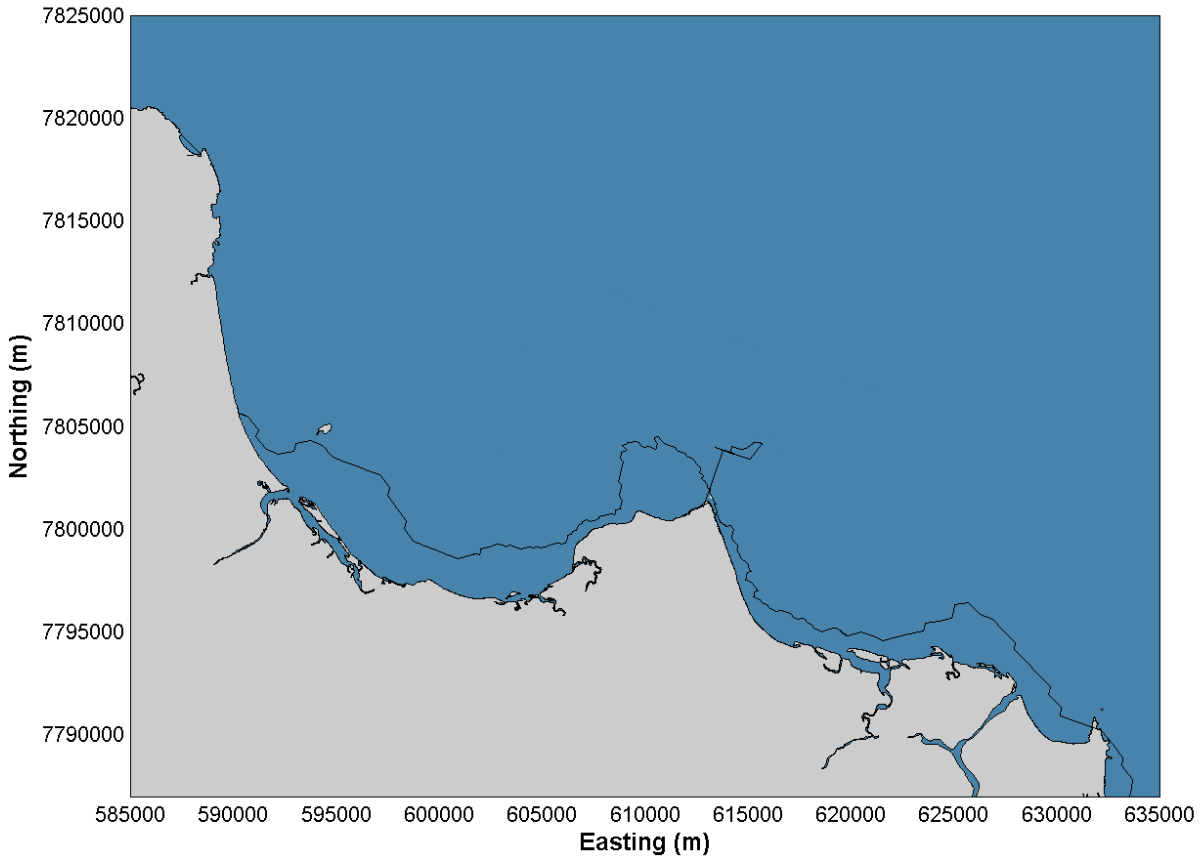

Figure 45 Benthic PAR threshold exceedance for nearshore seagrass species during the growing season for a 6 week dredging duration in a Neutral ENSO year (2007), showing baseline exceedance (black contour) and the difference resulting from the dredging activity (cream areas). Note: only a small difference occurs at the approximate return water discharge location.

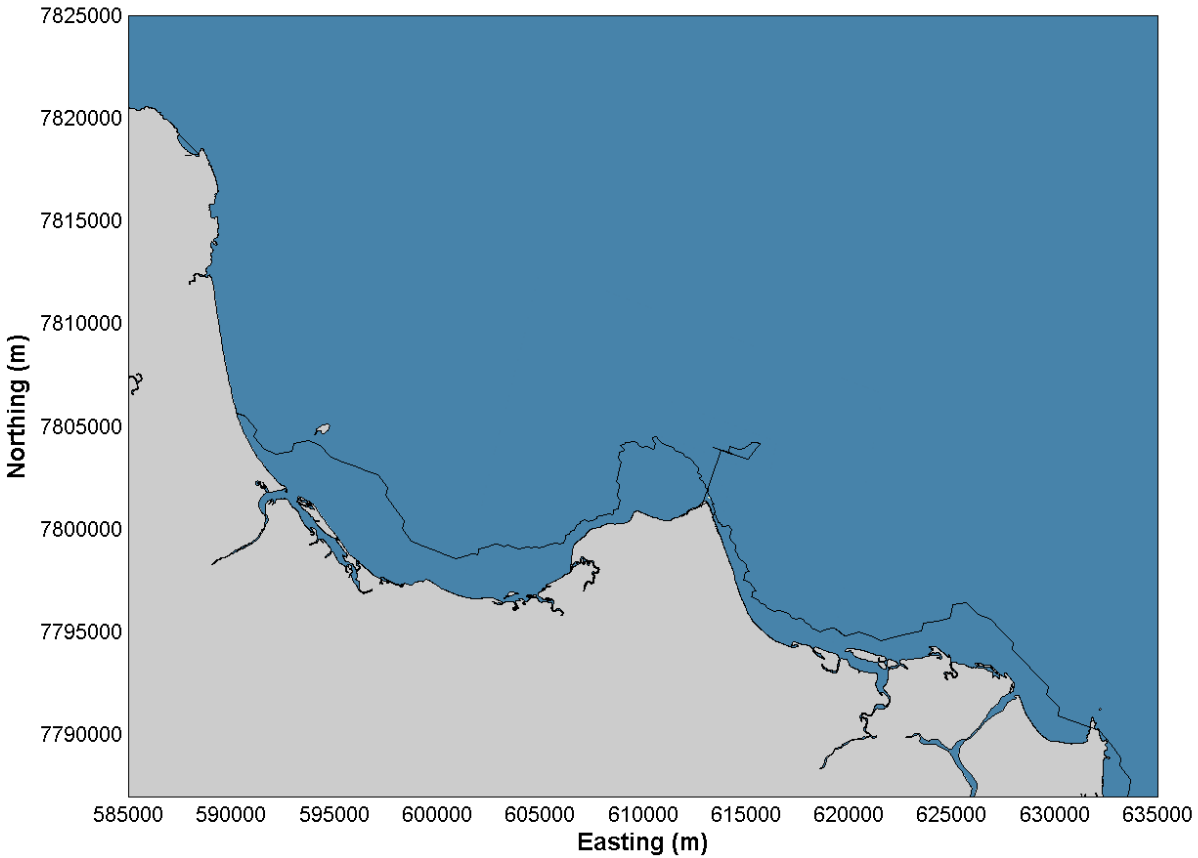

Figure 46 Benthic PAR threshold exceedance for nearshore seagrass species during the growing season for a 13 week dredging duration in a Neutral ENSO year (2007), showing baseline exceedance (black contour) and the difference resulting from the dredging activity (cream areas). Note: only a small difference occurs at the approximate return water discharge location.

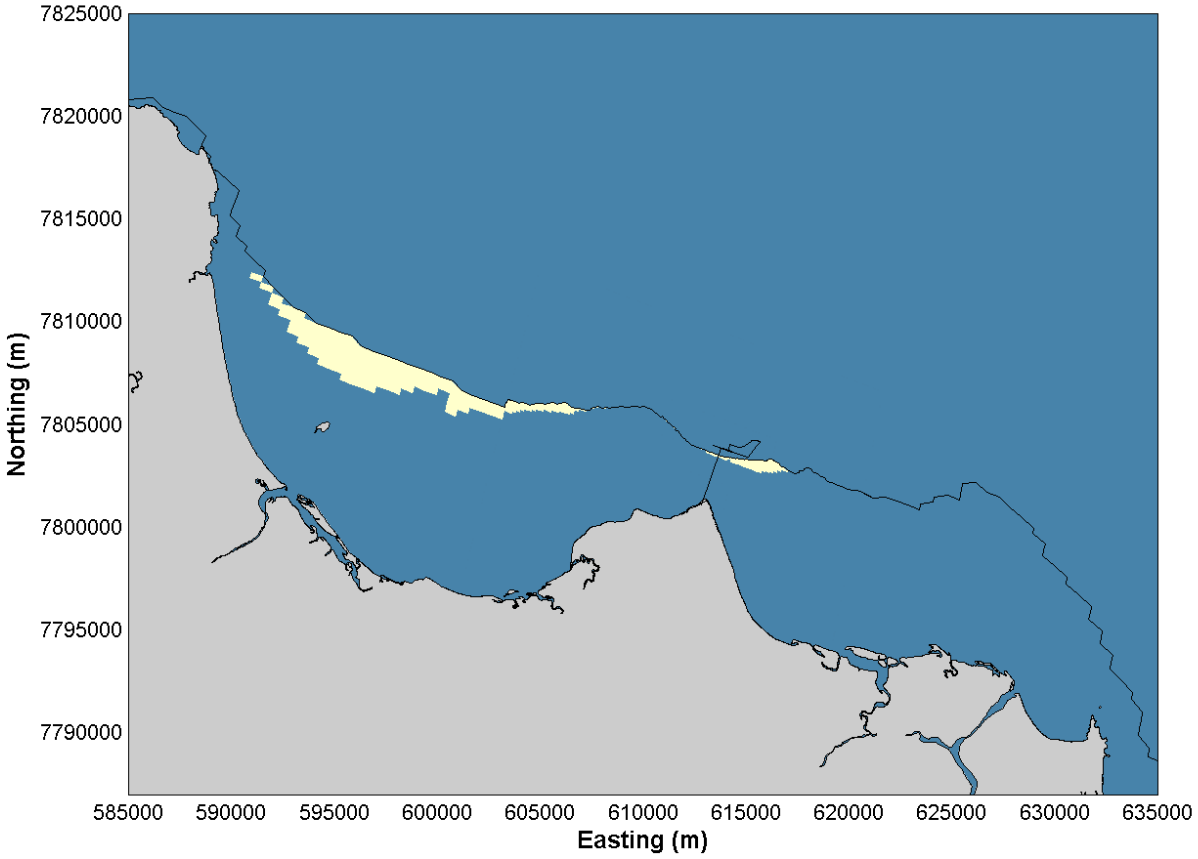

Figure 47 Benthic PAR threshold exceedance for offshore seagrass species during the growing season for a 6 week dredging duration in a Neutral ENSO year (2007), showing baseline exceedance (black contour) and the difference resulting from the dredging activity (cream areas).

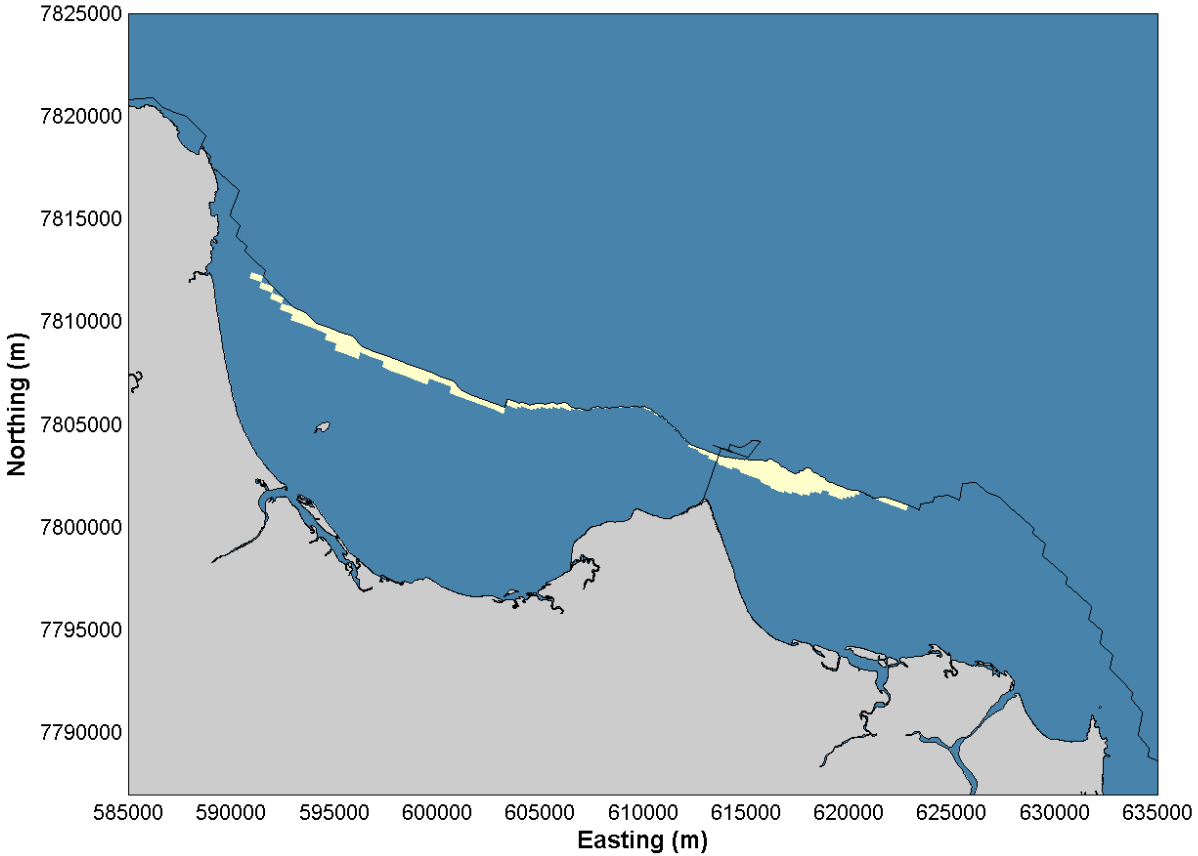

Figure 48 Benthic PAR threshold exceedance for offshore seagrass species during the growing season for a 13 week dredging duration in a Neutral ENSO year (2007), showing baseline exceedance (black contour) and the difference resulting from the dredging activity (cream areas).

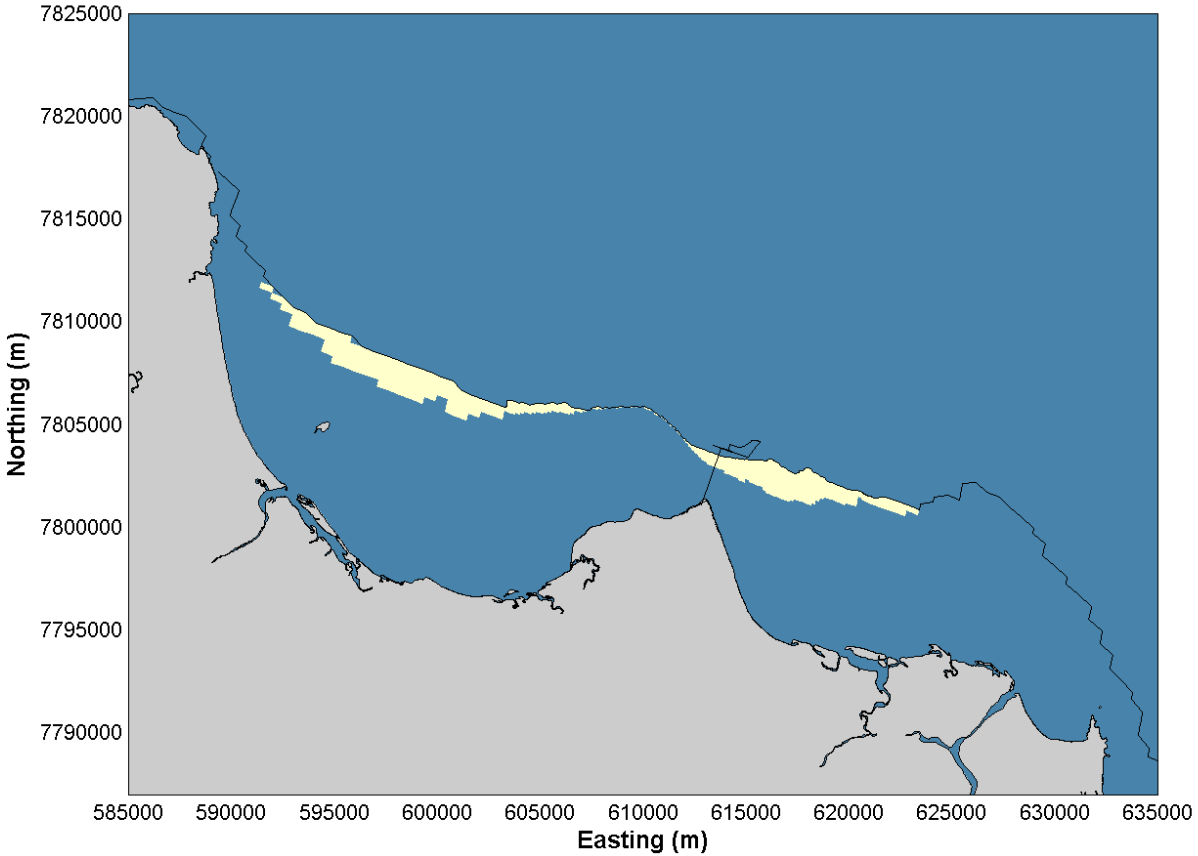

Figure 49 Benthic PAR threshold exceedance for offshore seagrass species during the growing season (approximately 6 weeks later than results shown in Figure 47) for a 6 week dredging duration in a Neutral ENSO year (2007), showing baseline exceedance (black contour) and the difference resulting from the dredging activity (cream areas).

5 DREDGING RATES

To represent the dredging activity for the onshore material placement and the discharge from the return pipeline outflow in the numerical modelling it is necessary to define the amount, location, duration and frequency of material released. Pro Dredging and Marine Consultants (PDMC) provided details of a potential dredging strategy, enabling the location, duration, amount and frequency of material released to be approximately known. The amount of material (referred to herein as the source term) which will become suspended in the water column during the dredging activity was estimated based on experience and information from previous dredging projects.

Realistic but conservative dredging source terms are generally determined based on the Dredging Contractors previous dredging experience and through interpretation of the relevant geotechnical information and the proposed dredging strategy. As part of the Ichthys Project the Dredging Contractor, Van Oord, conducted extensive data collection plume characterisation campaigns to measure the actual source terms to compare with those assumed in the numerical modelling (INPEX, 2013). The measurements showed that 2.9% of fines were lost in suspension at the cutter head when dredging with a Cutter Suction Dredger (CSD) and pumping to a Trailing Suction Hopper Dredger (TSHD) and 2% of fines were lost in suspension at the drag head when dredging with a TSHD.

The measurements from the Ichthys Project were based on the dredging of material with a similar composition as recorded for the material to be dredged at Abbot Point. An average of 36% of the dredging material was made up of silts and clays for the Ichthys Project, while at Abbot Point the latest analysis of geotechnical data at T0 and T3 found that 40% of the dredging material is silts and clays (PDMC, 2014). As such, the measured 2.9% and 2% losses of fines during the dredging activity as part of the Ichthys Project have been increased to 3% losses of fines for the modelling simulations reported herein. In this case fines have been assumed to represent any material of coarse silt and finer (<63 µm). The fine material released into suspension as a result of the dredging activity was released in the bed layer of the modelled water column.

Based on the information provided by PDMC, the following assumptions have been made with regard to the dredging activity and return water outflow for the numerical modelling:

- total in situ volume to be dredged is 1.1 million m^3 (including 0.5 m over dredge);
- dredging will be continuous for 16 hours per day, 13 days per fortnight;
- the average dredging rate will be 1,700 m^3/hr for the apron and 2,400 m^3/hr for the berth (**Table 9**);
- based on the dredging approach and associated volumes for the dredging scenario, the apron has been calculated to take 4 weeks to dredge and the berth 1.6 weeks;
- the amount of material suspended by the cutter head during the dredging activity will be 3% losses of fines. In this case fines have been assumed to represent any material of coarse silt and finer (<63 µm);
- 40% of the material to be dredged is made up of fine grained material (silts and clays);
- a conservative conversion factor of 1.1 has been adopted to convert the in-situ volume of fine grained material in cubic metres to dry mass in tonnes;
- the return pipeline outflow will be continuous for 24 hours a day throughout the duration of the dredging;

- the outflow discharge will be 8,300 m^3/hr throughout the duration of the dredging (**Table 9**);
- the outflow will be located at -4 m LAT;
- the concentration of the outflow will be 100 mg/L throughout the duration of the dredging; and
- following cessation of the dredging the outflow will continue discharging for an additional 7 days at 50% of the discharge during dredging.

Table 9 Assumed dredging and outfall discharge rates

Parameter	Per hour	Per day
Bulk Dredging Rate (16 hours per day)	14,000 m^3/hr	224,000 m^3/day
Solids Dredging Rate (16 hours per day)	1,700 – 2,400 m^3/hr	27,200 – 37,400 m^3/day
Outfall Discharge Rate (24 hours per day)	8,300 m^3/hr	199,200 m^3/day

Based on the assumptions detailed above, the total mass of material released into the model to represent suspended sediment resulting from the dredging and onshore placement activities for the 1.1 million m^3 was approximately 15,900 tonnes. The majority of this mass was material suspended by the dredging activity (cutter head), with only 780 tonnes resulting from the return water discharge.

One way of quantifying the difference between the amount of material discharged to the environment from dredging of the area with a Cutter Suction Dredger as is proposed for the Project versus dredging using a Trailing Suction Hopper Dredger with offshore placement of dredging material (which has previously been proposed) is to compare the modelling results and inputs for each activity. As the dredging plume modelling undertaken for the PER was for the offshore disposal of material using a Trailing Suction Hopper Dredger (TSHD), the modelling included the release of sediment into suspension by:

- the drag head during dredging;
- overflow during dredging through an adjustable overflow fitted with a Green Valve; and
- relocation of the dredged material at the offshore disposal site.

Based on the rates provided in the PER, the sediment suspended by the drag head represents approximately 3.5% of the total mass of material suspended by the dredging activity with the remaining mass being released by the overflow (GHD, 2012). The onshore placement of material does not require any overspill as the material is pumped directly to land and as a result the only material suspended during the dredging activity as part of the onshore placement is at the drag head. Due to the inclusion of overspill required to fill the dredge hopper for the offshore disposal an average mass of material released into the model during the dredging activity (excluding any disposal/placement) as applied in the PER was approximately 17,700 tonnes/day. In contrast, for the onshore placement with no overspill the average mass of material released into the model during the dredging activity was approximately 435 tonnes/day. Therefore, the mass of material released into the model as a result of the dredging activity for the onshore placement is significantly lower than in the offshore disposal modelling presented in the PER.

6 RESULTS

Results from the stochastic modelling and the dredging duration sensitivity testing are presented in this section. Results are presented showing:

- TSS;
- sedimentation rates;
- bed thickness;
- TSS exceedance for specific intensity, duration and frequency conditions; and
- benthic PAR impacts resulting from the dredging and onshore placement activities.

The dredging associated with the Abbot Point Growth Gateway is planned to occur either in 2016 or in a subsequent year. On the 12th May 2015 the Bureau of Meteorology (BoM) declared that an El Nino phase had commenced. The El Nino phases generally develop between autumn and winter and start to decay over the summer, lasting until the following autumn. However, the El Nino phase can last for between 6 months and 2 years and so the El Nino phase could either end near the start of 2016 or could last until the following autumn in 2017. Following an El Nino phase a Neutral period is usually experienced and as a result it is expected that 2016 will start by being El Nino and then in autumn could switch to Neutral or remain El Nino. Based on this, it is likely that the dredging will be undertaken during either El Nino wet or dry seasons or the Neutral dry season.

6.1 Stochastic Modelling

As detailed in **Section 3.3,** a total of 38 numerical model simulations were undertaken to represent the proposed dredging activities and dredging material relocation activity during different metocean conditions. The results were processed to present the TSS throughout the dredging activity when the TSS concentrations are at their highest. The model results show that following cessation of the dredging activity the TSS and sedimentation levels reduce rapidly as a result of the largest suspended sediment input (from the drag head) no longer occurring. Therefore, the period immediately following the dredging activity was not included as it would have resulted in a reduction in the values obtained through the statistical analyses. The results have been processed to separate the dredging during the wet and dry seasons. The wet season has been assumed to include January to April, while the dry season includes May to October. Slightly different periods were selected to calculate benthic PAR impacts to reflect the growing (1st July to 31st October) season for seagrass to make the results more ecologically relevant for the key sensitive receptor (seagrass).

To determine how the TSS varies through the water column, results were extracted at a location 200 m away from the dredging area for one of the simulations[5] (**Table 10**). The table clearly shows that even away from the dredging area the TSS concentration is much higher in the bed layer of the model than in the surface layer. As such, all the results presented in this report are for the bed layer of the model[6], this represents the location where the TSS is highest and so can be considered a worst case.

[5] Results were not presented at the dredge location as the sediment source in the numerical model is at the near-bed layer and so 200 m away from the dredge location the concentrations will still be relatively high but the material has also had the opportunity to spread through the water column.

[6] Excluding the benthic PAR plots which have adopted a depth averaged TSS as benthic PAR is dependent on the suspended sediment through the water column and not just in the bed layer.

It is important to note that a low critical erosion threshold of 0.1 N/m^2 was applied throughout the modelling to represent any of the suspended sediment released by the dredging activity and return water when it is deposited. This value represents very loosely consolidated material which is readily available for resuspension and is expected to be frequently resuspended by the currents. Adopting such a low value for the critical erosion threshold provides a conservative representation of the resuspension of the relocated material.

To demonstrate how the visual plume resulting from the dredging and onshore placement activity will appear, instantaneous TSS is shown for the surface layer of the model at weekly intervals throughout the dredging period in **Figure 50** to **Figure 54**. These plots are from a simulation which was shown to result in the largest extent and highest TSS concentration in the 95th percentile TSS plots; this was the final simulation for the dry season of the Neutral year. Plots were also created for the TSS the week after cessation of the dredging activity and for bed thickness throughout the duration of the simulation but these plots are not included as they do not show anything other than low rates of deposition in the dredging area. The plots show that over time the plume varies spatially with TSS concentrations less than 10 mg/L except for directly adjacent to the dredging area. Based on the visual appearance of water clarity for a range of TSS concentrations shown in **Figure 16** it is thought to be unlikely that surface layer TSS concentrations of less than 10 mg/L would result in a clearly defined visual plume. The variability in the plume extent and concentration shown in the plots is primarily a result of the variability in the metocean conditions which act to transport the plume away from the sources of suspended sediment at the dredging area and discharge location. Due to the variability in the metocean conditions and the influence of this on the transport of the plume it is necessary to undertake the stochastic modelling approach to include this variability in the modelling.

Table 10 Variation in TSS through the water column at a site 200m away from the dredging area (D02, see **Figure 96**).

Model Layer	Median TSS (mg/L)	Mean TSS (mg/L)	Max TSS (mg/L)
Surface	0.8	1.5	12.1
Mid	4.4	5.4	22.3
Bed	13.9	16.1	79.2

6.1.1 Suspended Sediment

The 95th percentile TSS above background levels as a result of the material relocation activity have been calculated over the duration of the dredging activity (**Figure 55** to **Figure 66**). The plots do not show an actual dredging plume at any point in time, the instantaneous TSS plots in **Figure 50** to **Figure 54** show this for the surface layer, but they are duration-based plots which show statistical summaries of the dredging plume dispersion over the entire dredging period. The percentile plots show the value for which TSS throughout the dredging duration is less than, a given percentage of the time. For example, the 95th percentile shows the value throughout the dredging duration for which the TSS is below for 95 percent of the time. Plots are presented for the three different years (El Nino, La Nina and Neutral) and for the wet season, dry season and entire dredging period to determine the

variability in the transport of the dredging plume due to seasonal and inter-annual variability in the metocean conditions.

The 95th percentile plots show that the area where the background TSS can be increased by more than 5 mg/L due to the proposed dredging activity covers a similar extent irrespective of the season or year. The area where the TSS is more than 5 mg/L extends in a north-west and south-east direction from the dredging location, ranging in total length from 5.3 to 8.2 km with an average width of approximately 1.2 km and a residual direction to the north-west.

The area where the lower concentrations (<5 mg/L) can occur due to the dredging is more variable both seasonally and annually. The area extends up to 17 km to the west of the dredging area and 7 km to the south-east of the dredging area, with the average extent over all the simulations being 10.9 km to the west-north-west and 4.4 km to the south-east.

The plots show that the area with increased TSS of more than 2.5 mg/L due to the dredging is largest in 2007, the Neutral ENSO year, and smallest in 2011, the strong La Nina year. The reason for this difference is a result of the metocean conditions (specifically the wind and waves); the Neutral ENSO year was subject to the lowest wind and wave energy out of the three years while the La Nina year was subject to the highest wind and wave energy. Higher wind and wave energy results in higher current speeds and increased resuspension, which results in the sediment released by the dredging operations and return water discharge being transported further from its source. The increase in transport results in a reduction in the TSS concentrations as it becomes diluted by being transported over a larger area. As a result the material is transported away from the main plume extent and so the TSS concentration is reduced and therefore the percentile plots do not show such a large plume extent. Based on these plots it appears that the worst case for assessing the potential impacts of the plume on the seagrass communities is the dry season in 2007, the Neutral ENSO year, when the largest area of TSS concentrations above 2.5 mg/L occurs.

Immediately adjacent to the discharge location is the only area where the TSS resulting from the return water can be more than 5 mg/L. The area with increased TSS of between 2.5 and 5 mg/L resulting from the return water extends up to 1.7 km to the south-west and 1.2 km to the south-east of the discharge location. The plots show that there is little variability in the extent of this area regardless of the season or year.

The results show that there is little to no interaction between the suspended sediment plumes resulting from the dredging and the return water, the areas with increased TSS remain separate.

These plots show that although there is some variability in the results due to differences in the inter-annual metocean conditions, this variability only results in significant changes to the low concentration areas in the 95th percentile plots (<5 mg/L). For the mean and 80th percentile plots there is little inter-annual variability and as such, these will only be presented as combined results for all the years.

The mean and the 80th percentile TSS above background levels as a result of the onshore placement activity have been calculated over the duration of the dredging activity, these are shown for the wet and dry seasons in **Figure 67** to **Figure 70**. The results show that the area impacted by the increased TSS is mainly localised to the dredging area. There is a small extent low concentration (<5 mg/L) plume extending to the north-west from the

dredging area, up to 0.6 km for the mean TSS and 4.4 km for the 80th percentile TSS. These plots show a much smaller extent and lower concentration plume than the 95th percentile plots, indicating that the larger area with increased TSS shown in the 95th percentile plots occur infrequently.

6.1.2 Sedimentation

The 80th and 95th percentile daily deposition rates are shown for the Neutral ENSO year in **Figure 71** to **Figure 74**. Plots are only presented for this year as it represents the highest rates (due to the lower metocean energy conditions during this year) and therefore the worst case compared to the other two years. The 80th percentile daily deposition rates for both the wet and dry season are similar with low daily deposition rates (only more than 0.5 mg/cm^2/day within the dredging area).

The 95th percentile plots are also similar in both the wet and dry seasons with generally low daily deposition rates. The rates were more than 0.5 mg/cm^2/day within the dredging area and in a localised area to the west of the discharge location, adjacent to the Abbot Point headland. The rates in these two locations were up to 10 mg/cm^2/day. The area to the west of the discharge location, adjacent to the Abbot Point headland, is subject to occasional high rates of deposition due to both the metocean conditions and the local bathymetry. Due to the sheltering effect of Clark Shoal and the Abbot Point headland this area is subject to relatively low wind and wave energy and is also relatively shallow. This results in material being deposited in this area at slack water, with the shallow bathymetry allowing more material to settle in a shorter period of time, and then resuspending on the subsequent flood or ebb currents.

The GBRMPA (2010) water quality guideline trigger values for sedimentation (deposition) rates are a maximum mean annual sedimentation rate of 3 mg/cm^2/day and a daily maximum of 15 mg/cm^2/day. These threshold values were applied to the model to predict the extent of a zone of moderate impact. Sensitive receptors within this zone are predicted to experience deposition conditions which may cause sub-lethal impacts only. The maximum mean annual sedimentation rate upper limit of 3 mg/cm^2/day was applied across the period of the dredging campaign and not over the entire year; which represents a conservative approach to the application of this annual rate. Based on these thresholds **Figure 75** and **Figure 76** show the zone of moderate impact based on the daily sedimentation rate. Plots are only provided from 2007 as this represents the period with the highest sedimentation rates and therefore the largest areas where the thresholds are exceeded. The plots show that the thresholds are only exceeded within the dredging area and to the west and south-east of the discharge location. The thresholds are only exceeded up to 1.4 km away from the discharge location. The wet and dry season plots have similar threshold exceedance areas.

The bed thickness at the cessation of the dredging activity was similar for all of the years; therefore plots are only shown for the average bed thickness for the three years in **Figure 77** and **Figure 78**. The plots show that at the cessation of dredging the only area where a bed thickness of more than 0.25 mm occurs is within the dredging area for both the wet and dry seasons.

These plots all show that the deposition rates resulting from the dredging operations and return water discharge are relatively low and that the areas with higher rates are restricted to within and close to the dredging area, and close to the discharge location.

6.1.3 TSS Intensity, Duration and Frequency

Intensity, duration and frequency thresholds for TSS have been provided by WorleyParsons based on available measured data for the area and through discussions with experts at TropWATER. These thresholds provide a better indication of areas with potential ecological impacts compared to percentile plots as they represent conditions which are ecologically relevant to seagrass and other benthic flora and fauna. The values which were selected for the area of influence[7] are provided in **Table 11** and for the zone of moderate impact in **Table 12**.

Plots showing the area of influence based on the intensity, duration and frequency thresholds for TSS for the wet and dry season are shown for each of the three years in **Figure 79** to **Figure 84**. The plots show that the area of influence, which is the area where there is a slight decrease in water quality without causing significant impact to biota, differs significantly with both the year and the season. The largest area of influence occurs during the dry season of the Neutral ENSO year, where the area extends approximately 33 km to the west-north-west and 1.8 km to the south-east of the dredging area. This agrees with the 95th percentile TSS plots which showed that the largest area with increased TSS due to the dredging operations and return water discharge occurred during the dry season of the Neutral ENSO year.

Table 11 Summary of Intensity, Duration and Frequency values to delineate the area of influence (Daylight hours only).

Season	Intensity TSS value	Duration (continuous hrs)	Frequency (every 6 weeks)
Wet	>2 mg/L	10 hrs	1 time
Dry	>2 mg/L	10 hrs	1 time

The median and 95th percentile zones of moderate impact for TSS do not show much variability between years and as a result plots are only shown for all the years averaged together for the wet and dry seasons (**Figure 85** and **Figure 88**). The plots show that both the median and 95th percentile zones of impact are restricted to the dredging area and the area immediately adjacent to the north-west up to 0.7 km from the dredging area. The results are similar for both the wet and the dry seasons. The return water discharge results in a small zone of moderate impact to the west of the discharge location during both the wet and dry seasons for the median thresholds but no impact for the 95th percentile thresholds.

[7] Area of influence is the area in which changes in water quality due to the dredging and dredge material relocation operations are predicted to occur, but these changes will not result in a detectable impact on benthic biota. This will most likely encompass a large area, but at any given time the actual dredge plume will be restricted to a small area.

Table 12 Summary of Intensity, Duration and Frequency values to delineate the zone of moderate impact (Daylight hours only)

Season	Intensity TSS value	Duration (continuous hrs)	Frequency (every 6 weeks)
Wet – Median[8]	>2.6 mg/L	5 hrs	18 times
Wet – 95th Percentile[9]	>14.5 mg/L	5 hrs	3 times
Dry – Median	>1.5 mg/L	5 hrs	24 times
Dry – 95th Percentile	>12.6 mg/L	5 hrs	2 times

These results show that the dredging operations and return water discharge have the potential to result in a relatively large area of influence based on the thresholds provided. However, the zone of moderate impact is restricted to the dredging area and the area immediately adjacent to the north-west up to 0.7 km from the dredging area. The return water discharge results in a small zone of moderate impact to the west of the discharge location.

6.1.4 Benthic PAR

The growth and distribution of seagrass is primarily driven by the availability and quality of light and if this is changed it can result in the loss of seagrass. The total daily benthic photosynthetically active radiation (PAR) provides a good measure of the light at the seabed. Site specific thresholds for benthic PAR have been developed by TropWATER based on benthic PAR measurements collected at Abbot Point in 2013 and 2014 (McKenna et al., 2015). Different thresholds have been developed for nearshore (<6m AHD) and offshore (>6m AHD) seagrass sites as the different species which grow in these areas have different light requirements (**Table 13**). When the average daily benthic PAR over the durations noted in **Table 13** drop below the thresholds due to impacts from the dredging activity and return water discharge, the area is considered to be a zone of moderate impact to the seagrass.

Table 13 Summary of benthic PAR threshold values used to define the zone of moderate impact to seagrass.

Location	Daily PAR threshold (mol/m²/day)	Duration (moving average period)	Frequency
Shallow inshore areas	3.5 mol/m²/day	14 days	1
Deeper offshore areas	1.5 mol/m²/day	7 days	1

[8] This threshold is based on the measured median TSS.
[9] This threshold is based on the measured 95th percentile TSS.

The background PAR attenuation coefficient (k_d) was calculated using measured data from Abbot Point at a shallow inshore seagrass site and at two deeper offshore seagrass sites to define the existing PAR conditions. Various statistical representations of the k_d coefficient were derived for the growing season (1st July to 31st December) at Abbot Point using data collected since 2013. A range of percentile values for k_d were used to calculate benthic PAR for the shallow nearshore seagrass areas and compared with all available measured data including data collected prior to 2013. The comparison shows that using the median of the measured data to define the k_d coefficient resulted in a good representation of the typical range in measured daily benthic PAR at all of the nearshore sites (**Figure 89** and **Figure 90**). For the offshore seagrass areas the monitoring sites are not located in the deepest water where seagrass occurs at Abbot Point and as such it is known that seagrass can exist under lower light than at these sites. Based on this the minimum k_d from the offshore seagrass sites was adopted to provide a conservative estimate of the baseline conditions in the offshore areas (i.e. clearer water and so more potential for increased TSS from the dredging to impact on the benthic PAR).

The Beer-Lambert Law was applied along with the model depth values and the surface PAR (based on BoM measurements at Bowen) to define the baseline daily benthic PAR. The benthic PAR including the modelled increase in the depth averaged TSS concentration due to the dredge activity and return water discharge was calculated for all time steps of the model simulations using the Beer-Lambert Law with a site specific attenuation coefficient for suspended dredge material of 0.025. The modelled benthic PAR was then used to define when the thresholds specified in **Table 13** were exceeded using a 7 and 14 day moving average of the benthic PAR values. Results from the different scenarios were combined by averaging when the thresholds were exceeded for the growing season.

A contour showing where the baseline (existing case) benthic PAR thresholds are exceeded for the offshore and nearshore areas during the growing season during El Nino and Neutral years (as the dredging is most likely to occur within these ENSO conditions, see **Section 4** for further details) is shown in **Figure 91** to **Figure 94**. The figures also show the difference which the dredge activity and return water discharge cause to the benthic PAR threshold exceedance, this is considered to represent the zone of moderate impact to the seagrass.

The plots show that there is very little difference in the benthic PAR threshold exceedance resulting from the project for the nearshore areas in both the El Nino and Neutral years, with a very small zone of moderate impact close to the return water discharge and small localised patches of impact to the west of Clark Shoal during Neutral year. There are greater differences for the offshore areas, with both the El Nino and Neutral years showing likely impacts to the west and south-east of the dredge area. The area to the west is larger in the Neutral year, while the area to the south-east is slightly larger in the El Nino year. The zones of moderate impact for the offshore areas are located adjacent to the baseline benthic PAR threshold exceedance contour indicating that the difference is the result of low TSS concentrations from the dredging causing areas which under existing conditions are close to the threshold to exceed the threshold. If the difference was the result of high TSS concentrations then differences away from the baseline contour would be expected as not only areas which are just above the threshold would be influenced. These zones of moderate impact to seagrass are further considered in terms of ecological impacts by WorleyParsons (2015).

6.1.5 Time Series

TSS, bed thickness and deposition rate data has been extracted from the model simulations at discrete locations to provide further information as to how the conditions change between the sites. The locations of the sites where data has been extracted are shown in **Figure 95** and **Figure 96**. Due to the stochastic nature of this assessment the time series results have been combined for all the simulations and converted to histograms, these are included in **Appendix D** for all the locations with only a few key locations included in the main body of this report.

The histograms show that the TSS rapidly reduces with distance away from the dredging area and the discharge location.

At the dredging location (site D01) the average TSS is approximately 80 mg/L and the maximum value is close to 160 mg/L. While at a location 200 m to the north-west (site D02) the average TSS has reduced to approximately 10 mg/L with a maximum of around 25 mg/L (**Figure 97** and **Figure 98**).

Likewise, at the discharge location (site OF1) the average TSS is approximately 7 mg/L and the maximum is just over 10 mg/L. While at a location 200 m to the west (site OF5) the average TSS has reduced to approximately 1.75 mg/L with a maximum TSS of less than 4 mg/L (**Figure 99** and **Figure 100**).

These results show how rapidly the TSS reduces away from the source of the suspended sediment.

The deposition and resuspension rates are significantly higher at the dredging location (D01) than at any other locations. The rates at the dredging location are ±150 mg/cm^2/day, while at the adjacent site D02 which is 200 m to the north-west the rates are only ±10 mg/cm^2/day.

The deposition and resuspension rates at the discharge location are low compared with the dredging location, with rates of only ±1 mg/cm^2/day. To the south-west of the discharge location, on the west side of the Abbot Point headland at site IM9 the deposition and resuspension rates are higher than at the discharge location, with rates of up to ±3 mg/cm^2/day (**Figure 101**). This agrees with the sedimentation map results (**Section 6.1.2**) which show that higher rates of deposition occur on this side of the headland. This is likely to be a result of the sheltering of the area by Clark Shoal, in terms of waves and wind driven currents. The rates at all of these sites exhibit an approximate balance between deposition (+) and resuspension (-) which shows that the net deposition rates are low as the majority of material which is deposited is subsequently resuspended.

The maximum bed thickness at the dredging location (D01) is much higher than at any other sites, with bed thickness of up to 40 mm occurring. There is significant variability in the bed thickness frequencies between the wet and dry season at the dredging location, with higher thicknesses occurring more frequently in the dry season and lower thicknesses in the wet season. This indicates that there is less wind and wave energy in the dry season at the dredging location, resulting in calmer conditions and a greater tendency for deposition resulting in higher bed thicknesses occurring more frequently. At site D02, which is located 200 m to the north-west of the dredging location, the bed thicknesses are much lower than at site D01 with maximum rates of up to 1 mm.

The bed thicknesses are again lower at the discharge location (OF1) where the maximum rates are only up to 0.025 mm. This agrees with the bed thickness map results where the only location with thicknesses of more than 0.25 mm at the cessation of the dredging was within the dredging area.

6.1.6 Tropical Cyclones

As detailed in **Section 2.6** TCs can result in short term (in the order of days to weeks) increases in TSS concentration due to the resuspension of natural bed material. If a TC occurred during or immediately after the dredging at Abbot Point it is likely that resuspension of any deposited material would occur. However, measured water quality data has shown that extensive resuspension of the existing bed material also occurs during these extreme events, due to increased currents and wave activity, with TSS concentrations exceeding 100mg/l during the peak of the events. In addition, the measured data indicates that the natural resuspension of the existing bed material occurs on a regional scale, likely influencing areas of hundreds of kilometres or more. The modelling results have shown that the sediment released by the dredging activity and the return water discharge results in a small, local scale increase in suspended sediment and does not result in significant deposition at any location except for at the dredging location immediately after the dredging finishes (this material will then be subsequently resuspended, dispersed and redeposited). Therefore, although resuspension of any deposited dredging material is expected to occur during a TC it is not expected that this would result in an increase in the resultant TSS concentrations during the event or change any impacts of the suspended sediment on the environment. In addition, there is a significant difference in the spatial scale of any impacts resulting from the resuspension of natural existing bed material during a TC which is regional compared to the resuspension of deposited material released during the dredging which is local.

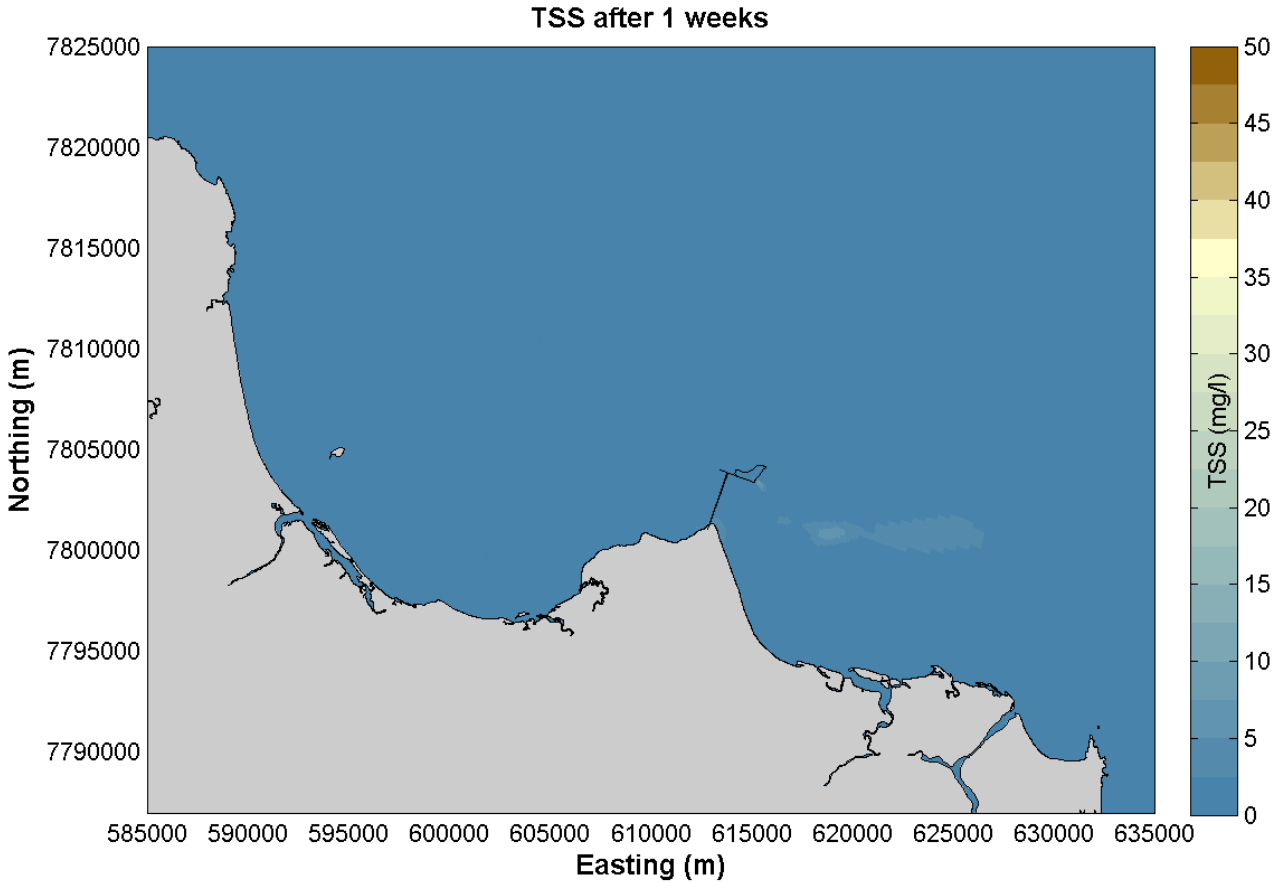

Figure 50 Instantaneous TSS in the surface layer for a single scenario 1 week after the dredging commenced (2007, dry season).

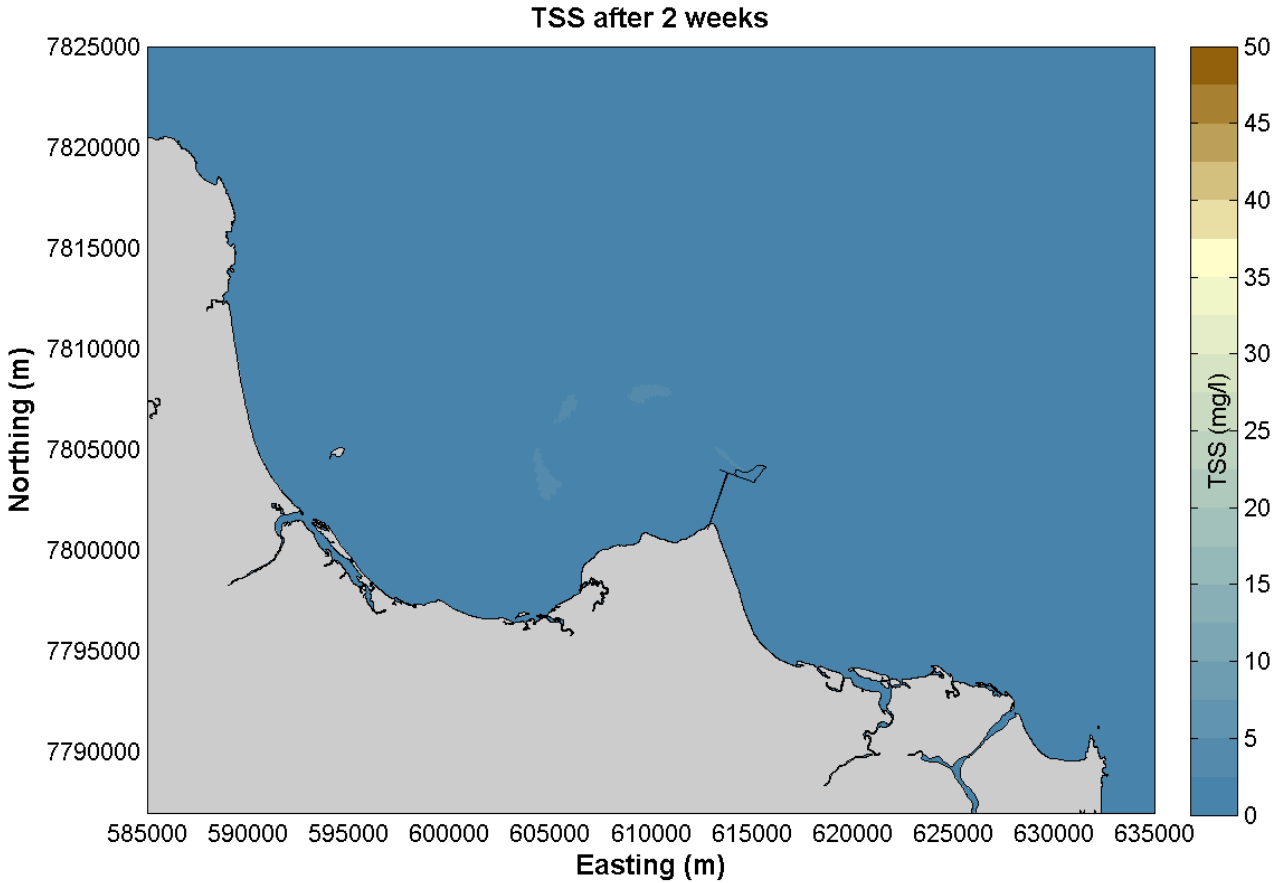

Figure 51 Instantaneous TSS in the surface layer for a single scenario 2 weeks after the dredging commenced (2007, dry season).

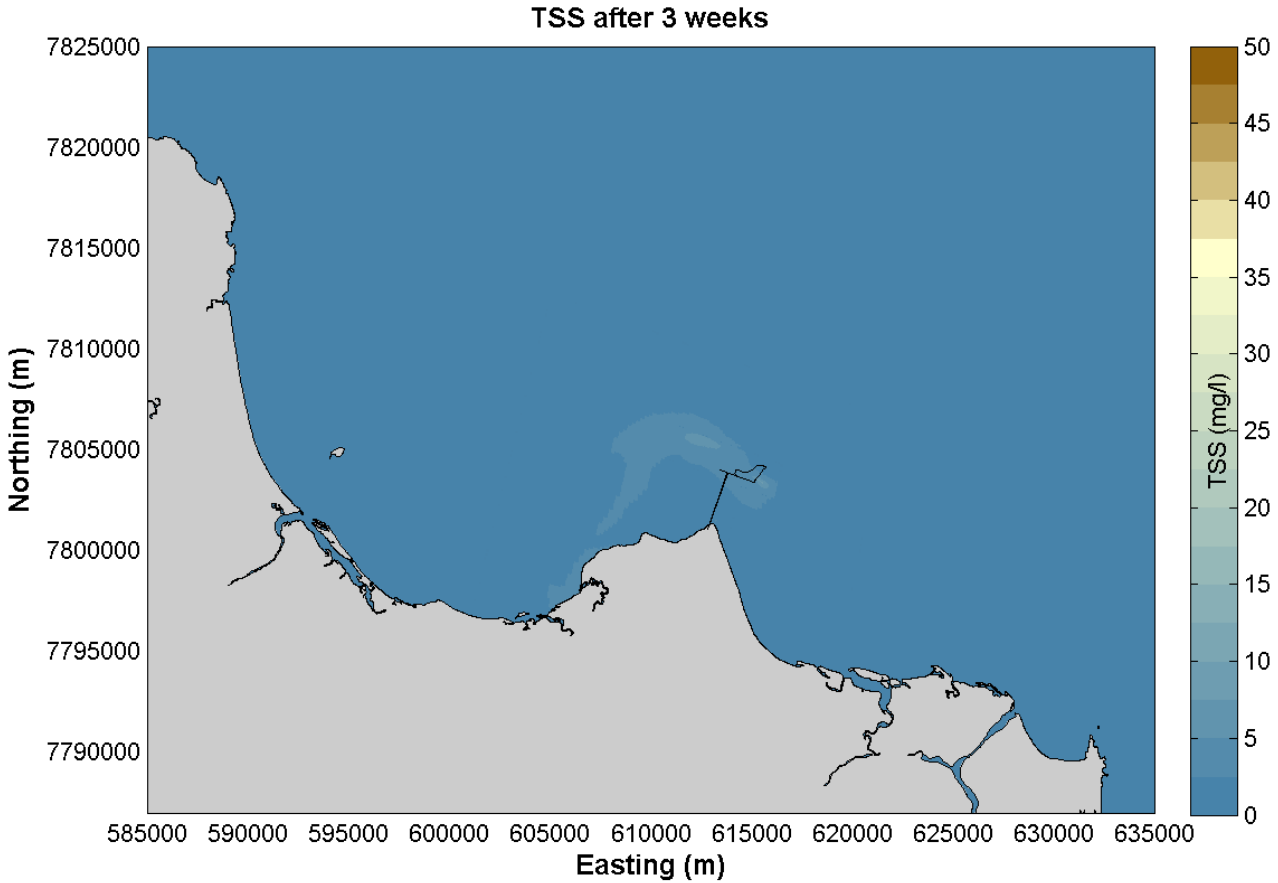

Figure 52 Instantaneous TSS in the surface layer for a single scenario 3 weeks after the dredging commenced (2007, dry season).

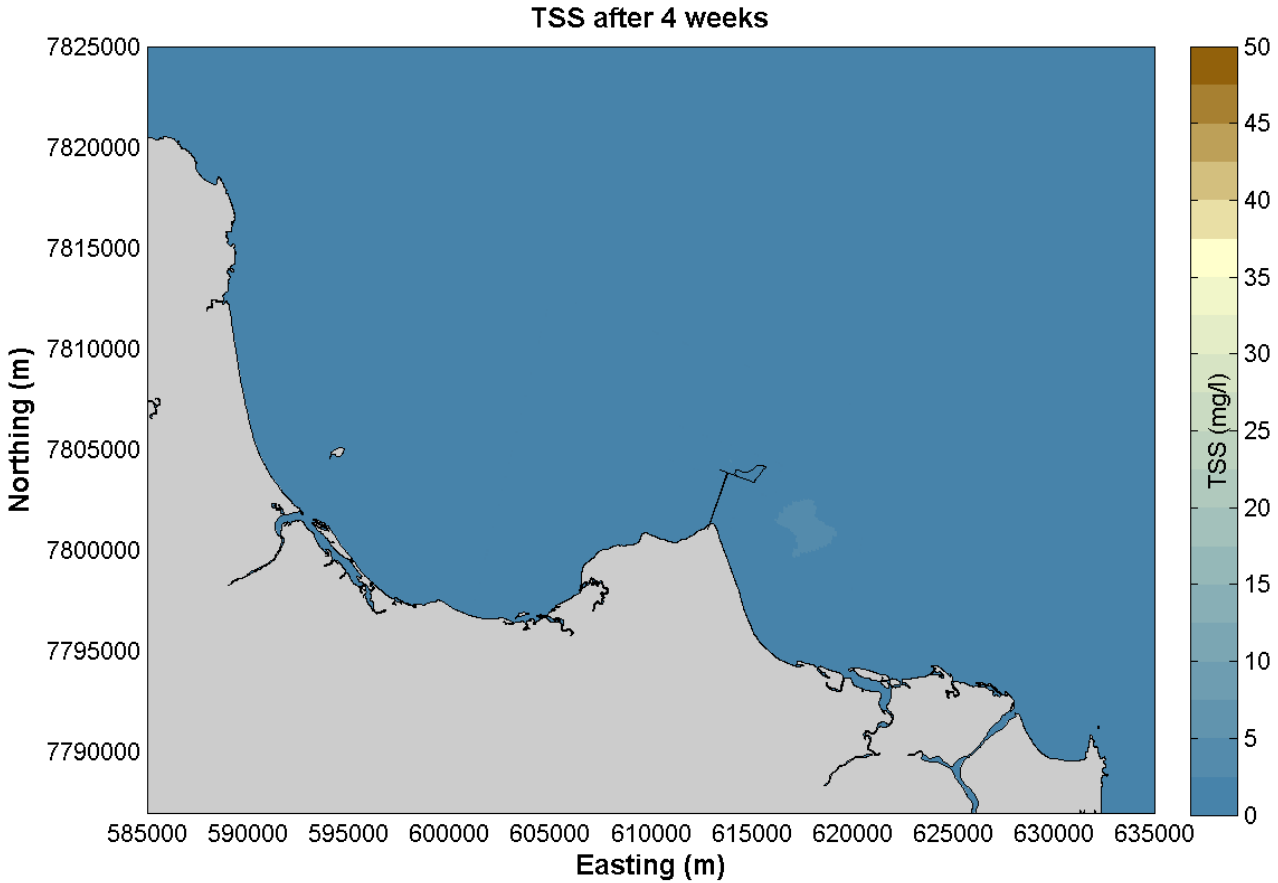

Figure 53 Instantaneous TSS in the surface layer for a single scenario 4 weeks after the dredging commenced (2007, dry season).

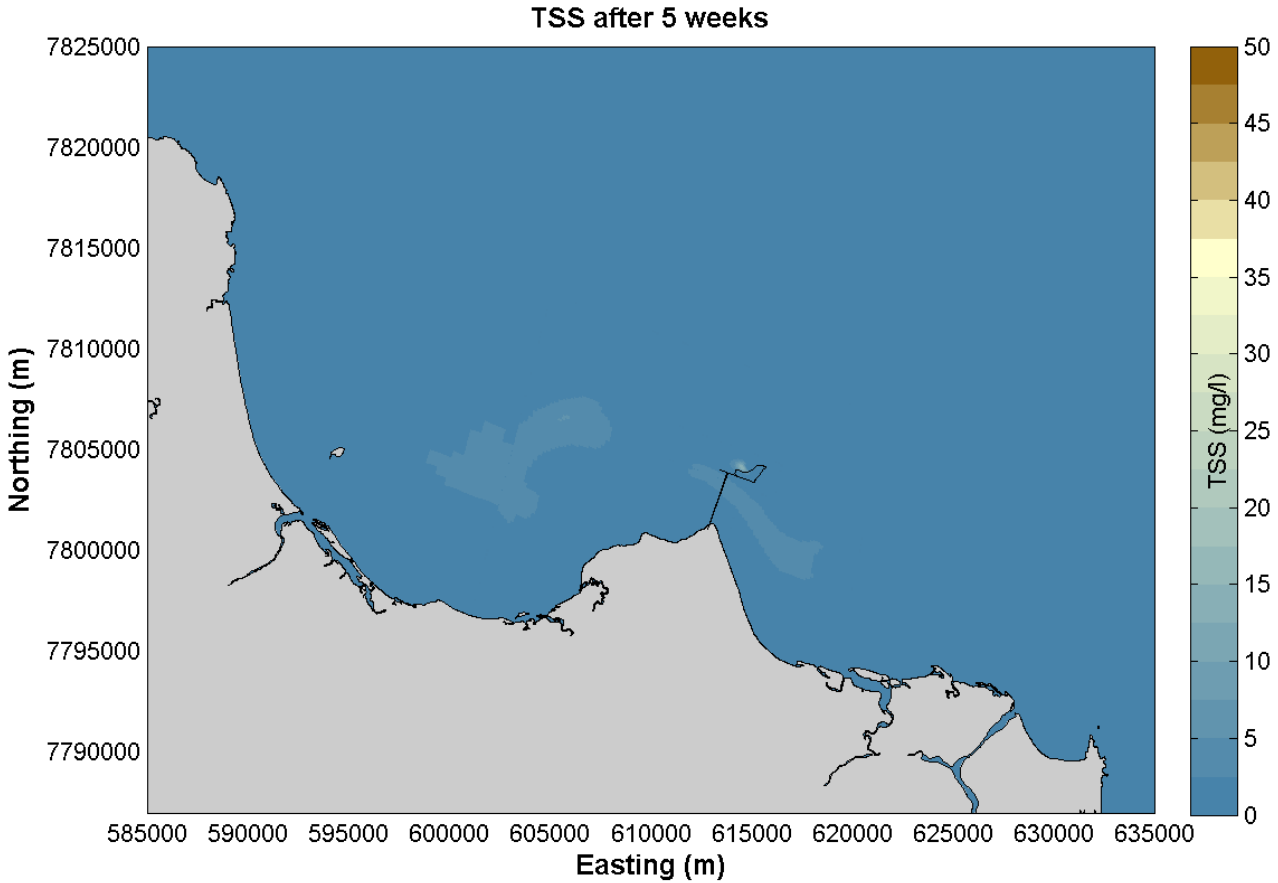

Figure 54 Instantaneous TSS in the surface layer for a single scenario 5 weeks after the dredging commenced (2007, dry season).

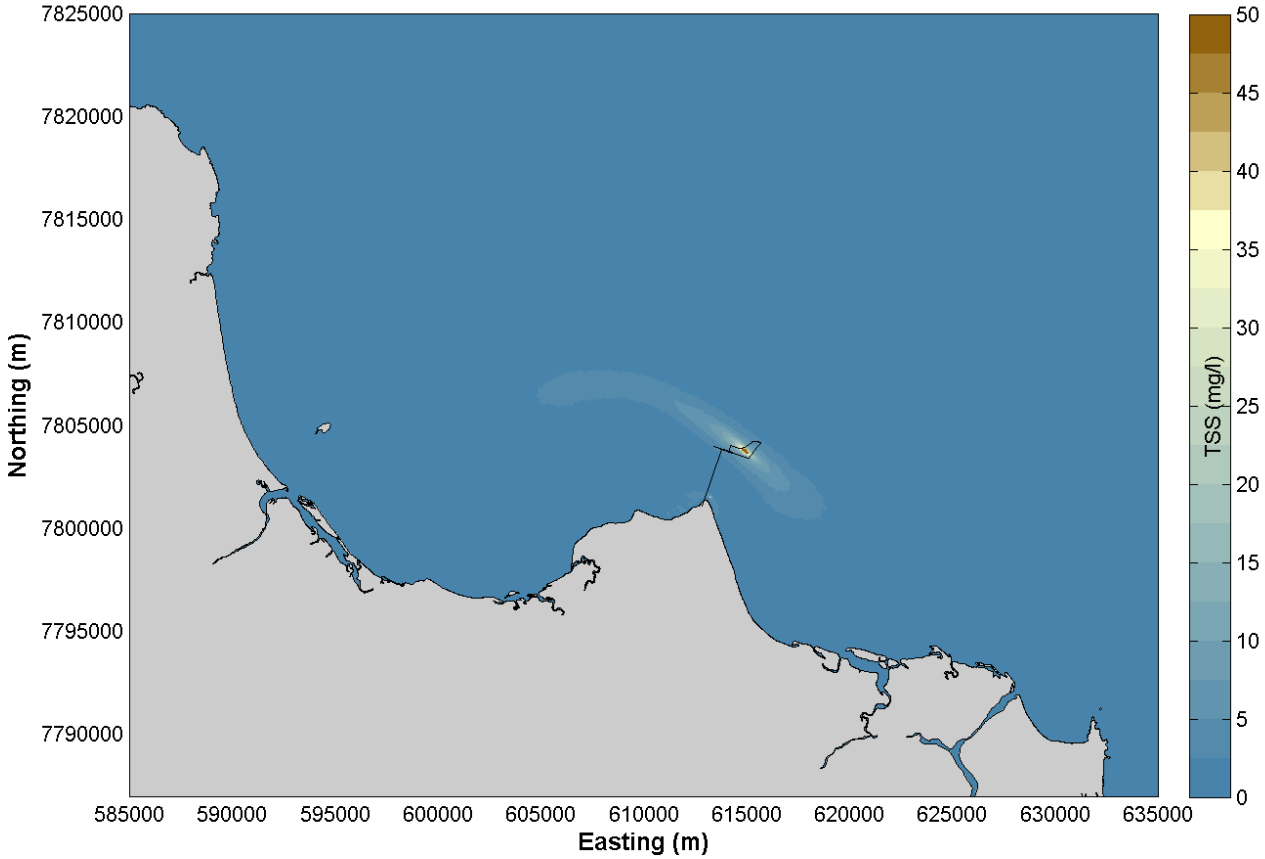

Figure 55 95th percentile TSS for the entire dredging period for the strong El Nino year (1997).

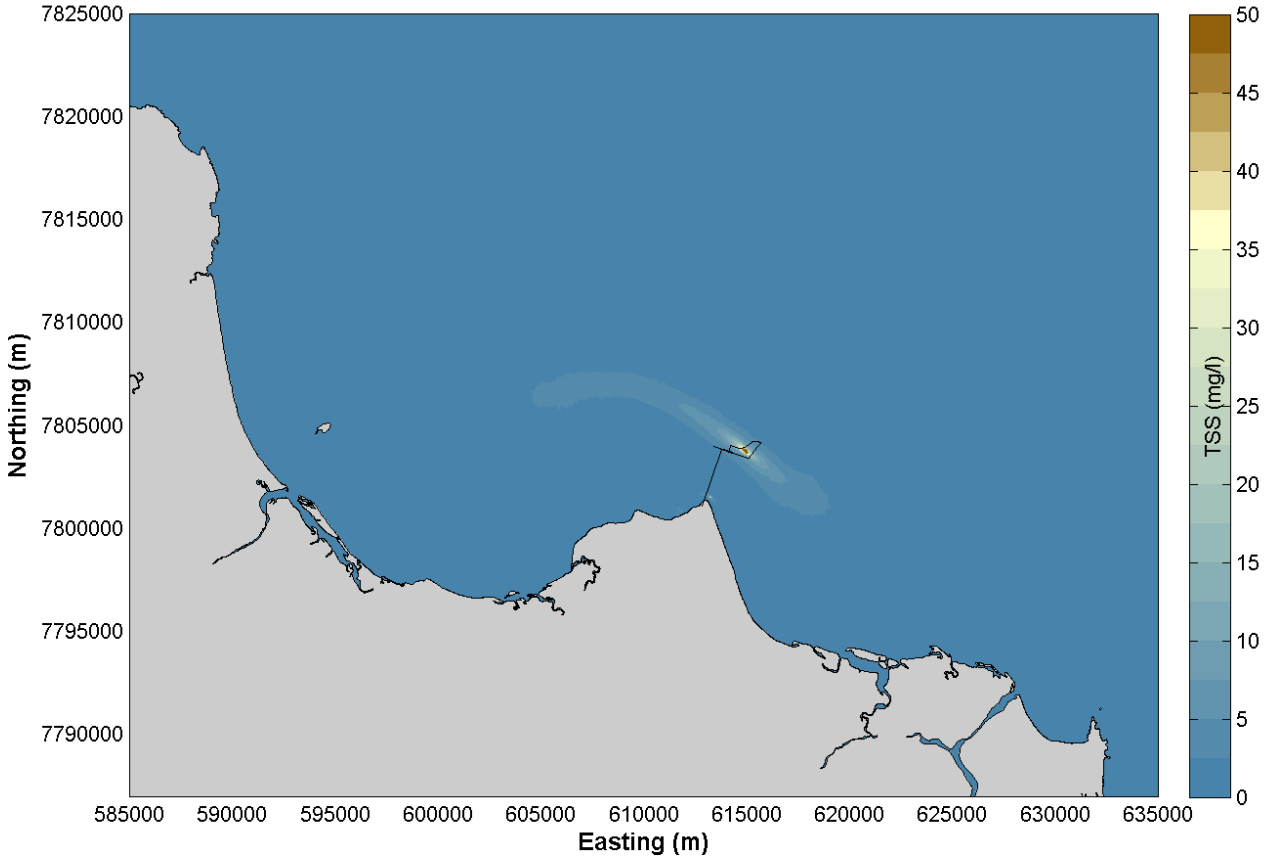

Figure 56 95th percentile TSS for the wet season for the strong El Nino year (1997).

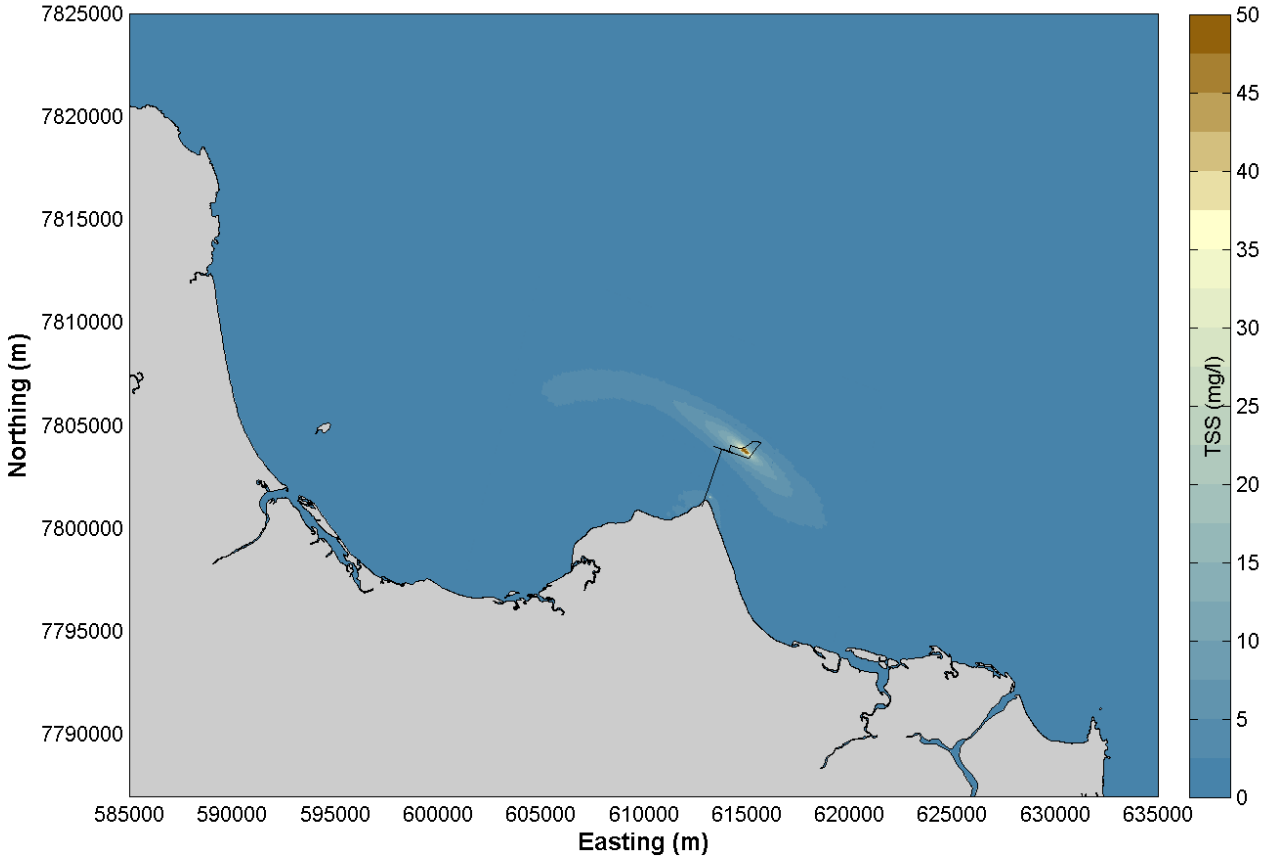

Figure 57 95th percentile TSS for the dry season for the strong El Nino year (1997).

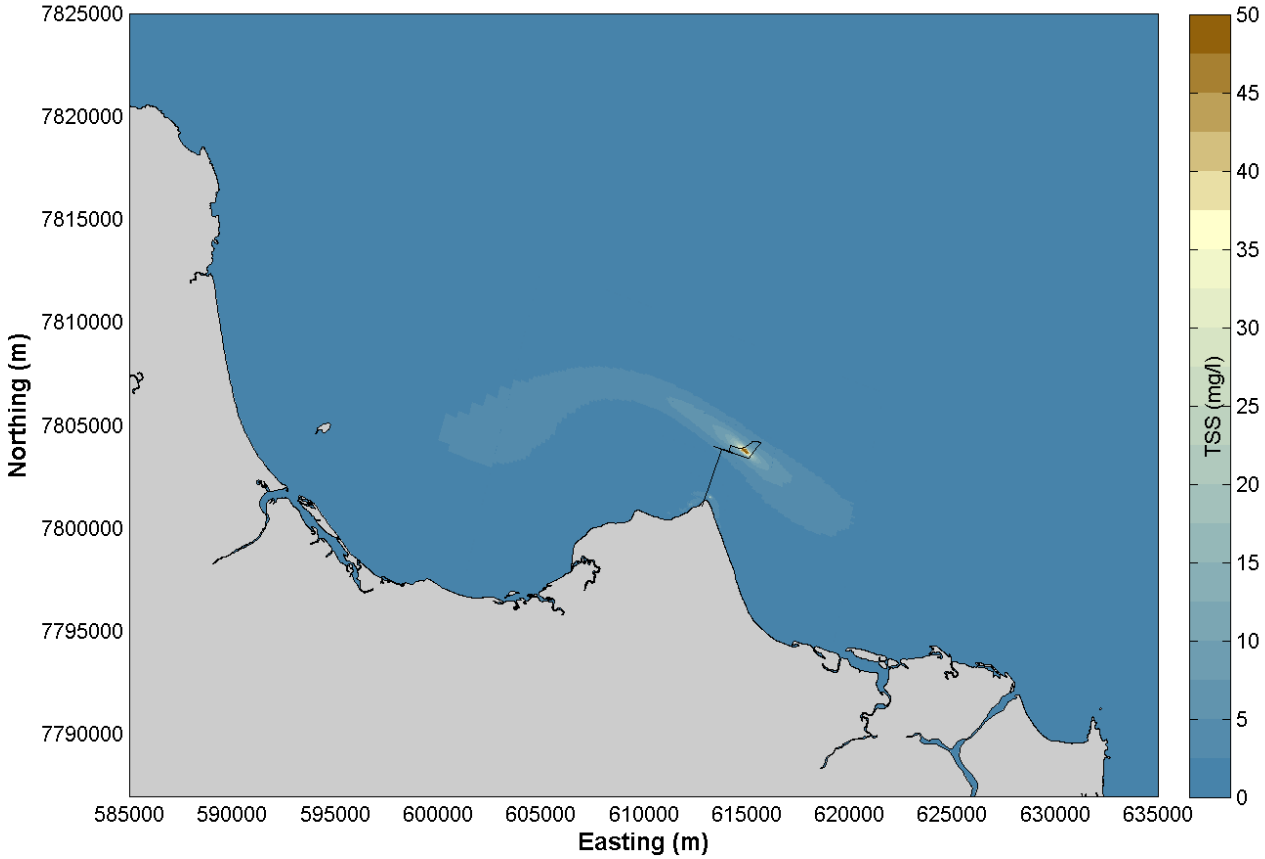

Figure 58 95th percentile TSS for the entire dredging period for the Neutral ENSO year (2007).

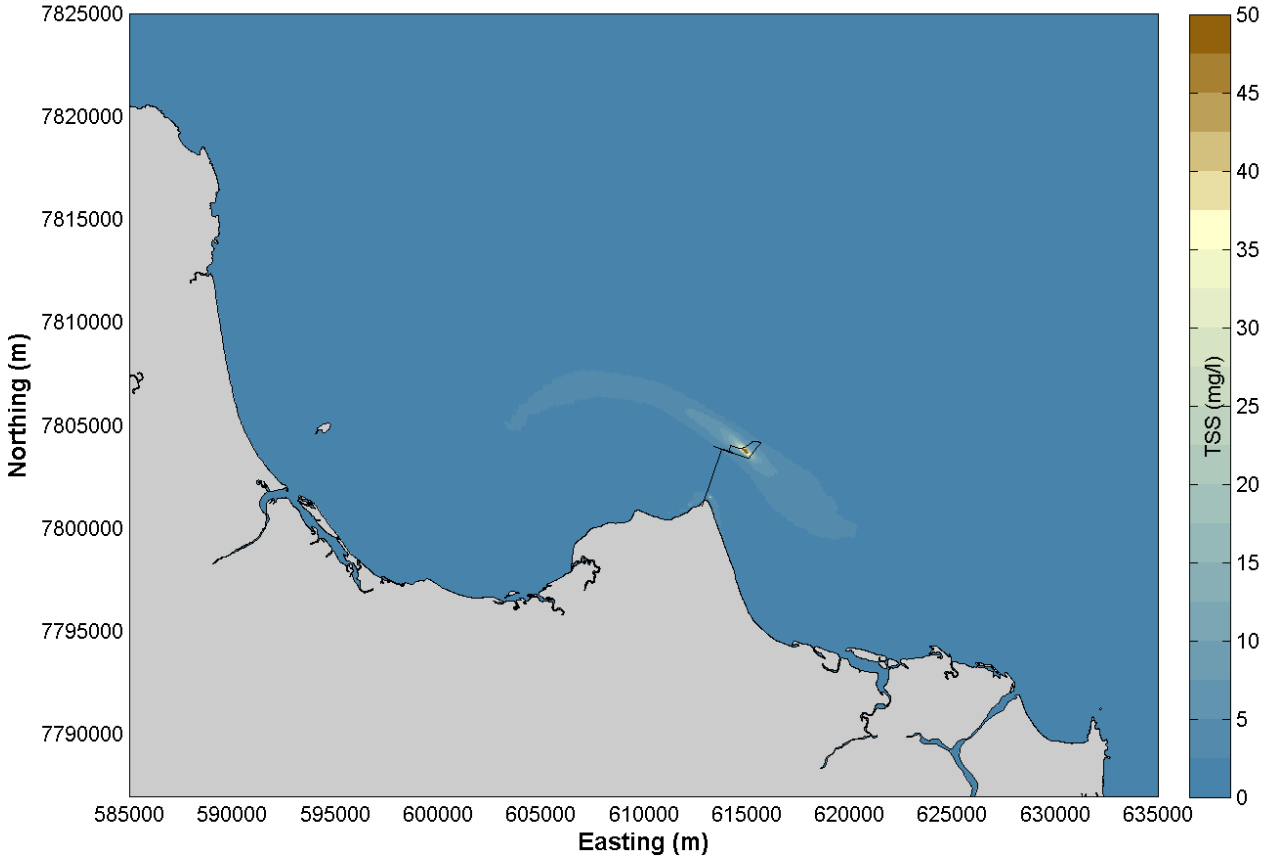

Figure 59 95th percentile TSS for the wet season for the Neutral ENSO year (2007).

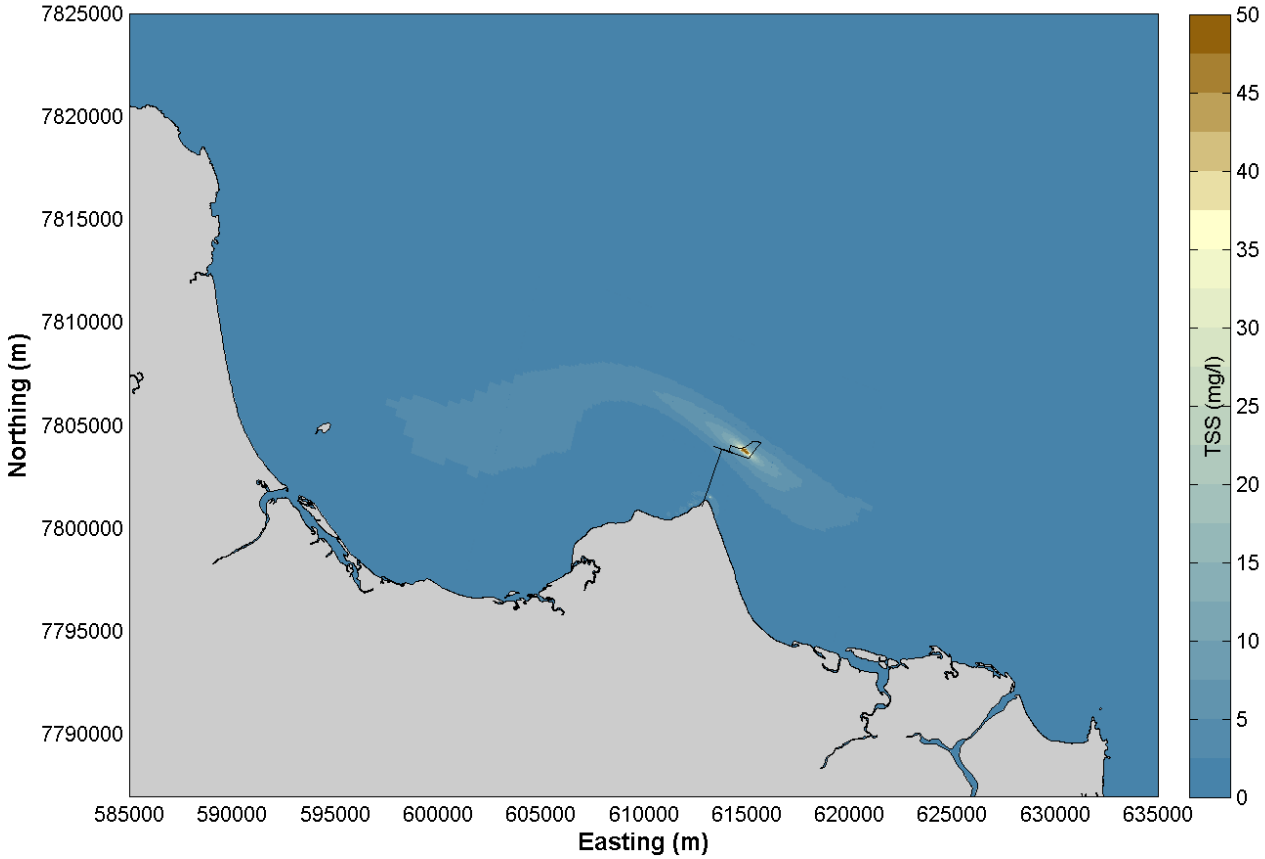

Figure 60 95th percentile TSS for the dry season for the Neutral ENSO year (2007).

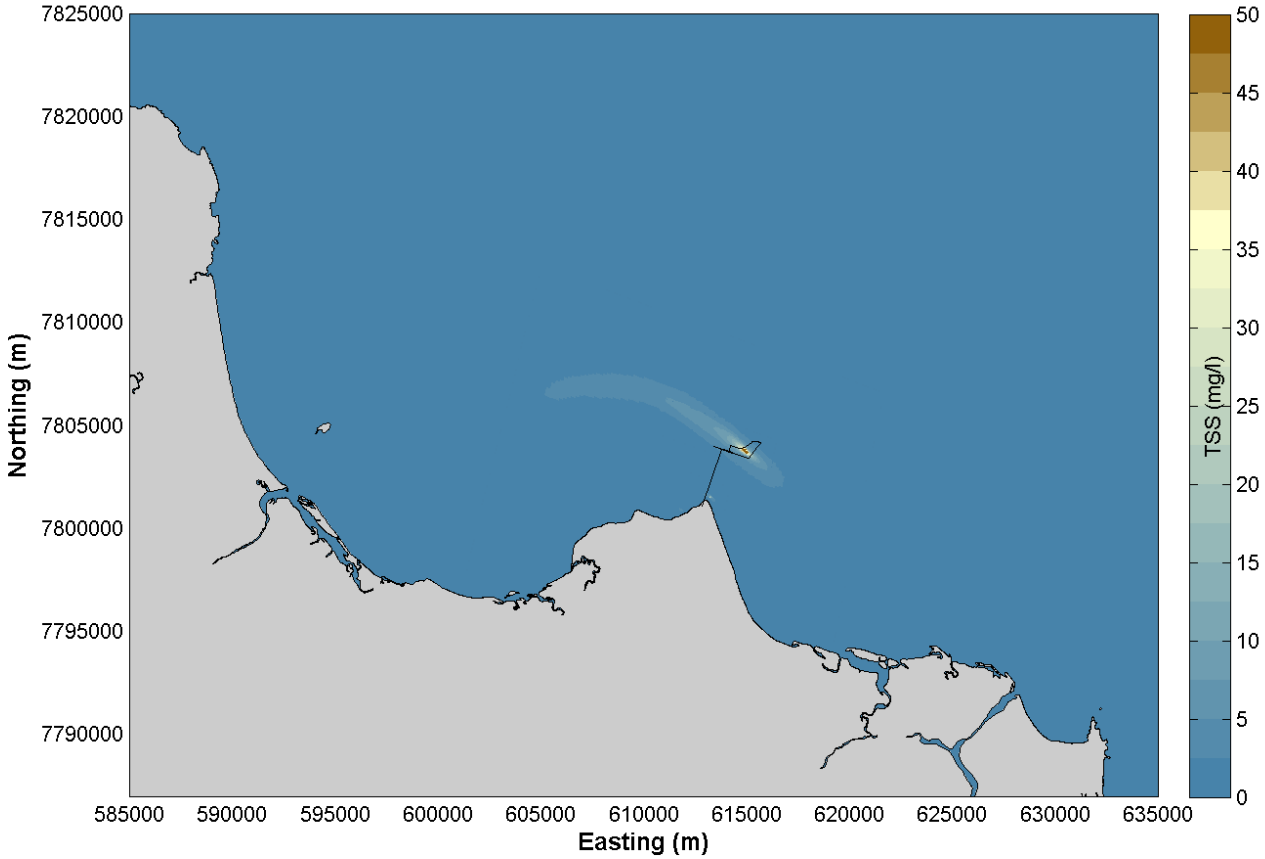

Figure 61 95th percentile TSS for the entire dredging period for the La Nina year (2011).

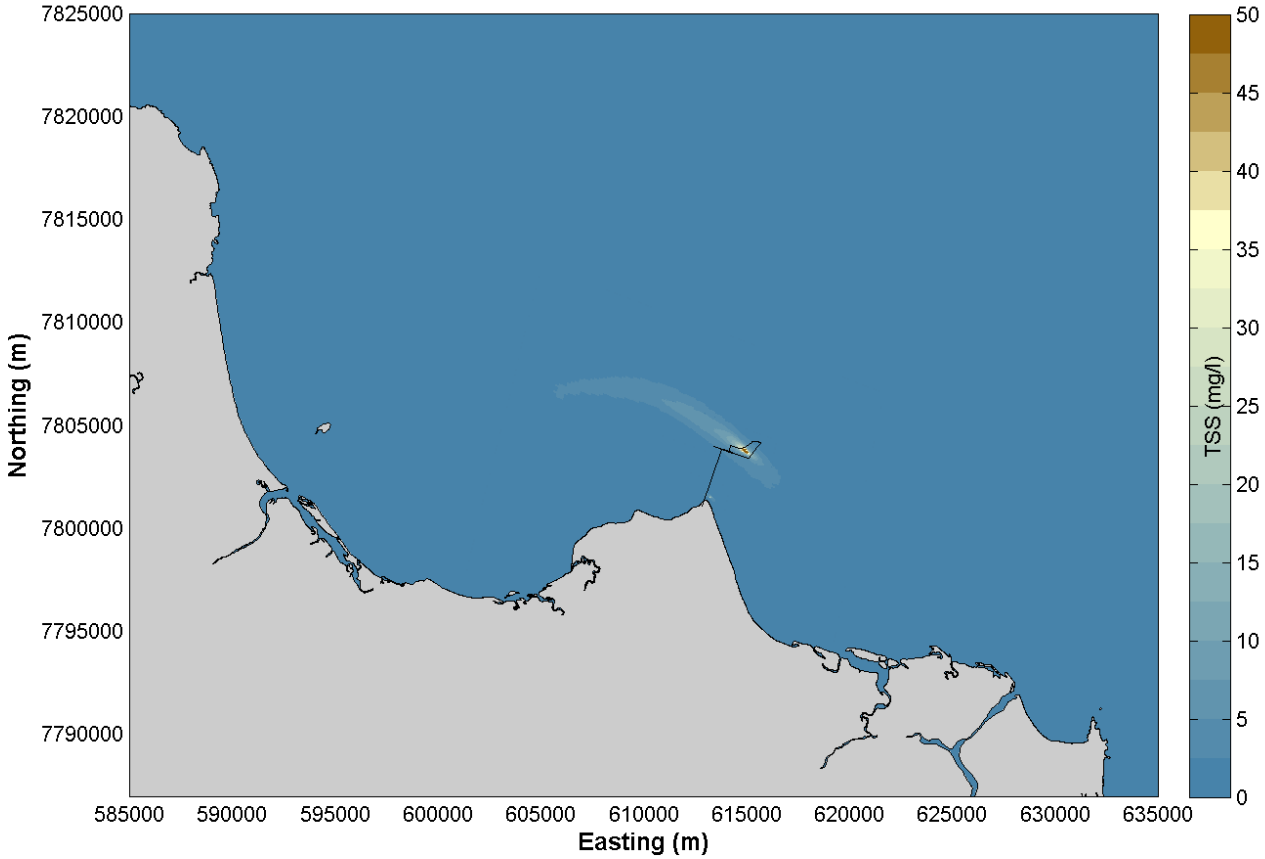

Figure 62 95th percentile TSS for the wet season for the La Nina year (2011).

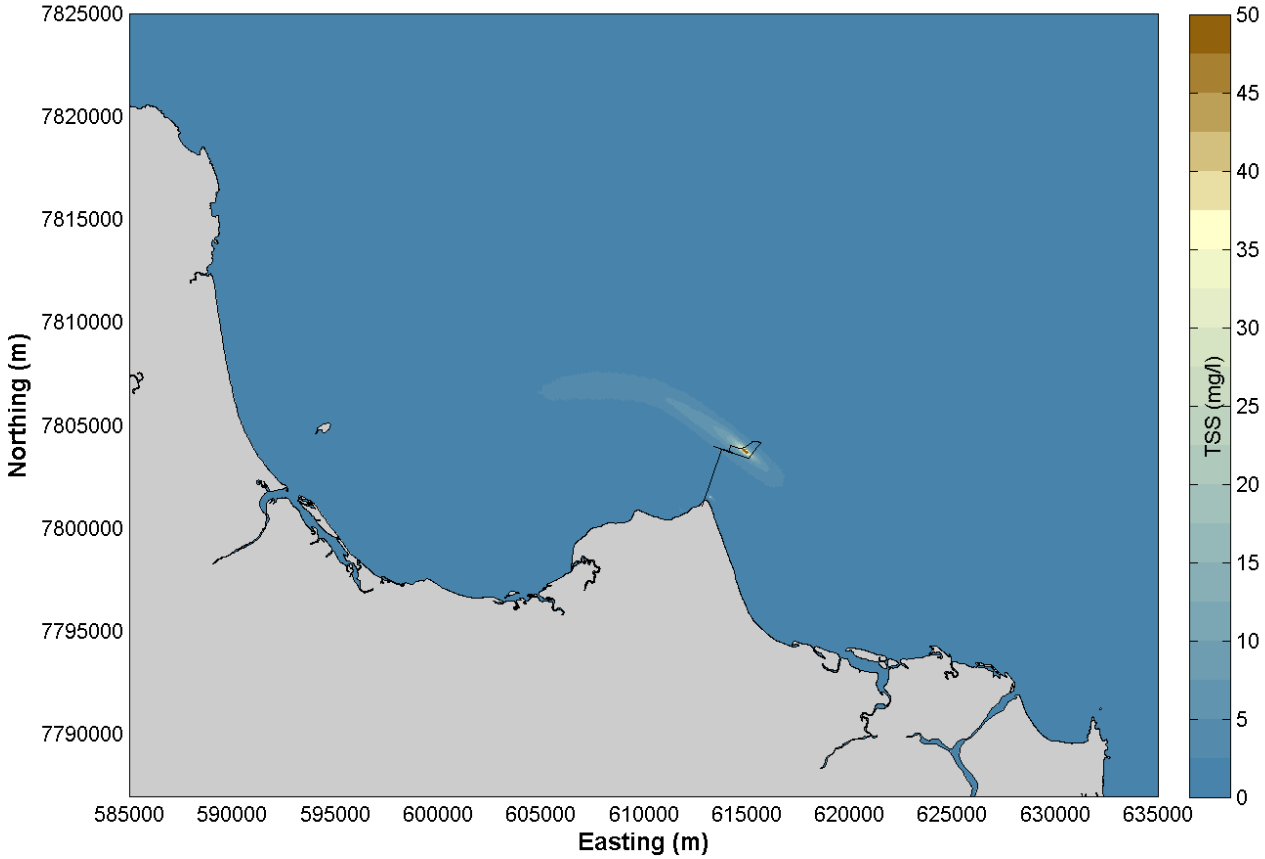

Figure 63 95th percentile TSS for the dry season for the La Nina year (2011).

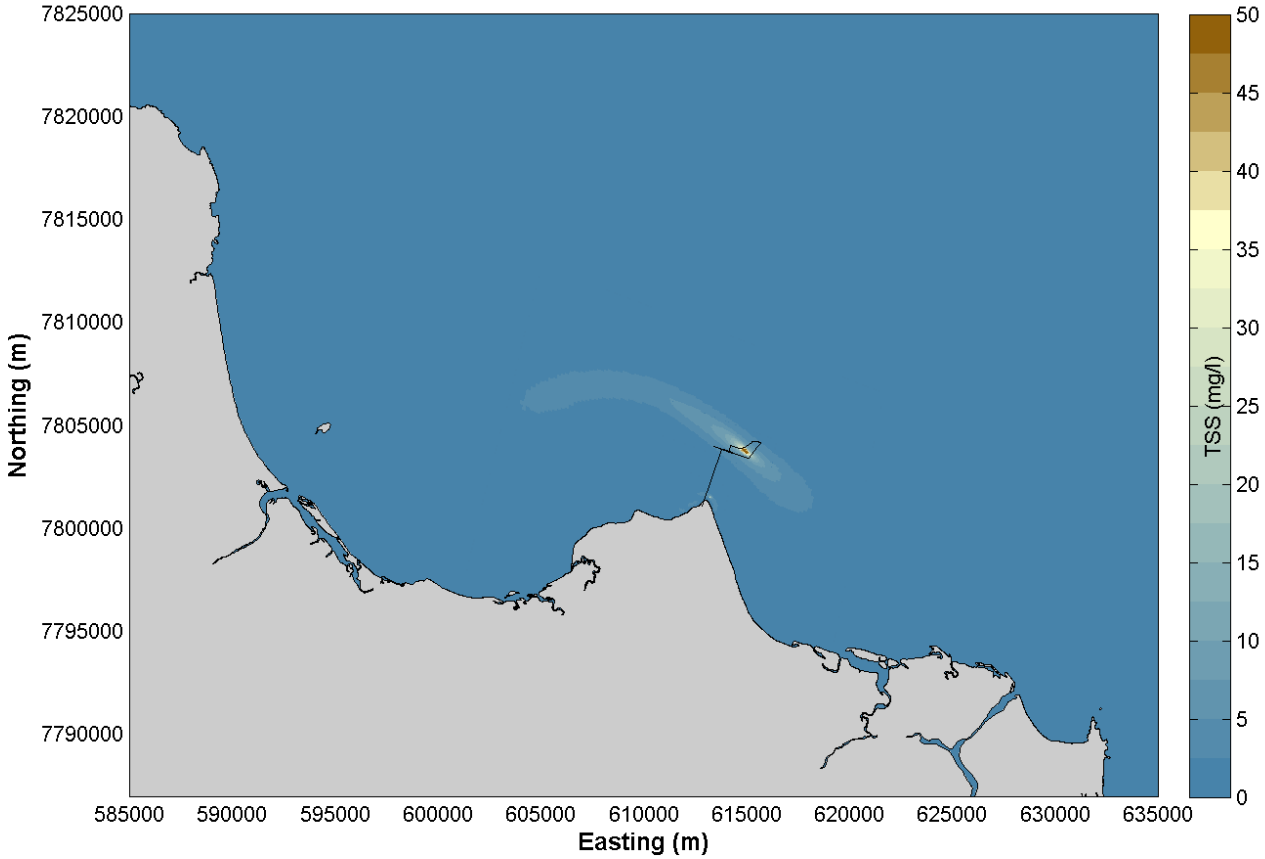

Figure 64 95th percentile TSS for the entire dredging period for all three years.

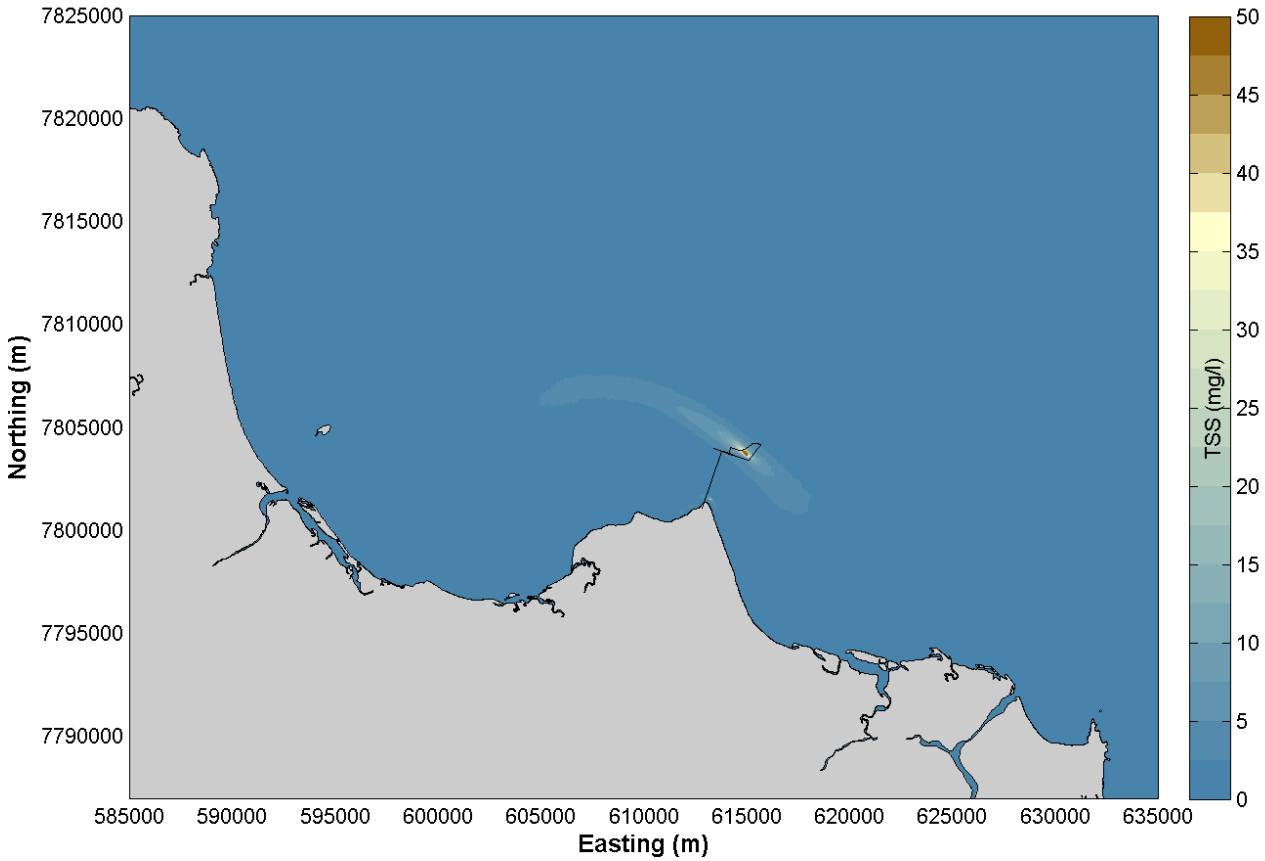

Figure 65 95th percentile TSS for the wet season for all three years.

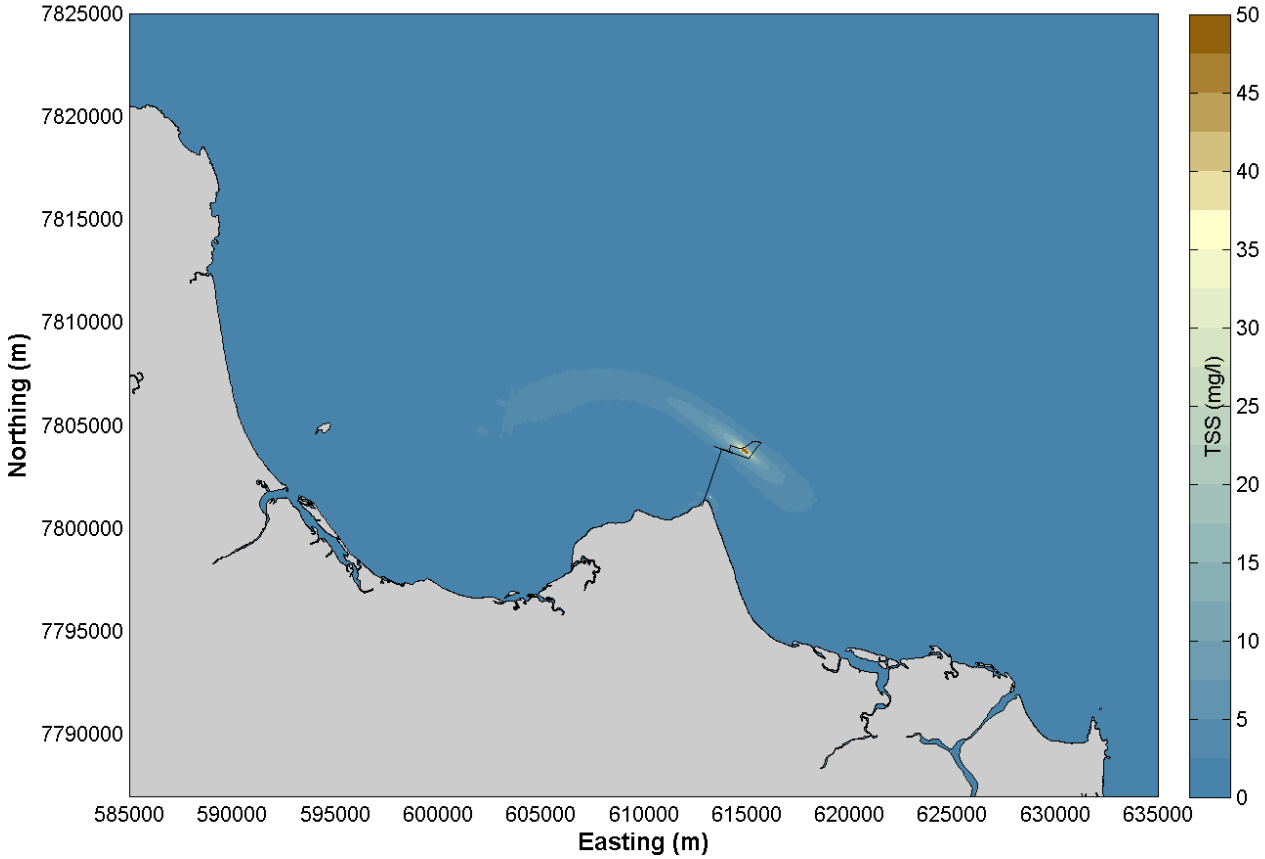

Figure 66 95th percentile TSS for the dry season for all three years.

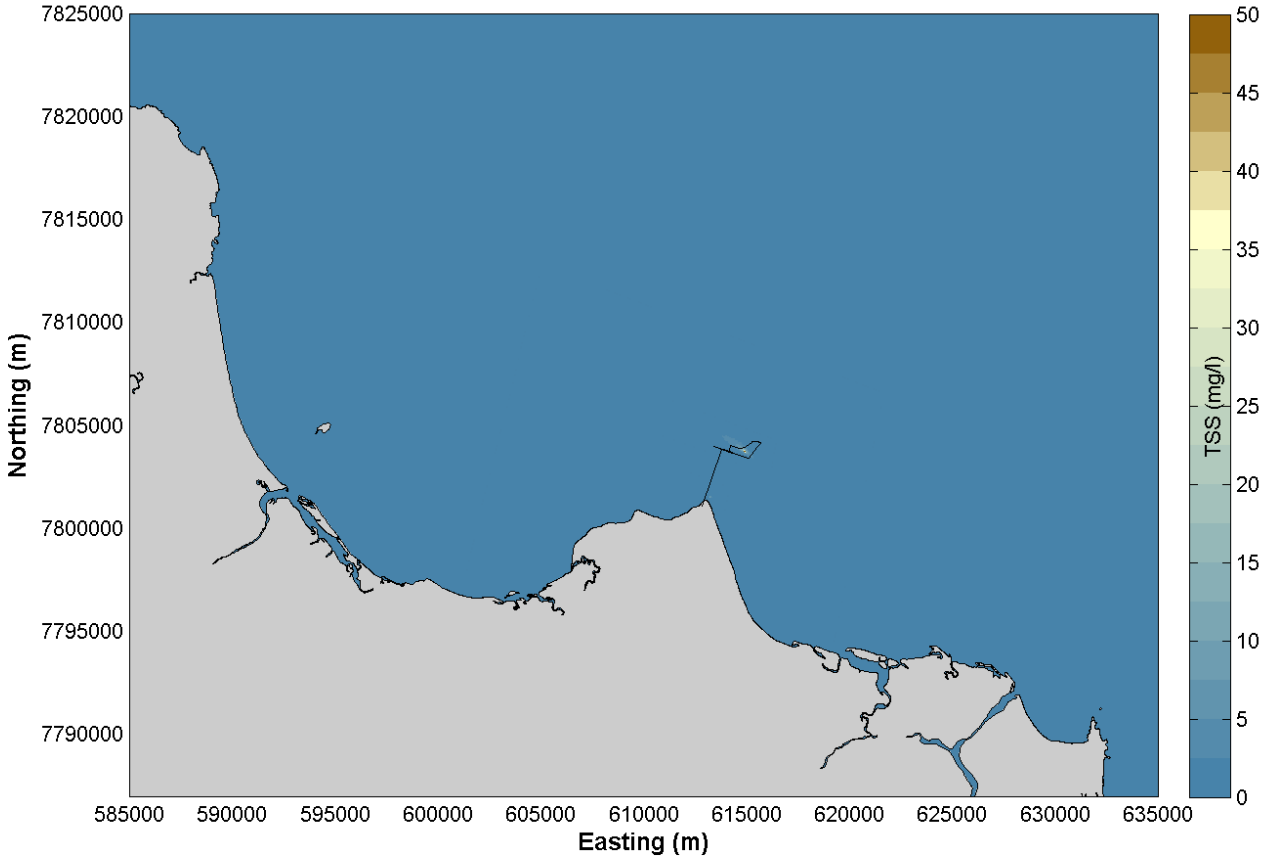

Figure 67 Mean TSS for the wet season for all three years.

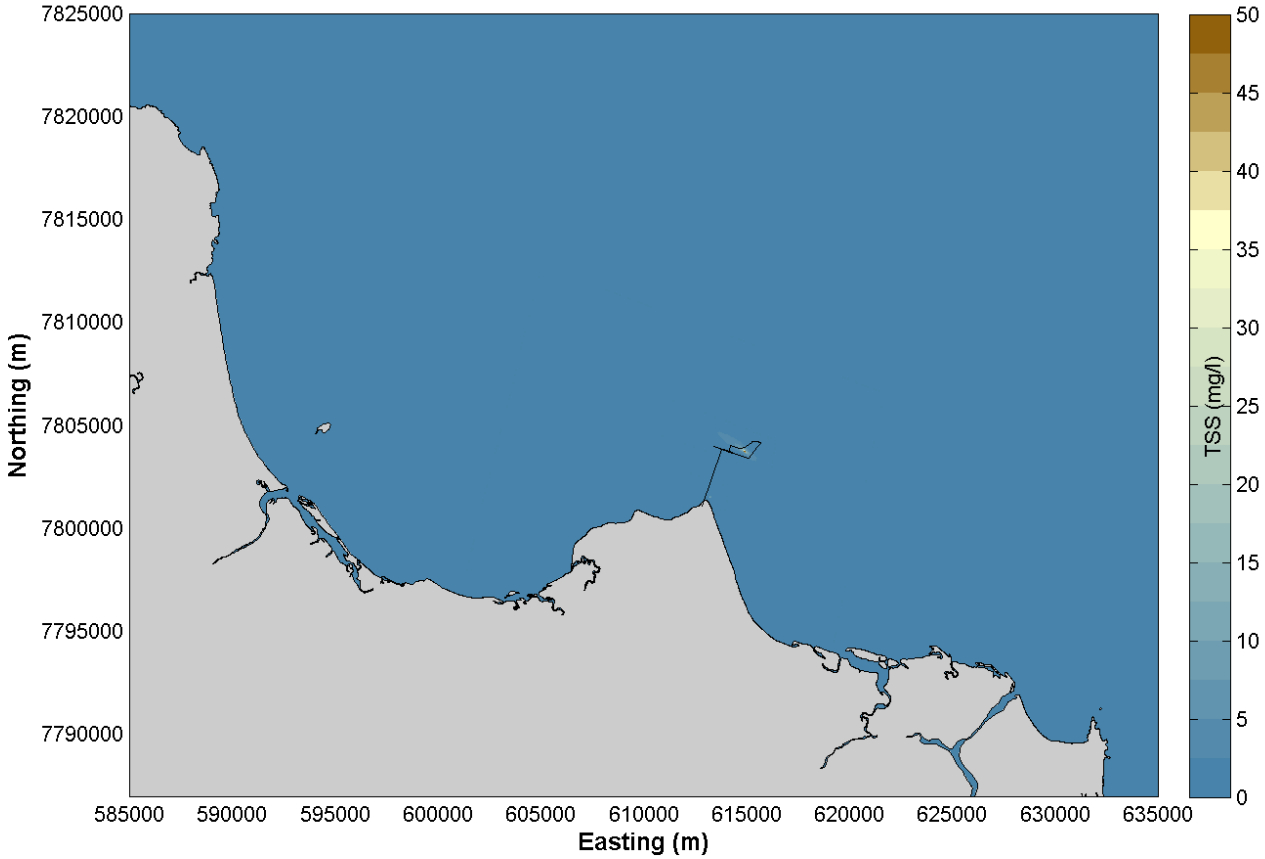

Figure 68 Mean TSS for the dry season for all three years.

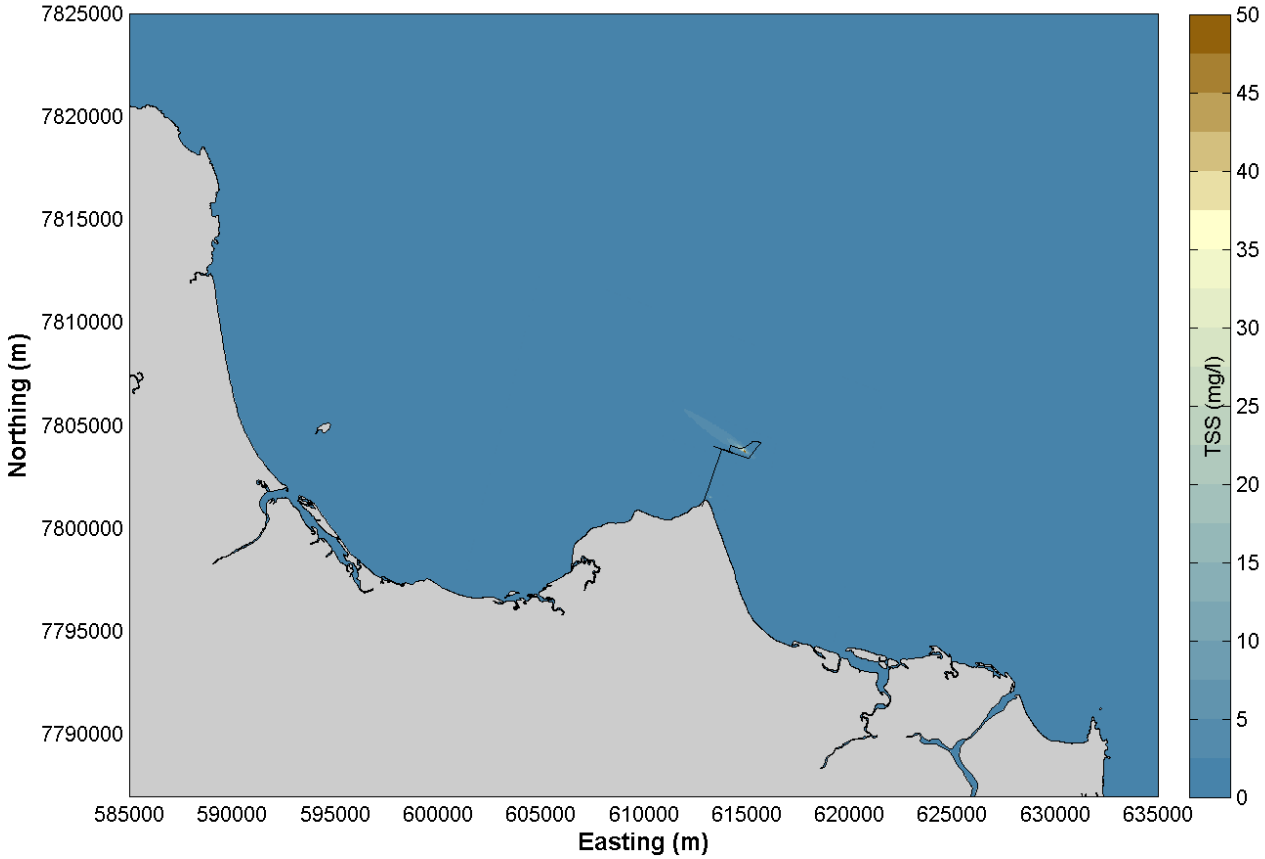

Figure 69 80th percentile TSS for the wet season for all three years.

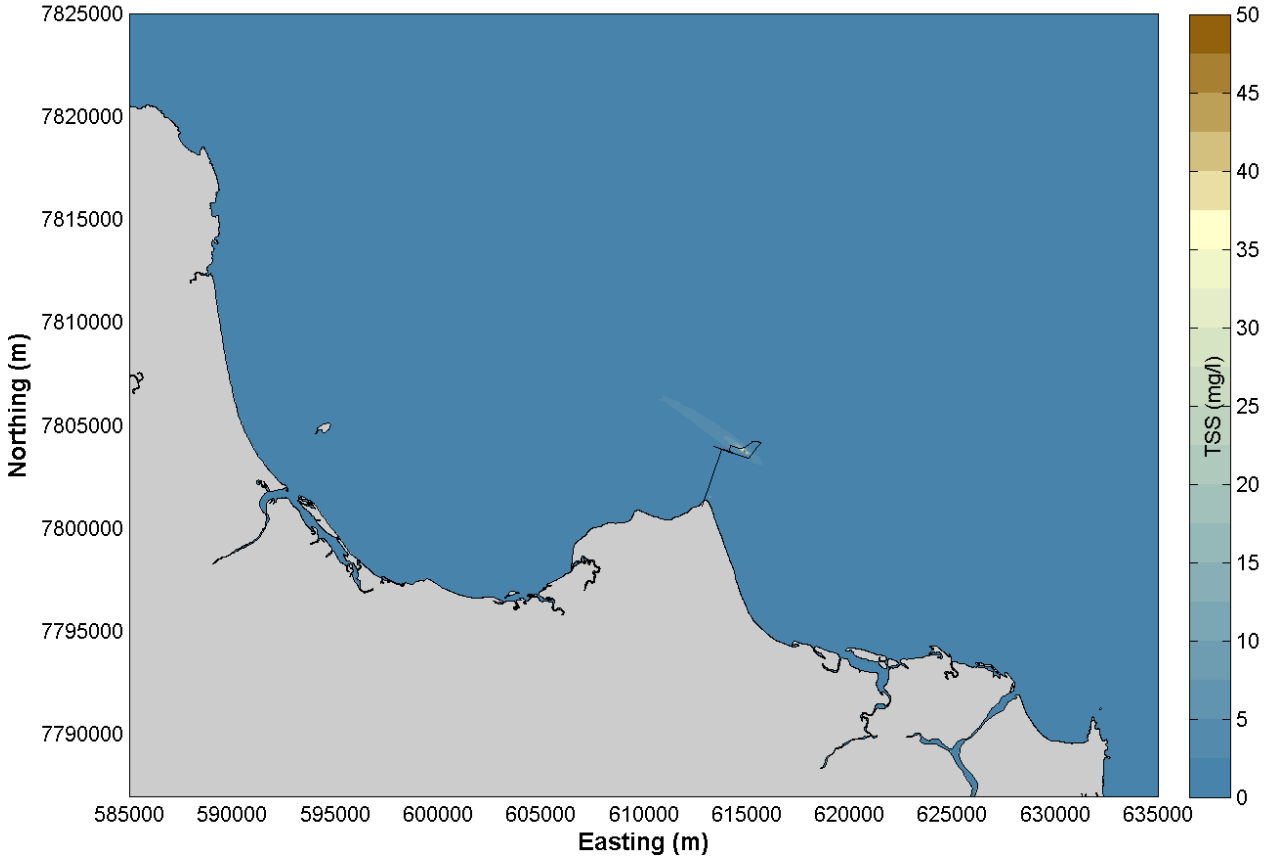

Figure 70 80th percentile TSS for the dry season for all three years.

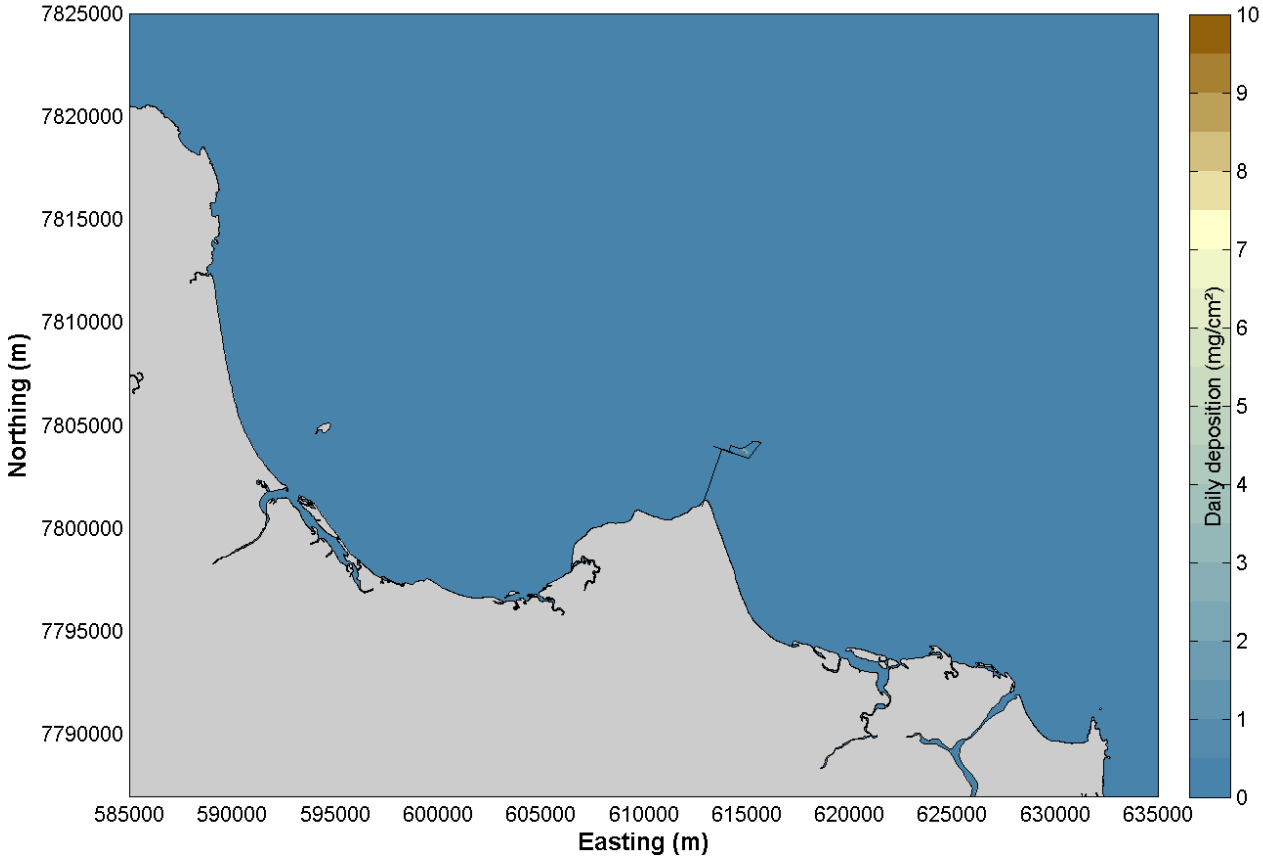

Figure 71 80th percentile sedimentation for the wet season for the Neutral ENSO year (2007).

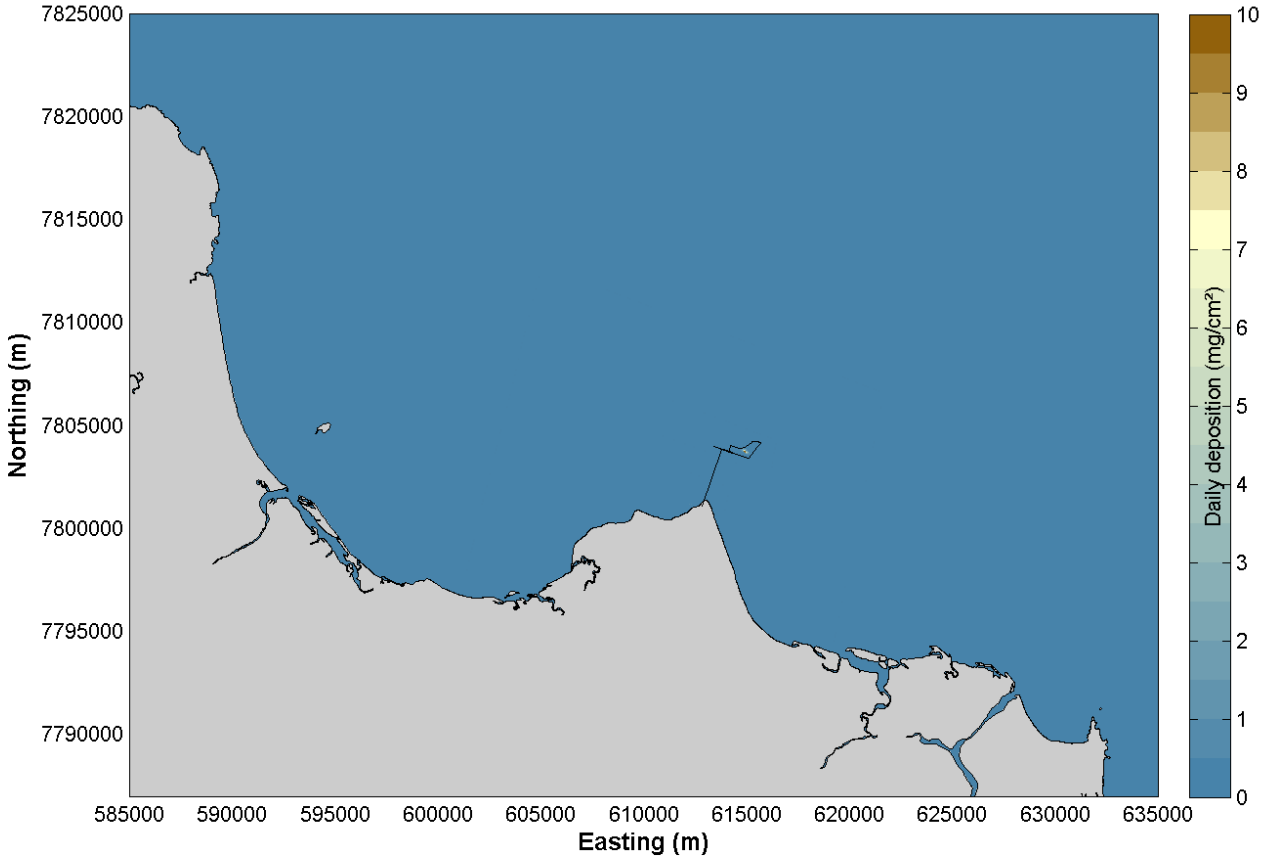

Figure 72 80th percentile sedimentation for the dry season for the Neutral ENSO year (2007).

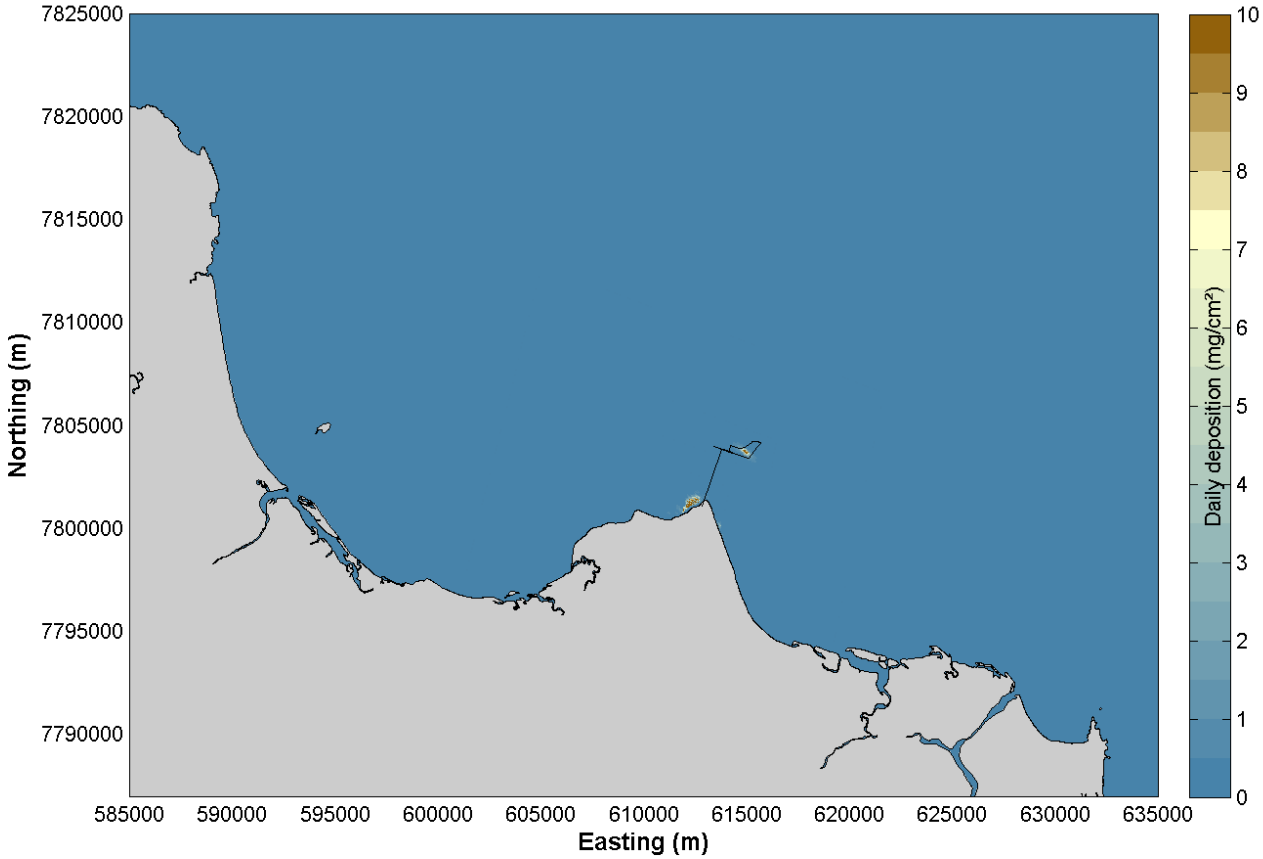

Figure 73 95th percentile sedimentation for the wet season for the Neutral ENSO year (2007).

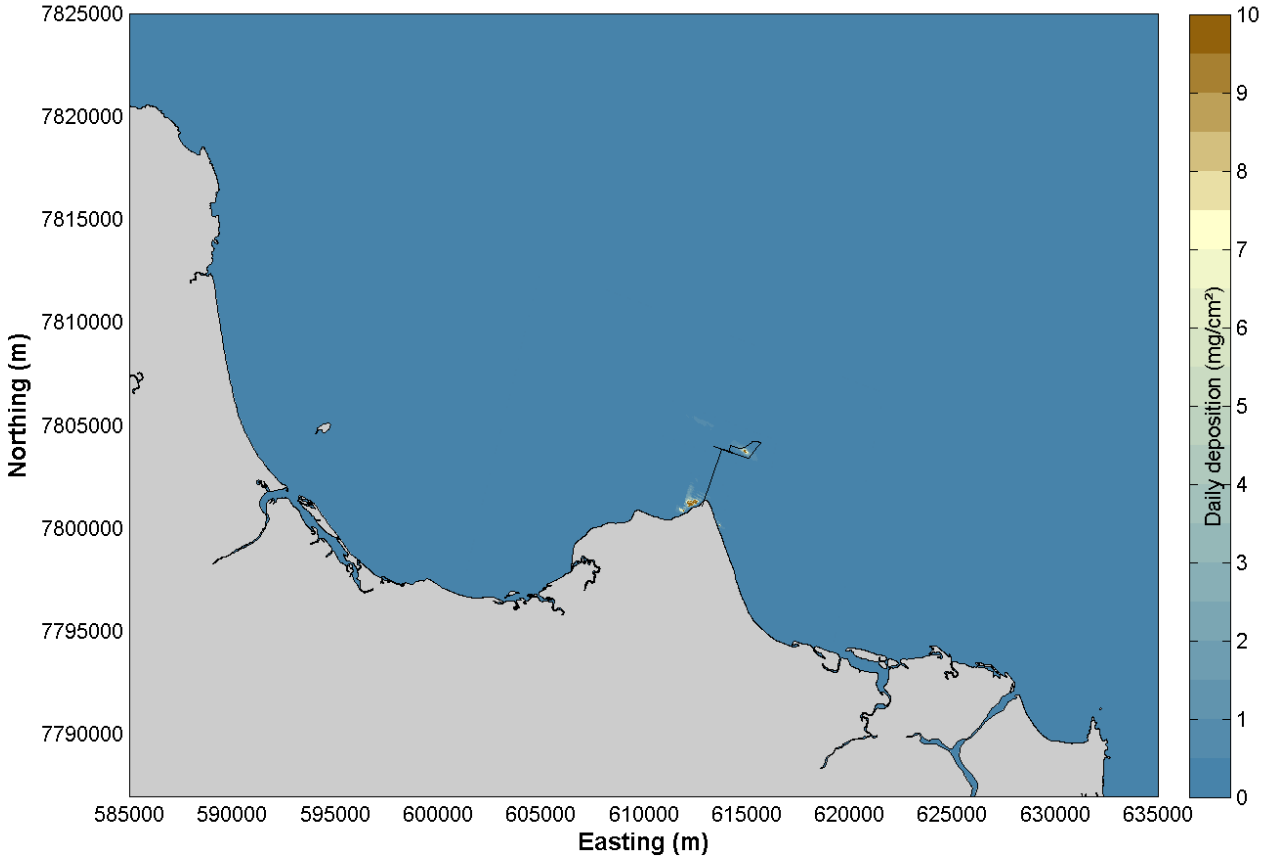

Figure 74 95th percentile sedimentation for the dry season for the Neutral ENSO year (2007).

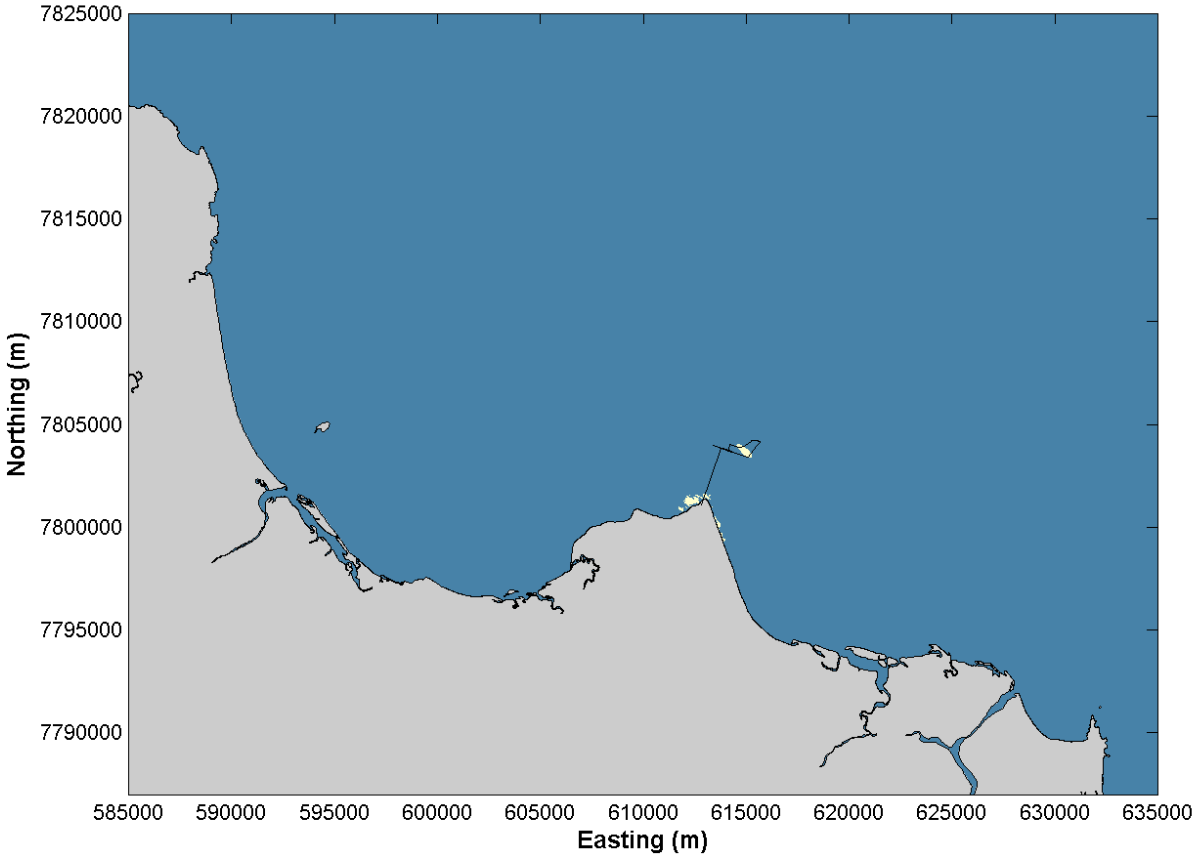

Figure 75 Zone of moderate impact based on daily sedimentation rate for the wet season for the Neutral ENSO year (2007).

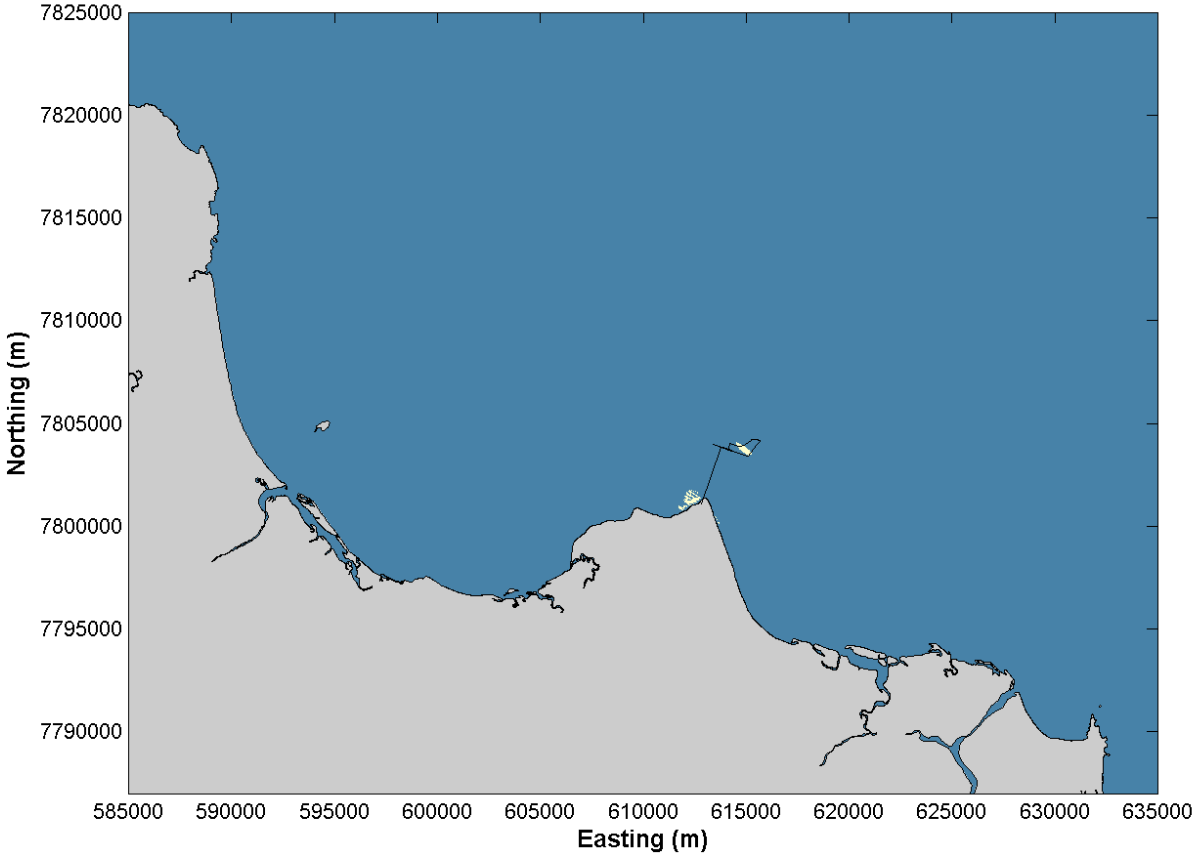

Figure 76 Zone of moderate impact based on daily sedimentation rate for the dry season for the Neutral ENSO year (2007).

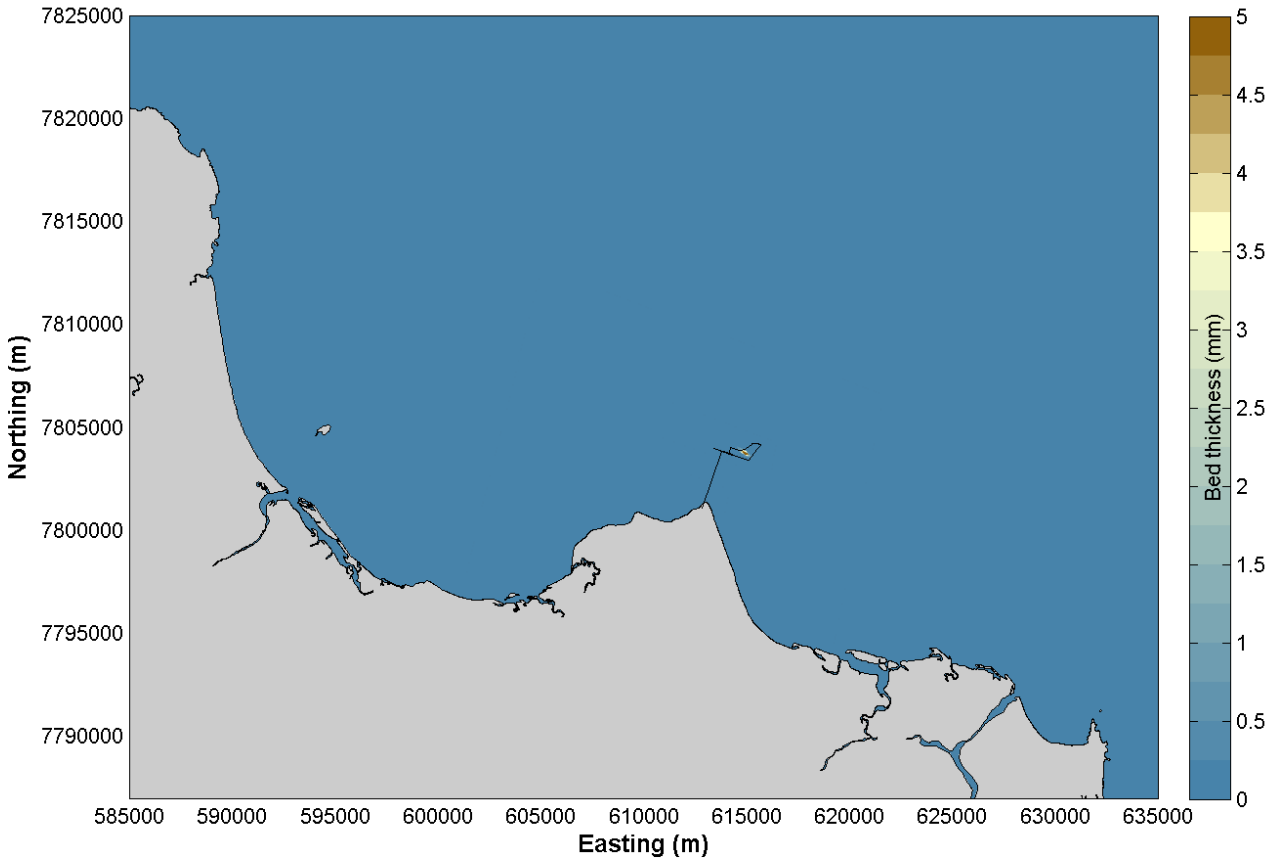

Figure 77 Bed thickness map at the cessation of dredging for the wet season for all three years.

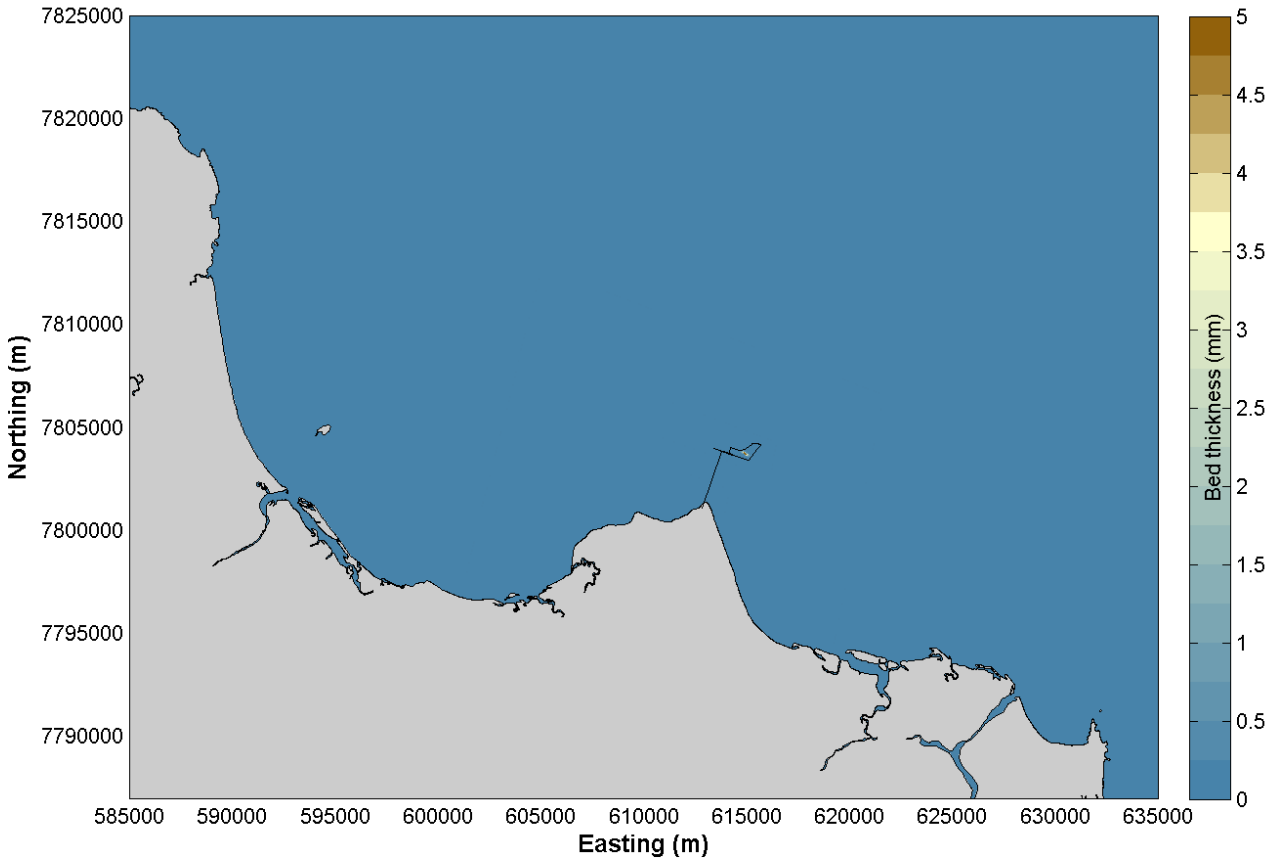

Figure 78 Bed thickness map at the cessation of dredging for the dry season for all three years.

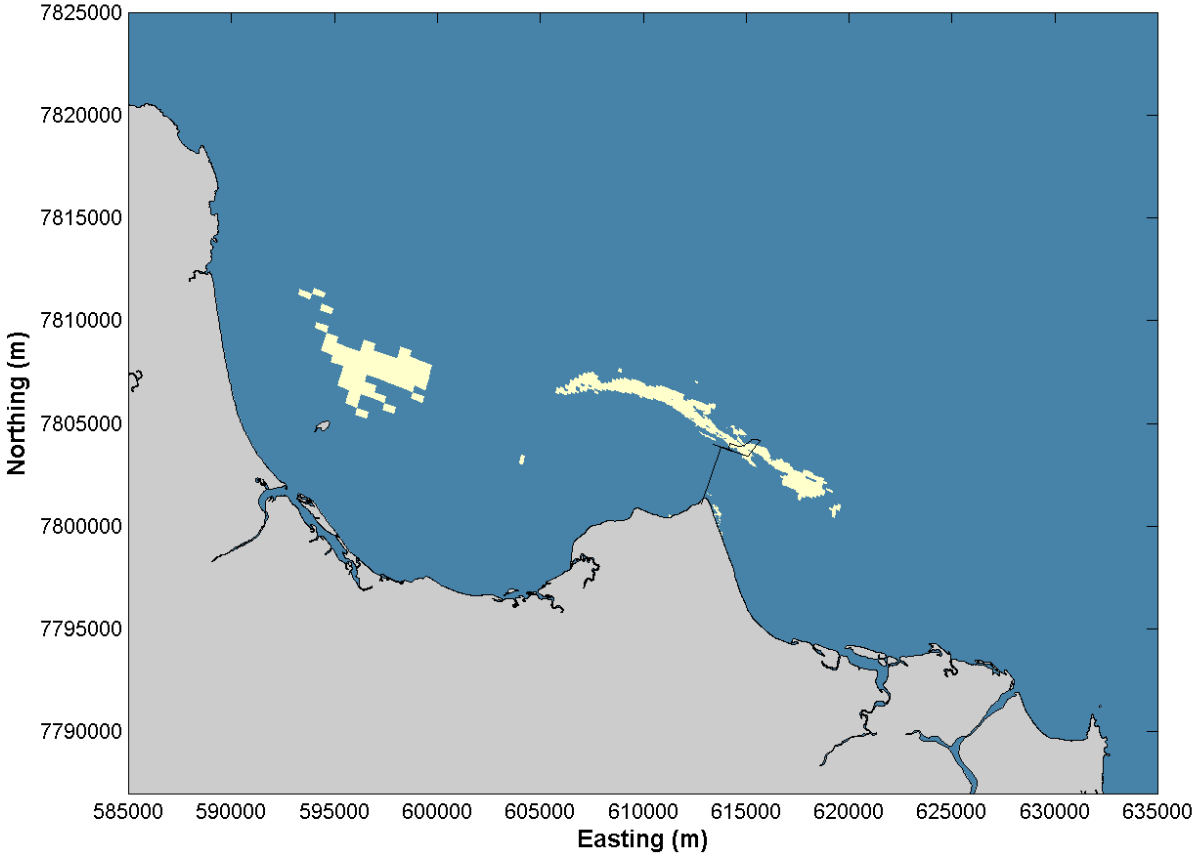

Figure 79 Area of influence for TSS for the wet season for the El Nino year (1997).

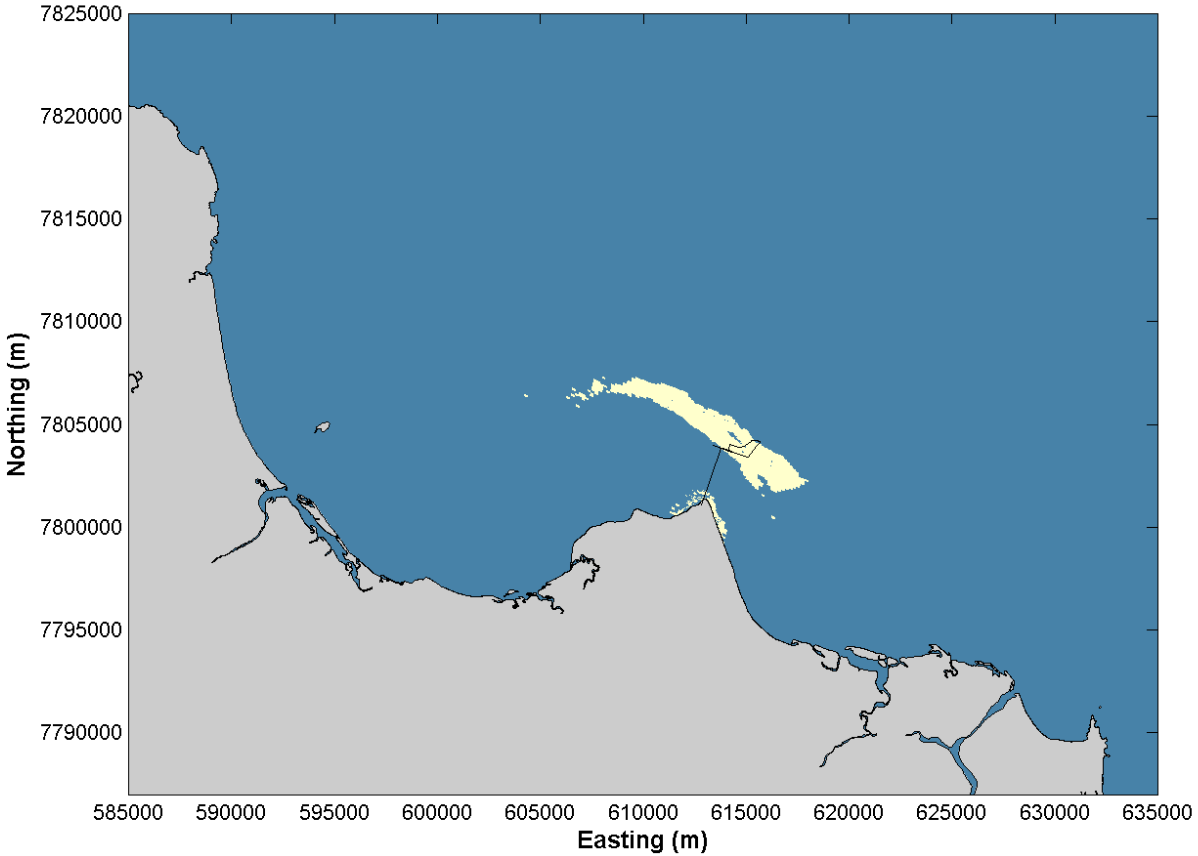

Figure 80 Area of influence for TSS for the dry season for the El Nino year (1997).

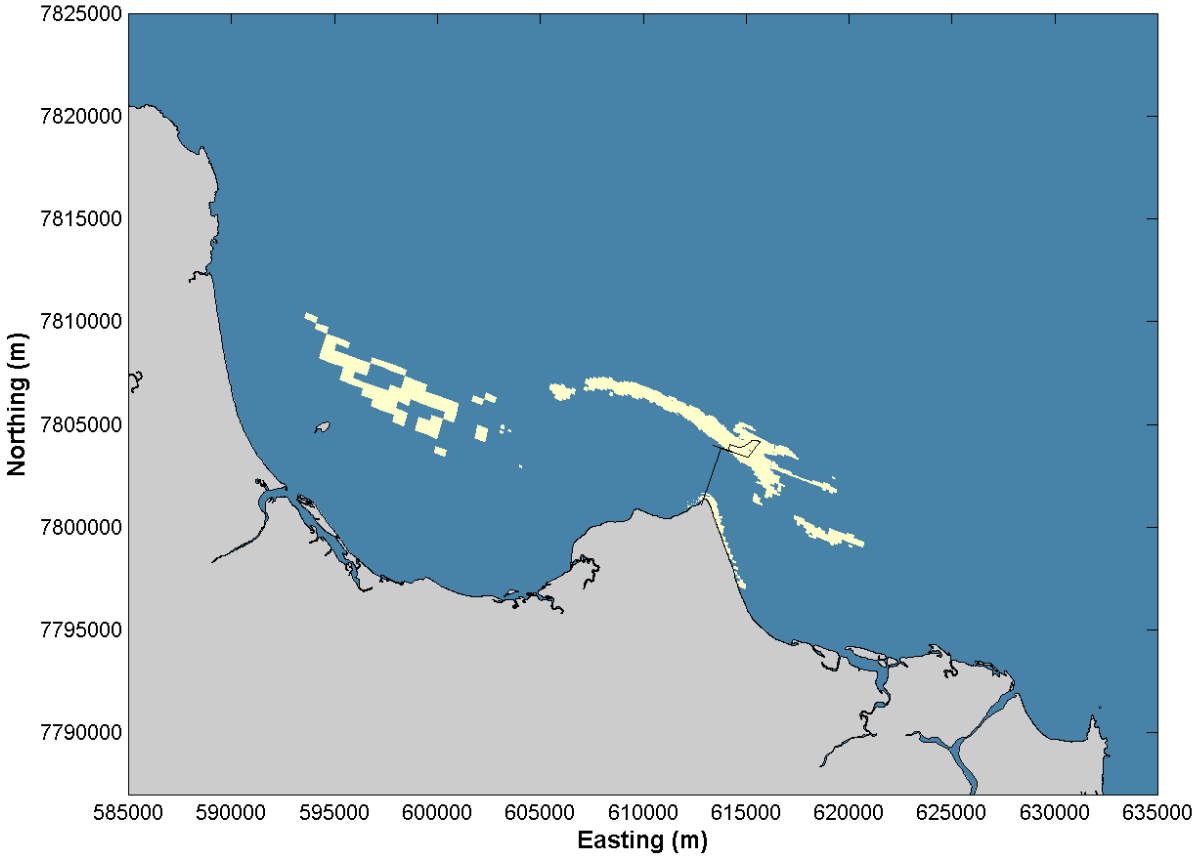

Figure 81 Area of influence for TSS for the wet season for the Neutral ENSO year (2007).

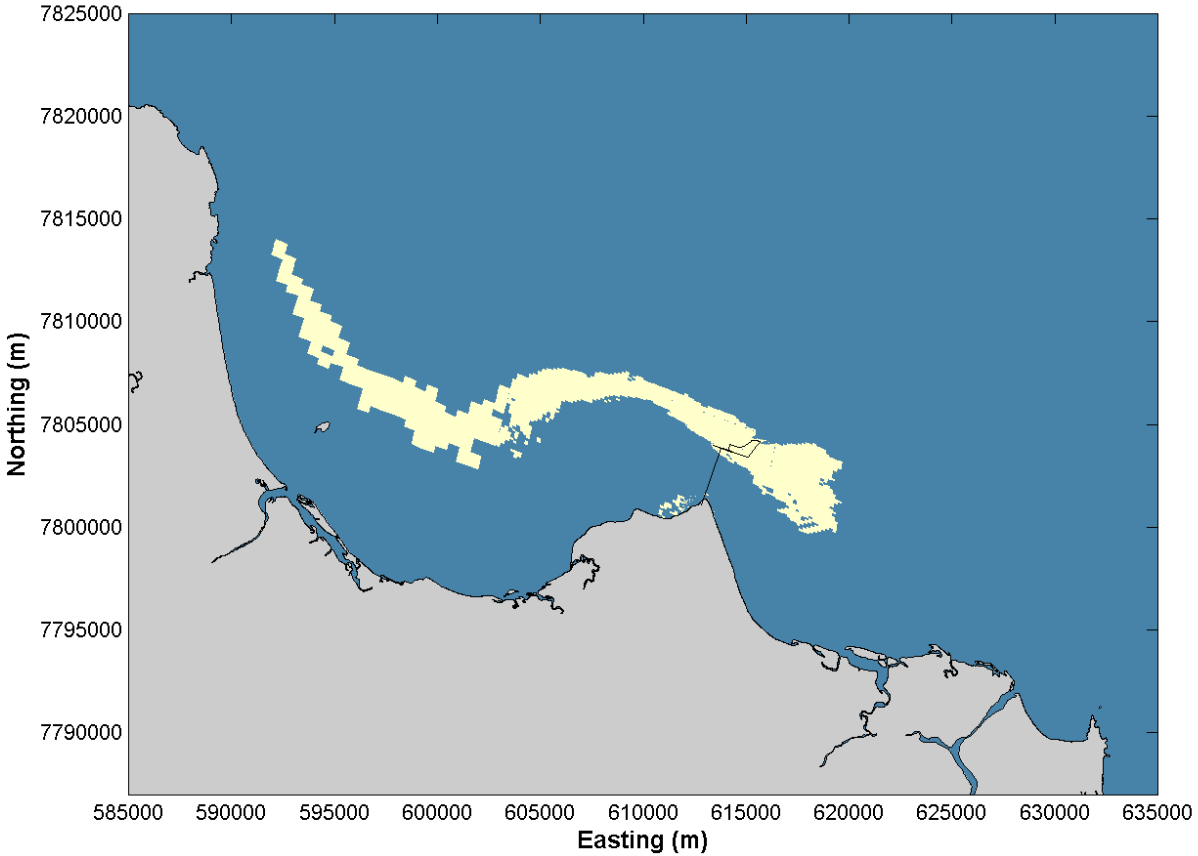

Figure 82 Area of influence for TSS for the dry season for the Neutral ENSO year (2007).

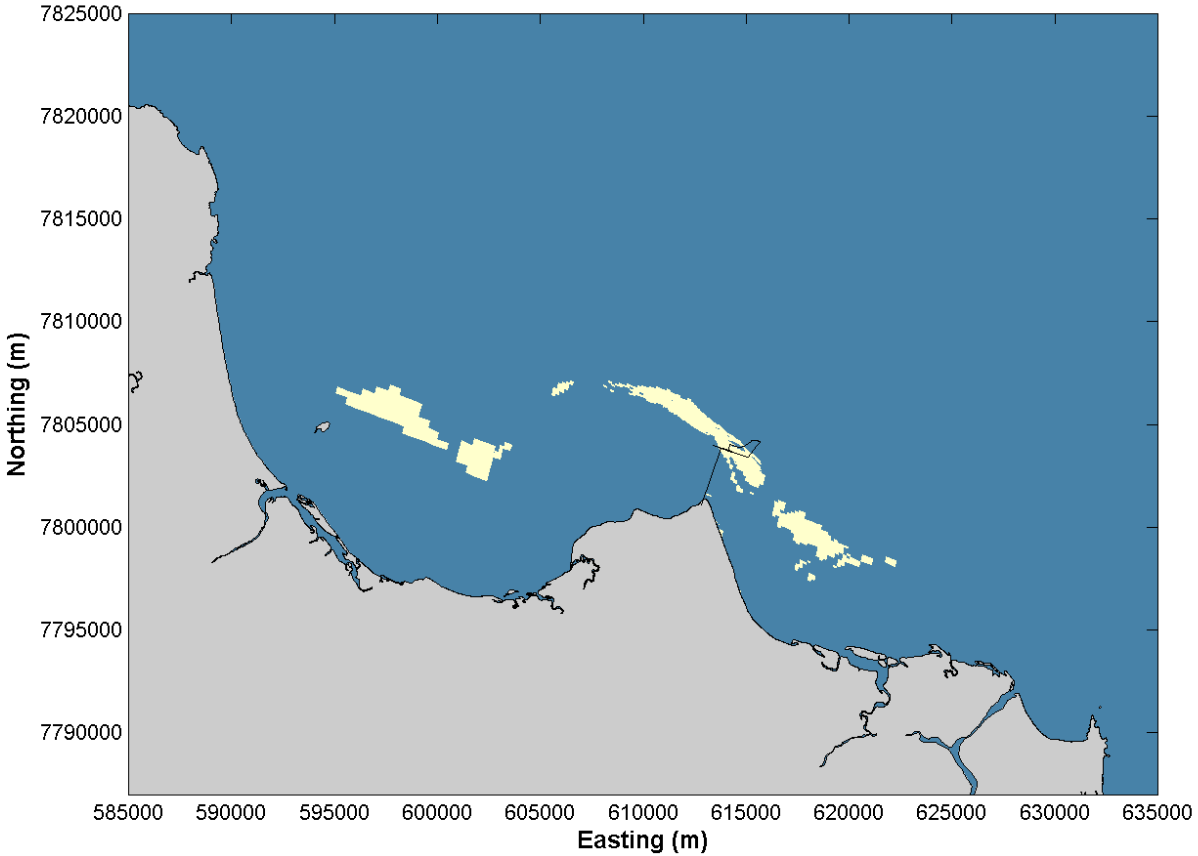

Figure 83 Area of influence for TSS for the wet season for the La Nina year (2011).

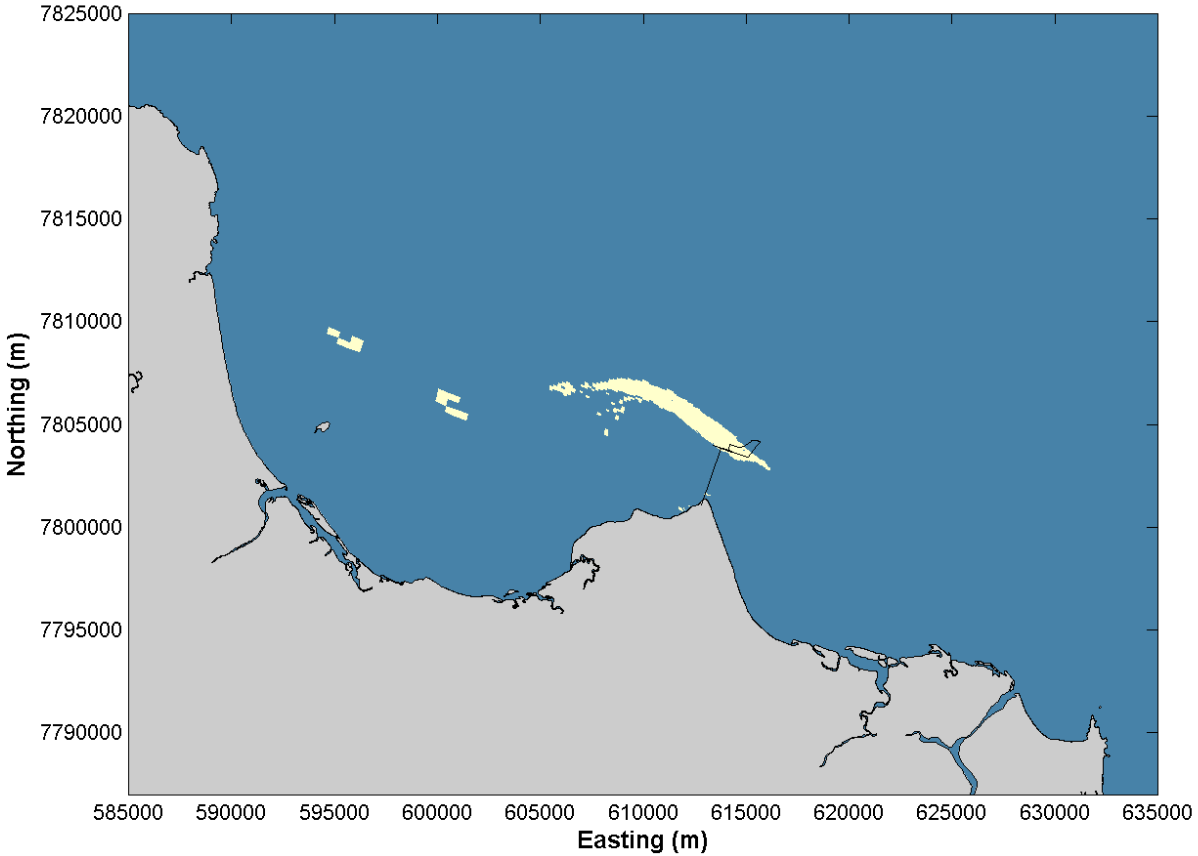

Figure 84 Area of influence for TSS for the dry season for the La Nina year (2011).

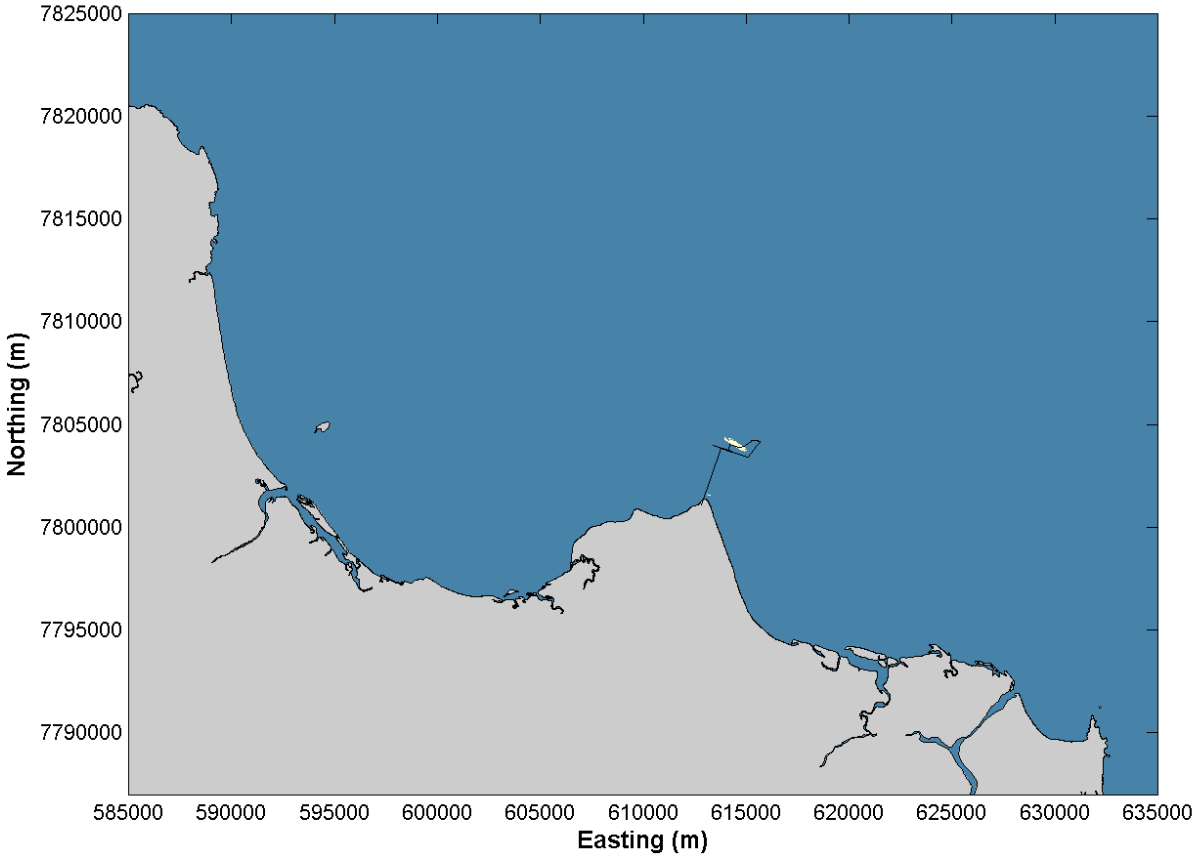

Figure 85 Median zone of moderate impact for TSS for the wet season for all years.

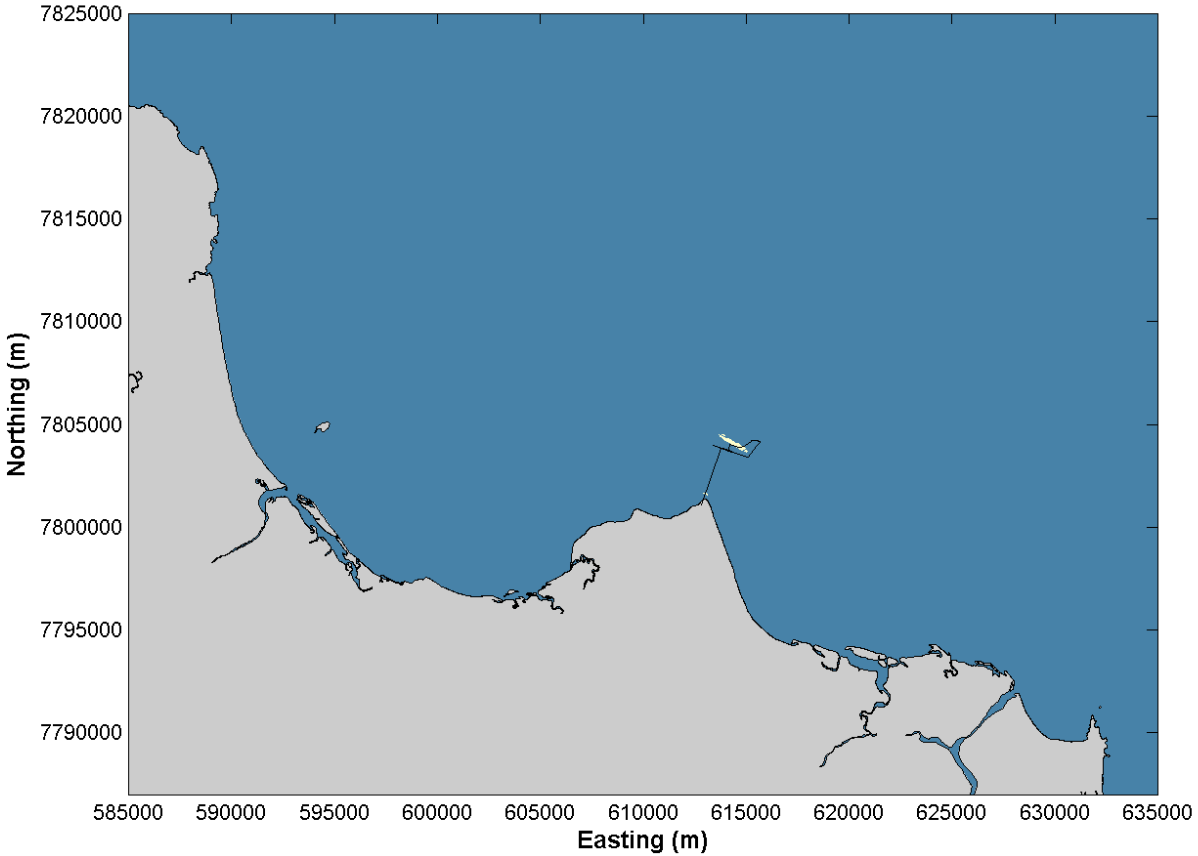

Figure 86 Median zone of moderate impact for TSS for the dry season for all years.

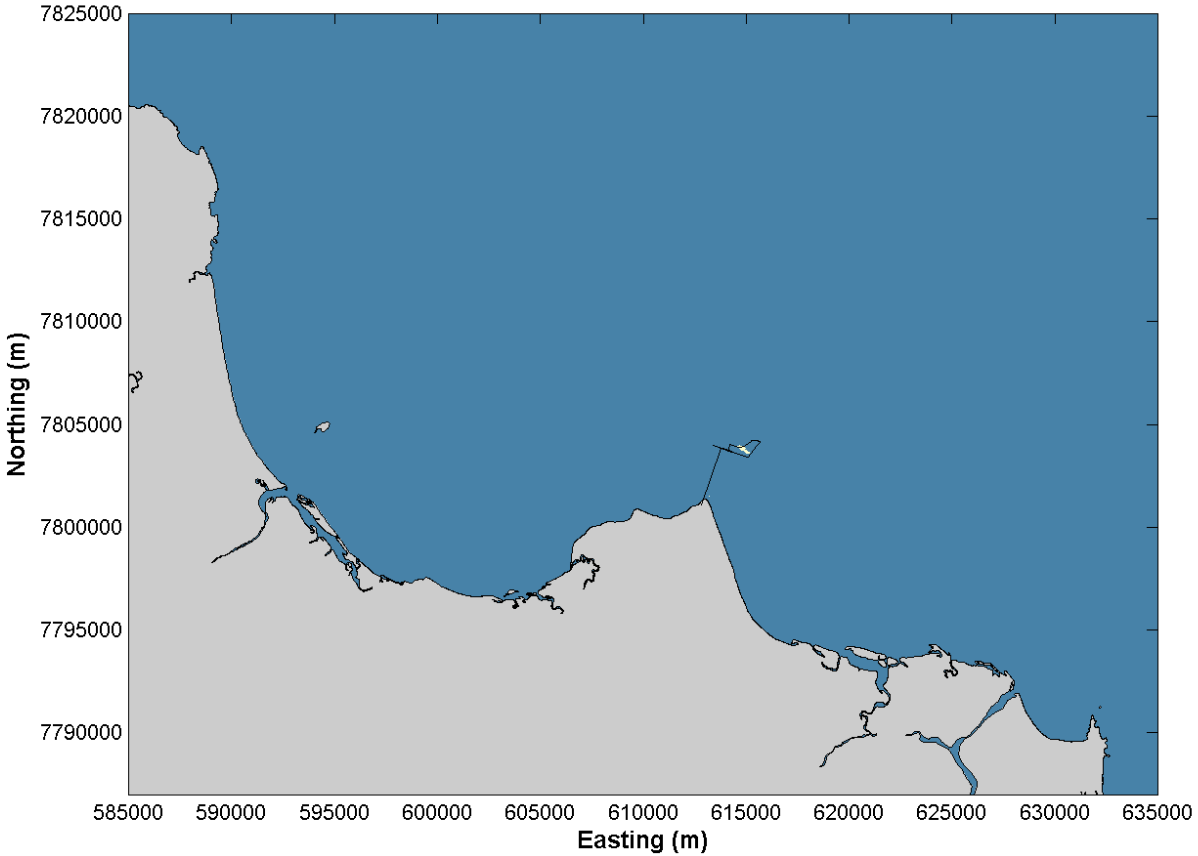

Figure 87 95th percentile zone of moderate impact for TSS for the wet season for all years.

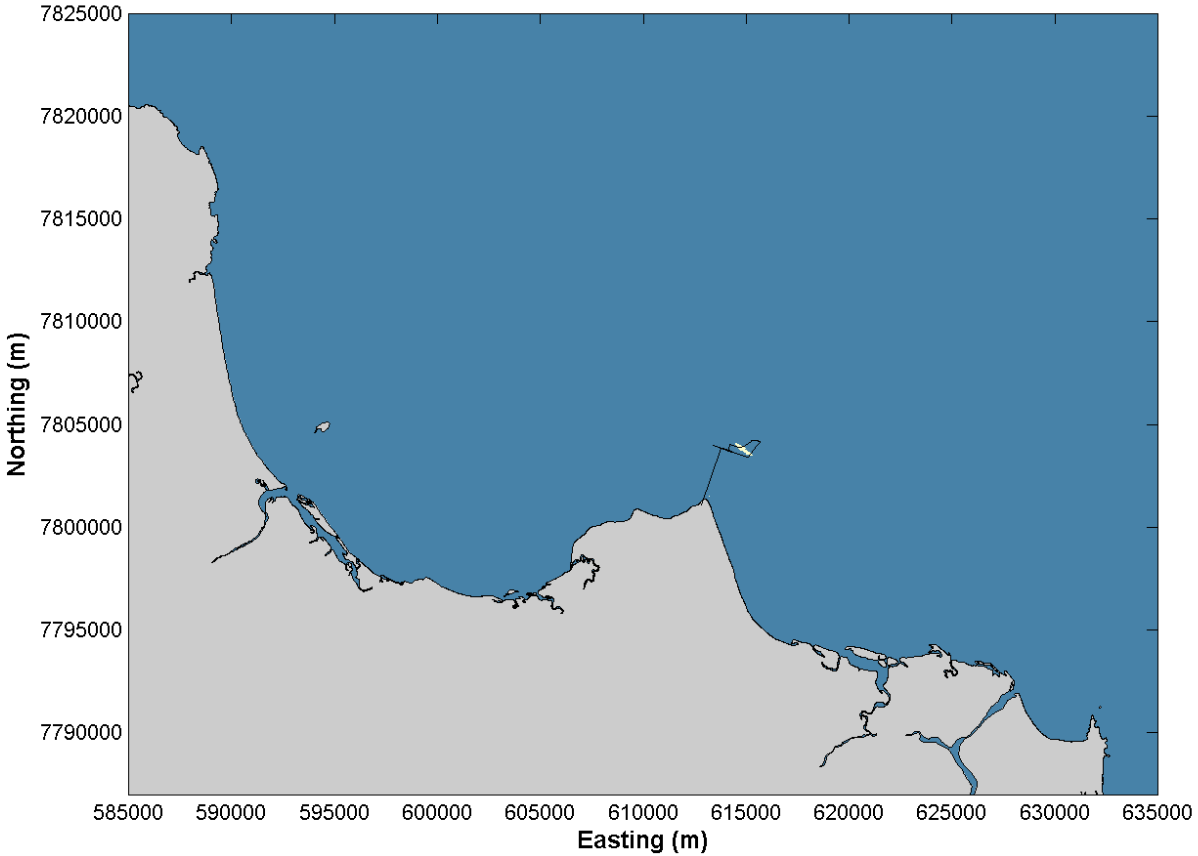

Figure 88 95th percentile zone of moderate impact for TSS for the dry season for all years.

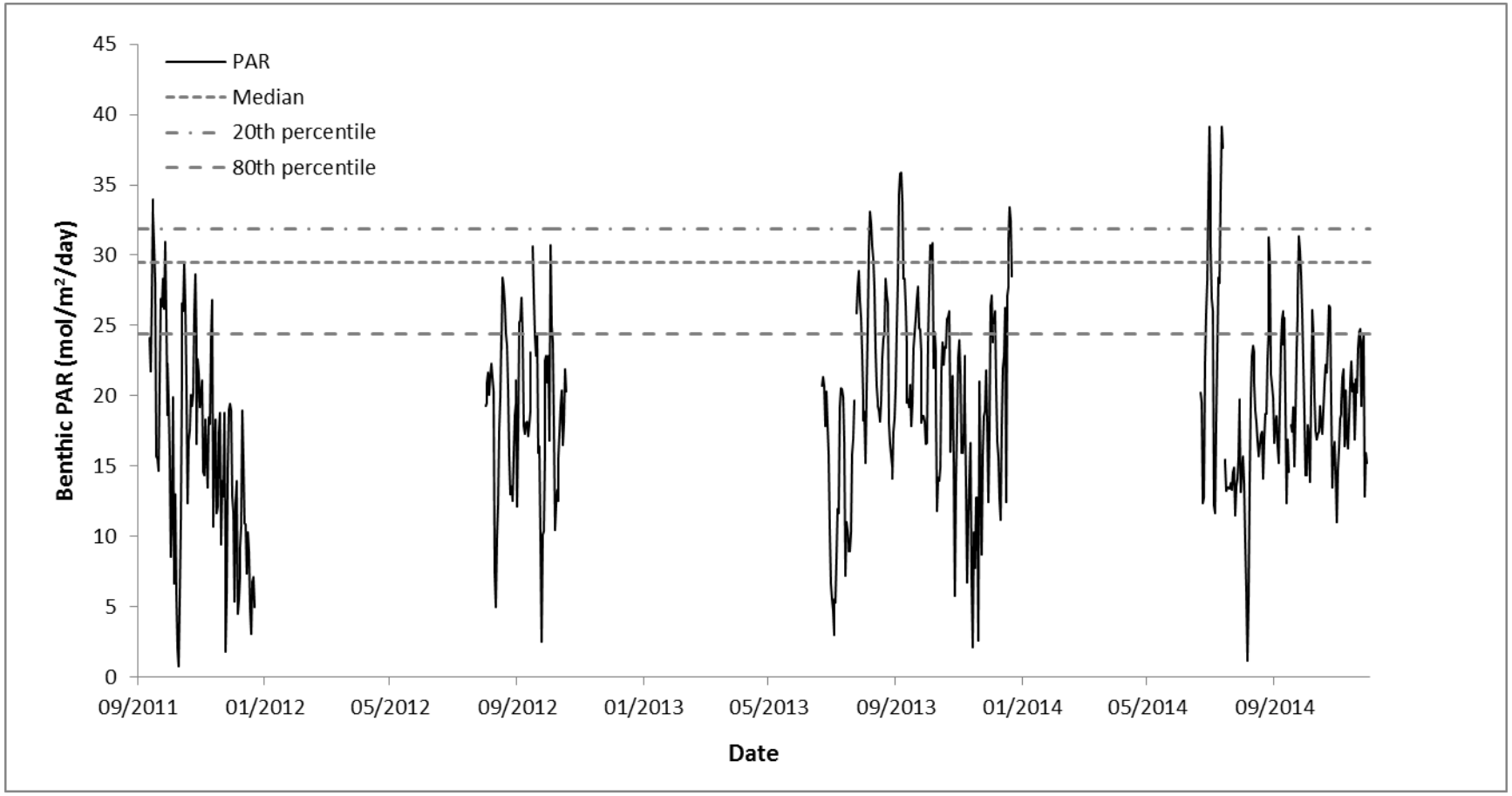

Figure 89 Comparison of measured daily benthic PAR at Nearshore Site 3 (see McKenna et al. (2015) for locations) during the growing season with statistical representations of k_d used to calculate daily benthic PAR.

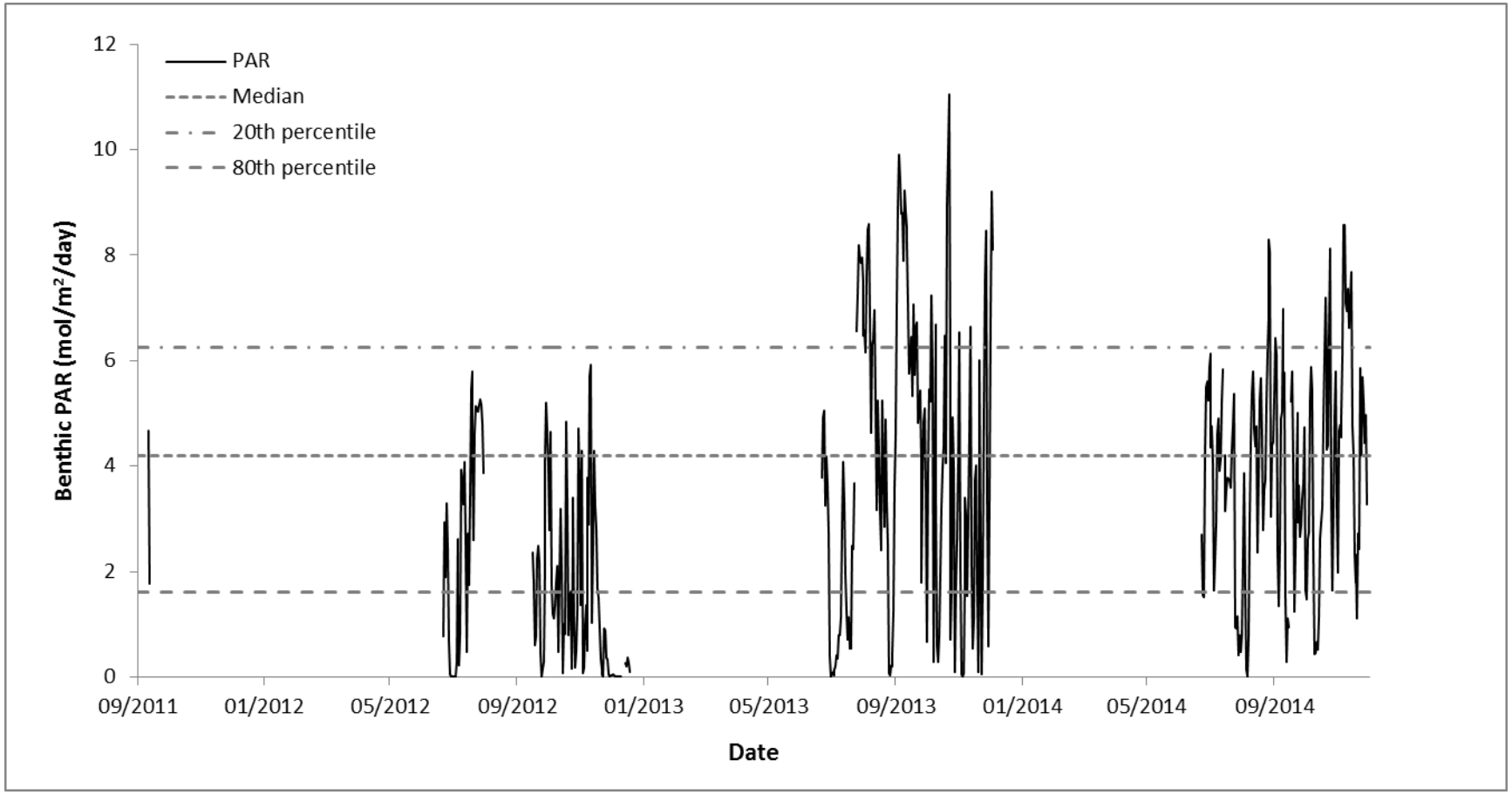

Figure 90 Comparison of measured daily benthic PAR at Nearshore Site 7 (see McKenna et al. (2015) for locations) during the growing season with statistical representations of k_d used to calculate daily benthic PAR.

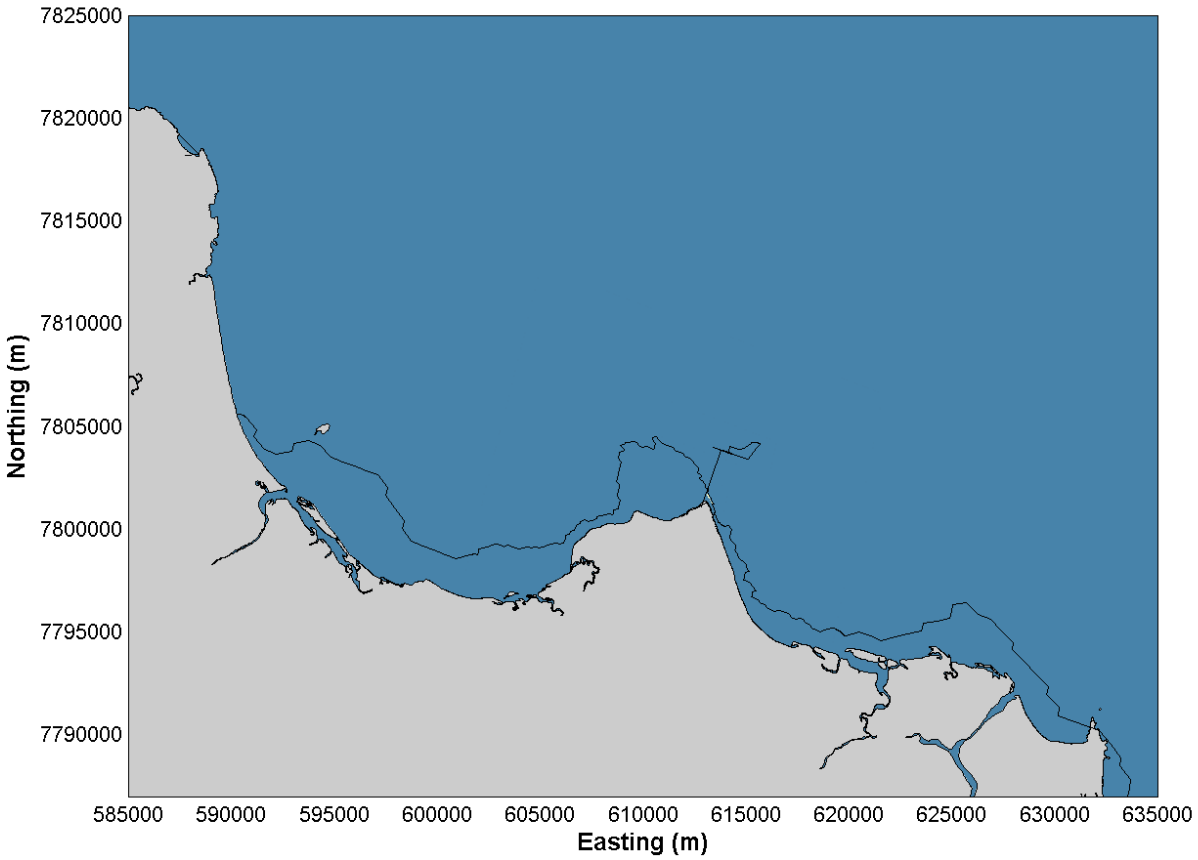

Figure 91 Benthic PAR threshold exceedance for nearshore seagrass species during the growing season for an El Nino year (1997), showing baseline exceedance (black contour) and the difference resulting from the dredging activity (cream areas). Note: only a small difference occurs at the approximate return water discharge location.

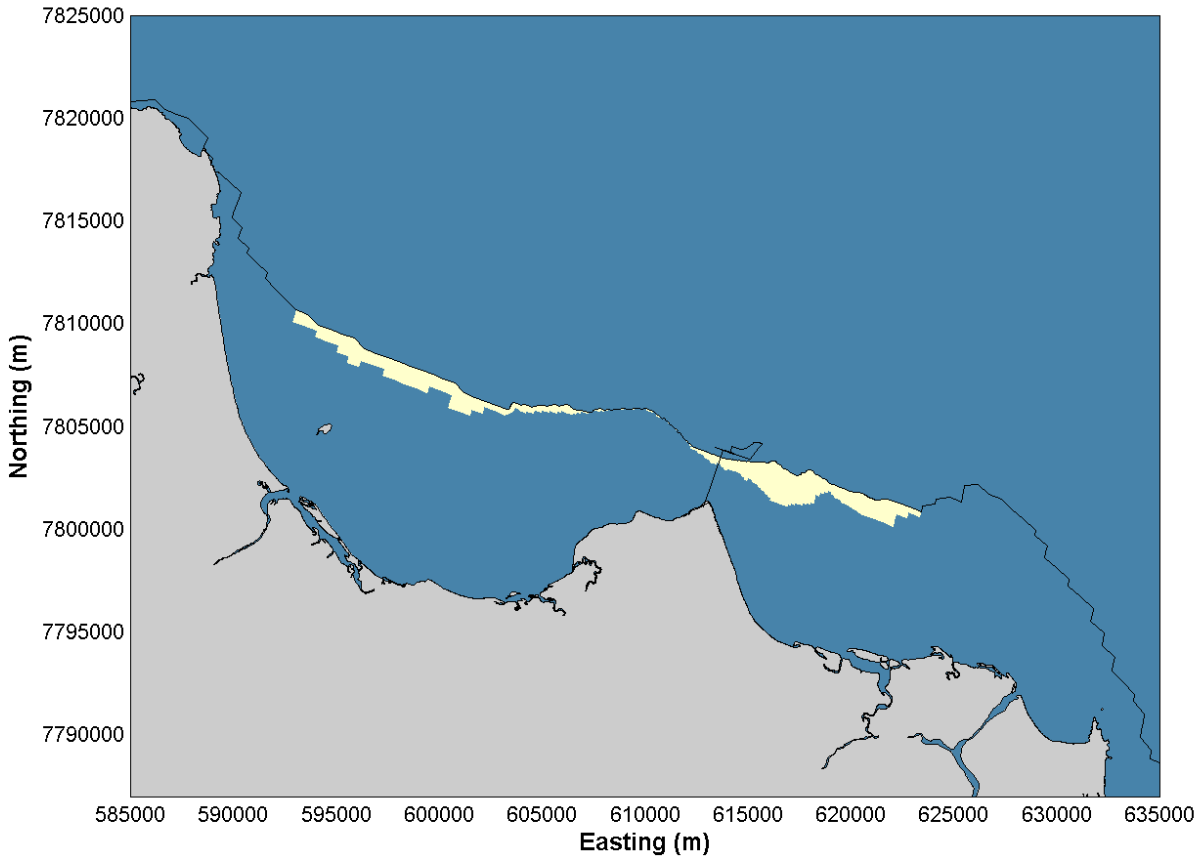

Figure 92 Benthic PAR threshold exceedance for offshore seagrass species during the growing season for an El Nino year (1997), showing baseline exceedance (black contour) and the difference resulting from the dredging activity (cream areas).

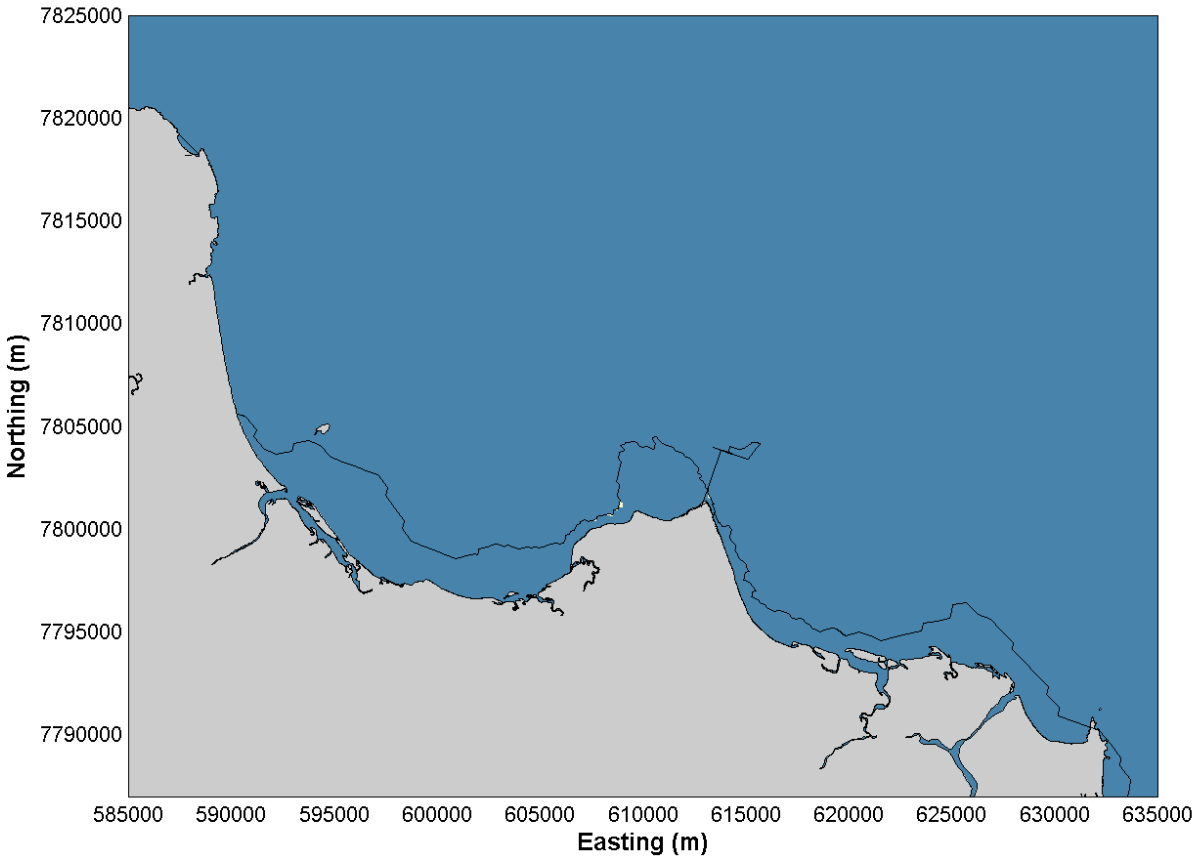

Figure 93 Benthic PAR threshold exceedance for nearshore seagrass species during the growing season for a Neutral ENSO year (2007), showing baseline exceedance (black contour) and the difference resulting from the dredging activity (cream areas).

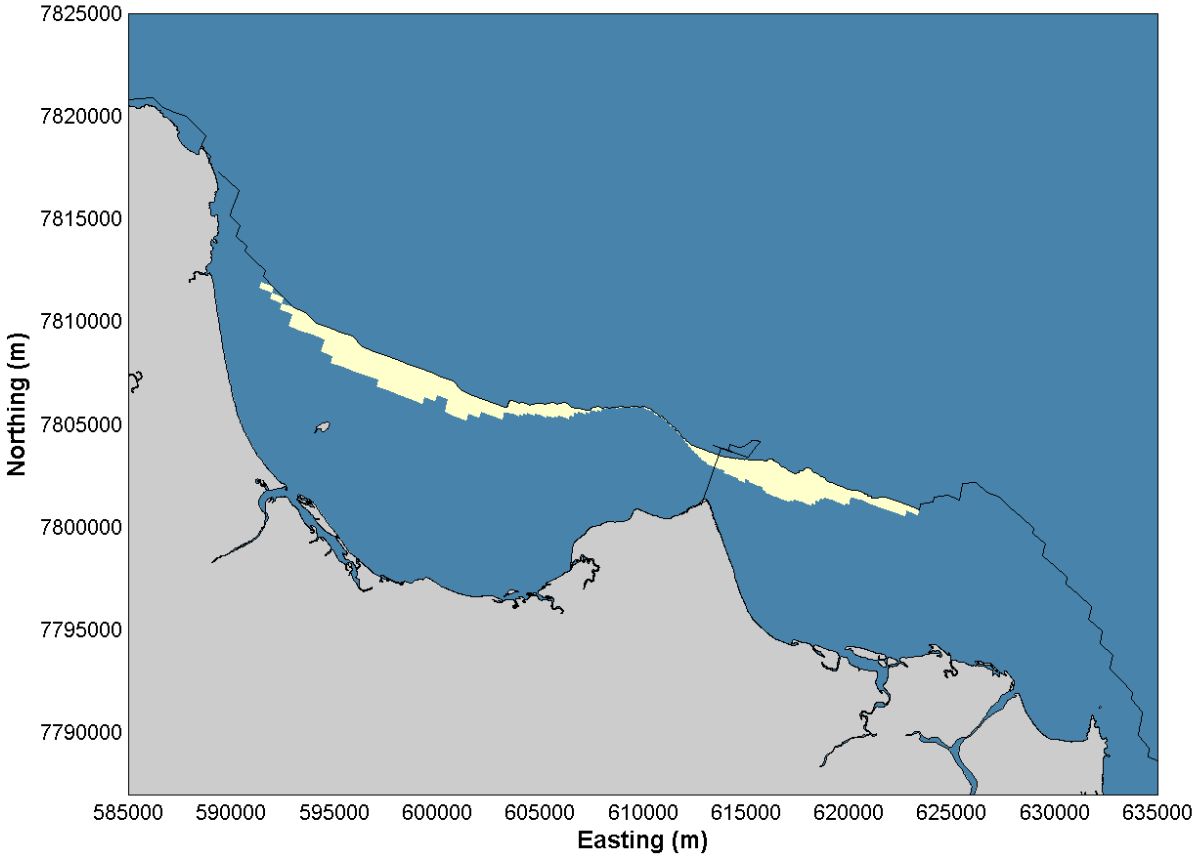

Figure 94 Benthic PAR threshold exceedance for offshore seagrass species during the growing season for a Neutral ENSO year (2007), showing baseline exceedance (black contour) and the difference resulting from the dredging activity (cream areas).

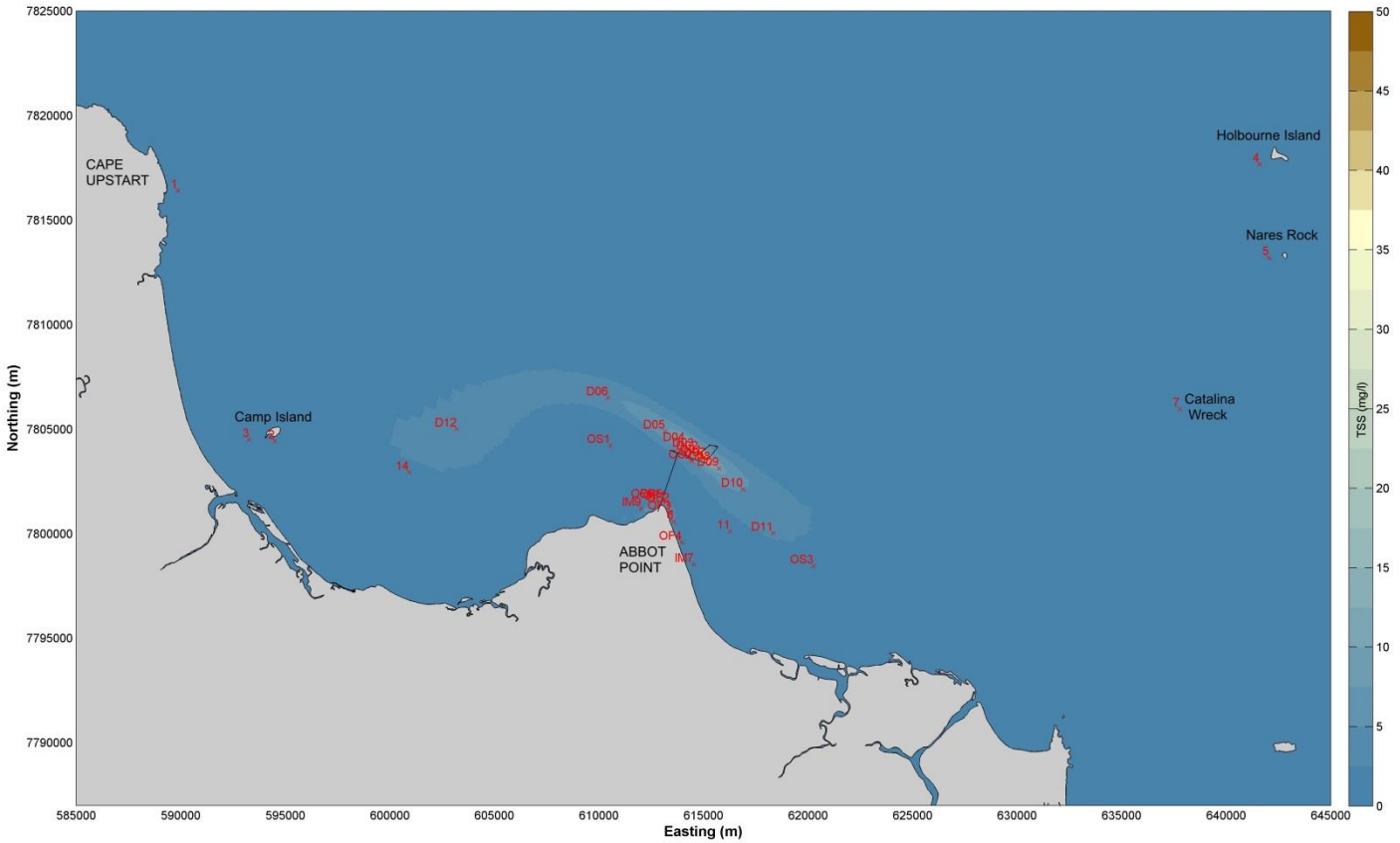

Figure 95 Time series output locations superimposed on the Neutral year average 95th percentile TSS.

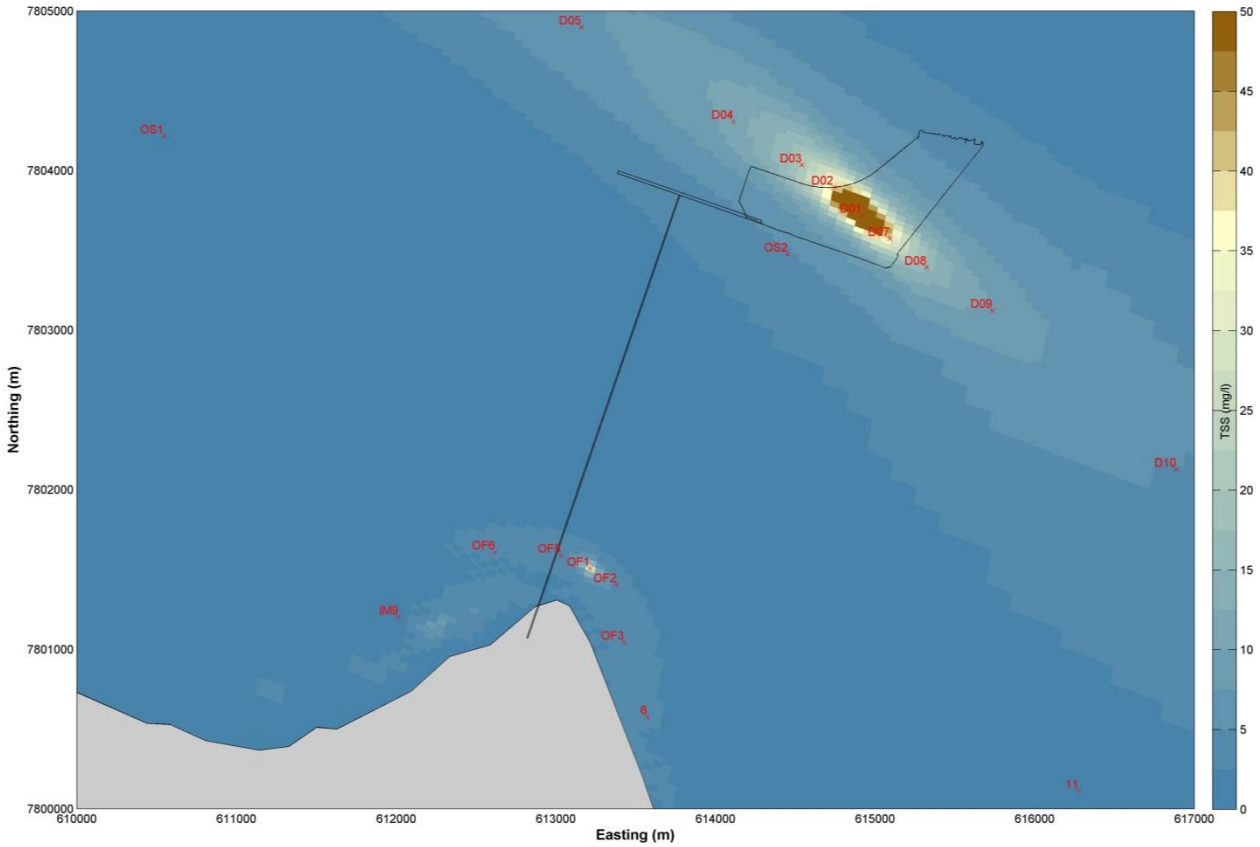

Figure 96 Time series output locations zoomed in to the dredging area (D01) and discharge location (OF1) superimposed on the all year average 95th percentile TSS.

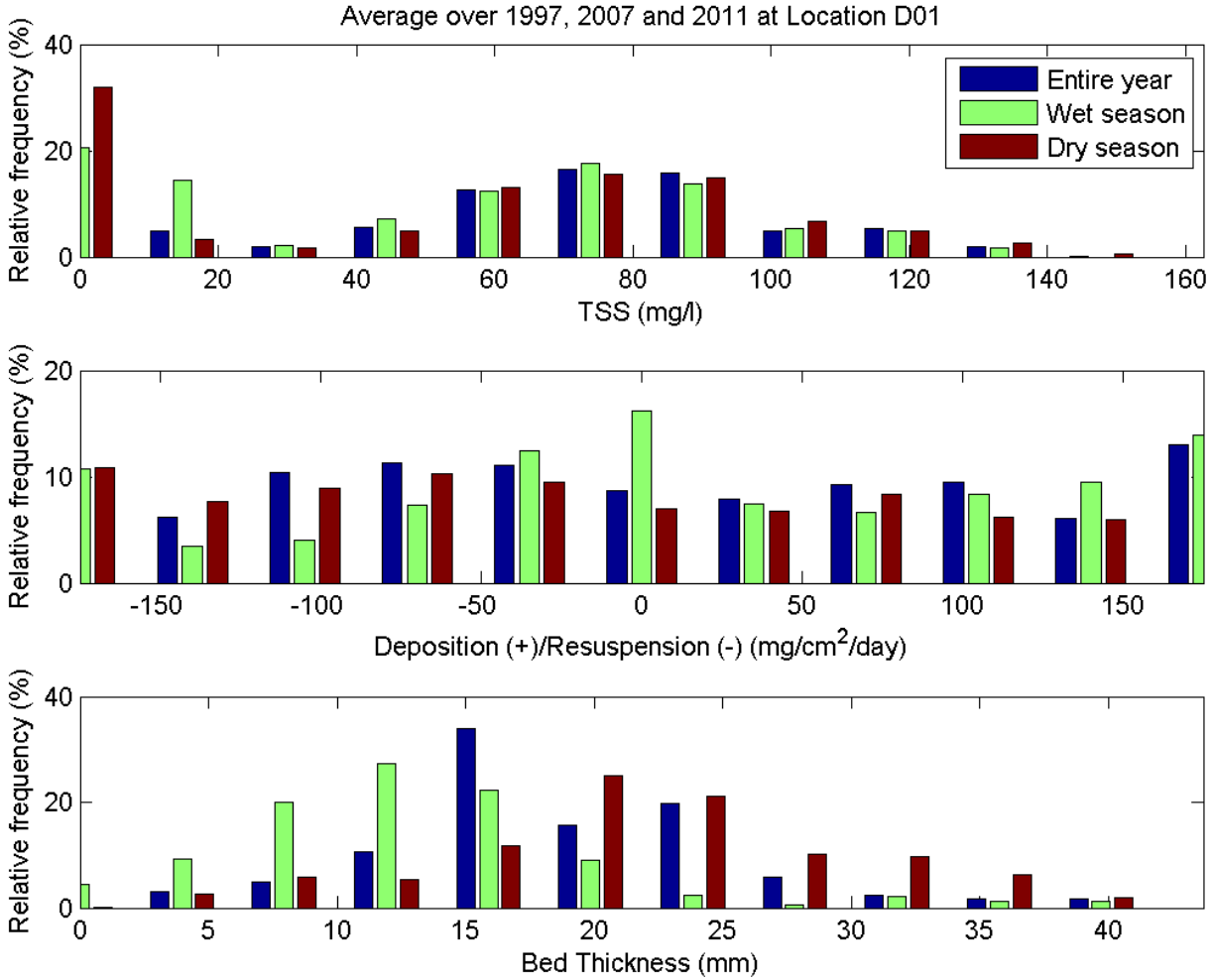

Figure 97 Histogram of TSS, deposition/resuspension and bed thickness for all simulations at site D01.

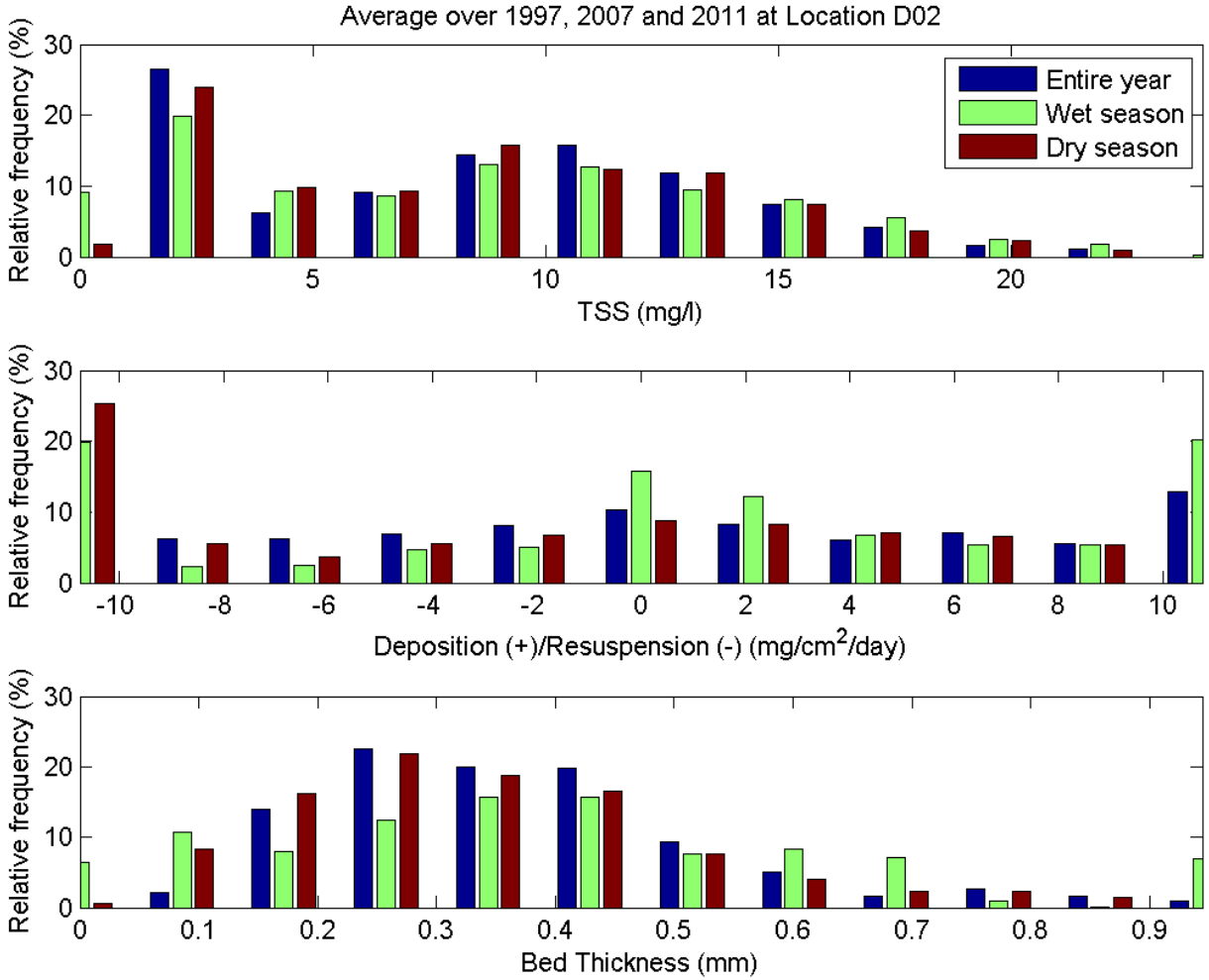

Figure 98 Histogram of TSS, deposition/resuspension and bed thickness for all simulations at site D02.

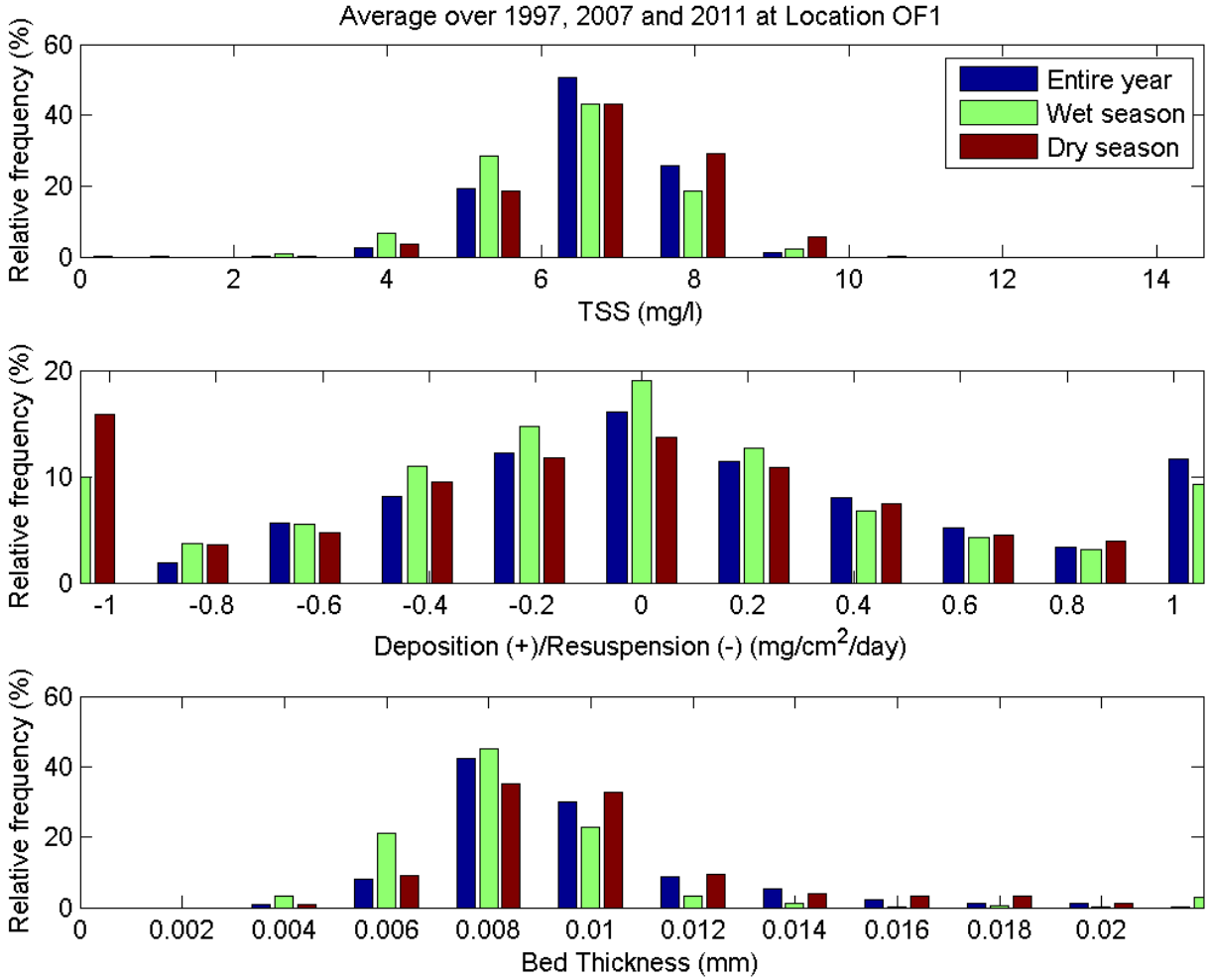

Figure 99 Histogram of TSS, deposition/resuspension and bed thickness for all simulations at site OF1.

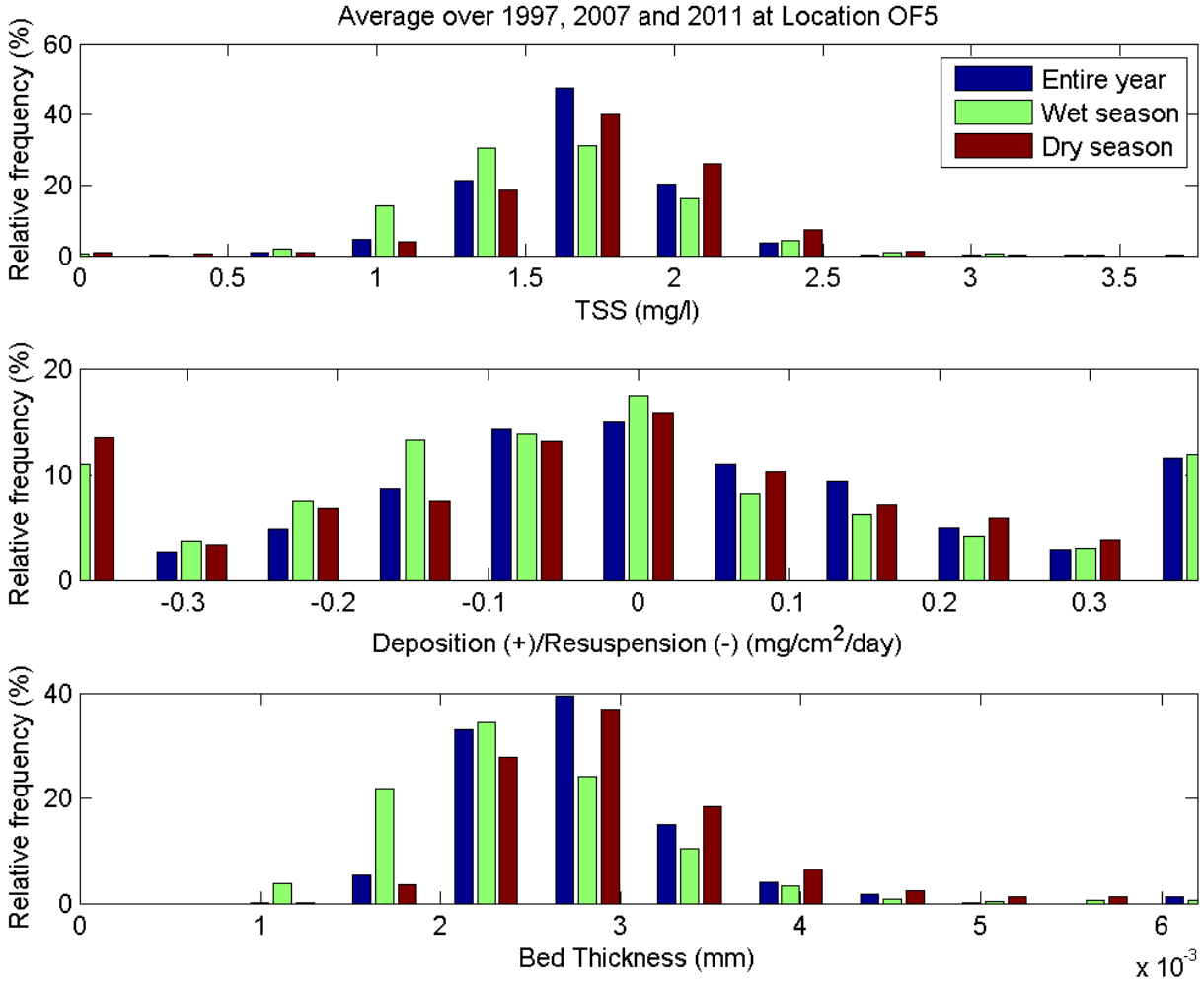

Figure 100 Histogram of TSS, deposition/resuspension and bed thickness for all simulations at site OF5.

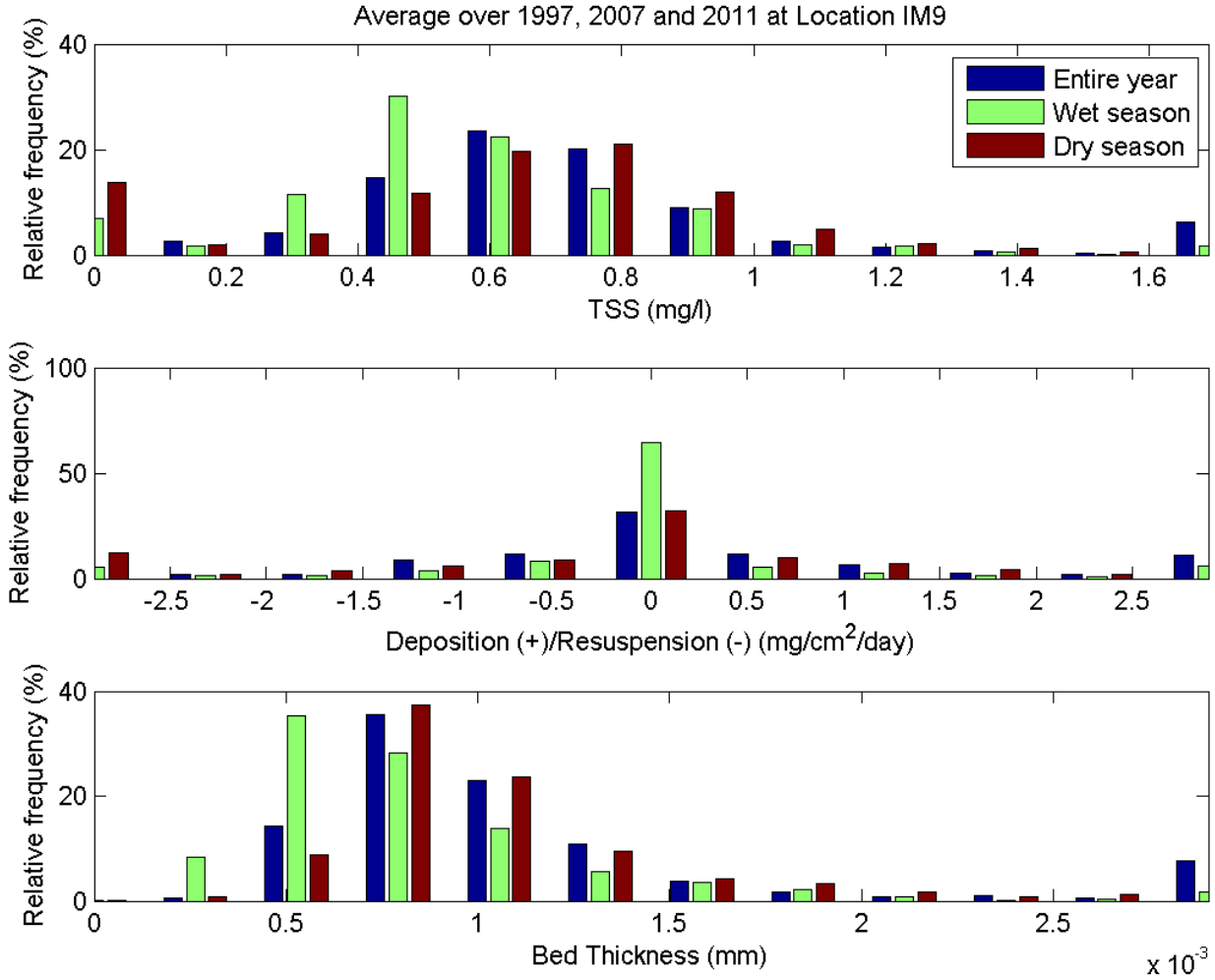

Figure 101 Histogram of TSS, deposition/resuspension and bed thickness for all simulations at site IM9.

7 CONCLUSIONS

This report has detailed a numerical modelling assessment for the proposed dredging and return water discharge associated with the onshore placement of dredging material.

The assessment applied a stochastic approach for the modelling of sediment plumes and as such is considered to be leading practise. This approach takes into account the inter-annual and seasonal variability in metocean conditions for modelling the dispersion of material during the relocation activity, significantly increasing the confidence in the modelling and reducing risk of the dredging material behaving in an unpredicted manner. In addition, the model verification process undertaken as part of this assessment has successfully demonstrated that the model can accurately represent the regional scale GBR Lagoon circulation processes.

The size of the dredge vessel that will undertake the T0 dredging is not known at this stage, although it is likely that it will be either a large or medium sized dredger. As such, sensitivity testing was undertaken to determine the difference between using a large and medium sized dredge vessel. The dredging duration is considerably longer when using a medium sized vessel compared to a large vessel, with total dredging durations ranging from 13 weeks to approximately 6 weeks, respectively.

The shorter dredging duration was found to result in increased TSS concentration impacts compared to the longer dredging duration, although the impacts lasted for a shorter duration of 6 weeks compared to 13 weeks for the longer dredging duration. Both dredging durations were found to show similar impacts in terms of sedimentation rates and impacts to benthic PAR. Therefore, adopting the large dredge vessel with a shorter dredging duration of approximately 6 weeks for the stochastic modelling represents the worst case scenario in terms of the intensity and extent of potential impacts. As a result, the modelling detailed in this report has been based on the larger dredge vessel with a dredging duration of approximately 6 weeks.

Instantaneous TSS plots have been presented at weekly intervals from the simulation which was shown to result in the largest extent and highest TSS concentration in the 95th percentile TSS plots. The plots showed that over time the plume in the surface layer of the model varies spatially with TSS concentrations less than 10 mg/L except for directly adjacent to the dredging area. It is unlikely that such low surface layer TSS concentrations would result in a clearly defined visual plume.

The stochastic modelling undertaken as part of this assessment has shown the following:

- Suspended sediment released by the dredging activity is transported from the dredging area in a north-west and south-east direction due to the influence of Clark Shoal on the current directions. The residual transport is to the north-west due to the dominant south-easterly winds;
- Suspended sediment released at the discharge location is transported in both a south-westerly and south-easterly direction, with residual transport to the south-west;
- The sediment suspended at the dredging area and at the discharge location do not interact, with the areas with increased total suspended solids (TSS) due to these activities remaining in separately identifiable plumes;

- The area where the background TSS has the potential to be increased by more than 5 mg/L due to the dredging activity and return water is relatively small. Based on the scenarios tested, the area where TSS can be increased by over 5 mg/L for more than 5 percent of the dredging duration can be up to 8.2 km in length and 1.2 km in width centred at the dredging location. The discharge location only results in a very small localised area where the TSS is greater than 5 mg/L, with the extent of this area being similar regardless of season or year;
- The modelling results show that the dredging activities and return water discharge have the potential to result in a relatively large area of influence based on the thresholds provided. However, it must be noted that the adopted thresholds of 2mg/L are low compared to the natural background TSS, as all seven of the water quality monitoring sites at Abbot Point had median TSS concentrations higher than 2 mg/L. The zone of moderate impact for TSS is restricted to the dredging area and the area immediately adjacent to the north-west up to 0.7 km from the dredging area. The return water results in a small zone of moderate impact immediately to the west of the discharge location;
- Deposition rates resulting from the dredging activities and return water discharge are relatively low, with the higher rates being limited to areas close to the dredging area and the discharge location;
- The dredging activities and return water discharge may result in localised zones of moderate impact to seagrasses due to reductions in daily benthic PAR caused by suspended sediment. The largest zones of moderate impact are indicated to occur west and south-east of the dredging and return water discharge locations during the growing season of the Neutral El Nino Southern Oscillation (ENSO) year, correlating with the largest area and highest TSS concentration shown by the 95th percentile TSS plots; and
- The TSS, deposition/resuspension and bed thickness are highest at the dredging location, with a significant reduction in all of these just 200 m away from the dredging area.

Comparison of the results of this modelling with the dredging plume results presented in the PER shows that the plume resulting from the dredging and onshore placement activities is smaller and less intense than for the dredging associated with the offshore disposal. This difference is because the mass of material released into the model as a result of the dredging activity for the onshore placement is significantly lower than in the offshore disposal modelling presented in the PER.

8 REFERENCES

DELFT3D-WAQ Water Quality Manual, 2013. Water Quality. Processes library description. Technical Reference Manual.

Department of State Development (DSD), 2015. Referral of proposed action: Abbot Point Growth Gateway Project.

GBRMPA, 2010. Water quality guidelines for the Great Barrier Reef Marine Park. Revised Edition 2010.

GBRMPA, 2012. Guidelines: The use of hydrodynamic numerical modelling for dredging projects in the Great Barrier Reef Marine Park. August 2012.

GHD, 2009. North Queensland Bulk Ports Corporation Limited, Report on Proposed Abbot Point Multi Cargo Facility, Hydrodynamic and Sediment Transport Modelling.

GHD, 2012. Abbot Point Terminals 0, 2 and 3 Capital Dredging Project. Public Environmental Report. Appendix H1: GHD 2012, Hydrodynamic and Sediment Transport Analysis Report.

INPEX, 2013. Dredging and spoil disposal management plan – east arm. Document No.: C075-AH-PLN-0028. December 2013.

Krone, R., 1962. Flume studies of transport of sediment in estuarial shoaling processes (Final report). Tech. rep., University of California, Hydraulics Engineering and Sanitary Engineering Laboratory, Berkeley, USA. 224, 227, 232, 373

McKenna, S.A., Chartrand, K.M., Jarvis, J.C., Carter, A.B., Davies, J.N. and Rasheed, M.A., 2015. Port of Abbot Point: Initial light thresholds for modelling impacts to seagrass from the Abbot Point Growth Gateway Project. TropWATER Report No. 15/23, May 2015.

Morton, R., Kettle, B., Jones, A. and Stump, R., 2014. Dredging by Queensland Ports – needs, methods and environmental effects. Report to Queensland Ports Association, Brisbane, Australia, 104pp.

Partheniades, E., 1962. A study of erosion and deposition of cohesive soils in salt water. Ph.D. thesis, University of California, Berkeley, USA. 182 p. 224, 228, 373

Partheniades, E., 1965. Erosion and deposition of cohesive soils, Journal of the Hydraulic Division, Vol. 91, No.1, S.105 – 139.

PDMC, 2014. Technical memorandum Abbot Point, dredge materials. November 2014.

SMEC, 2012. Abbot Point Water Quality Assessment: T0, T2 and T3. for: North Queensland Bulk Ports Corporation. July 6th 2012.

Tolhurst, T.J., Black, K.S. and Paterson, D.M., 2009. Muddy sediment erosion: Insight from Field Studies. J. Hydraul. Eng. 2009.135:73-87.

Van Rijn, L.C., 1993. Principles of sediment transport in rivers, estuaries and coastal seas. Aqua Publications, Amsterdam.

Winterwerp, J. and W. van Kesteren, 2004. Introduction to the physics of cohesive sediments in the marine environment. Developments in Sedimentology, 56.

WorleyParsons, 2014. Baseline Abbot Point Water Quality Report. Abbot Point Dredging and Onshore Placement of Dredged Material Project. Report prepared for NQBP.

WorleyParsons, 2015. Marine Ecology Technical Report, Abbot Point Growth Gateway Project. Report prepared for Department of State Development.

APPENDIX A
Representation of Regional Circulation

Technical Note

To	:	Dr Richard Brinkman (AIMS)
From	:	Andrew Symonds, Dan Messiter
Cc	:	Paul Doyle (NQBP)
Date	:	20/06/2014
Subject	**:**	**Abbot Point DSAP Modelling: GBR Lagoon Residual Circulation Representation**

Introduction

This technical note describes the proposed approach for representing the regional scale ocean circulation, which occurs within the Great Barrier Reef (GBR) Lagoon, in the Royal HaskoningDHV (RHDHV) Abbot Point numerical model. Possible approaches have been discussed previously with Dr Richard Brinkman, who is advising GBRMPA in terms of the numerical modelling. One of the approaches which Dr Brinkman suggested applying was superimposing a residual water level slope onto the astronomical tidal boundary as a way of representing the regional GBR Lagoon scale circulation. Results from this approach are presented here and demonstrate that it is valid and can realistically represent the circulation. This note provides details of the approach and its results as it was agreed that the final proposed approach would be run by Dr Brinkman again prior to the modelling commencing.

The purpose of this technical note is to:

- detail the proposed approach for representing regional scale circulation; and
- demonstrate the proposed approach provides realistic current speeds and directions in the RHDHV Abbot Point model.

Event Identification

Initially it was necessary to determine what processes the RHDHV local scale numerical model was not able to reproduce by applying typical model forcing parameters. Periods when atypical residual processes occurred were identified and methods to represent these were investigated through more sophisticated model forcing.

The typical model forcing investigation involved running the numerical model with just astronomical tidal forcing and then with astronomical tidal and local wind forcing for all periods with available measured data at Abbot Point:

- 11/07/2008 to 14/11/2008 - measured current data available at three nearshore sites (only two sites simultaneously), located to the east and west of the existing Abbot Point jetty (**Figure 1**); and
- 20/12/2013 to ongoing - measured current data available at three offshore sites (only two sites simultaneously), alternate disposal Sites 1 and 2 from December 2013 to mid-February 2014 and at alternate disposal Site 2 and the PER Site from mid-February 2014 onwards (**Figure 1**).

During periods of December 2013 and January 2014 the model was not able to replicate the measured currents at Sites 1 and 2 through astronomical and local wind forcing. For these two sites:

- **Figures 2** to **3** show measured currents and modelled currents as a result of astronomical tidal forcing; and
- **Figures 4** and **5** show measured currents and modelled currents as a result of astronomical tidal and local wind forcing.

Figures 2 to **5** show that from 24/12/2013 to 08/01/2014 and from 20/01/2014 to 26/01/2014 the model consistently under-predicts the measured current speed and is not able to represent the east to east-south-east dominance in the measured current directions.

To determine the influence of regional scale residual circulation patterns during these periods, data from the Integrated Marine Observing System (IMOS) were used. As part of the IMOS OceanCurrent dataset, maps showing sea level anomaly and geostrophic current velocity are available for the east coast of Queensland from 1993 to the present day. The maps use a combination of altimetry and tide gauge data to determine the spatial variability in both sea level anomaly and geostrophic currents. The IMOS maps show that the periods identified coincided with a strong residual circulation through the GBR Lagoon to the south-east (**Figures 6** and **7**). As a result of the circulation there was also a slope in sea level anomaly, with lower sea levels to the south.

Validation

The change in sea level anomaly over the approximate model extent (shown in **Figure 1**) was determined based on the IMOS maps for the periods when the model was not able to represent the measured currents. This slope in residual sea level was added to the existing astronomical tidal water level boundaries to create combined astronomical tide and residual sea level boundaries to drive the RHDHV numerical model. The model was then run using the combined boundary conditions along with local wind conditions. Accordingly, the model included astronomical tides, the regional GBR Lagoon circulation and the local winds.

The resultant output plots (**Figures 8** and **9**) show that by including a slope in residual sea level, determined based on the IMOS sea level anomaly maps, along with the existing astronomical tidal boundaries and local wind, the model can accurately represent current speeds and directions during periods when regional GBR Lagoon circulation occurs. Comparison of **Figures 8** and **9** with **Figures 2** to **5** demonstrates that each of the three driving forcing mechanisms can be important to ensure that the currents offshore Abbot Point are accurately represented by the RHDHV numerical model.

Table 1 provides a statistical summary of the differences between the modelled and measured current speeds and directions when different forcing is included in the RHDHV numerical model. The table highlights the significant improvement in the models ability to represent the measured current speeds and directions when all three types of forcing are included.

Table 1 Difference between modelled and measured current speeds at Site 2.

Current Parameter Assessed	RHDHV Model Forcing		
	Tide (**Figure 3**)	Tide + Wind (**Figure 5**)	Tide + Wind + Circulation (**Figure 9**)
Mean Ebb Current Speed Difference (modelled – measured)	0.00	-0.02	0.01
Mean Flood Current Speed Difference (modelled – measured)	-0.12	-0.09	-0.01
Percent Difference of Mean Modelled Ebb Current Speed Relative to Maximum Measured	-0.7	-4.6	1.5
Percent Difference of Mean Modelled Flood Current Speed Relative to Maximum Measured	-17.8	-13.5	-1.5
Ebb Current Speed RMS Error	0.09	0.07	0.05

Current Parameter Assessed	RHDHV Model Forcing		
	Tide (**Figure 3**)	Tide + Wind (**Figure 5**)	Tide + Wind + Circulation (**Figure 9**)
Flood Current Speed RMS Error	0.16	0.11	0.06
Mean Ebb Direction Difference (modelled – measured)	65	57	12
Mean Flood Direction Difference (modelled – measured)	-18	10	-2

Future Implementation

The preceding section demonstrated that the proposed approach to include regional GBR Lagoon circulation is suitable by validating the approach using measured tidal current data from within the RHDHV numerical model domain. However, to undertake the stochastic dredge plume dispersion modelling it will be necessary to represent the circulation without having any measured data for validation. Accordingly, the following application of the approach described above is proposed to include the circulation in stochastic modelling:

- results from the circulation validation period will be used to determine the relationship between the slope in residual sea level along the model boundaries and the resultant daily residual current within the model domain;
- a manual assessment of the regional GBR Lagoon circulation will be undertaken using the IMOS OceanCurrent maps for all periods that the model will be run;
- periods when the residual circulation is in a south-easterly direction (residual circulation in other directions can be replicated in the model through just astronomical tide and local wind forcing) will be identified and the change in sea level anomaly and the residual current speed over the approximate model domain will be recorded;
- the relationship from the circulation validation period will be used to ensure a suitable slope in residual sea level is applied to represent the residual current speed; and
- the final slope in residual sea level will be added to the existing astronomical tidal water level boundaries to create combined astronomical tide and residual sea level boundaries to drive the RHDHV numerical model in addition to local wind forcing over the model domain.

Summary

This technical note has outlined RHDHV's proposed approach for including the regional scale GBR Lagoon circulation in the RHDHV local scale numerical model. The approach has been validated using measured data from the proposed alternate disposal Sites 1 and 2. The validation demonstrates that the numerical model can accurately represent the regional scale circulation by using a slope in residual sea level along the model boundaries which is determined from the IMOS OceanCurrent data. The validation also demonstrates the relative importance of astronomical tides, local winds and the regional scale circulation on the currents at the proposed alternate disposal sites. Finally, an approach to include the regional scale circulation in the stochastic dredge plume modelling has been provided. Even though measured data is not available to further validate the model during these periods, information from the validation presented in this technical note can be used to ensure that the regional scale circulation is included in the model in a manner representative of realistic onsite conditions.

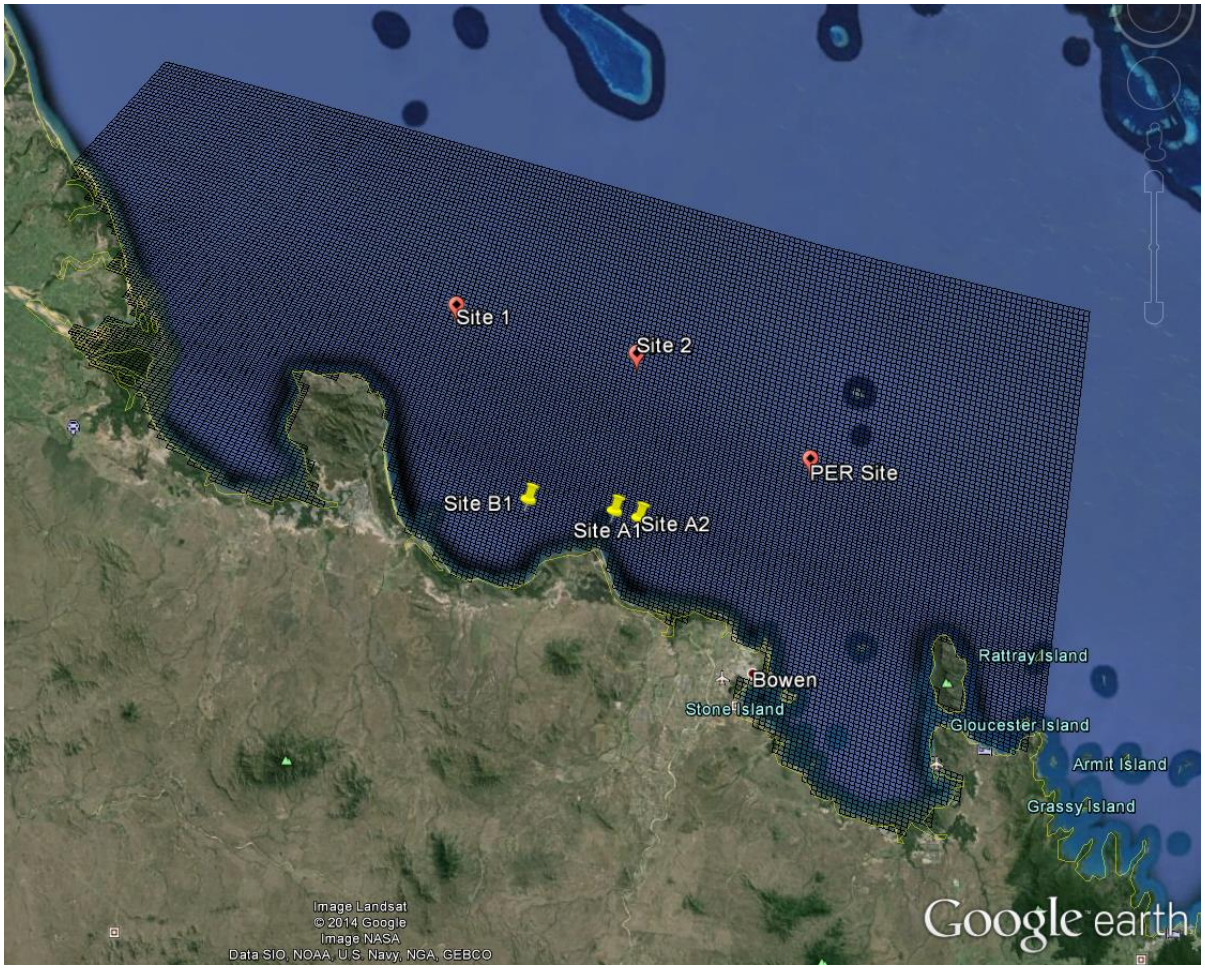

Figure 1 Extent of the RHDHV Abbot Point numerical model domain and locations of the ADCP data available within the model domain.

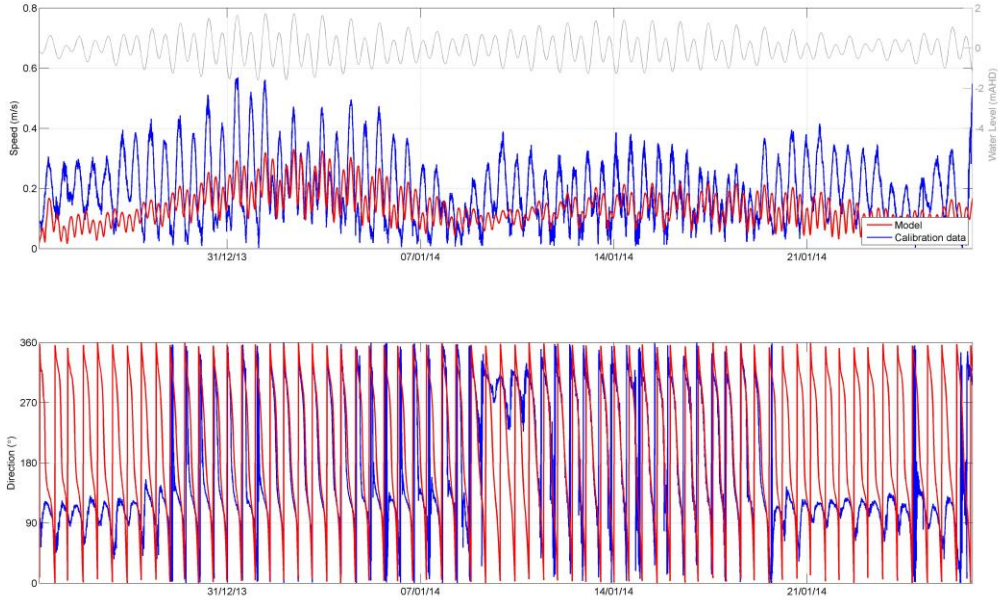

Figure 2 Site 1 measured (blue) and modelled (red) currents. Model forcing - astronomical tides.

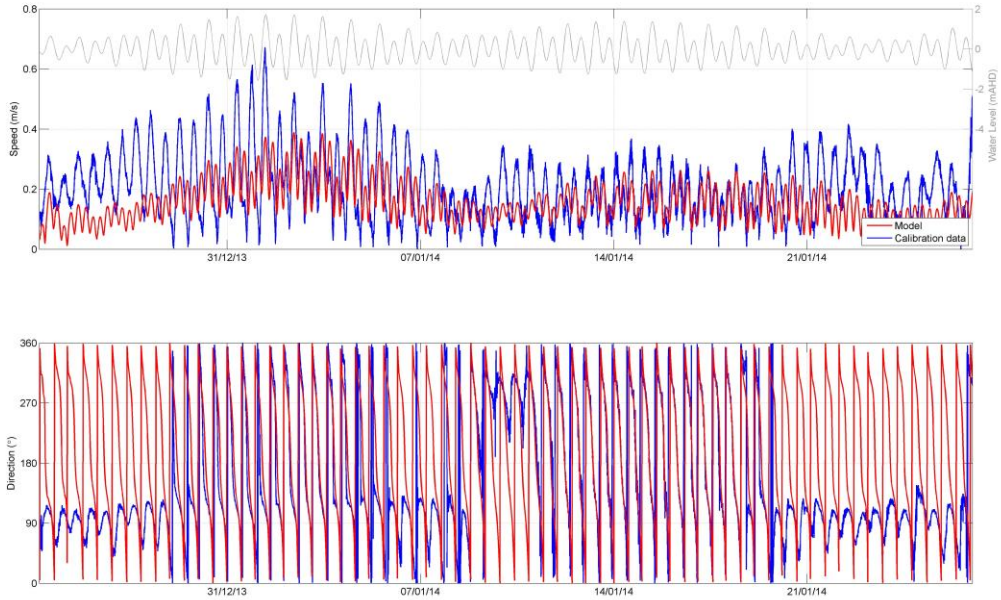

Figure 3 Site 2 measured (blue) and modelled (red) currents. Model forcing - astronomical tides.

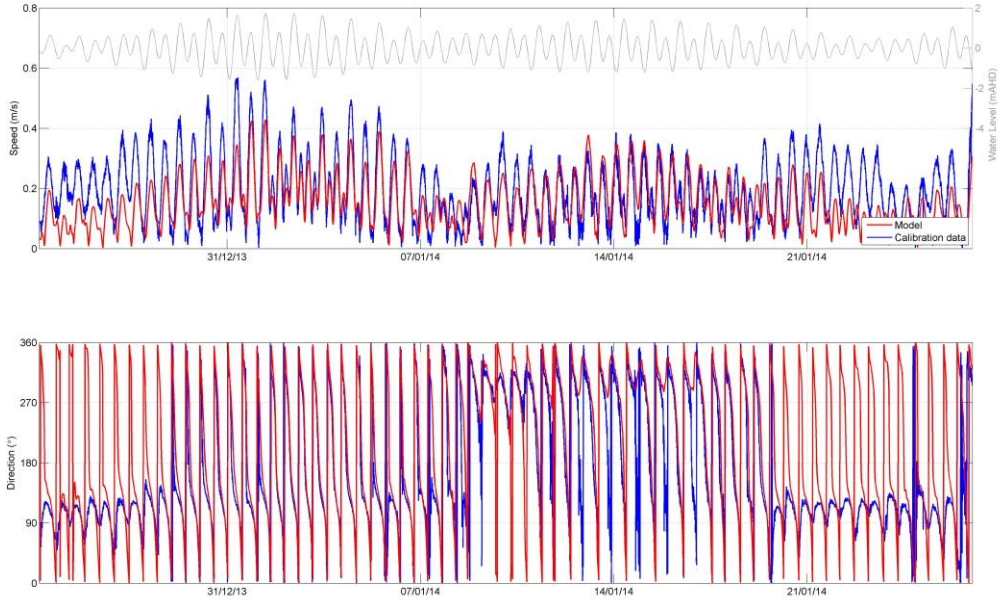

Figure 4 Site 1 measured (blue) and modelled (red) currents. Model forcing - astronomical tides and local wind.

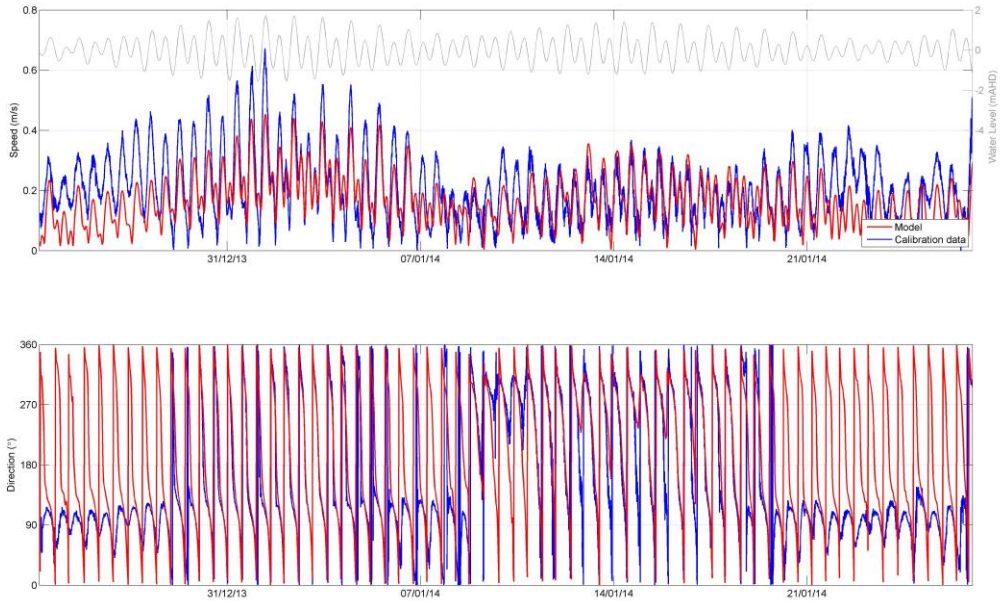

Figure 5 Site 2 measured (blue) and modelled (red) currents . Model forcing - astronomical tides and local wind.

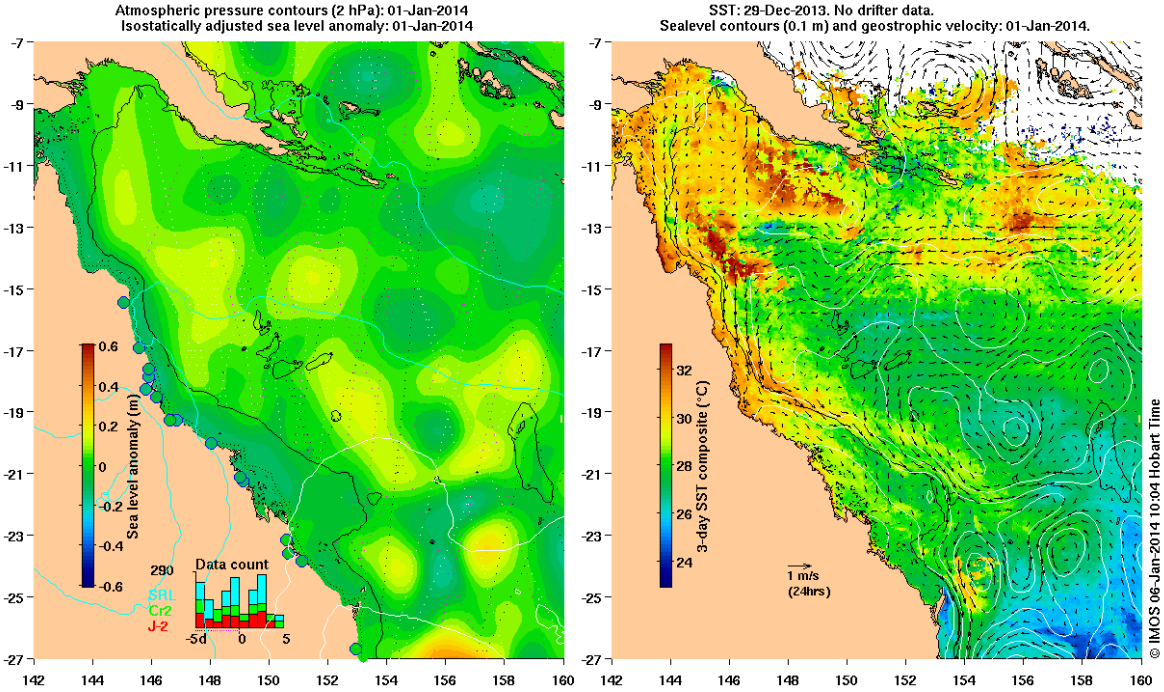

Figure 6 Sea level anomaly (left) and vectors showing geostrophic current velocity superimposed over sea surface temperature (right) on 01/01/2014. Source: http://oceancurrent.imos.org.au

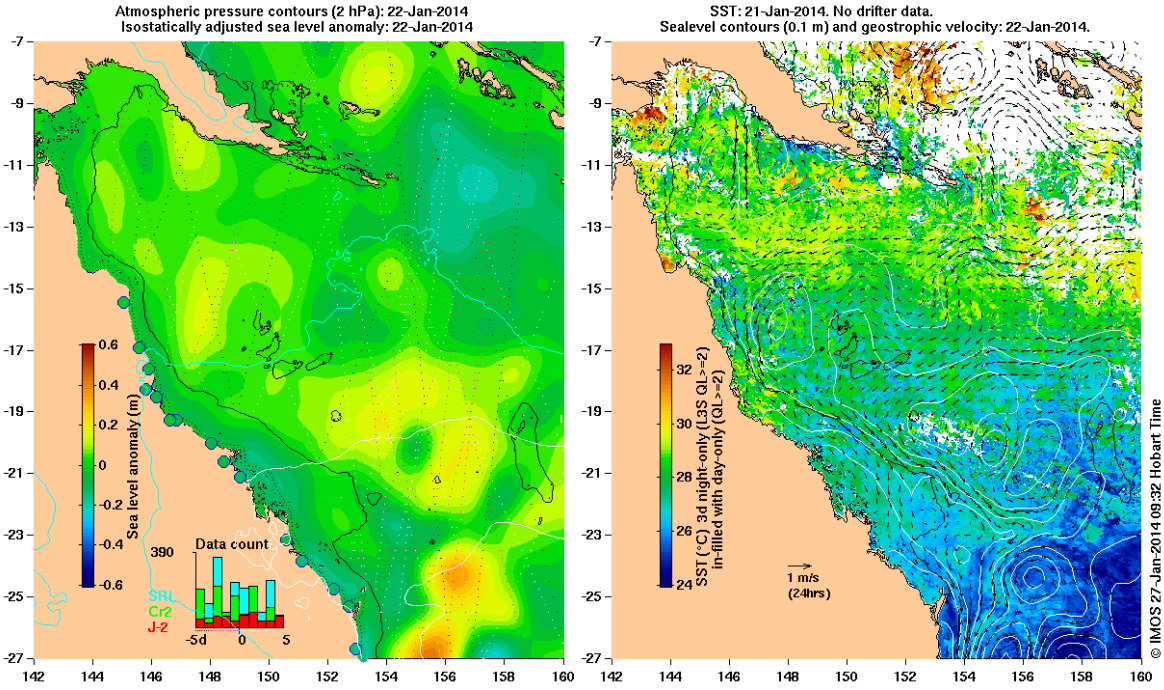

Figure 7 Sea level anomaly (left) and vectors showing geostrophic current velocity superimposed over sea surface temperature (right) on 22/01/2014. Source: http://oceancurrent.imos.org.au

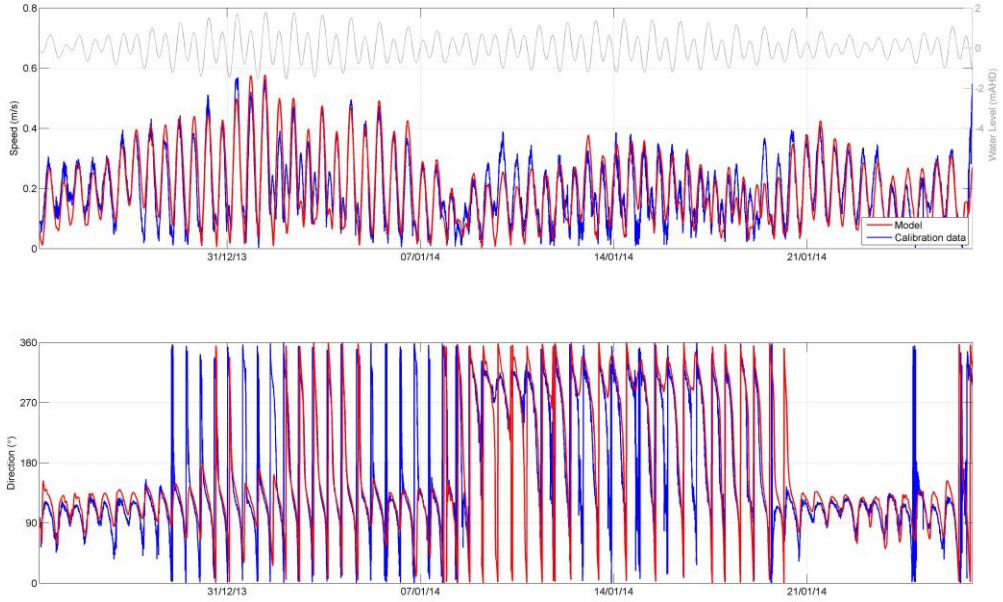

Figure 8 Site 1 measured (blue) and modelled (red) currents. Model forcing - astronomical tides, local wind and regional GBR Lagoon circulation.

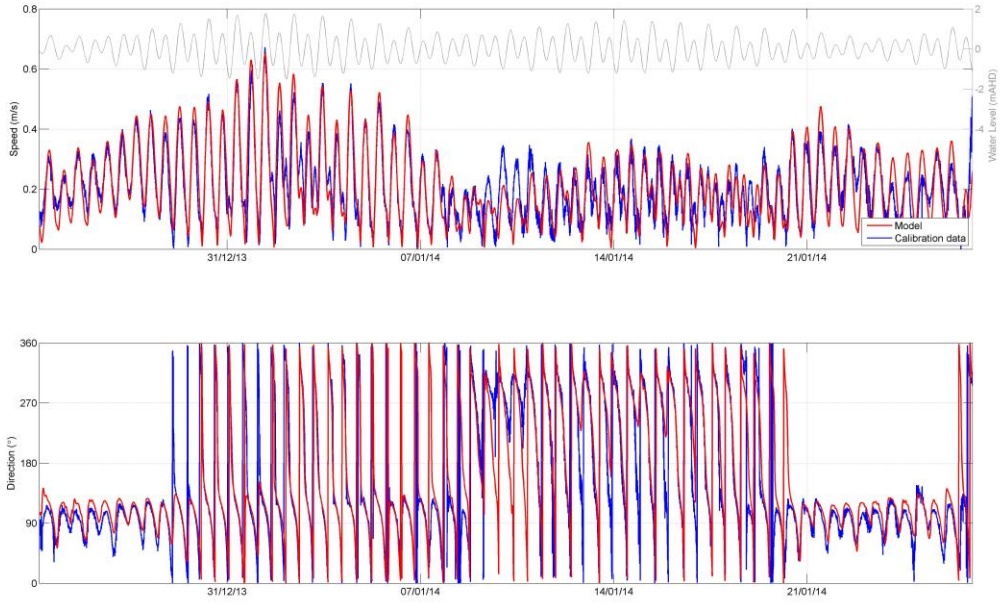

Figure 9 Site 2 measured (blue) and modelled (red) currents. Model forcing - astronomical tides, local wind and regional GBR Lagoon circulation.

APPENDIX B
Model Calibration and Validation

1 SUMMARY

The calibration and validation process presented in this report has demonstrated that:

- the hydrodynamic model provides a good representation of water levels and currents at the two nearshore sites close to Abbot Point and offshore;
- the hydrodynamic model can accurately represent the resultant currents due to forcing from astronomical tides, local wind and regional circulation;
- the hydrodynamic model is capable of accurately representing the vertical variations in currents through the water column; and
- the wave model provides a good representation of wave conditions at the disposal sites.

The good hydrodynamic and wave calibration achieved provides a high level of confidence in the modelling of the driving processes for the sediment transport modelling. However, the lack of suspended sediment calibration data during a dredging and disposal campaign means some uncertainty exists when estimating the resultant dredge plumes and sediment deposition. The implementation of the stochastic dredge plume modelling approach combined with the adoption of conservative values for the sediment transport modelling reduce this uncertainty.

2 INTRODUCTION

This appendix provides details of the calibration and validation process undertaken as part of the numerical modelling for the Abbot Point Growth Gateway onshore disposal assessment. The hydrodynamic, wave and sediment transport models are all discussed.

This onshore dredge material relocation study, with the dredge activity located within the Great Barrier Reef World Heritage Area, has applied a stochastic approach for the modelling of sediment plumes and as such this assessment is considered to be leading practise. This approach takes into account the inter-annual variability in metocean conditions for modelling the dispersion of material during the relocation activity. The modelling must still be considered as a predictive tool but this approach significantly increases the confidence in the modelling and reduces the risk of the dredge material behaving in an unpredicted manner.

2.1 Model Calibration and Validation

Model calibration is the process of setting physically realistic values for model parameters so that the model reproduces observed values to the desired level of accuracy. Model validation is used to confirm that the calibrated model continues to consistently represent the natural processes to the required level of accuracy in periods other than the calibration period without any additional adjustment to the model parameter settings. The process provides confidence in the model results and is essential for the accurate representation of the coastal hydrodynamics and for subsequent sediment transport calculations at Abbot Point. A calibration and validation exercise is required to demonstrate that the performances of the hydrodynamic and wave models are considered to be representative.

Hydrodynamic models are calibrated against measured water level and current data at a number of locations throughout the model domain. An assessment of the differences between the measured and modelled values is undertaken to enable the level of calibration achieved to be quantified. The calibration of a hydrodynamic model in which tidal forcing dominates requires a minimum of one spring neap tidal cycle (approximately 14 days) or preferably a full lunar cycle (approximately 29 days). Model validation would generally cover a similar period.

Locations of all the calibration and validation sites along with the extent of the model grid and the interpolated bathymetry are shown in **Figure 1**.

The hydrodynamic model was calibrated and validated against measured water level and current data. The model calibration has been undertaken at Sites A2 and B1, located to the east and west of the existing jetty at Abbot Point for the period 15/09/08 to 15/10/08. The model was then validated for a number of different periods to improve the confidence in the model's representation of the natural processes:

- Period 1: 15/07/2008 to 15/08/2008 at Sites A1 and B1;
- Period 2: 24/12/2013 to 27/01/2014 at Sites 1 and 2; and

- Period 3: 17/03/2014 to 15/04/2014 at the PER Site[1].

The wave model was calibrated using wave data collected at Site 2 and at the Abbot Point Waverider buoy (WRB in **Figure 1**) location from 24/12/2013 to 15/02/2014.

2.2 Calibration and Validation Standards

For quality control in the hydrodynamic model we have defined calibration performance criteria required to demonstrate that the model is capable of accurately representing the natural processes. For coastal waters such as Abbot Point, the following performance criteria have been defined and can be expressed in percentage terms as:

- Modelled peak current speeds should be within 10% of measured speeds over a lunar cycle;
- Modelled water levels should be within 10% of the tidal range over a lunar cycle; and
- Timing of high water and low water should be within 15 minutes.

These standards provide a good basis for assessing model performance, but experience has shown that sometimes they can be too prescriptive and it is also necessary for visual checks to be undertaken. Under certain conditions, models can meet statistical calibration standards but appear to perform poorly. Conversely, seemingly accurate models can fall short of the guidelines. Consequently a combination of both statistical calibration standards and visual checks has been used to ensure that the model is representative.

2.3 Hydrodynamic Model Calibration

The area of the Great Barrier Reef (GBR) Lagoon where the nominated disposal sites are located is subject to forcing by astronomical tides, wind[2] and GBR Lagoon regional circulation with all of these being capable of influencing the currents to some degree (see **Appendix A**). As such, it was important for the model calibration to include periods when all of these processes influence the currents. Therefore a 30 day period (i.e. more than one full lunar cycle) was required as this includes two periods where GBR Lagoon regional circulation processes occur. An assessment of the differences in phase and amplitude between the modelled and measured data was undertaken to assess the level of calibration achieved. For both water levels and currents, the modelled data was calibrated using measured data recorded at ADCPs. It is important to note that unlike a tide gauge it is not possible to accurately survey the level of an ADCP and as a result it is not possible to relate the water level to a specific datum such as Australian Height Datum (AHD). The water level measured by the ADCPs can be calculated relative to mean sea level (MSL), but as the bathymetry in the model is relative to AHD it is expected that there would be differences between the two.

[1] This third validation period is to demonstrate that the model can accurately represent flow conditions at the PER Site. Simultaneous data was only available at Sites 1 and 2 and so a separate validation period was selected to validate the model at the PER Site.

[2] Sensitivity testing has shown that the currents are influenced by wind but not by waves in this area. Waves cause an orbital current which can result in a stress on the bed, but does not result in a residual current.

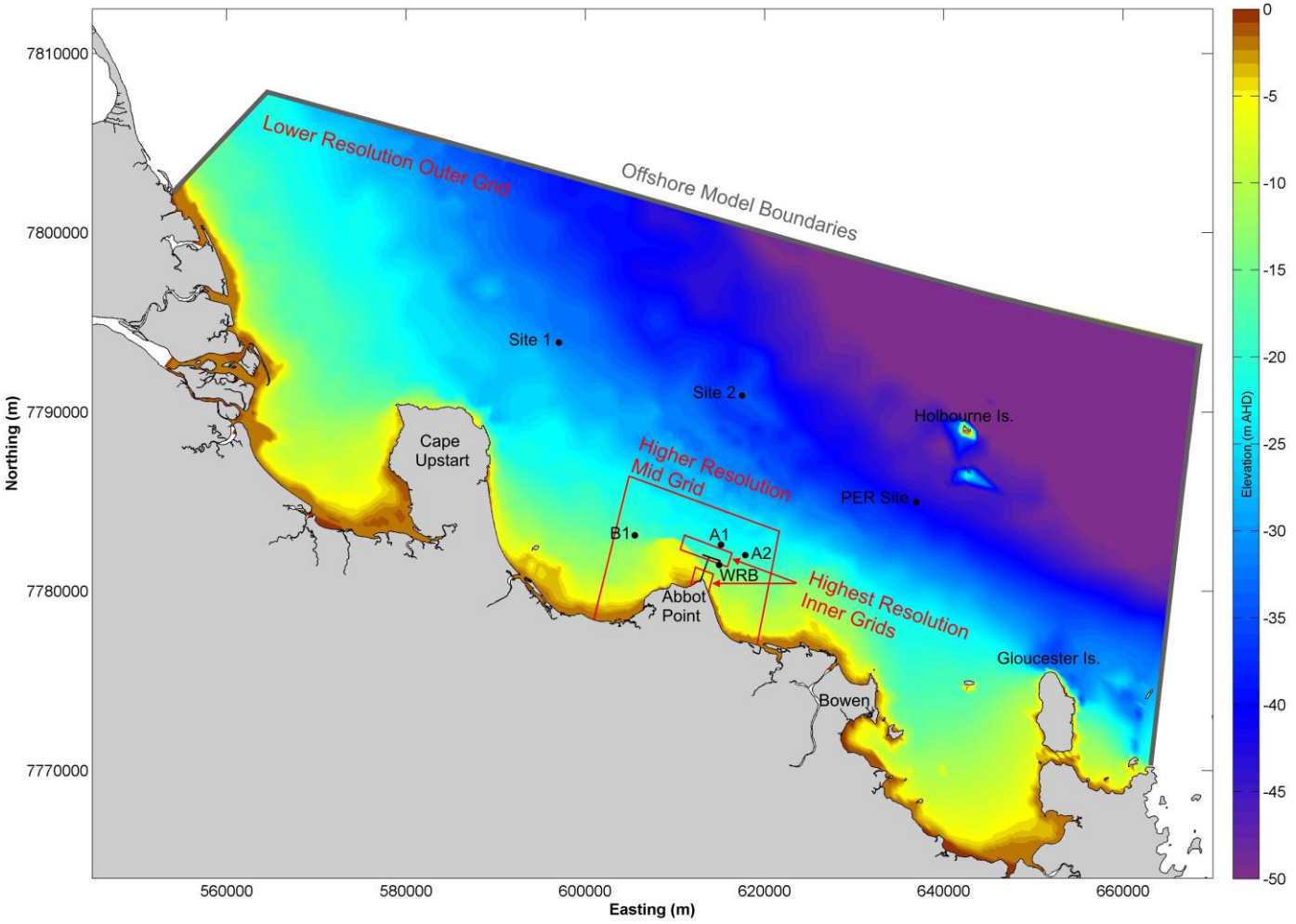

Figure 1 Model extent and bathymetry, and locations of the calibration and validation sites.

2.3.1 Water Levels

Time series plots of the modelled and measured water levels for Sites A2 and B1 are shown in **Figures 2** and **3**. As noted in the **Section 2.1** the measured water levels are relative to MSL while the modelled water levels are relative to AHD. In addition, the measured water levels include any residual water levels. Despite this the modelled water levels generally agree well with the measured data at both sites.

It order to further assess the level of calibration achieved, statistical analysis was undertaken to quantify the difference in elevation and timing between the modelled and measured high and low water values. The results of the analysis for the difference in water level at high water and low water are presented as absolute values in **Table 1**. Mean water level differences were less than 0.1m for both sites over the calibration period, indicating only small differences (<10%) relative to the tidal range. Over this period the difference in phasing at high water at Site A2 was greater than the threshold of 15 minutes, while at Site B1 it was 15 minutes. The reason for the significantly higher phase lag at Site A2 compared to Site B1 is a result of the statistical approach adopted. During the neap tides on the 4th to 6th October 2008 the second smaller high water is not always clearly defined as a peak in the model while the measurements consistently shows a clear peak, this results in the statistical approach comparing the timing of the measured second high with the timing of the nearest modelled high water which can be up to 12 hours before or after. When this period is not included in the stastical analysis and the initial 14 days are used the HW phase difference at Site A2 is reduced to 17 minutes which is much closer to the guideline of 15 minutes. Comparison of the modelled and measured data in **Figures 2** and **3** shows that at both sites the water levels tend to be approximately in phase during spring tides and become out of phase during neap tides, indicating that the model can accurately replicate the phasing during spring tides but cannot replicate it as accurately during neap tides. The Root Mean Square Deviation (RMSD) values show that there is some variation between the modelled and measured water levels through the calibration period and that this is comparable for high and low water.

Table 1 Water level calibration period statistics, September 2008.

Statistical Description	Site A2	Site B1
Mean HW Difference (m)	0.039	0.058
Mean HW Difference relative to Tidal Range (%)	2.4	3.5
Mean LW Difference (m)	0.009	0.007
Mean LW Difference relative to Tidal Range (%)	0.6	0.4
RMSD for HW (m)	0.166	0.165
RMSD for LW (m)	0.130	0.127
Mean HW Phase Lag (mins)	29*	15
Mean LW Phase Lag (mins)	9	6

* This is a result of the statistical approach for the comparison, described in more detail in Section 2.3.1.
Note: The differences in phase of the high and low waters were derived by subtracting the time of the measured value from the time of the model value. A negative value therefore indicates that the model is early compared to the measured data.

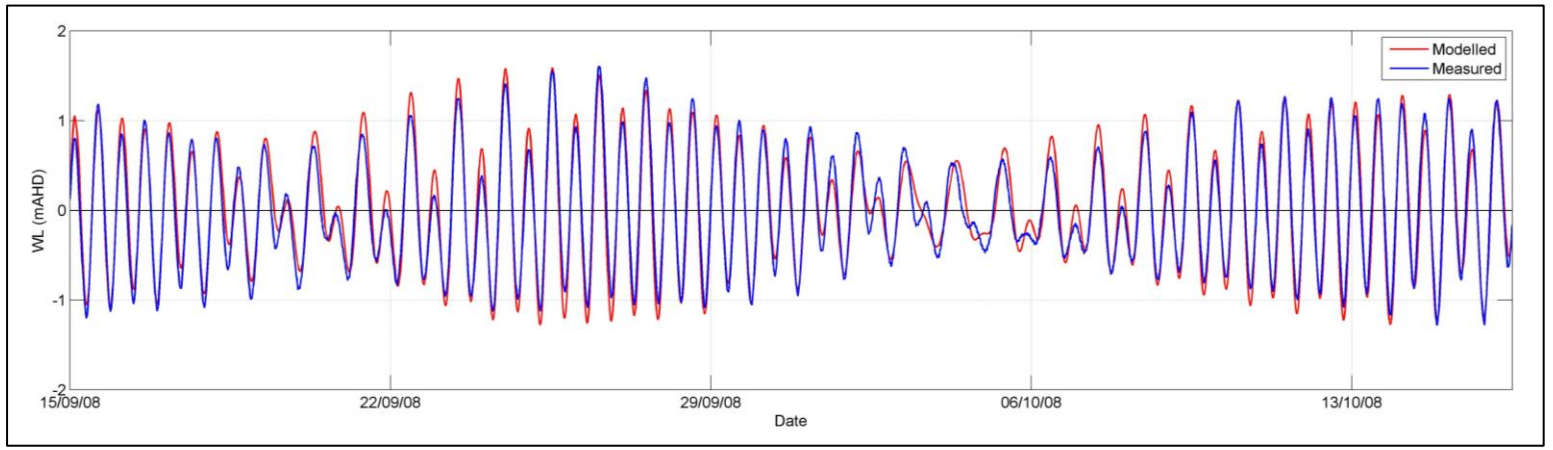

Figure 2 Site A2 water levels.

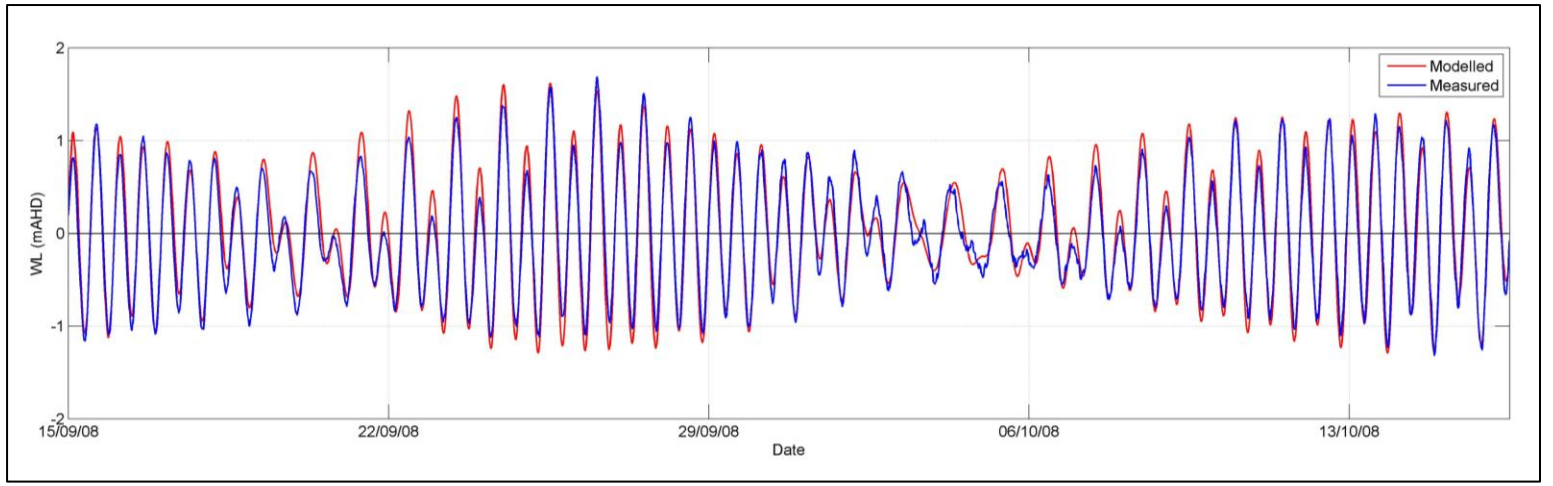

Figure 3 Site B1 water levels.

2.3.2 Current Speed and Direction

The current speeds and directions offshore of Abbot Point are influenced by forcing from astronomical tides, local winds and regional circulation. As such this is considered to be a highly complex hydrodynamic environment which requires understanding of all the forcings to be able to accurately replicate the current speeds and directions. Further details on the representation of these forcings in the model and their relative importance for the currents are provided in **Appendix A**.

Time series plots for the calibration of current speed and direction are shown in **Figures 4** and **5.** A statistical summary of the calibration is provided in **Table 2**. The mean differences in current speed and direction in **Table 2** for Sites A2 and B1 are within the calibration guideline ranges specified in **Section 2.2**. The RMSD values are relatively low showing that the modelled currents consistently replicate the measured currents. Given the high degree of variability in the measurements, indicating a complex interaction in the astronomical tide and the local wind processes which dominate the currents in this location, the overall model calibration achieved for current speed and direction is considered to be good.

Table 2 Current speed and direction calibration period statistics, September 2008.

Statistical Description	Site A2	Site B1
Mean Difference in Speed of Flood (m/s)	-0.01	-0.04
Mean Difference in Flood Speed Relative to Maximum Observed Speed (%)	-2.7	-9.3
Mean Difference in Speed of Ebb (m/s)	-0.03	-0.03
Mean Difference in Ebb Speed Relative to Maximum Observed Speed (%)	-8.2	-6.9
RMSD for Flood Speed (m)	0.05	0.07
RMSD for Ebb Speed (m)	0.06	0.06
Mean Difference in Direction of Flood (°)	-8	-19
Mean Difference in Direction of Ebb (°)	-14	-7

Note: The differences were derived by subtracting measured values from model values. A negative value therefore indicates that the model is under-predicting measured values.

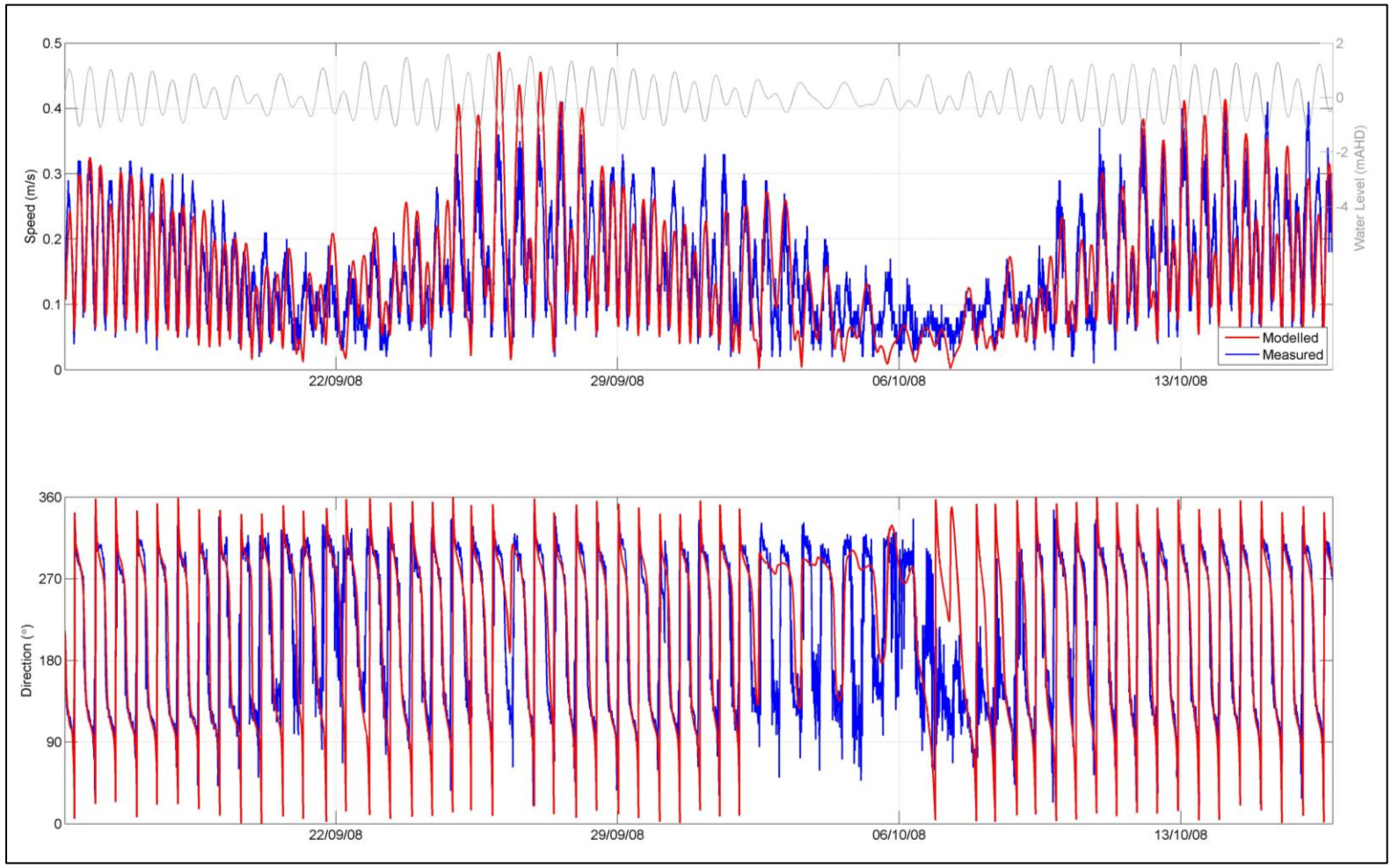

Figure 4 Site A2 current speed and direction.

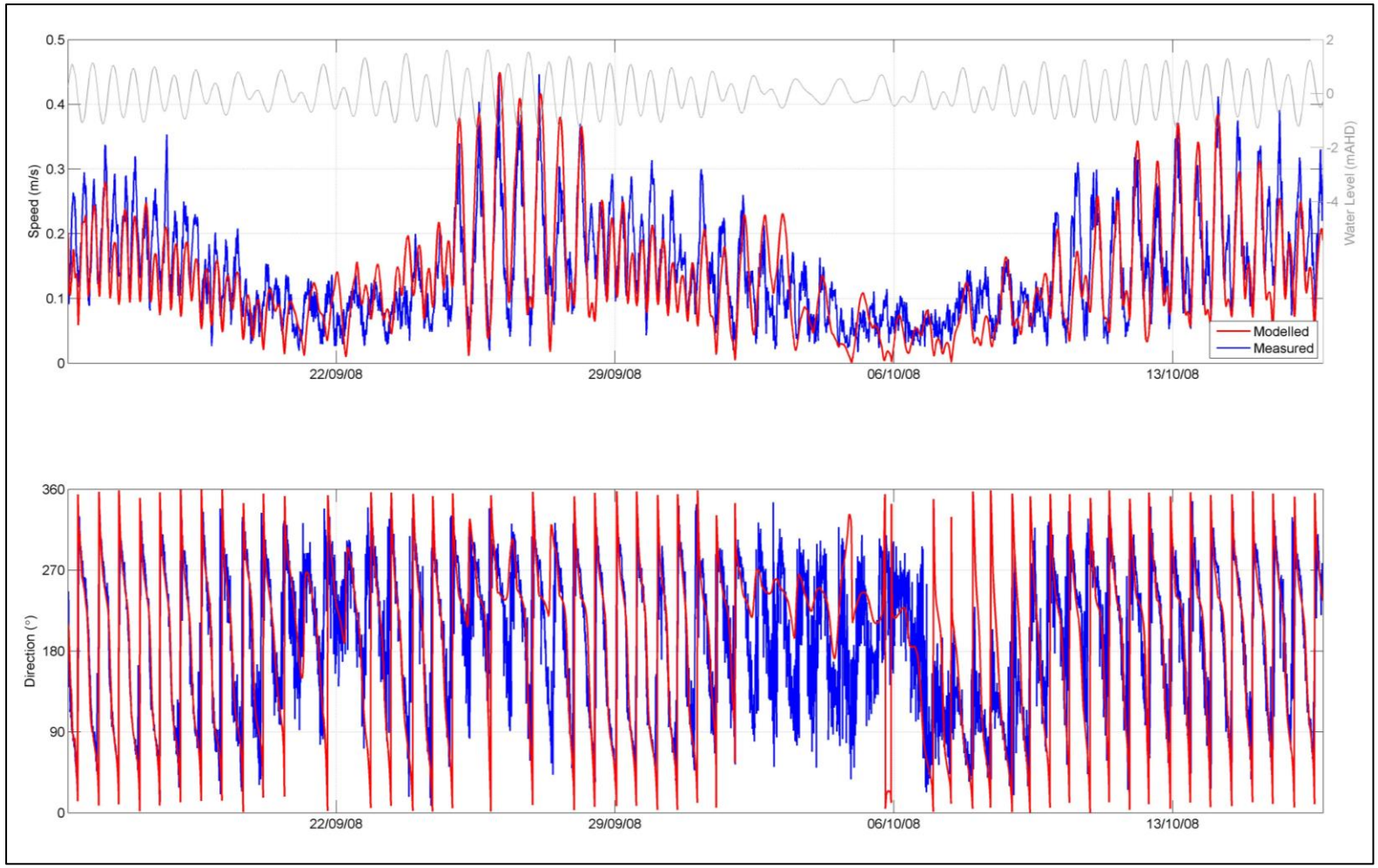

Figure 5 Site B1 current speed and direction.

2.3.3 Three Dimensional Calibration

To ensure current speed and direction are being accurately represented through the water column modelled and measured data have been compared at various layers at Site A2. This three dimensional calibration is only presented for one site, but as the depth averaged calibration is similar at Sites B1 and A2 a similar three dimensional calibration would also be expected for Site B1. The modelled current speeds and directions have been compared with the data measured by the ADCP at: the bed layer, mid water column layer and surface layer. Time series plots of modelled and measured data at these depths are shown in **Figures 6** to **8**. The plots show that the model provides a reasonable representation of the current speeds and directions through the water column despite the high degree of variability in the currents due to variations in the forcing conditions. The measured data at the surface layer shows some noise in the measurements which the model is not able to replicate, the model does provide a good representation of the average tidal current speeds when the noise in the measurements is ignored. At the mid and near-bed layers the noise in the measurements does not occur and as a result the model provides a much better representation of the current speeds. A statistical summary of the comparison is provided in **Table 3** which confirms that the currents are reasonably well represented by the model throughout the water column. Due to the noise in the measurements at the surface layer the statistics show that the model is underestimating the current speeds by more than 10%, while in the mid and near-bed layers the model is accurately representing the current speeds, with differences of 5% and less.

Table 3 Site A2 discrete layer current speed and direction calibration period statistics.

Statistical Description	Bed Layer	Mid Layer	Surface Layer
Mean Difference in Speed of Flood (m/s)	-0.02	0.00	-0.11
Mean Difference in Flood Speed Relative to Maximum Observed Speed (%)	-5.0	1.0	-18.6
Mean Difference in Speed of Ebb (m/s)	-0.01	-0.04	-0.10
Mean Difference in Ebb Speed Relative to Maximum Observed Speed (%)	-1.8	-9.3	-14.5
RMSD for Flood Speed (m)	0.05	0.05	0.13
RMSD for Ebb Speed (m)	0.06	0.07	0.13
Mean Difference in Direction of Flood (°)	-17	2	-9
Mean Difference in Direction of Ebb (°)	9	-11	-4

Note: The differences were derived by subtracting measured values from model values. A negative value therefore indicates that the model is under-predicting measured values.

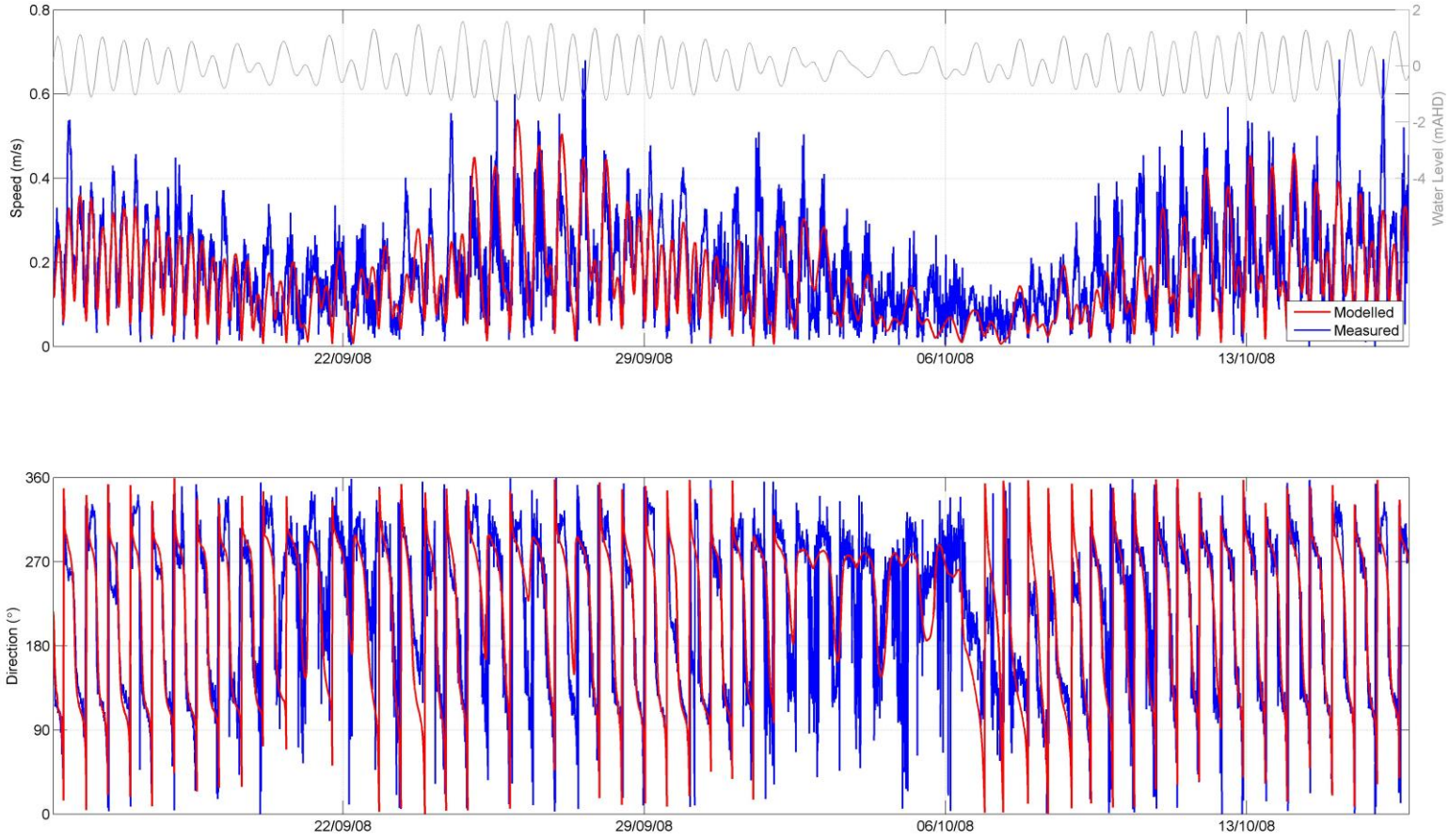

Figure 6 Site A2 surface layer current speed and direction.

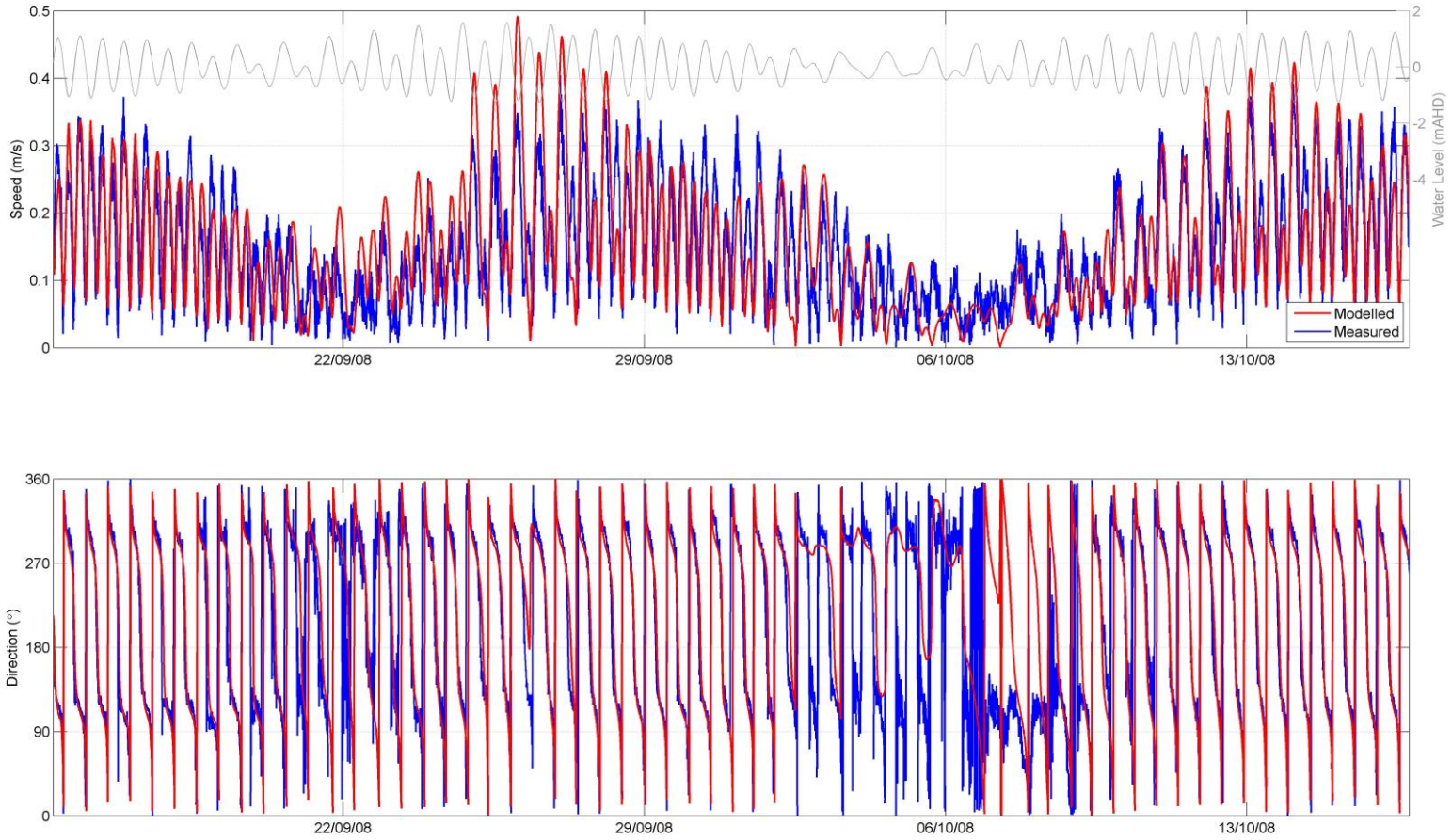

Figure 7 Site A2 middle layer current speed and direction.

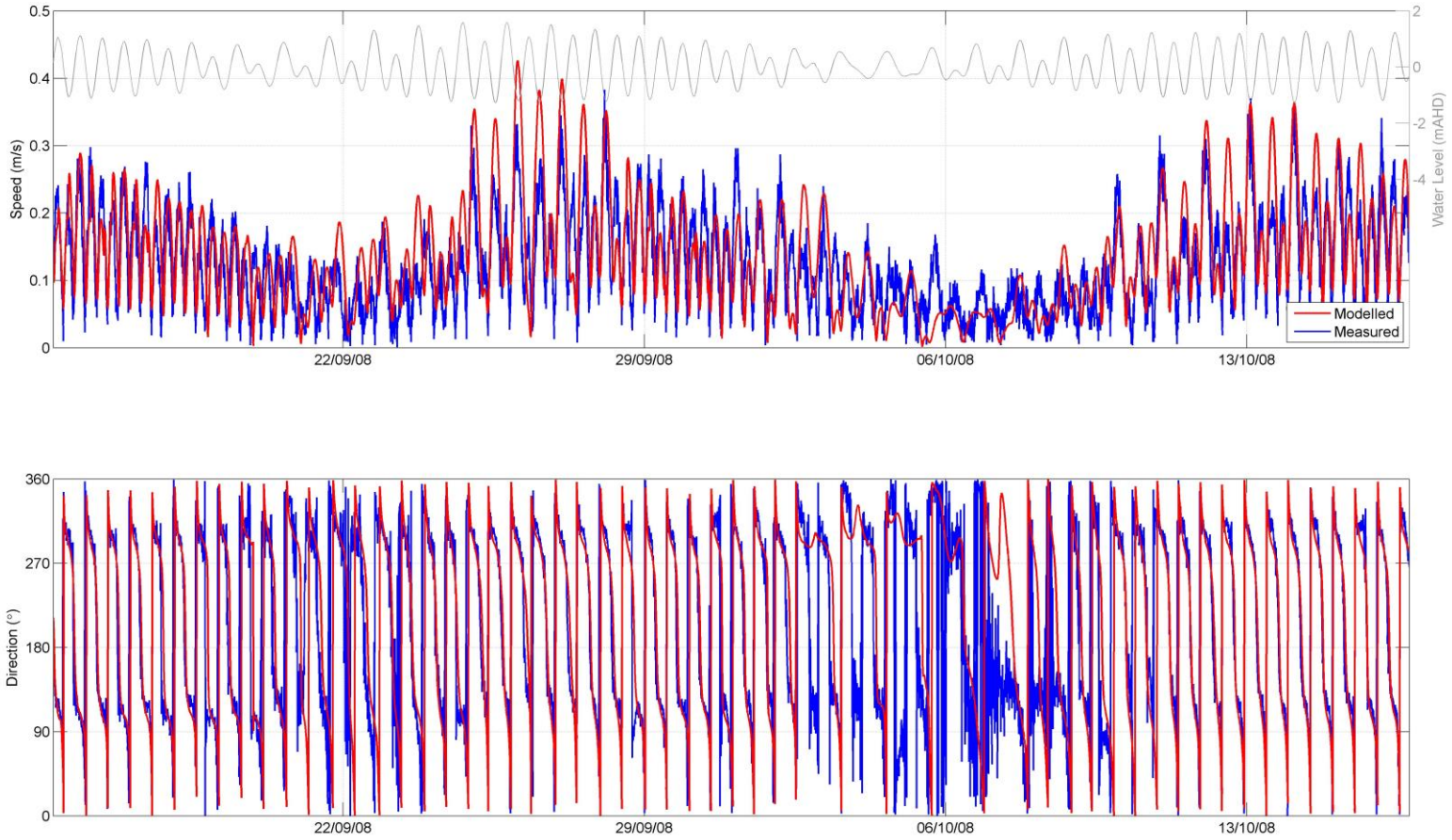

Figure 8 Site A2 bed layer current speed and direction.

2.4 Hydrodynamic Model Validation

Following the calibration period, the hydrodynamic model was validated at a number of different sites for the following periods:

- Period 1: 15/07/2008 to 15/08/2008 at Sites A1 and B1;
- Period 2: 24/12/2013 to 27/01/2014 at Sites 1 and 2; and
- Period 3: 17/03/2014 to 15/04/2014 at the PER Site.

No adjustments to the model parameter settings were applied for the model validation.

The current speeds and directions offshore of Abbot Point are influenced by forcing from astronomical tides, local winds and regional circulation.

The second model validation period was specifically selected as it includes periods when forcing from astronomical tides, local winds and regional circulation occur simultaneously:

- 24/12/13 to 08/01/14: currents are a combination of astronomical tidal, local wind and regional circulation forcings;
- 08/01/14 to 19/01/14: currents are a combination of astronomical tidal and local wind forcings; and
- 19/01/14 to 27/01/14: currents are a combination of astronomical tidal, local wind and regional circulation forcings.

2.4.1 Water Levels

Period 1

Figures 9 and **10** show the model validation for water levels at Sites A1 and B1, the model generally performs well. The results of the analysis for the difference in water level at high water and low water are presented as absolute values in **Table 4.** This statistical summary indicates that mean water level differences at both Site A1 and B1 were very small (<2%) relative to the tidal range. The RMSD values show that there is some variation between the modelled and measured water levels, but when considered along with mean differences it can be seen that the model is not consistently over or under-predicting the levels. The mean high and low water phase differences were between 10 and 21 minutes at the sites. The plots show that at both sites the phasing of the model compared to the measured data is good during spring tides. However, during neap tides the modelled high and low water levels occur later than the corresponding measured levels. This shows that, although generally representative of tidal processes, the model is not able to accurately reproduce the variable phasing of the tides during neap periods. As this assessment is related to the transport of suspended sediment, the phase difference between the measured and modelled HW and LW times is not considered an issue.

Period 2

Figures 11 and **12** show the model validation for water levels at Sites 1 and 2, the model generally performs well. The results of the analysis for the difference in water level at high water and low water are presented as absolute values in **Table 5.** This statistical summary indicates that mean water level

differences at both Site 1 and 2 were less than 10% relative to the tidal range. The RMSD values show that there is some variation between the modelled and measured water levels through the calibration period and that this is comparable for high and low water. Over this period the difference in phasing at both sites were less than 5 minutes, which lies well within the threshold of 15 minutes.

Table 4 Water level validation period statistics, July 2008.

Statistical Description	Site A1	Site B1
Mean HW Difference (m)	0.010	0.028
Mean HW Difference relative to Tidal Range (%)	0.6	1.8
Mean LW Difference (m)	0.022	-0.001
Mean LW Difference relative to Tidal Range (%)	1.4	-0.1
RMSD for HW (m)	0.147	0.143
RMSD for LW (m)	0.142	0.141
Mean HW Phase Lag (mins)	21	19
Mean LW Phase Lag (mins)	19	14

Note: The differences in phase of the high and low waters were derived by subtracting the time of the measured value from the time of the model value. A negative value therefore indicates that the model is early compared to the measured data.

Table 5 Water level validation period statistics, Period 1 2014.

Statistical Description	Site 1	Site 2
Mean HW Difference (m)	0.127	0.085
Mean HW Difference relative to Tidal Range (%)	8.2	5.4
Mean LW Difference (m)	0.091	0.108
Mean LW Difference relative to Tidal Range (%)	5.9	6.8
RMSD for HW (m)	0.175	0.149
RMSD for LW (m)	0.174	0.177
Mean HW Phase Lag (mins)	1	-4
Mean LW Phase Lag (mins)	-3	-3

Note: The differences in phase of the high and low waters were derived by subtracting the time of the measured value from the time of the model value. A negative value therefore indicates that the model is early compared to the measured data.

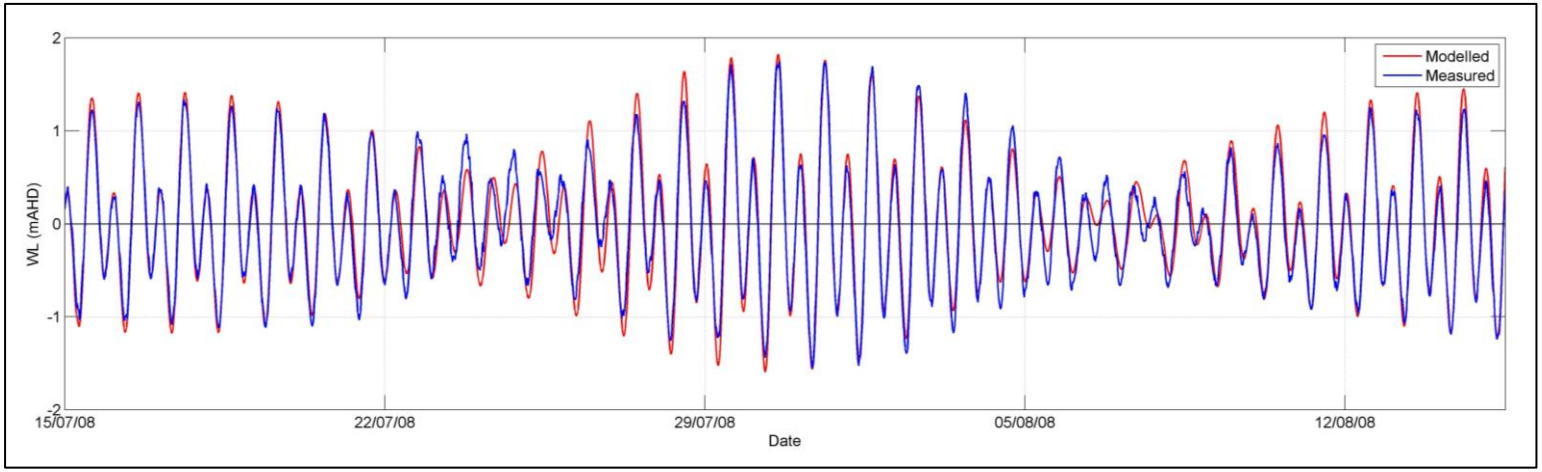

Figure 9 Site A1 water levels.

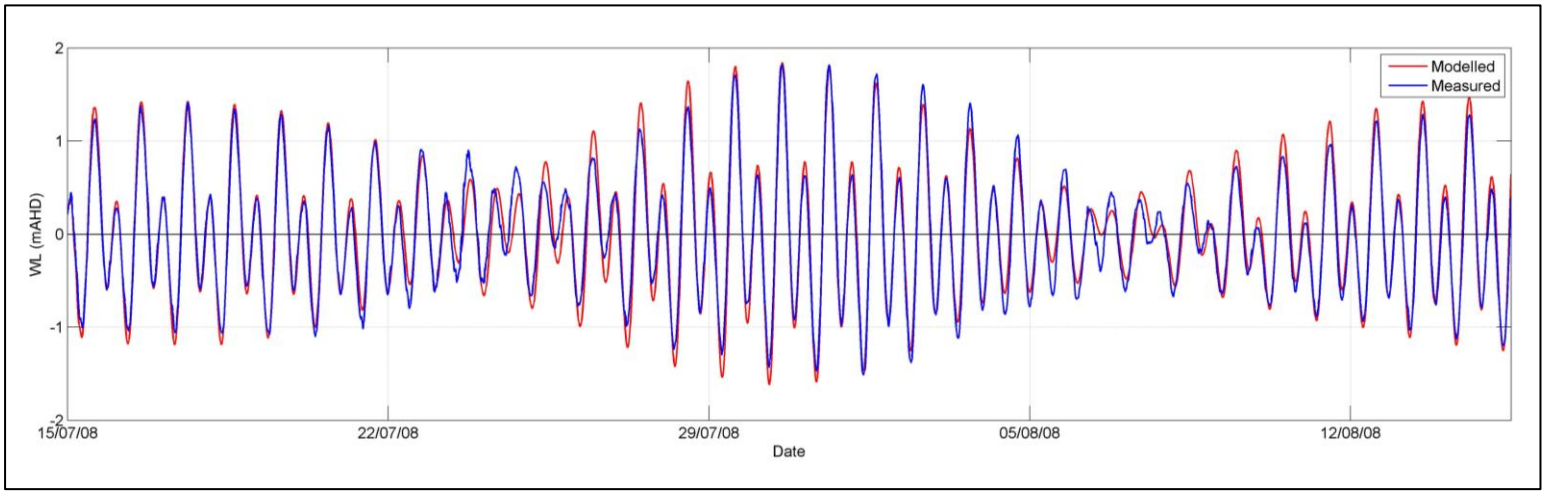

Figure 10 Site B1 water levels.

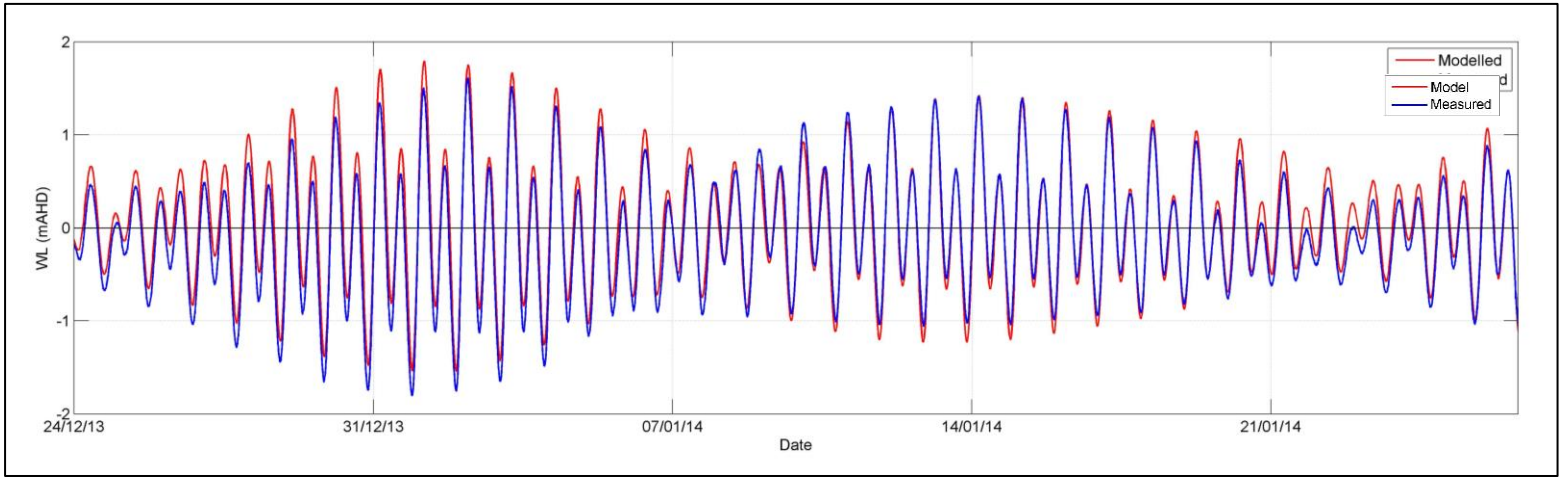

Figure 11 Site 1 water levels.

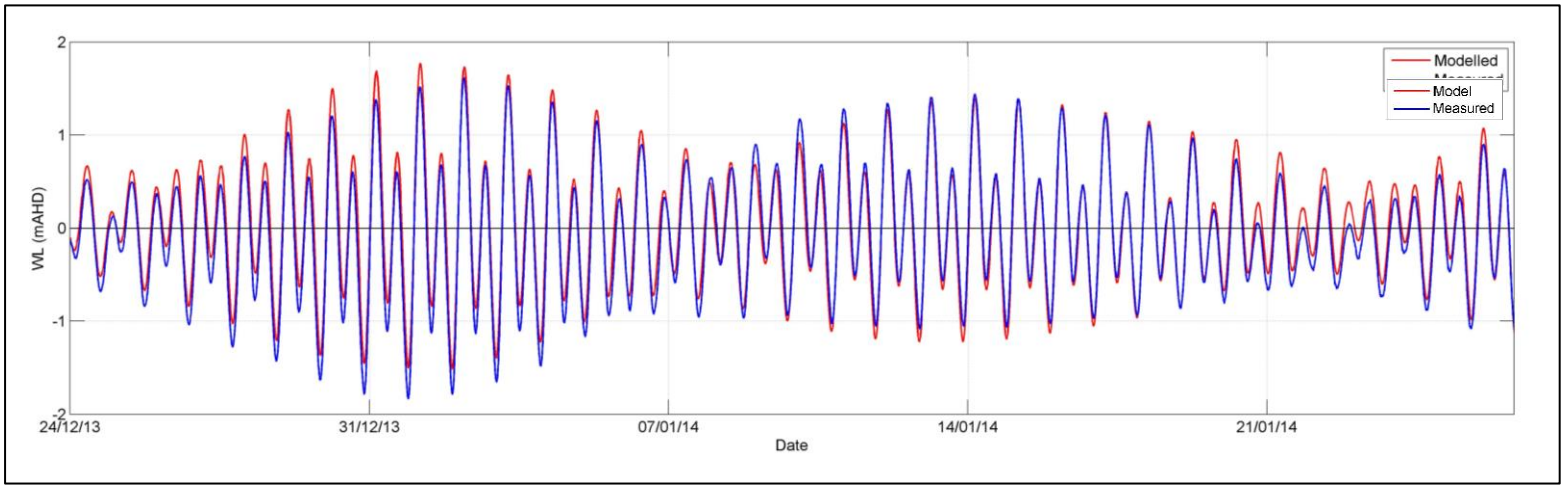

Figure 12 Site 2 water levels.

2.4.2 Current Speed and Direction

Period 1

The validation for current speed and direction for July 2008 was over a 29 day period to represent a full lunar cycle. Time series plots showing the modelled and measured speeds and directions are shown in **Figures 13** and **14.** A statistical summary is provided in **Table 6**. The model provides a good representation of the currents at both sites with differences between the modelled and measured currents of less than 10%. As such, the model validation at these sites is considered suitable for the present assessment.

Table 6 Current speed and direction validation period statistics, Period 1 in July 2008.

Statistical Description	Site A1	Site B1
Mean Difference in Speed of Flood (m/s)	-0.03	0.00
Mean Difference in Flood Speed Relative to Maximum Observed Speed (%)	-7.6	-0.3
Mean Difference in Speed of Ebb (m/s)	0.02	0.01
Mean Difference in Ebb Speed Relative to Maximum Observed Speed (%)	5.4	2.8
RMSD for Flood Speed (m)	0.06	0.06
RMSD for Ebb Speed (m)	0.05	0.06
Mean Difference in Direction of Flood (°)	-21	4
Mean Difference in Direction of Ebb (°)	-4	-11

Note: The differences were derived by subtracting measured values from model values. A negative value therefore indicates that the model is under-predicting measured values.

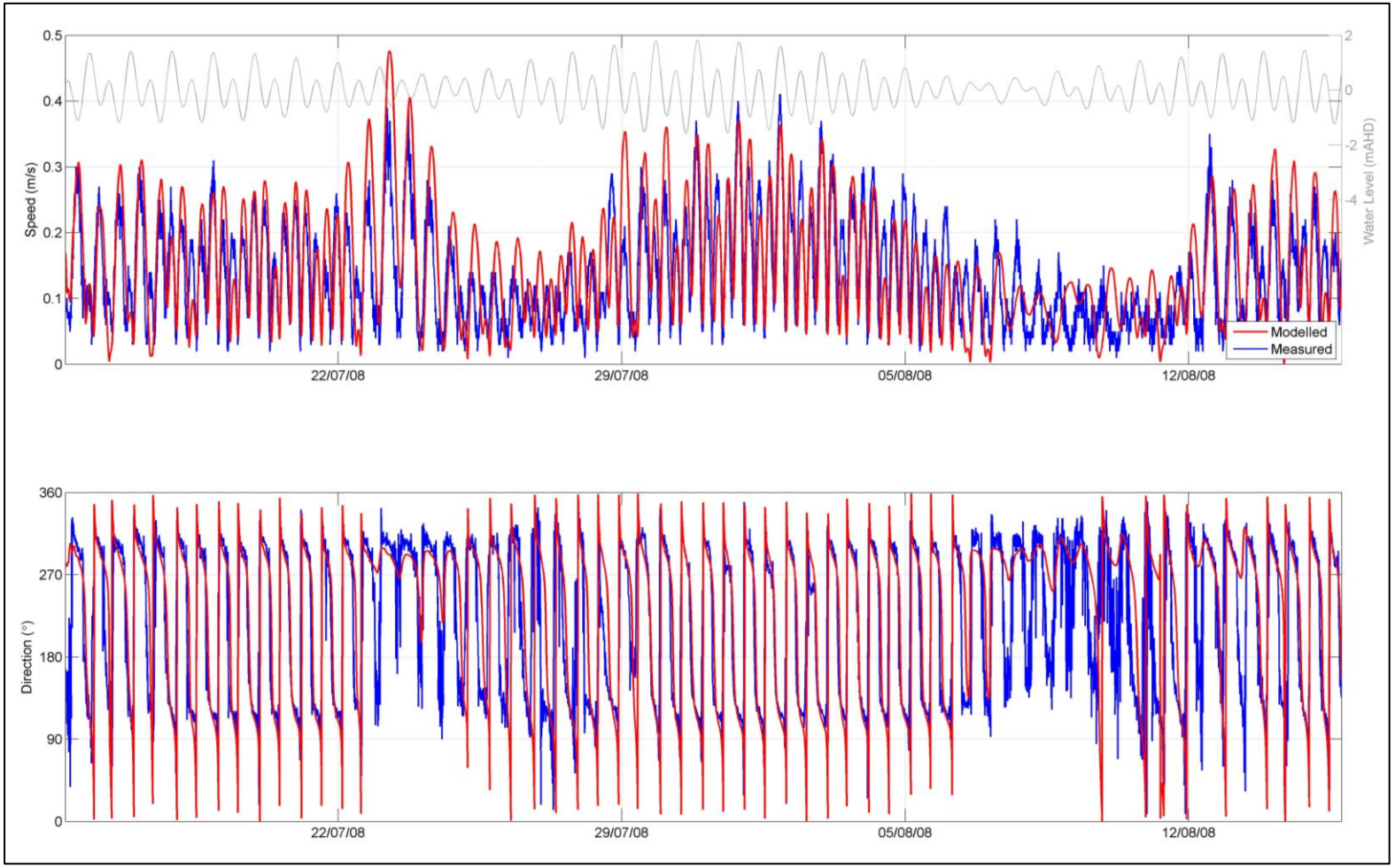

Figure 13 Site A1 current speed and direction.

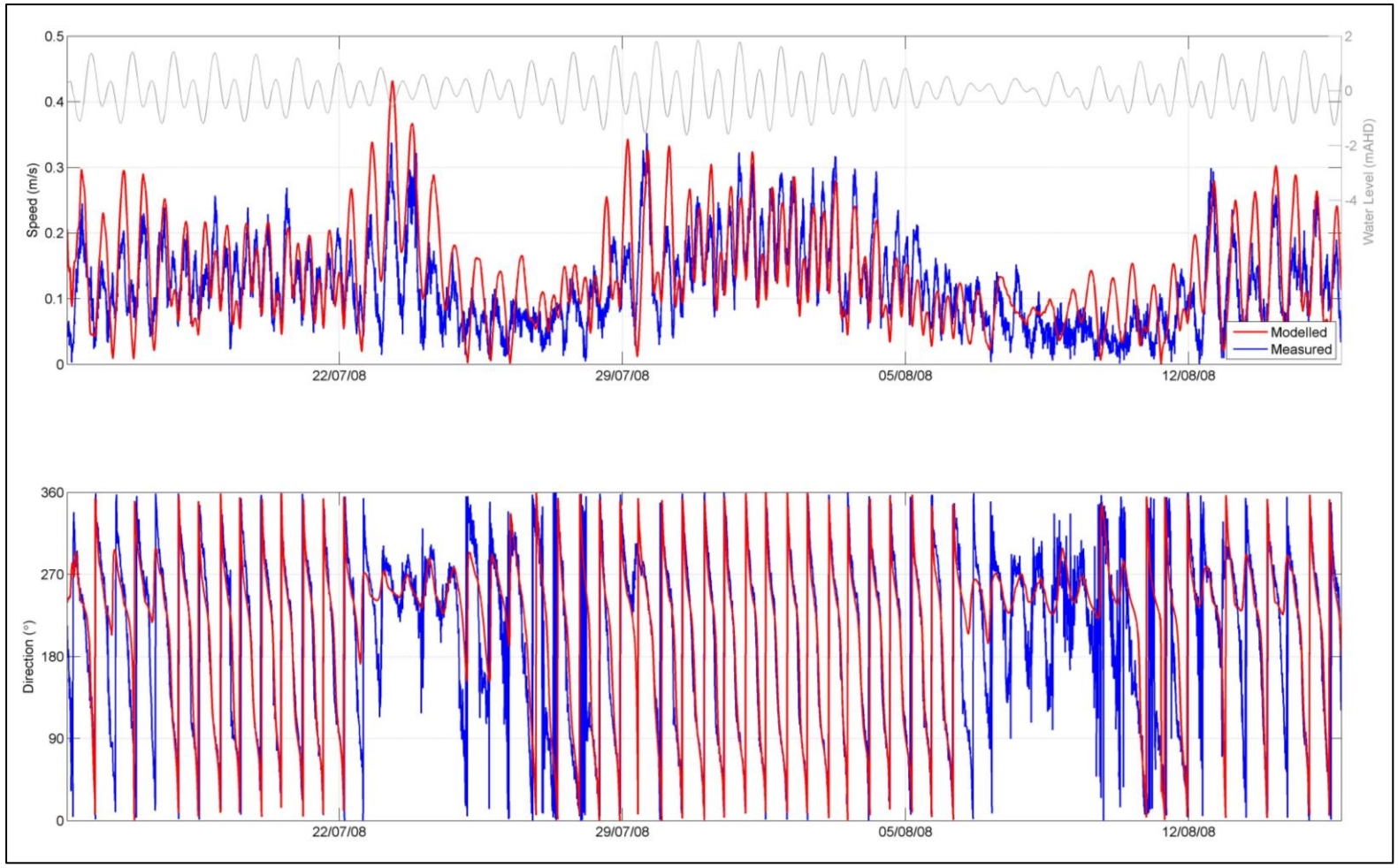

Figure 14 Site B1 current speed and direction.

Period 2

The validation for current speed and direction for Period 2 was over a 34 day period to represent a full lunar cycle as well as a number of periods where regional scale ocean circulation occurs. Time series plots showing the modelled and measured speeds and directions are shown in **Figures 15** and **16.** A statistical summary is provided in **Table 7**. The model provides a good representation of the currents at both sites, with similar measured and modelled conditions at the sites. As such, the model validation at these sites is considered suitable for the present assessment and demonstrates that the model is capable of accurately representing the currents in the area offshore of Abbot Point.

Table 7 Current speed and direction validation period statistics, Period 2 2014.

Statistical Description	Site 1	Site 2
Mean Difference in Speed of Flood (m/s)	-0.02	-0.03
Mean Difference in Flood Speed Relative to Maximum Observed Speed (%)	-4.6	-4.6
Mean Difference in Speed of Ebb (m/s)	-0.03	0.00
Mean Difference in Ebb Speed Relative to Maximum Observed Speed (%)	-6.1	-0.2
RMSD for Flood Speed (m)	0.07	0.06
RMSD for Ebb Speed (m)	0.06	0.04
Mean Difference in Direction of Flood (°)	19	8
Mean Difference in Direction of Ebb (°)	14	3

Note: The differences were derived by subtracting measured values from model values. A negative value therefore indicates that the model is under-predicting measured values.

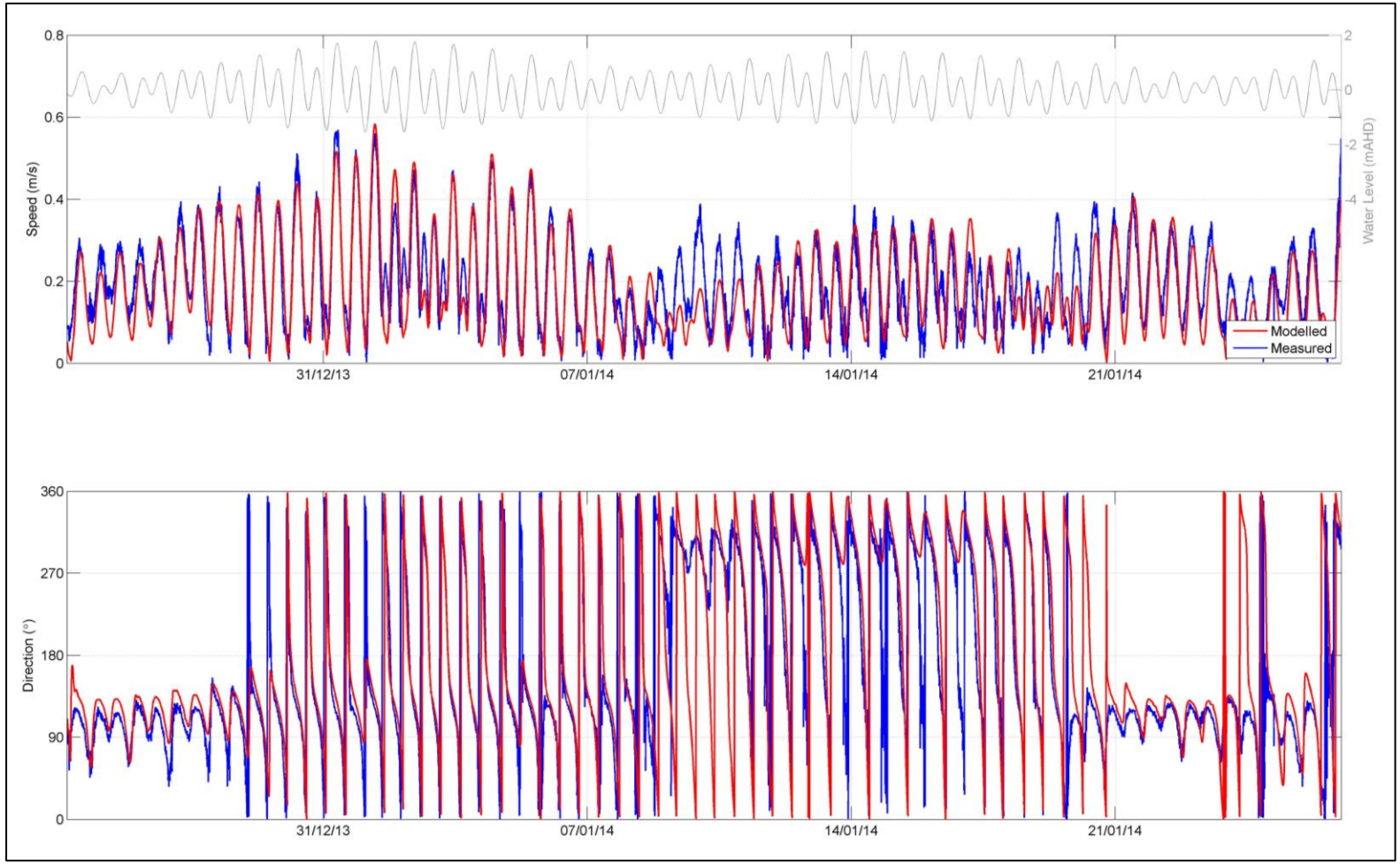

Figure 15 Site 1 current speed and direction.

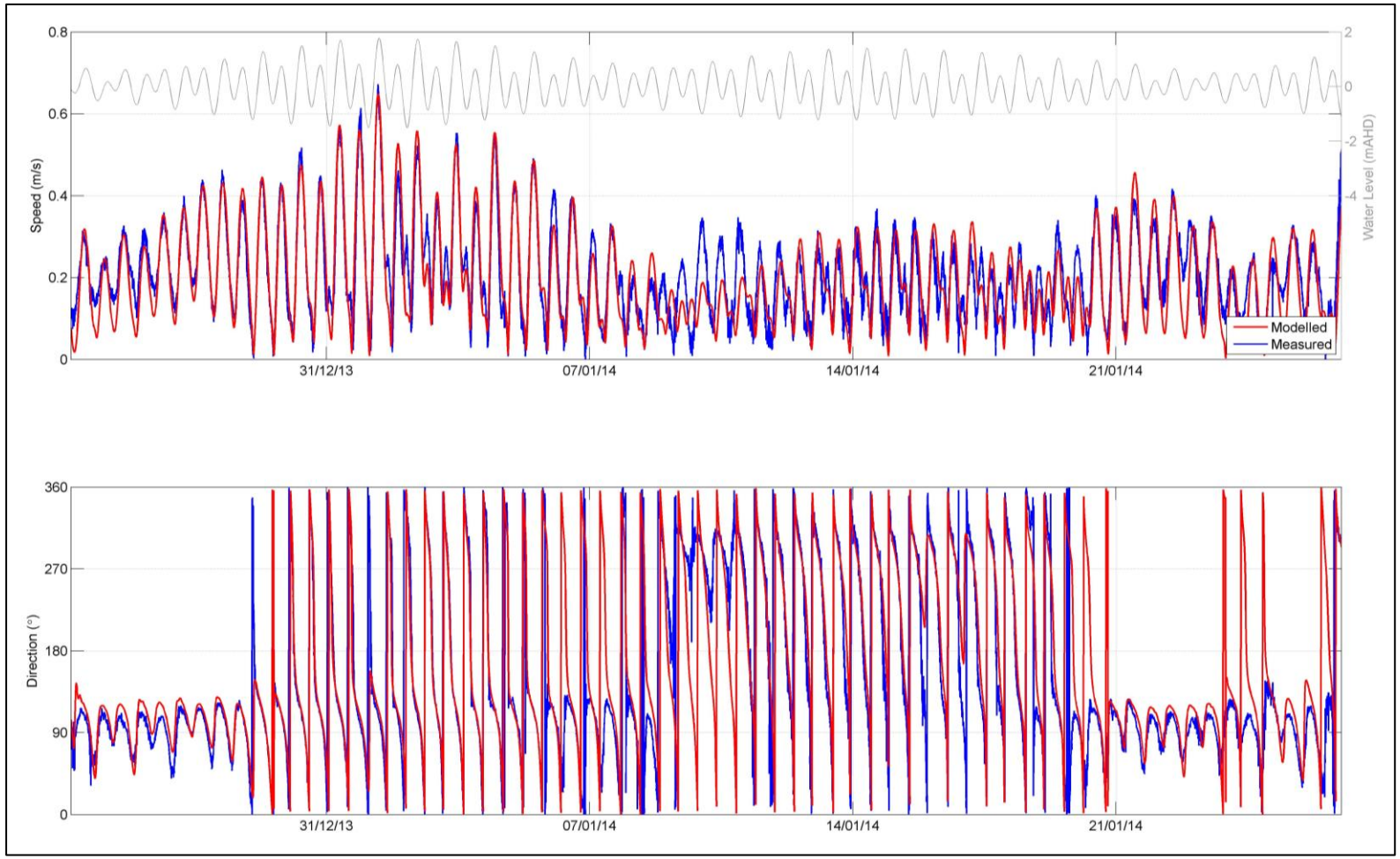

Figure 16 Site 2 current speed and direction.

Period 3

The validation for current speed and direction for Period 3 was over a 29 day period to represent a full lunar cycle. Time series plots showing the modelled and measured speeds and directions are shown in **Figure 17.** A statistical summary is provided in **Table 8**. The model provides a good representation of the currents at both sites, with similar measured and modelled conditions at the sites. As such, the model validation at these sites is considered suitable for the present assessment and demonstrates that the model is capable of accurately representing the currents in the area offshore of Abbot Point.

Table 8 Current speed and direction validation period statistics, Period 3 2014.

Statistical Description	PER Site
Mean Difference in Speed of Flood (m/s)	0.00
Mean Difference in Flood Speed Relative to Maximum Observed Speed (%)	0.6
Mean Difference in Speed of Ebb (m/s)	0.02
Mean Difference in Ebb Speed Relative to Maximum Observed Speed (%)	4.5
RMSD for Flood Speed (m)	0.06
RMSD for Ebb Speed (m)	0.07
Mean Difference in Direction of Flood (°)	-3
Mean Difference in Direction of Ebb (°)	6

Note: The differences were derived by subtracting measured values from model values. A negative value therefore indicates that the model is under-predicting measured values.

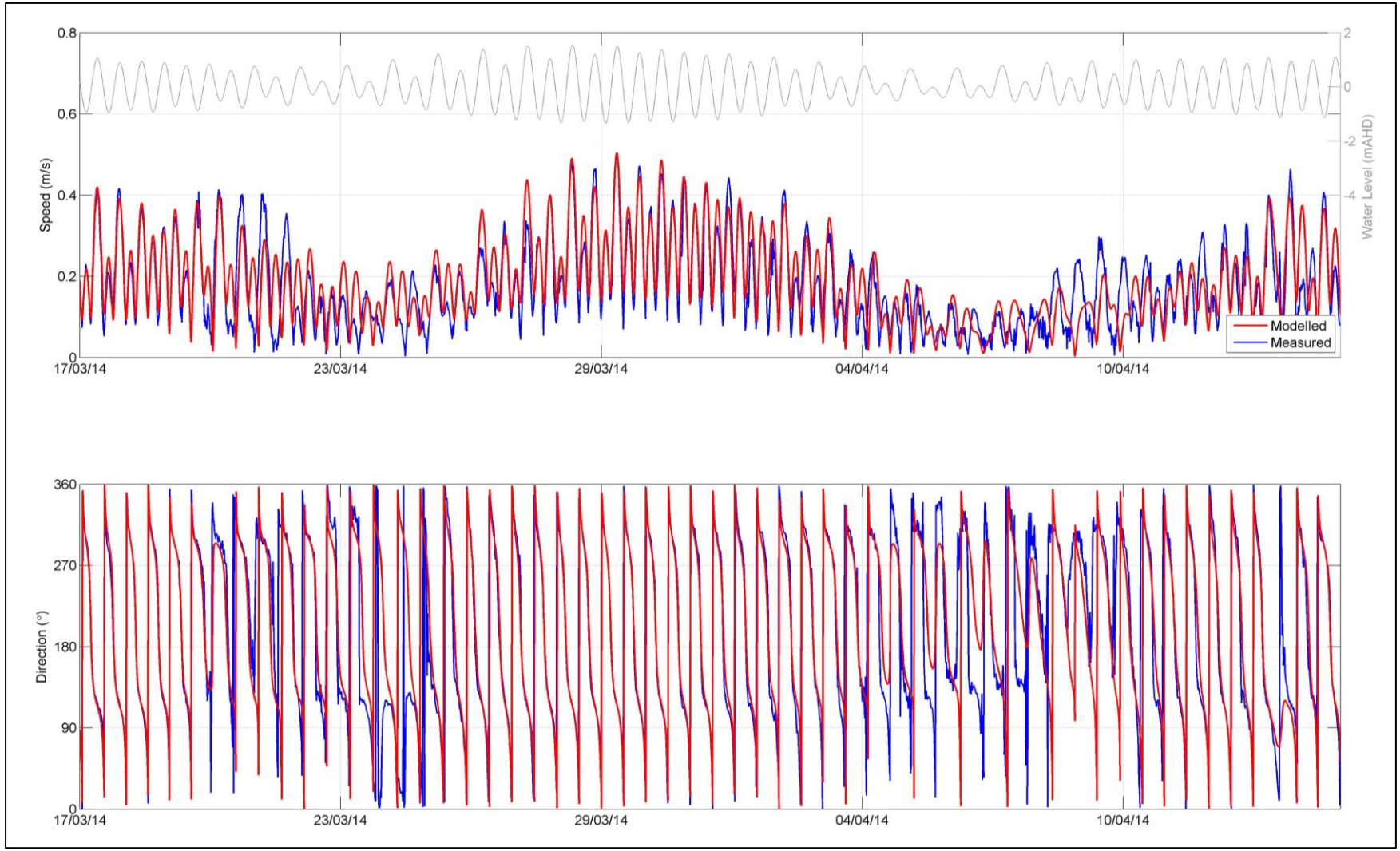

Figure 17 PER Site current speed and direction.

2.5 Wave Model Calibration

For calibration purposes the wave model was set up to represent the wave conditions at Site 2 and the Abbot Point Waverider Buoy from 24/12/2013 to 15/02/2014. This time period was chosen as it represents a period with a high degree of variability in the wave conditions and includes TC Dylan. Unfortunately the Waverider Buoy was removed during TC Dylan presumably due to the potential risk of instrument loss/damage, but measurements at Site 2 continued throughout the event.

The plots provided in **Figures 19** and **20** show that the model is achieving a good fit against the measured wave height, period and direction at both locations. The period from 26/01/14 to 03/02/14 is when TC Dylan occurred, the plots show that at Site 2 the model provides a very good representation of the significant wave height and mean wave direction during this event but results in a slight over-estimation of the peak wave period.

A quantitative assessment of the calibration at Site 2 is provided in **Table 9** (this only provided at Site 2 as this is the complete dataset)**,** with percent exceedance statistics presented for both measured and modelled significant wave height over the calibration period. The exceedance statistics show that the model generally agrees well with the measured data, except that it slightly over-estimates the largest significant wave heights (1% exceedance) and the smallest significant wave heights (80% and 95% exceedance).

The plots and statistics both show that the model is capable of accurately representing the wave conditions at Site 2 and the plots also show that the model is capable of accurately representing the wave conditions at the Abbot Point Waverider Buoy.

Table 9 Significant wave height (H_s) calibration period exceedance statistics.

Statistical Description	Measured H_s (m)	Modelled H_s (m)
Maximum	3.62	3.63
1% Exceedance	2.88	3.23
5% Exceedance	2.20	2.10
10% Exceedance	1.75	1.70
20% Exceedance	1.35	1.40
50% Exceedance	0.73	0.78
80% Exceedance	0.25	0.39
95% Exceedance	0.09	0.31

2.6 Sediment Model Calibration

No reliable suspended sediment concentration or sedimentation data is available during a dredging campaign to calibrate or validate the sediment transport module. As a result, some uncertainty will

exist in the results from the sediment transport modelling. To reduce the risk of this uncertainty, conservative values have been selected for the sediment transport modelling to ensure the model over estimates rather than underestimates the physical extent of the resultant sediment plume and deposition from the dredge disposal.

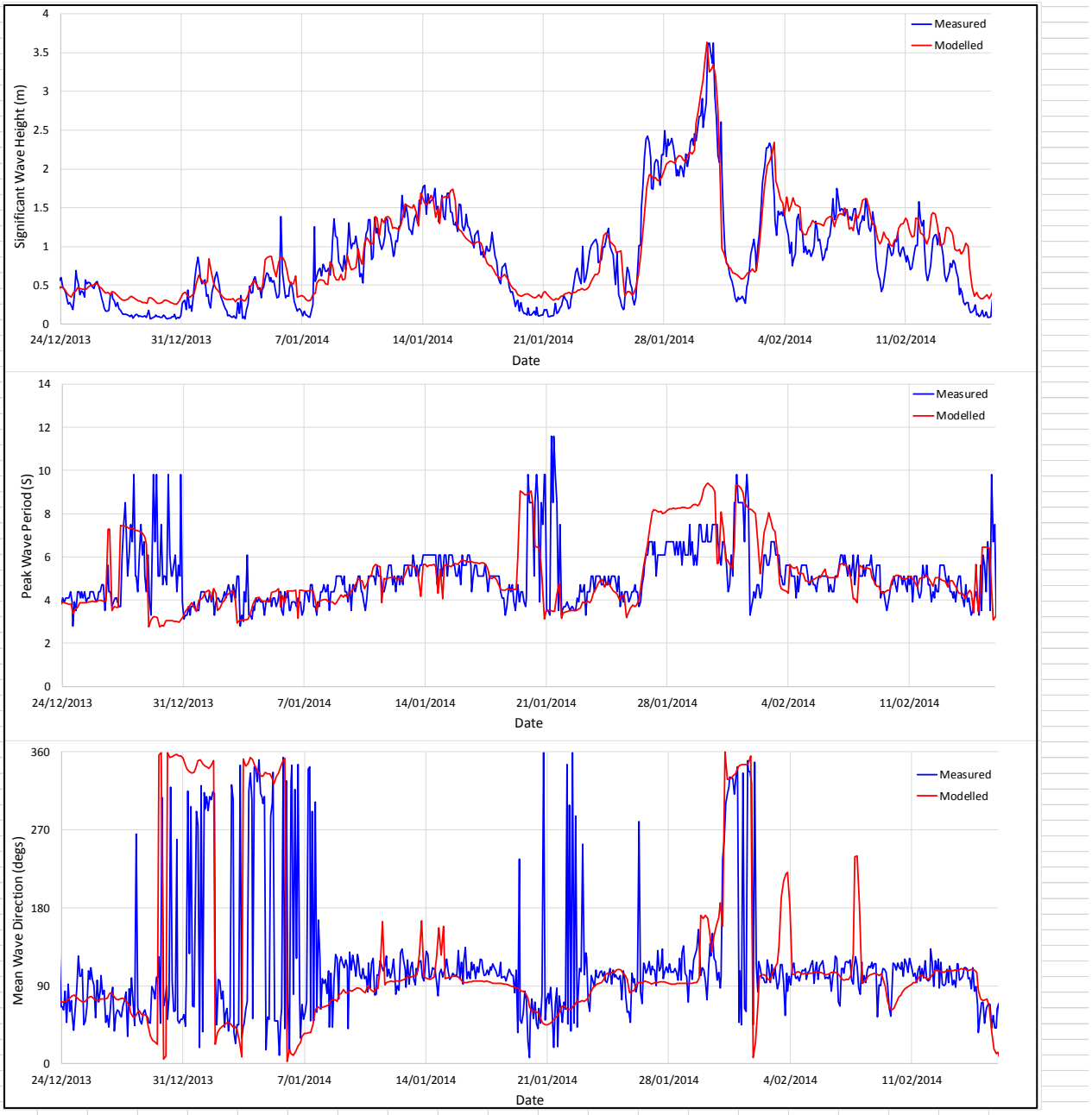

Figure 19 Wave calibration at Site 2.

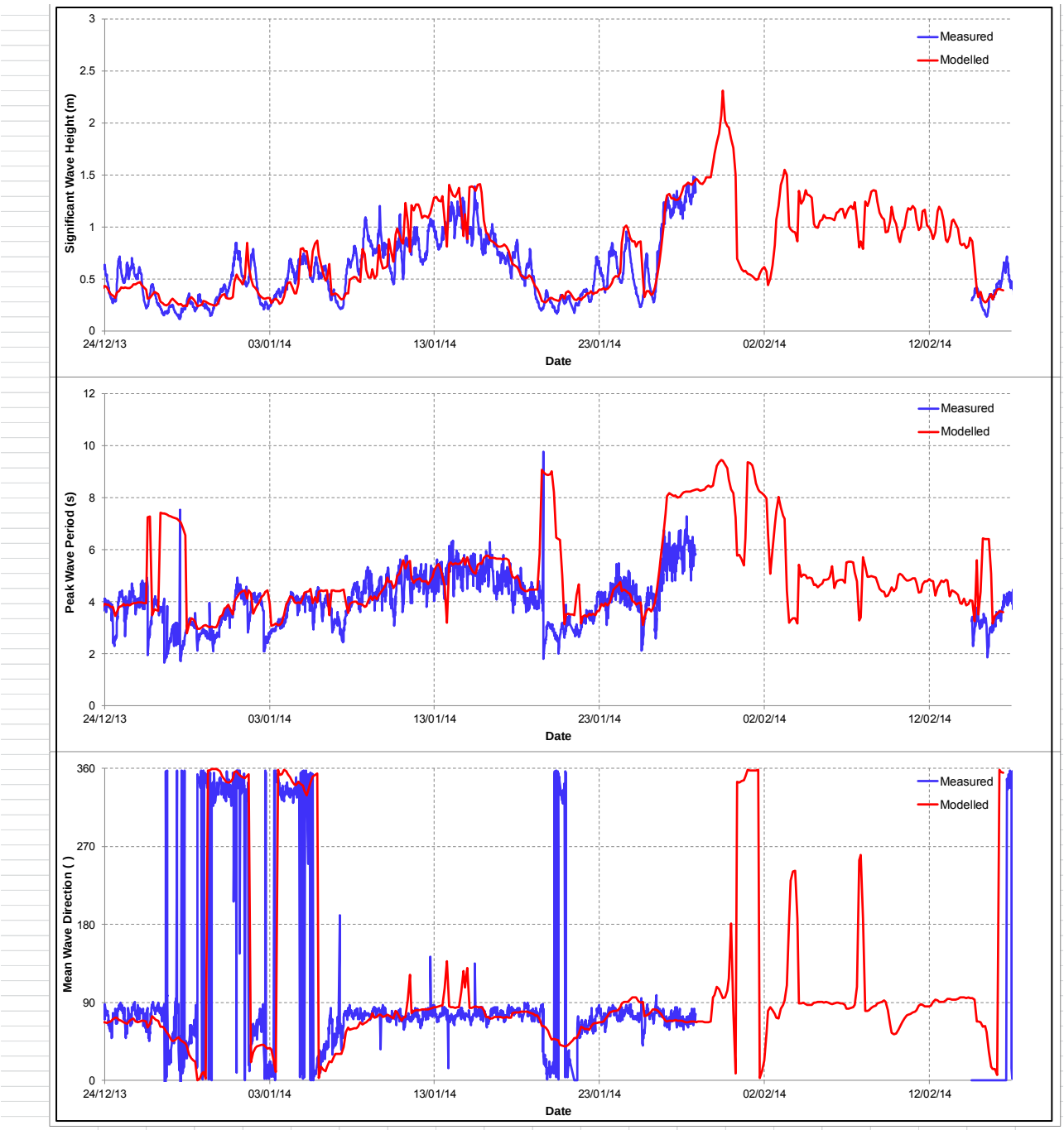

Figure 20 Wave calibration at the Abbot Point Waverider Buoy.

3 FINDINGS

This calibration and validation process has demonstrated that:

- the hydrodynamic model provides a good representation of water levels and currents at the two nearshore sites close to Abbot Point as well as offshore;
- the hydrodynamic model can accurately represent the resultant currents due to forcing from astronomical tides, local wind and regional circulation;
- the hydrodynamic model is capable of accurately representing the vertical variations in currents through the water column; and
- the wave model provides a good representation of wave conditions.

The good hydrodynamic and wave calibration achieved provides a high level of confidence in the modelling of the driving processes for the sediment transport modelling. However, the lack of suspended sediment calibration data during a dredging and disposal campaign means some uncertainty exists when estimating the resultant dredge plumes and sediment deposition. The implementation of the stochastic dredge plume modelling approach combined with the adoption of conservative values for the sediment transport modelling reduce this uncertainty.

APPENDIX C
Department of Environment Letter

Australian Government

Department of the Environment

Ref: EPBC 2011/6213

Mr Paul Doyle
Manager Environment Business Development
North Queensland Bulk Ports Corporation
GPO Box 409
BRISBANE QLD 4001

Dear Mr Doyle

Abbot Point Terminal 0, 2 and 3 Capital Dredging Project—EPBC 2011/6213

I refer to the draft Disposal Site Analysis Plan (DSAP) methodology dated 21 February 2014.

The Department has reviewed the draft methodology noting that since the document was submitted there have been discussions between your organisation and the Department about how the assessment of alternative disposal locations will be undertaken. In particular, the Hydrodynamic Modelling Scope has been revised incorporating comments from the Great Barrier Reef Marine Park Authority (GBRMPA) and the Australian Institute of Marine Science. The modelling is an important component of the comparative assessment and I note the changes adopted in the revised scope build on the work previously undertaken to identify disposal sites.

I also note that the proposed comparative assessment criteria broadly include the information requirements as outlined in the National Assessment Guidelines for Dredging (2009) and that the assessment will take into consideration the information in the Improved Dredge Material Management for the Great Barrier Reef Region (2013) report.

Therefore, given the level of consultation and general consensus on the approach going forward, the Department supports the further development of the draft DSAP and comparative assessment. I note that your organisation will continue to work with the Department, the GBRMPA and key stakeholders as necessary on the development of the DSAP and other plans required under the *Environment Protection and Biodiversity Conservation Act 1999* conditions of approval.

Should you have any questions please contact Chris Murphy, Director, Queensland and Sea Dumping Assessments, at Chris.Murphy@environment.gov.au or phone 02 6274 2014.

Yours sincerely

Deb Callister
Assistant Secretary
Queensland and Sea Dumping Assessment Branch

~~June~~ 2014
4 July

APPENDIX D
Time Series Results

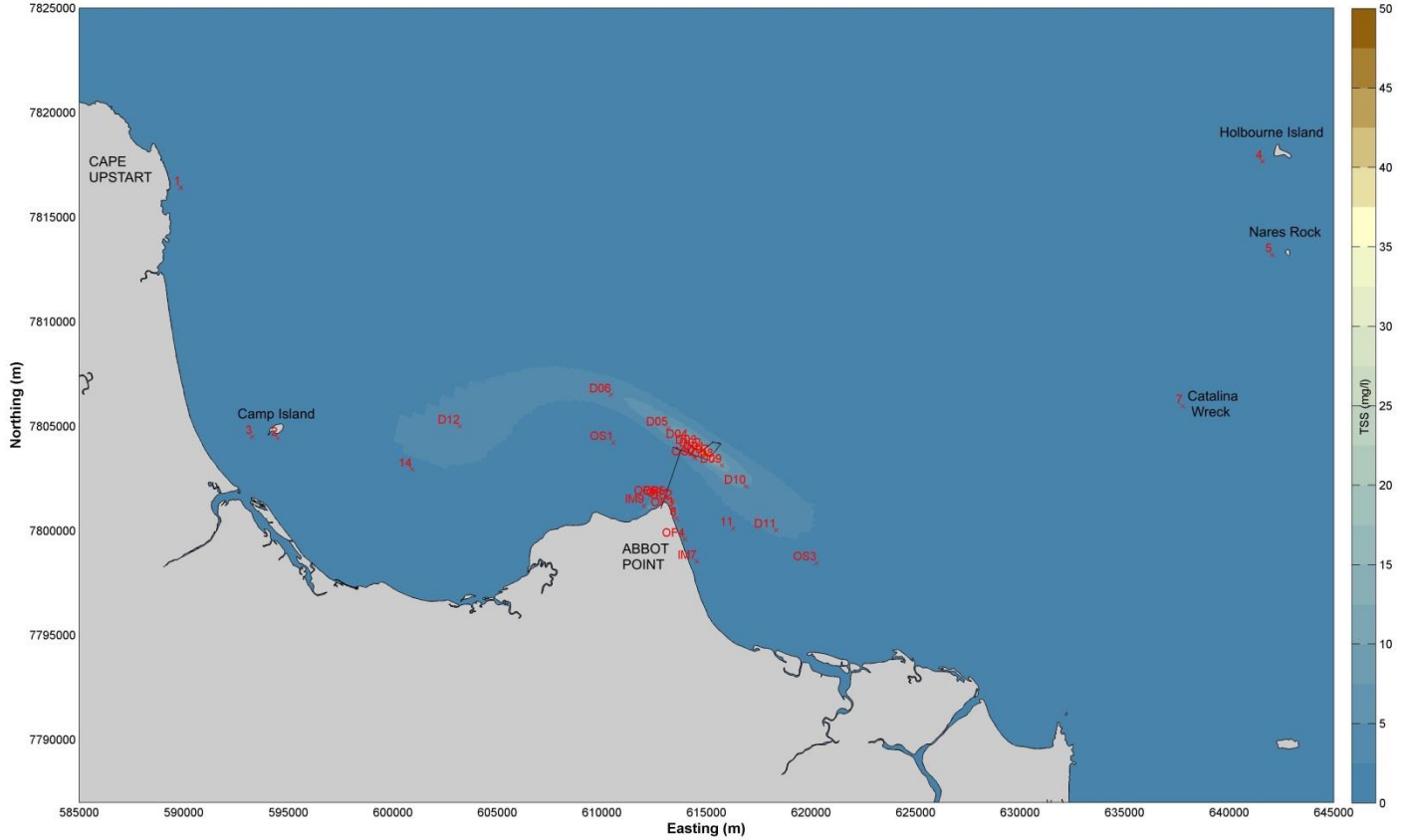

Figure 1 Time series output locations superimposed on the Neutral year average 95th percentile TSS.

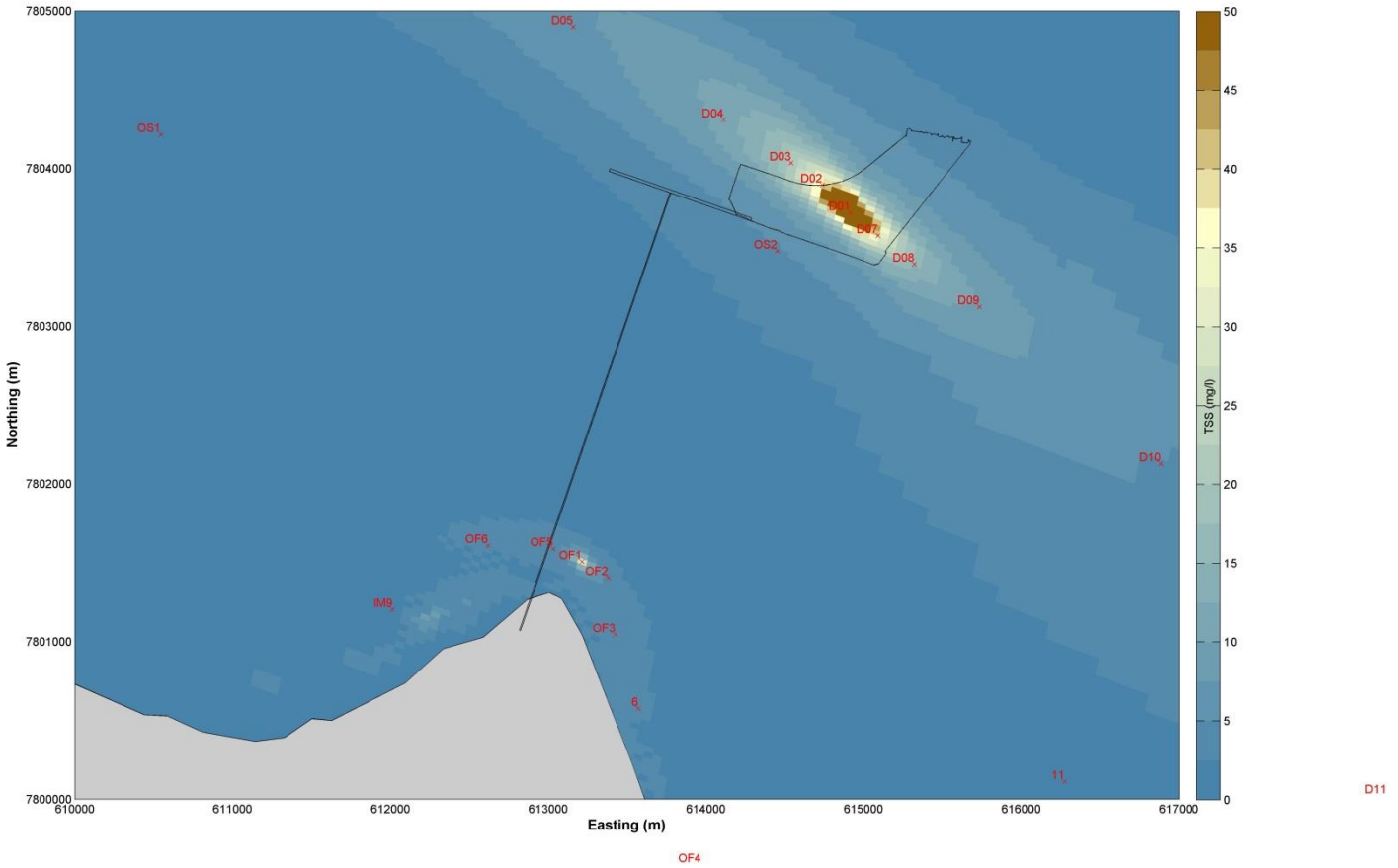

Figure 2 Time series output locations zoomed in to the dredge area and outfall superimposed on the all year average 95th percentile TSS.

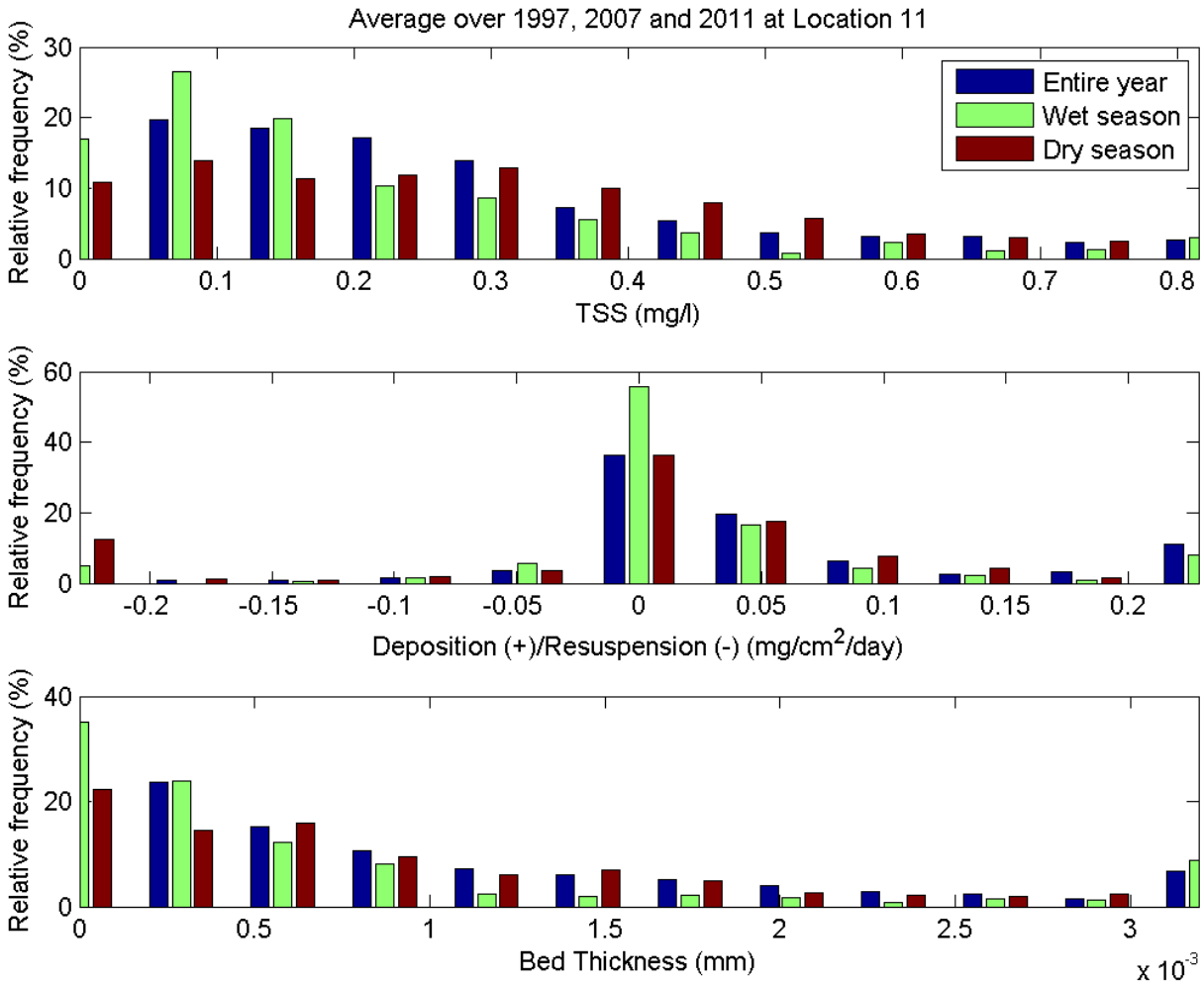

Figure 3 Histogram of TSS, deposition/resuspension and bed thickness for all simulations at site 11.

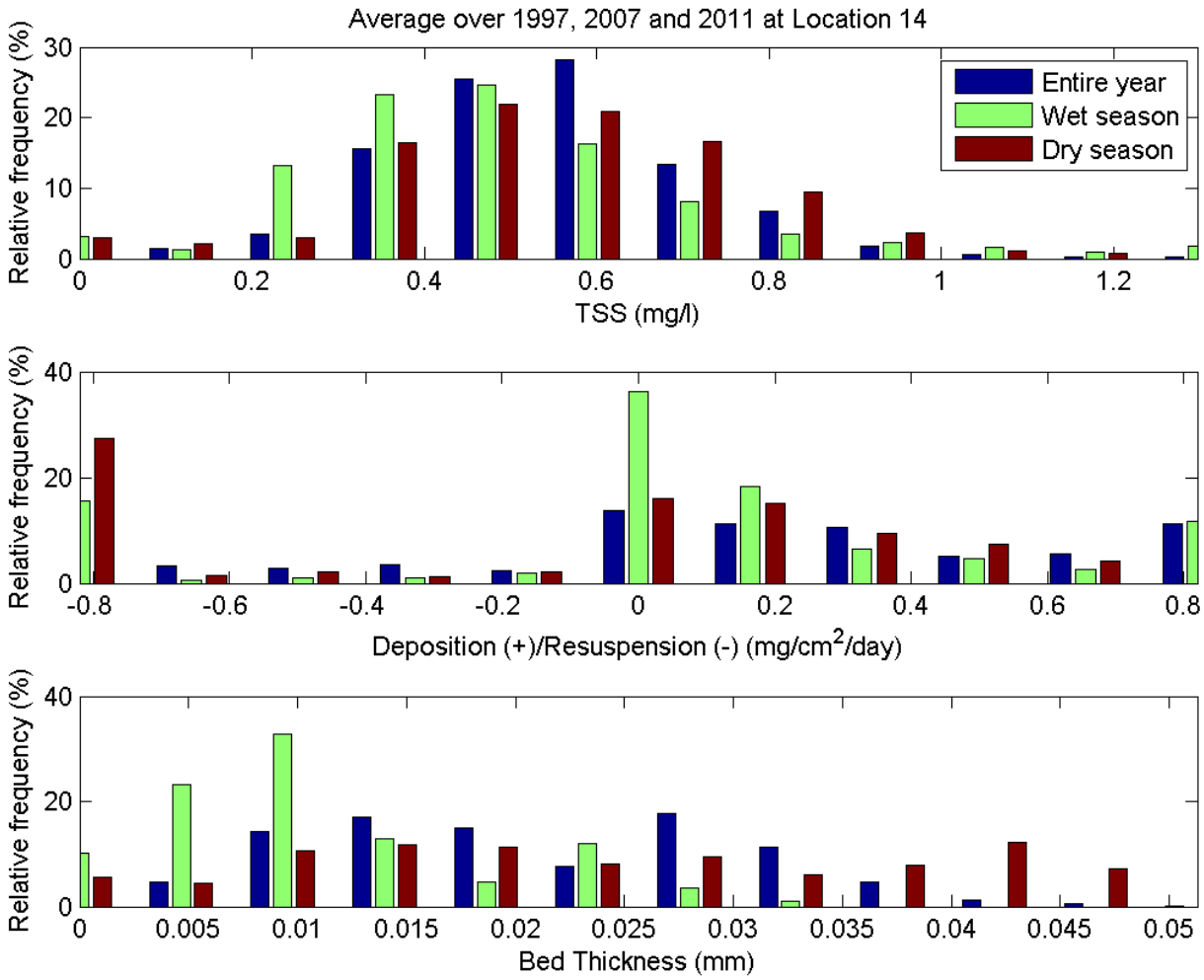

Figure 4 Histogram of TSS, deposition/resuspension and bed thickness for all simulations at site 14.

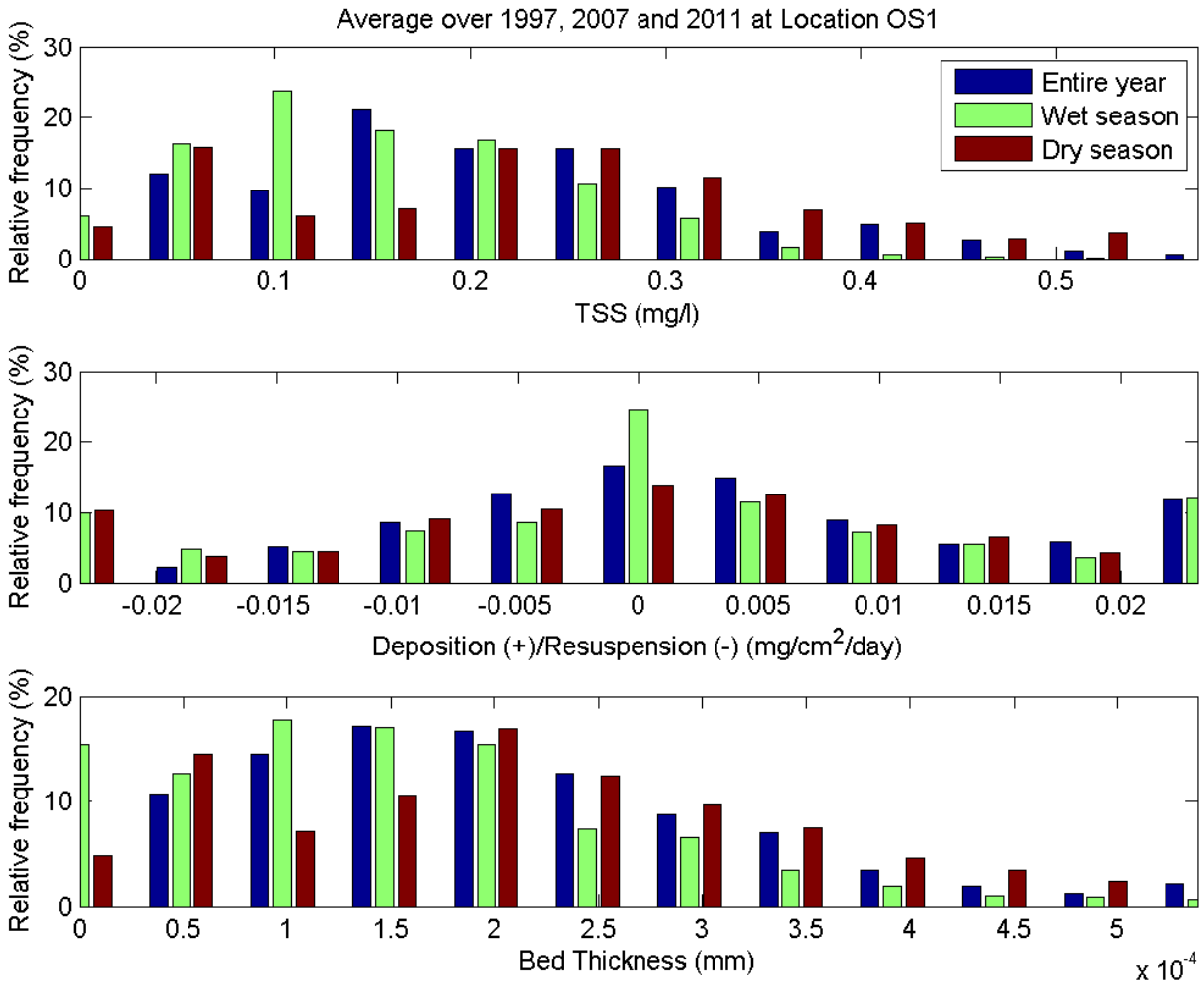

Figure 5 Histogram of TSS, deposition/resuspension and bed thickness for all simulations at site OS1.

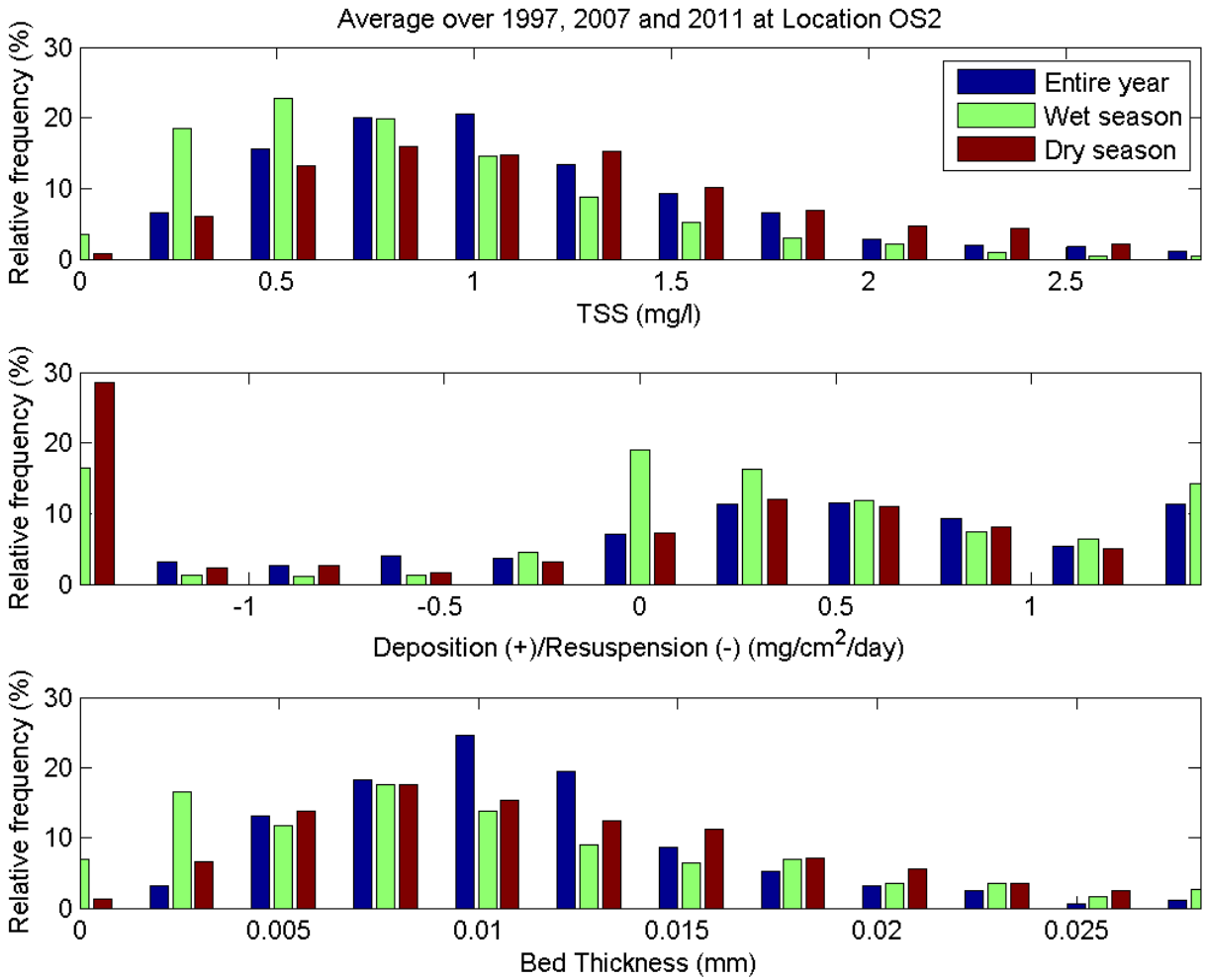

Figure 6 Histogram of TSS, deposition/resuspension and bed thickness for all simulations at site OS2.

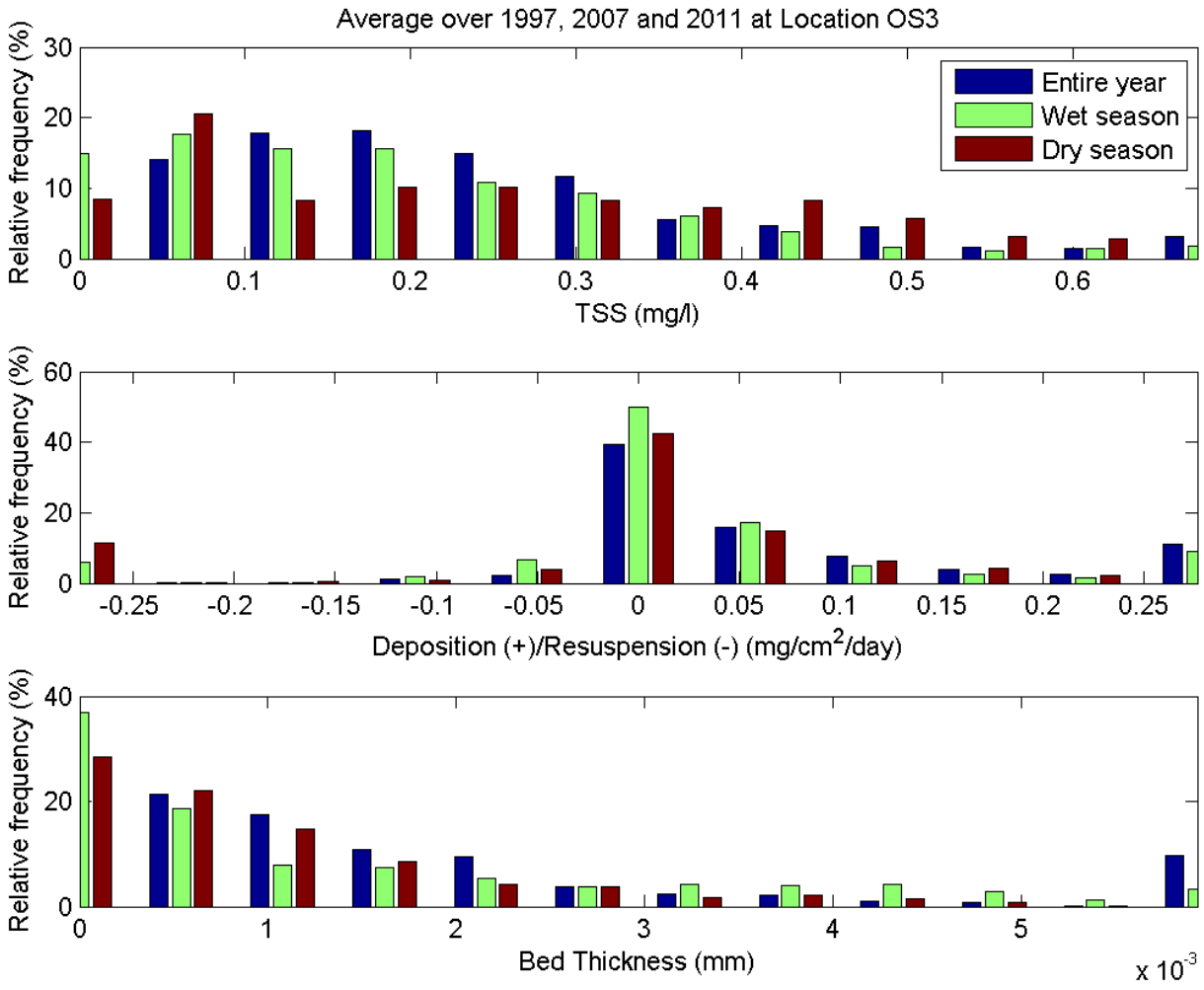

Figure 7 Histogram of TSS, deposition/resuspension and bed thickness for all simulations at site OS3.

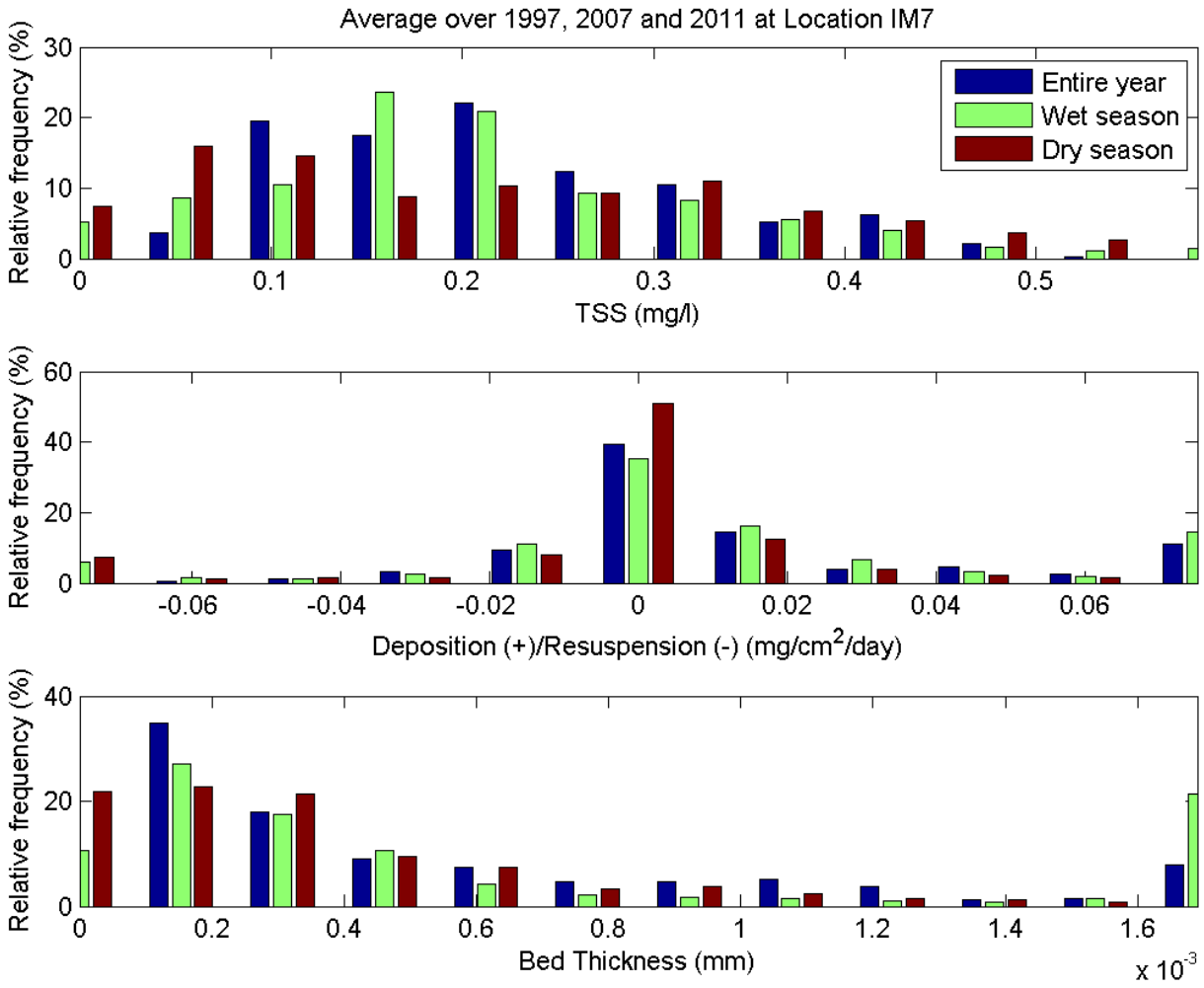

Figure 8 Histogram of TSS, deposition/resuspension and bed thickness for all simulations at site IM7.

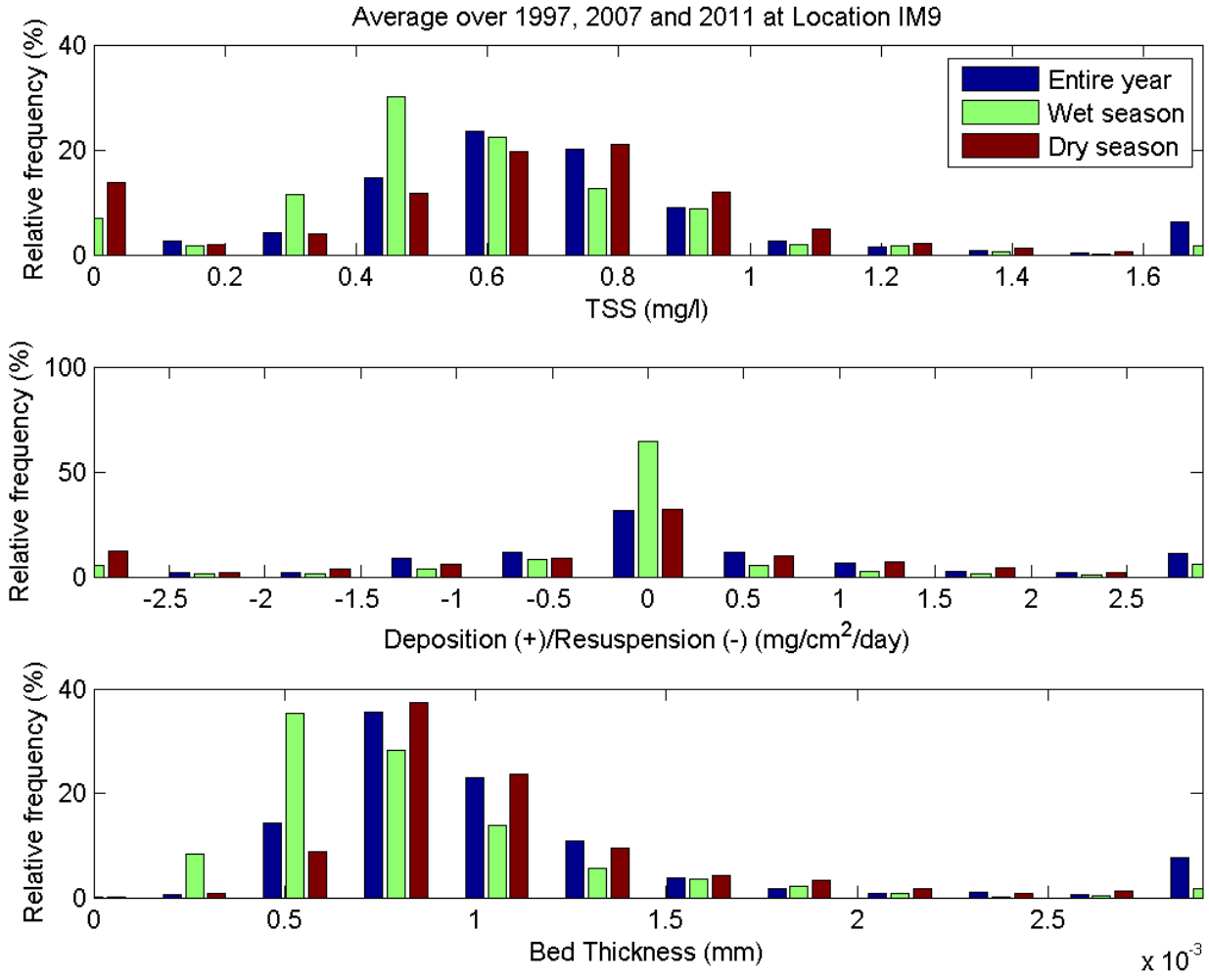

Figure 9 Histogram of TSS, deposition/resuspension and bed thickness for all simulations at site IM9.

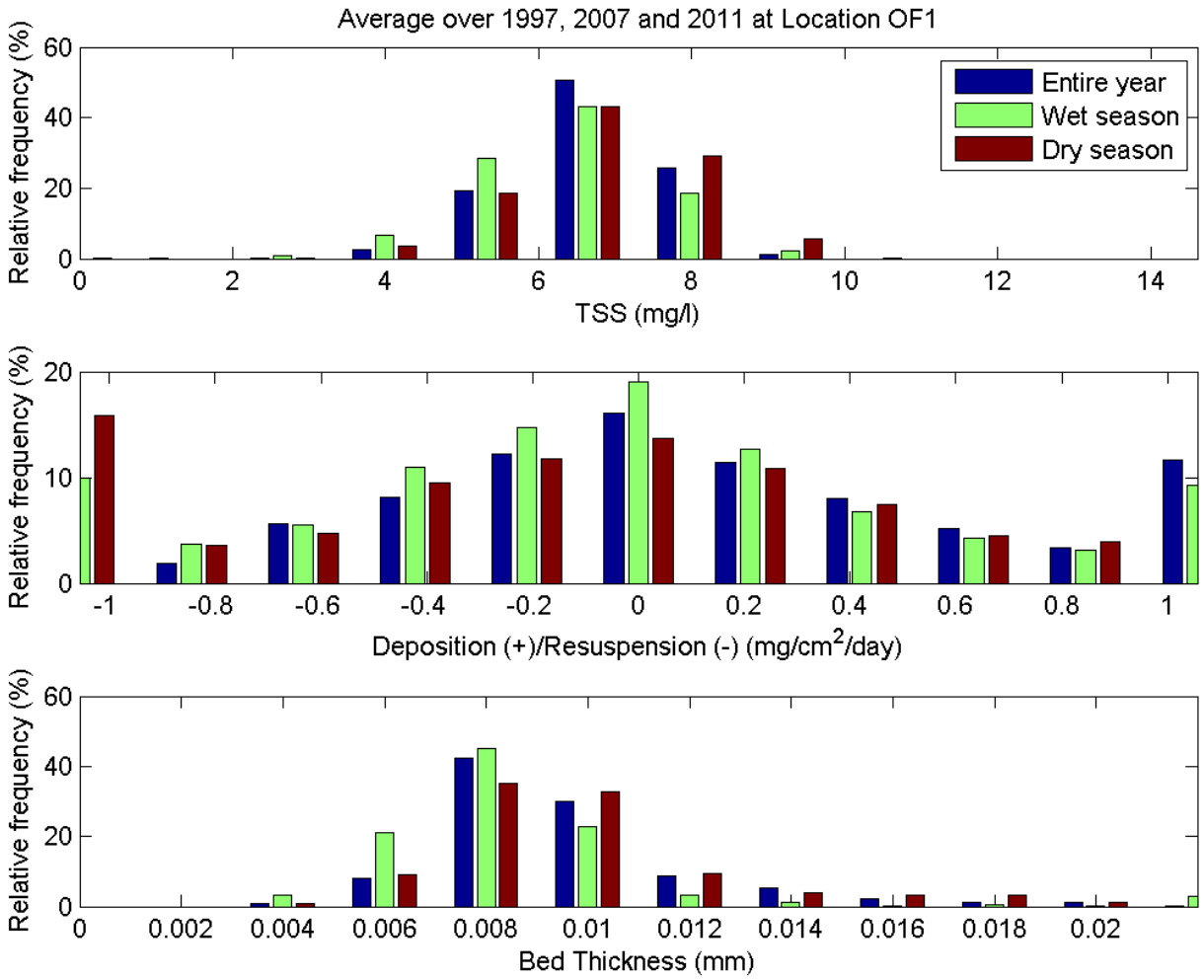

Figure 10 Histogram of TSS, deposition/resuspension and bed thickness for all simulations at site OF1.

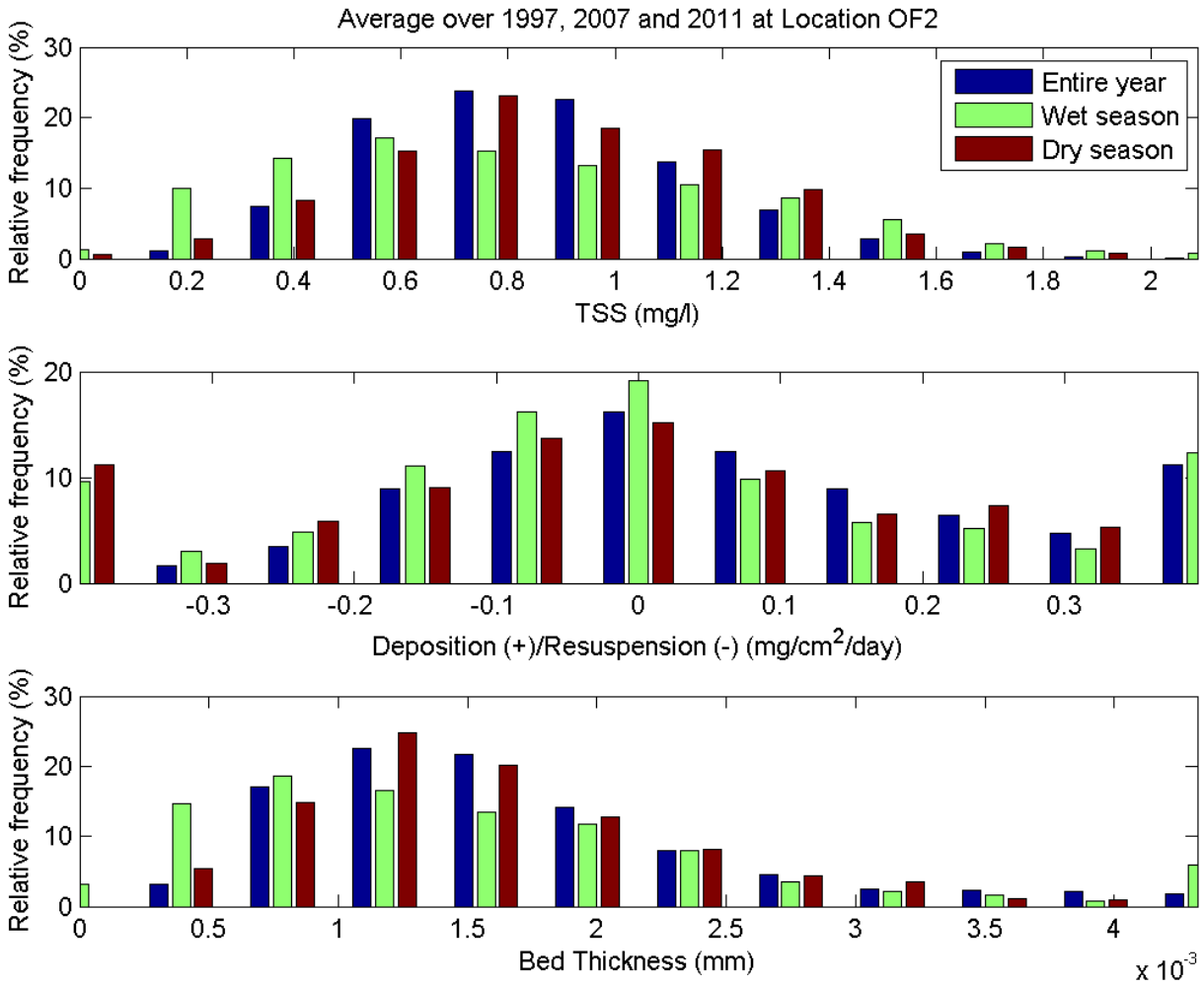

Figure 11 Histogram of TSS, deposition/resuspension and bed thickness for all simulations at site OF2.

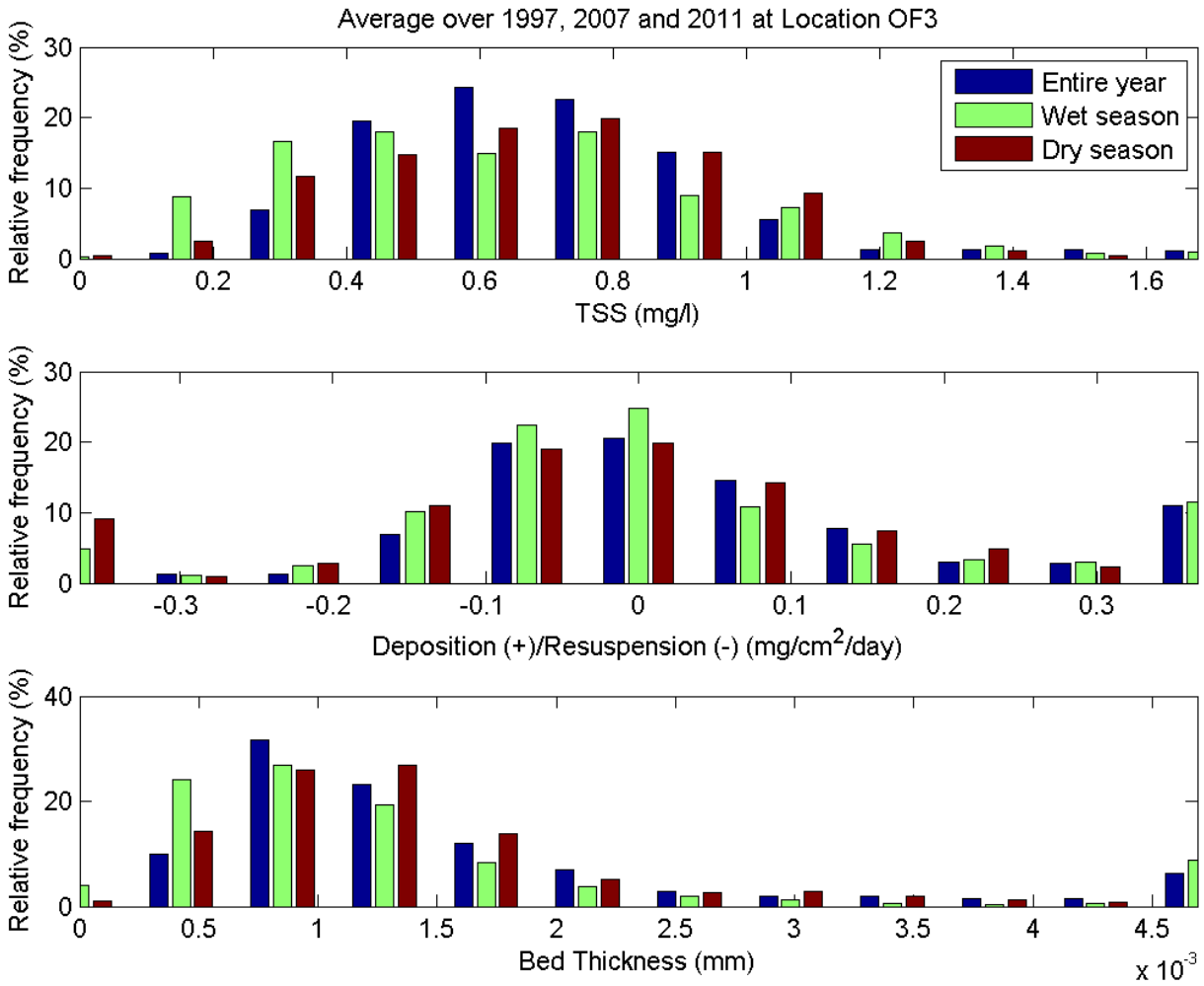

Figure 12 Histogram of TSS, deposition/resuspension and bed thickness for all simulations at site OF3.

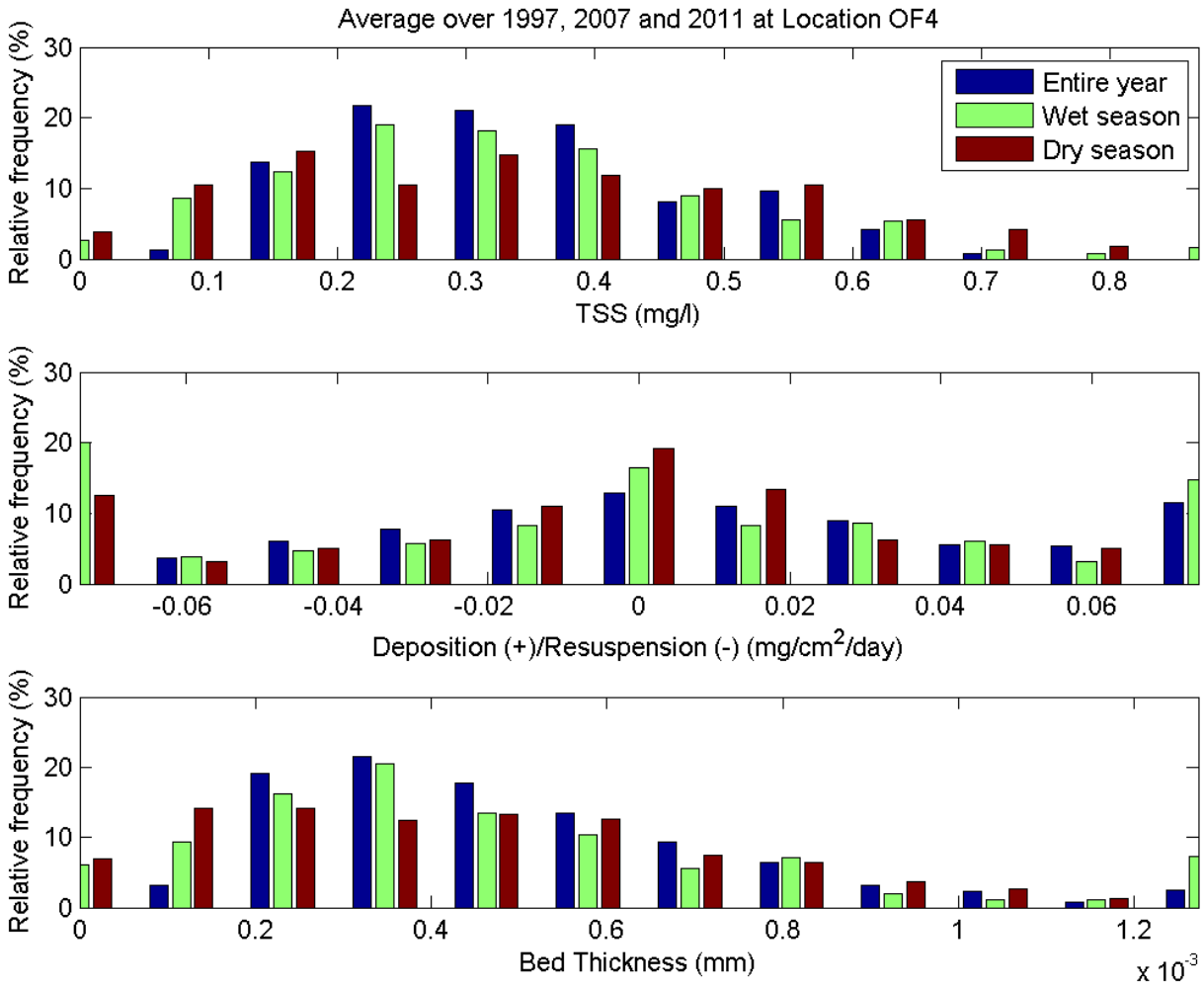

Figure 13 Histogram of TSS, deposition/resuspension and bed thickness for all simulations at site OF4.

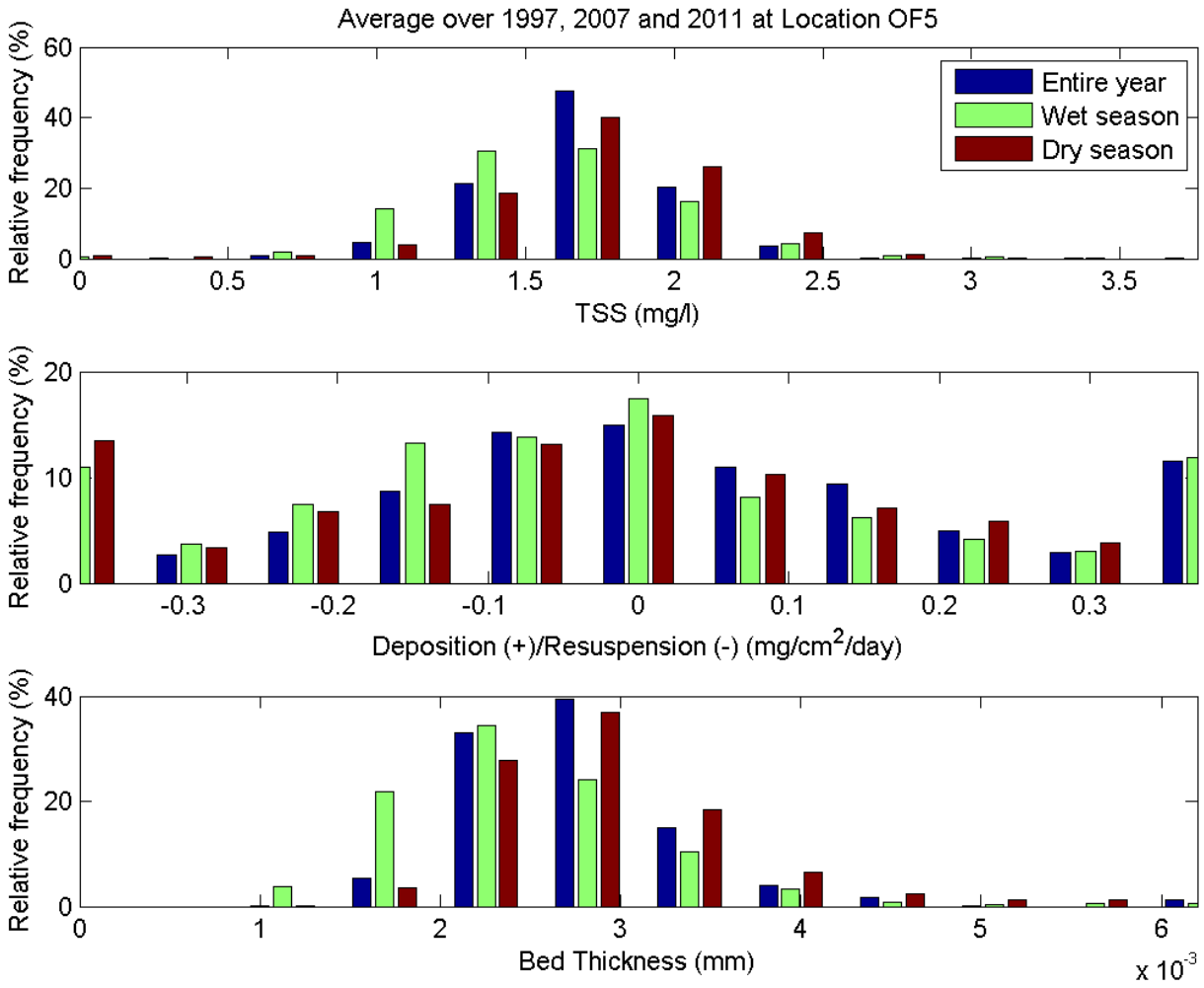

Figure 14 Histogram of TSS, deposition/resuspension and bed thickness for all simulations at site OF5.

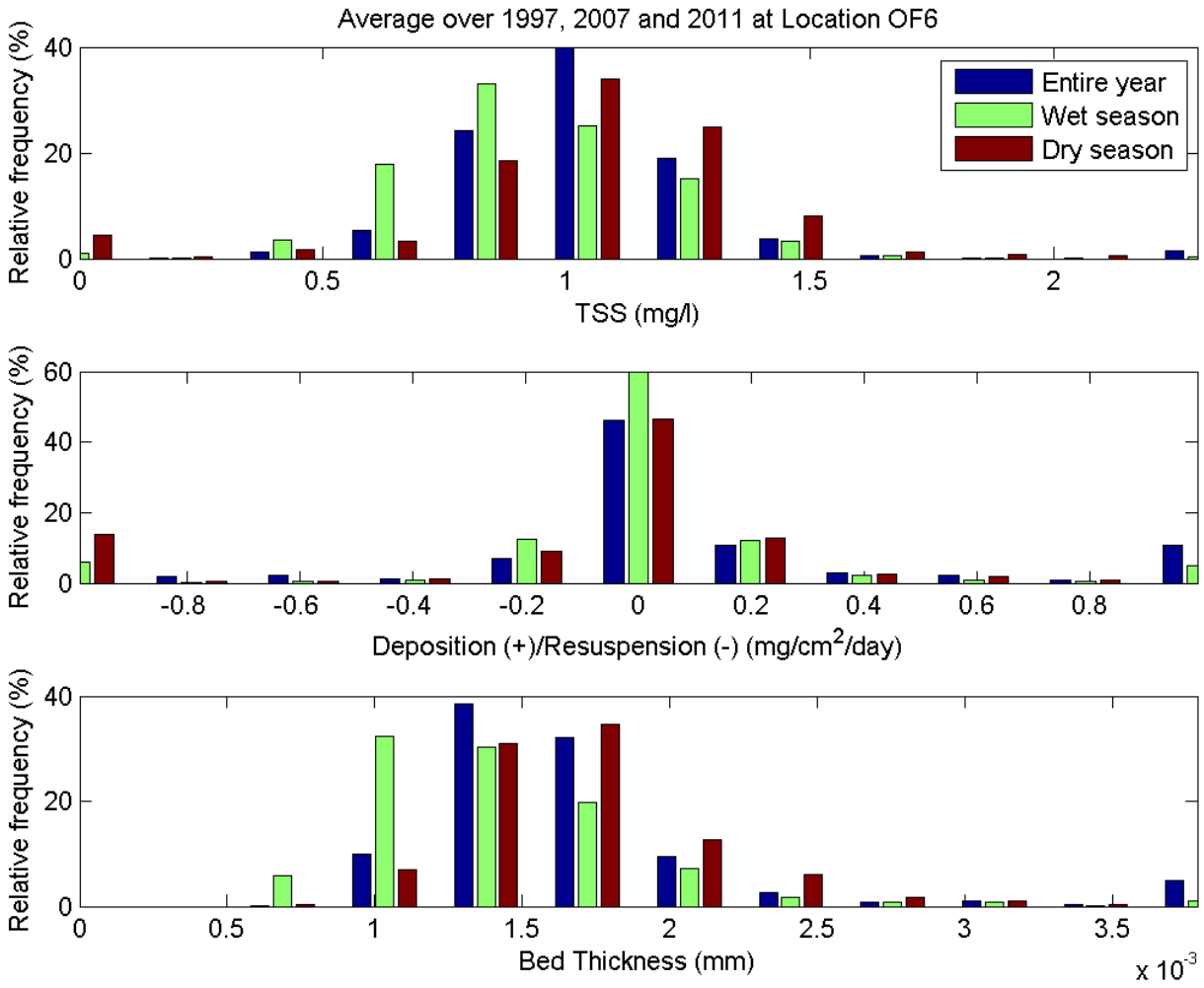

Figure 15 Histogram of TSS, deposition/resuspension and bed thickness for all simulations at site OF6.

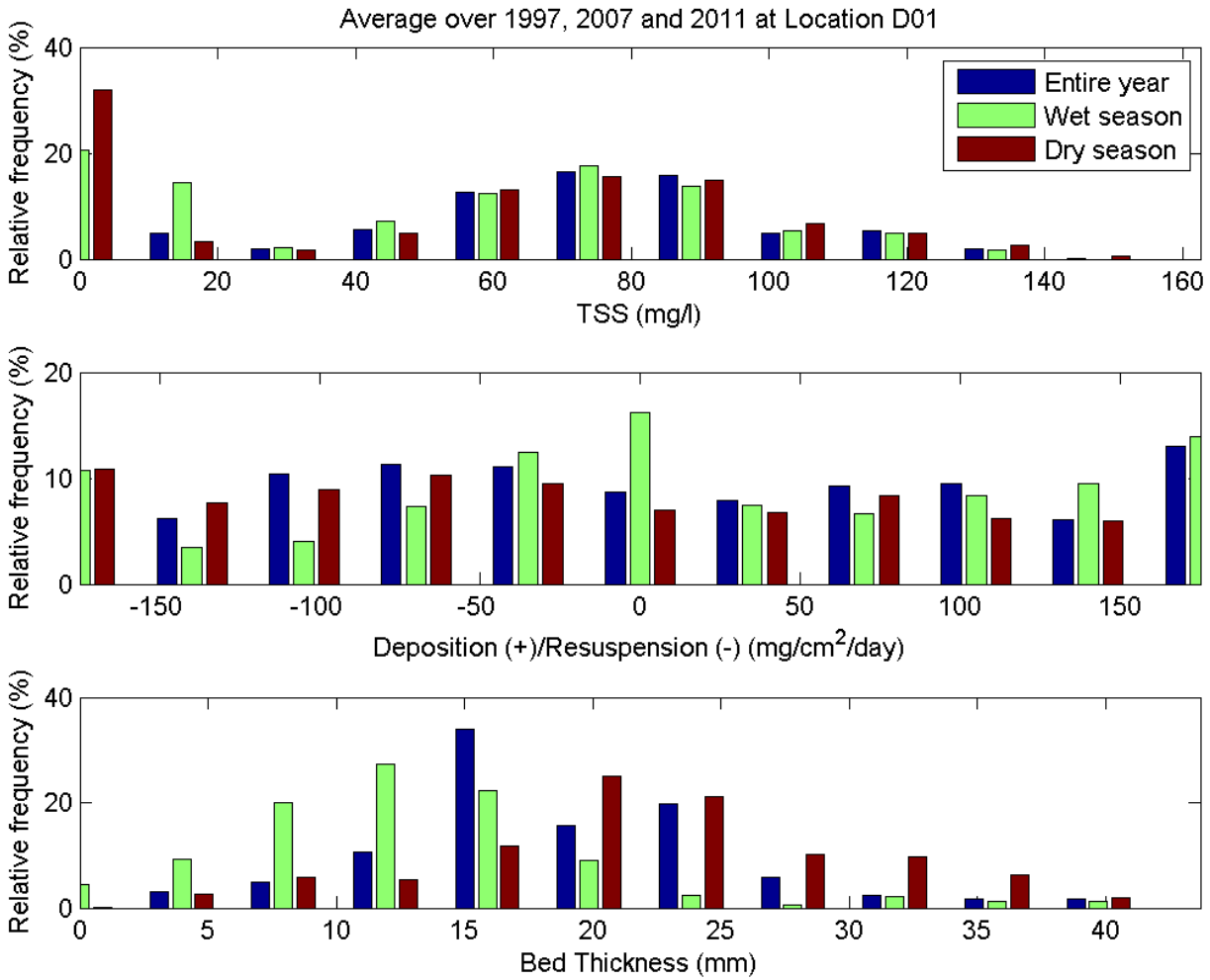

Figure 16 Histogram of TSS, deposition/resuspension and bed thickness for all simulations at site D01.

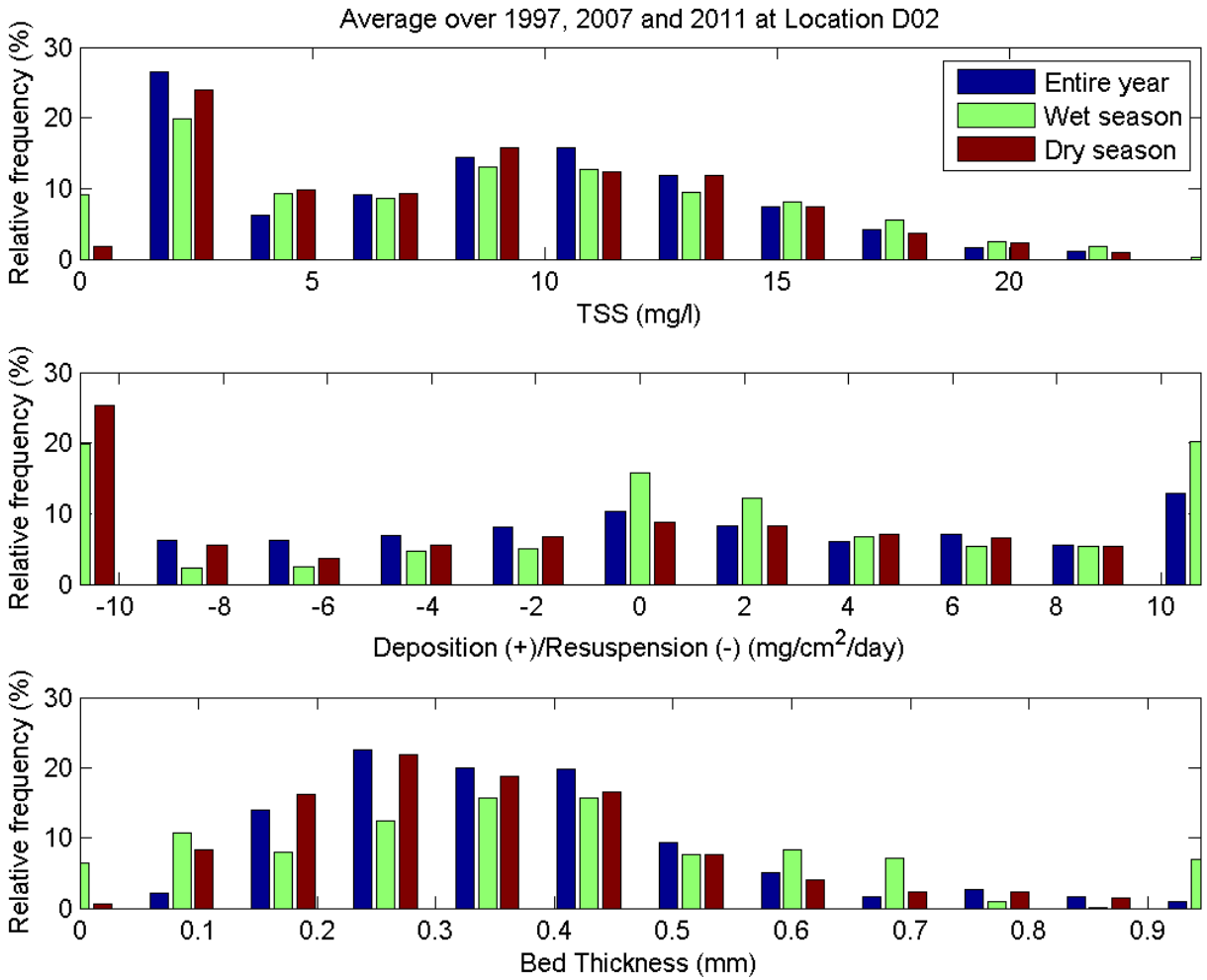

Figure 17 Histogram of TSS, deposition/resuspension and bed thickness for all simulations at site D02.

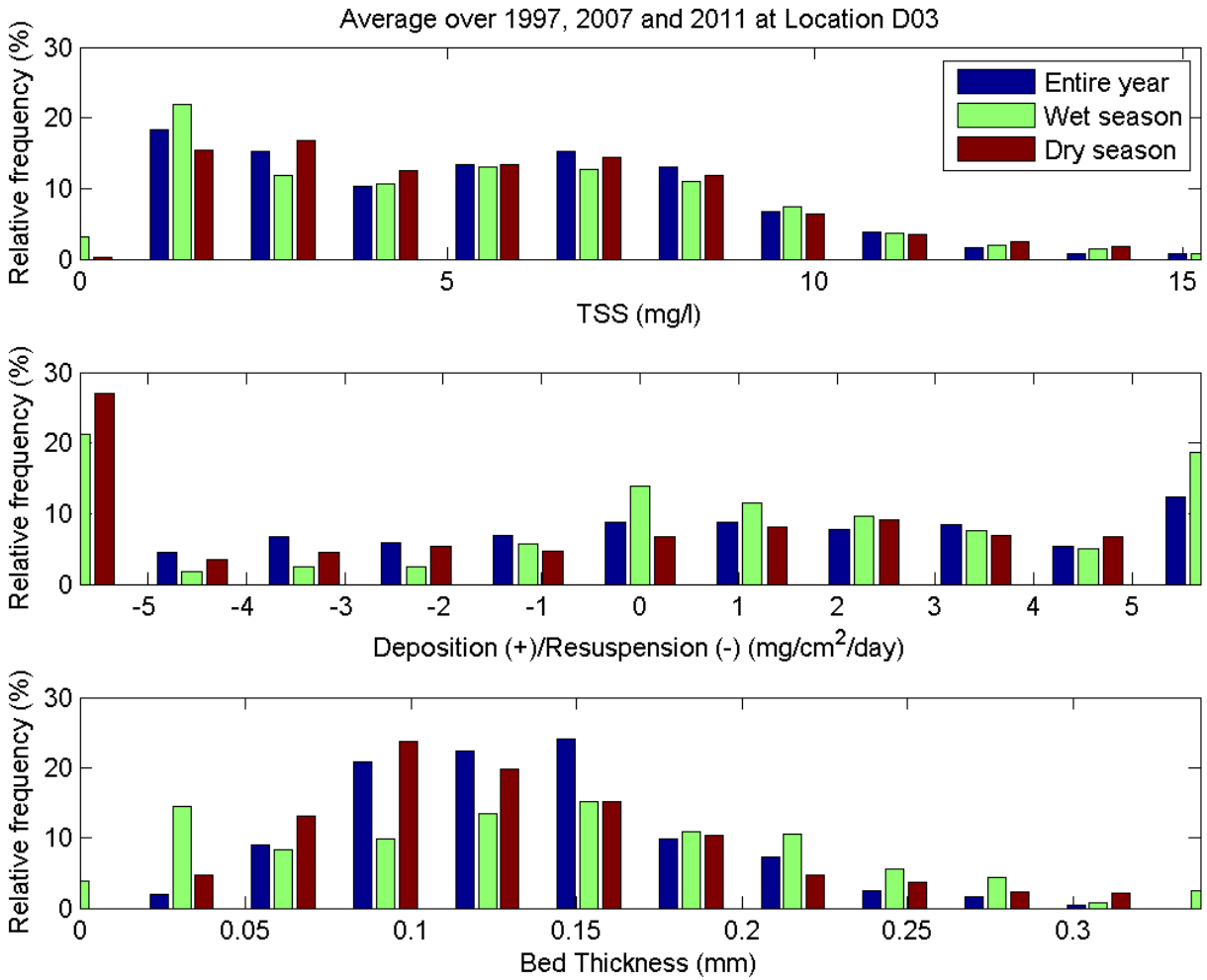

Figure 18 Histogram of TSS, deposition/resuspension and bed thickness for all simulations at site D03.

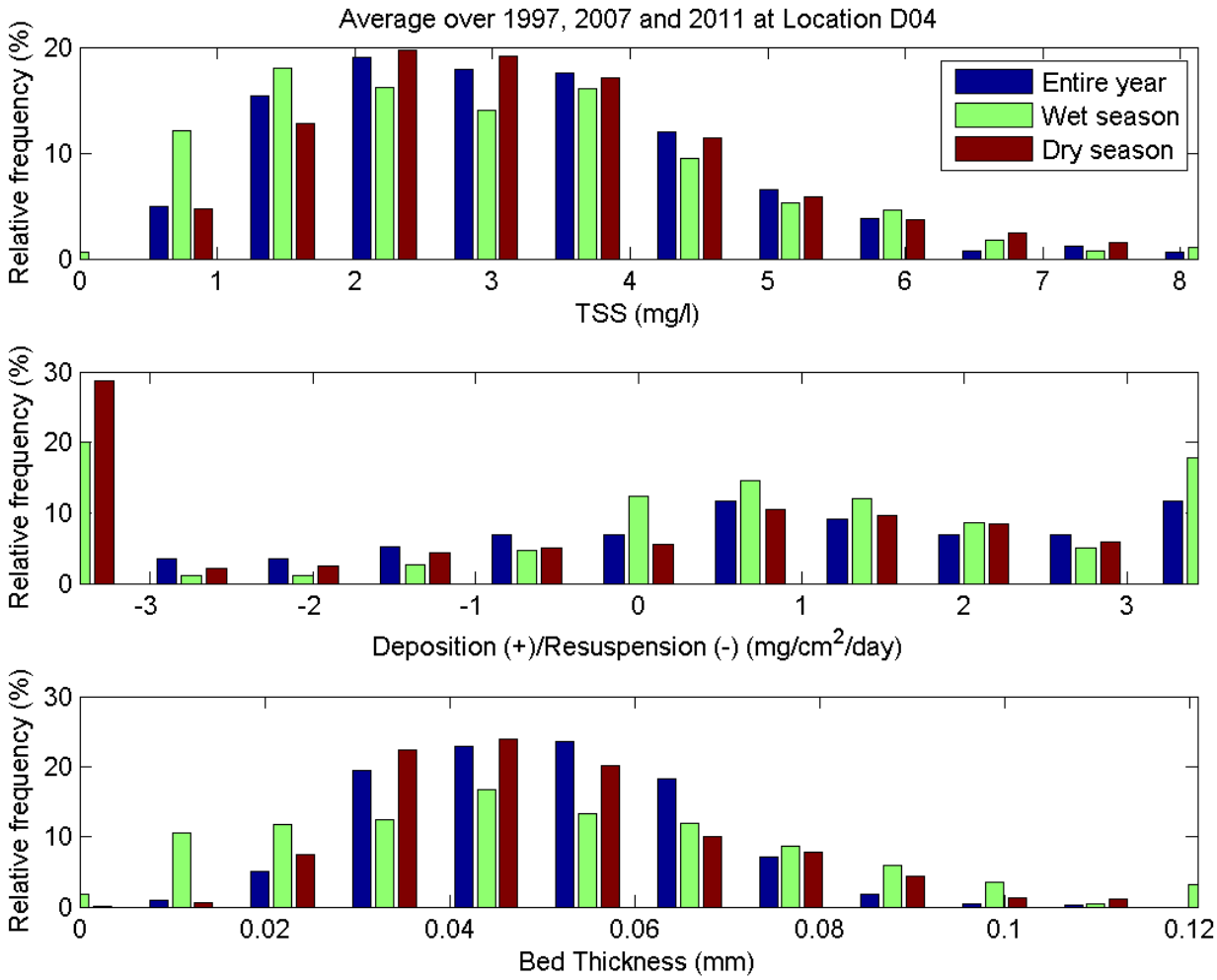

Figure 19 Histogram of TSS, deposition/resuspension and bed thickness for all simulations at site D04.

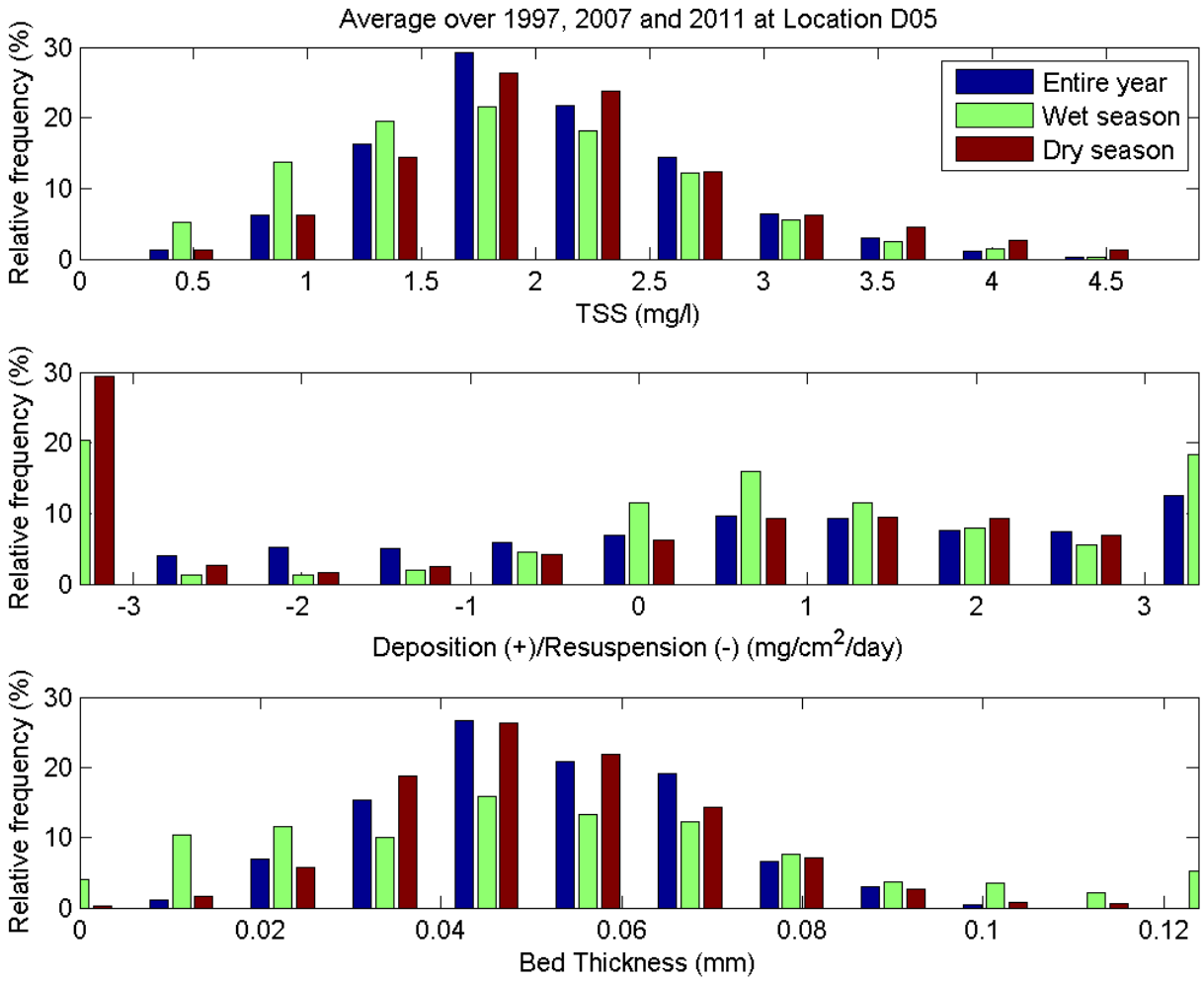

Figure 20 Histogram of TSS, deposition/resuspension and bed thickness for all simulations at site D05.

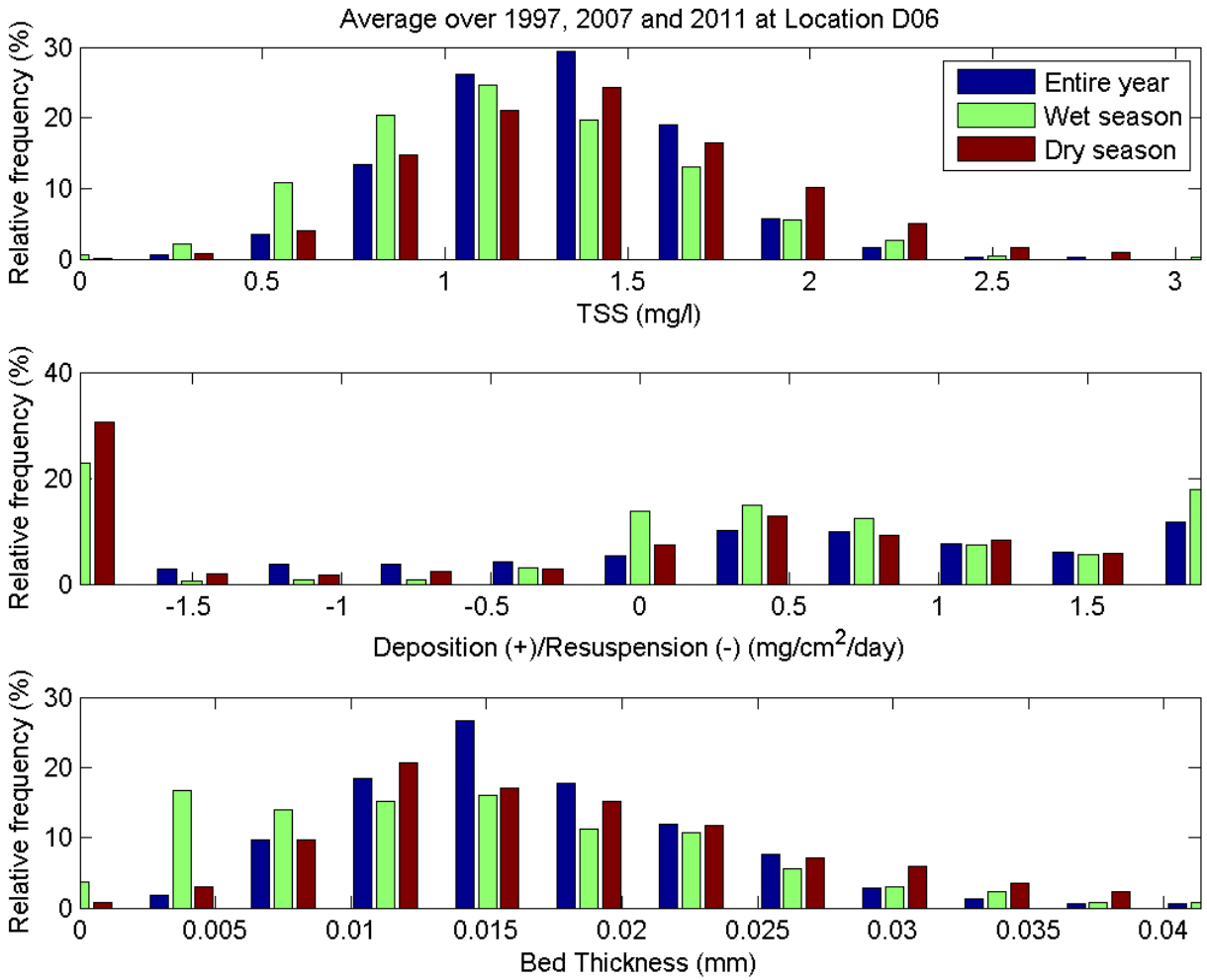

Figure 21 Histogram of TSS, deposition/resuspension and bed thickness for all simulations at site D06.

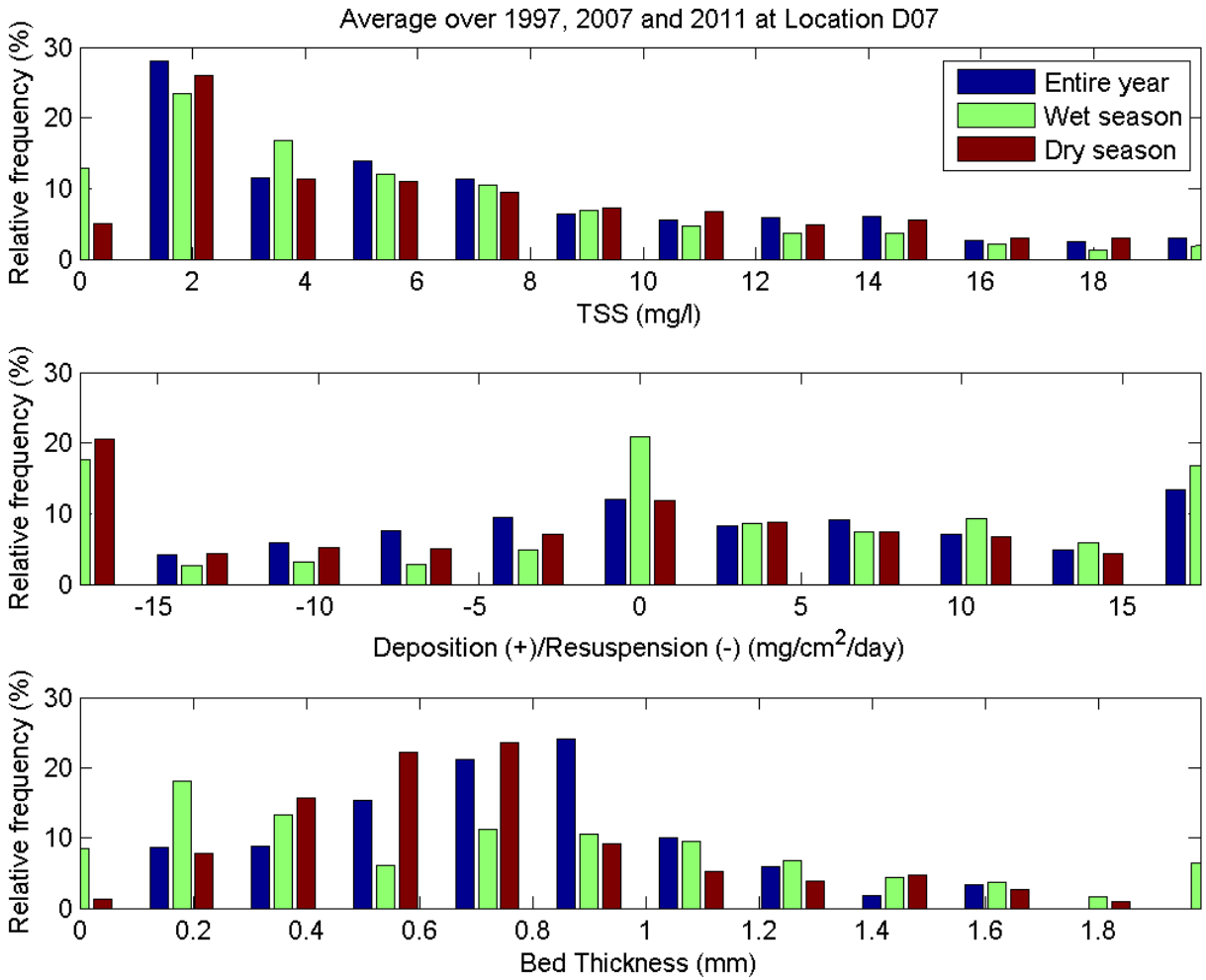

Figure 22 Histogram of TSS, deposition/resuspension and bed thickness for all simulations at site D07.

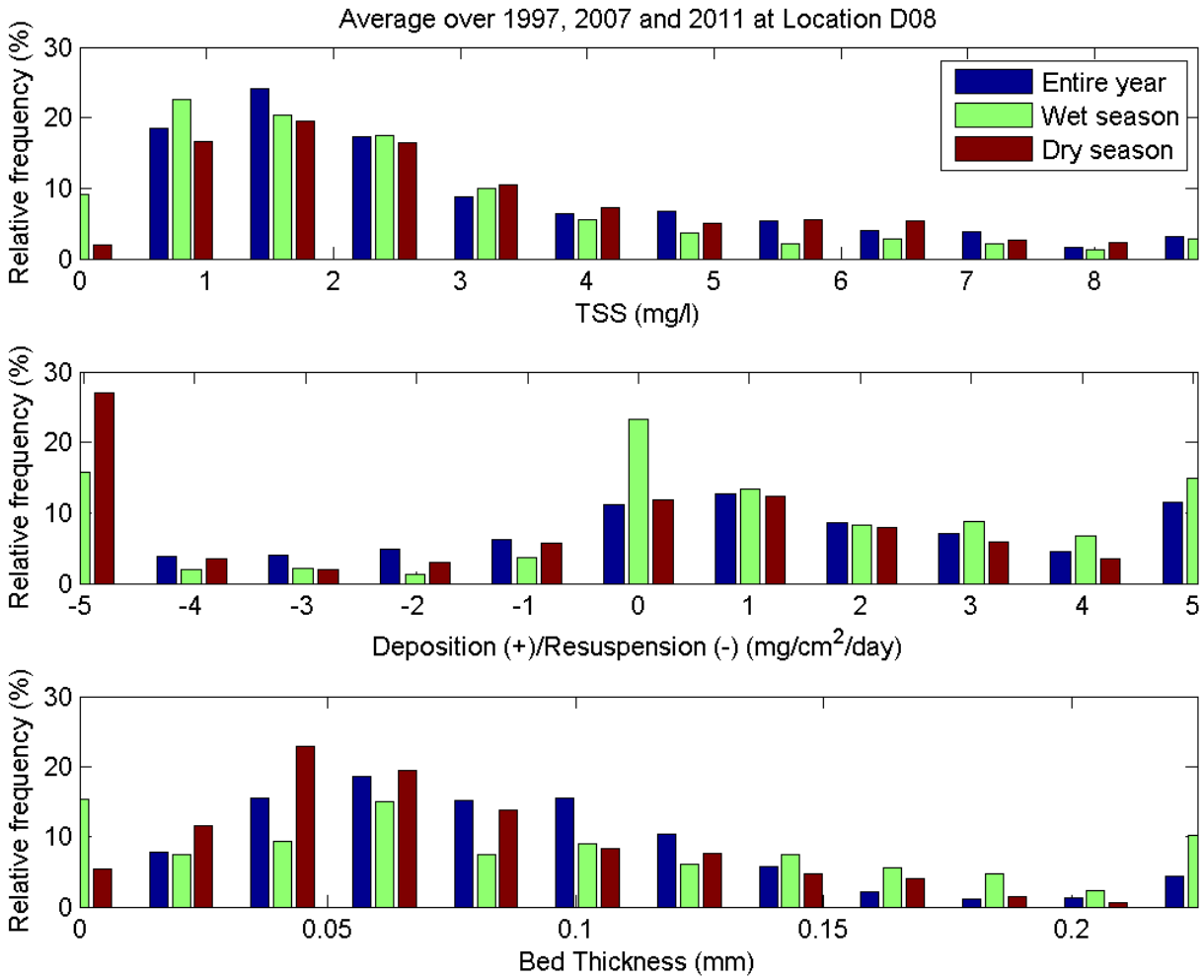

Figure 23 Histogram of TSS, deposition/resuspension and bed thickness for all simulations at site D08.

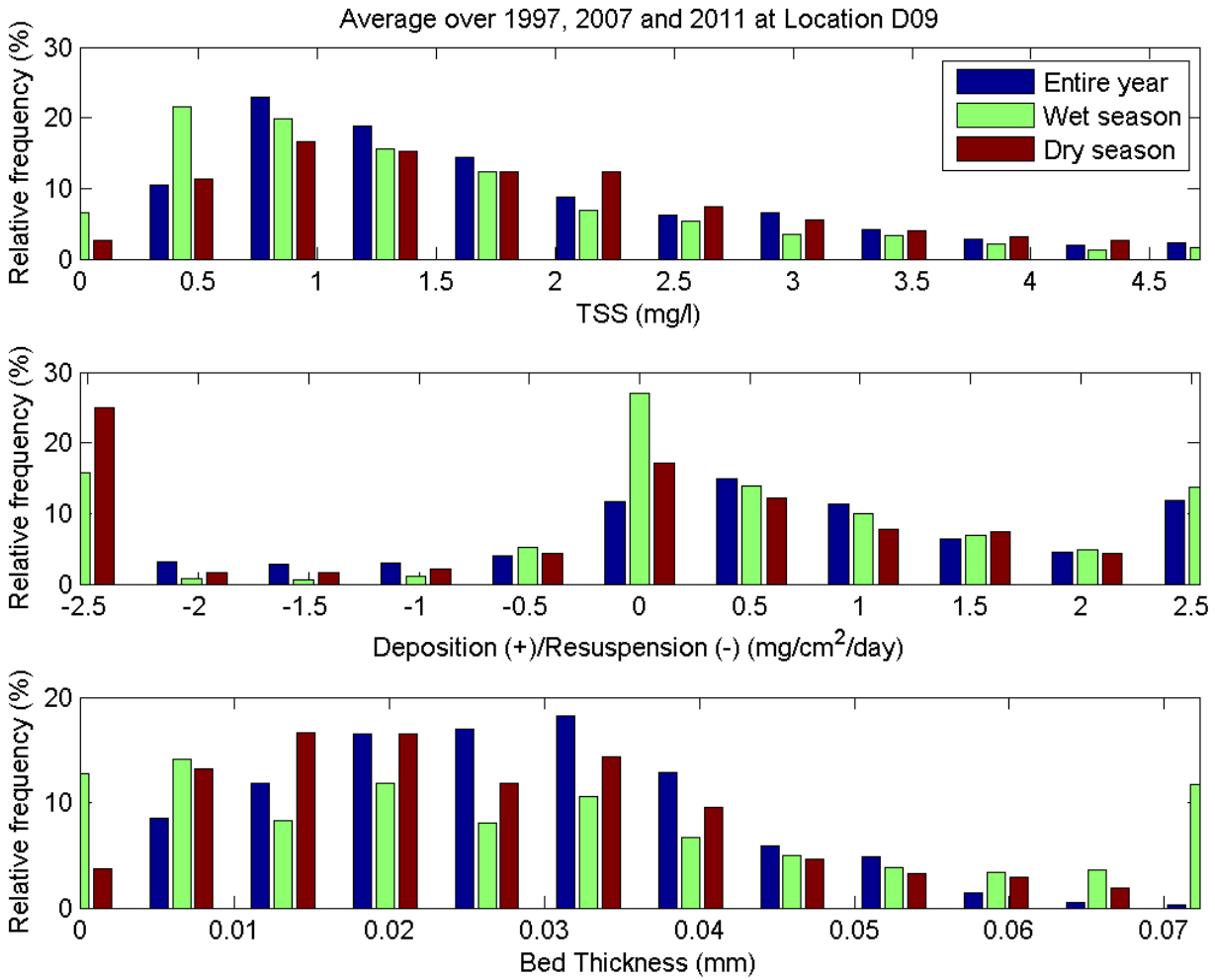

Figure 24 Histogram of TSS, deposition/resuspension and bed thickness for all simulations at site D09.

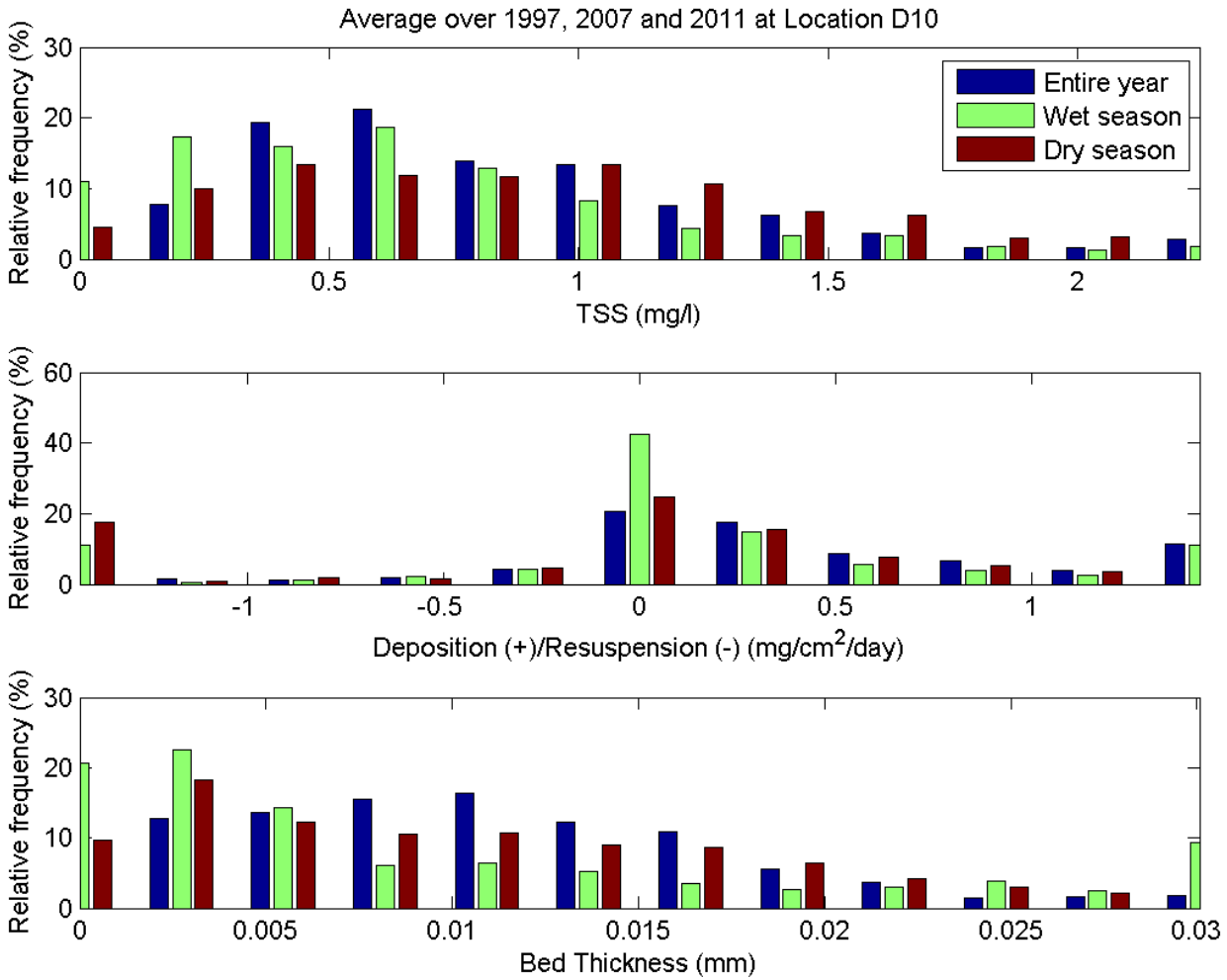

Figure 25 Histogram of TSS, deposition/resuspension and bed thickness for all simulations at site D10.

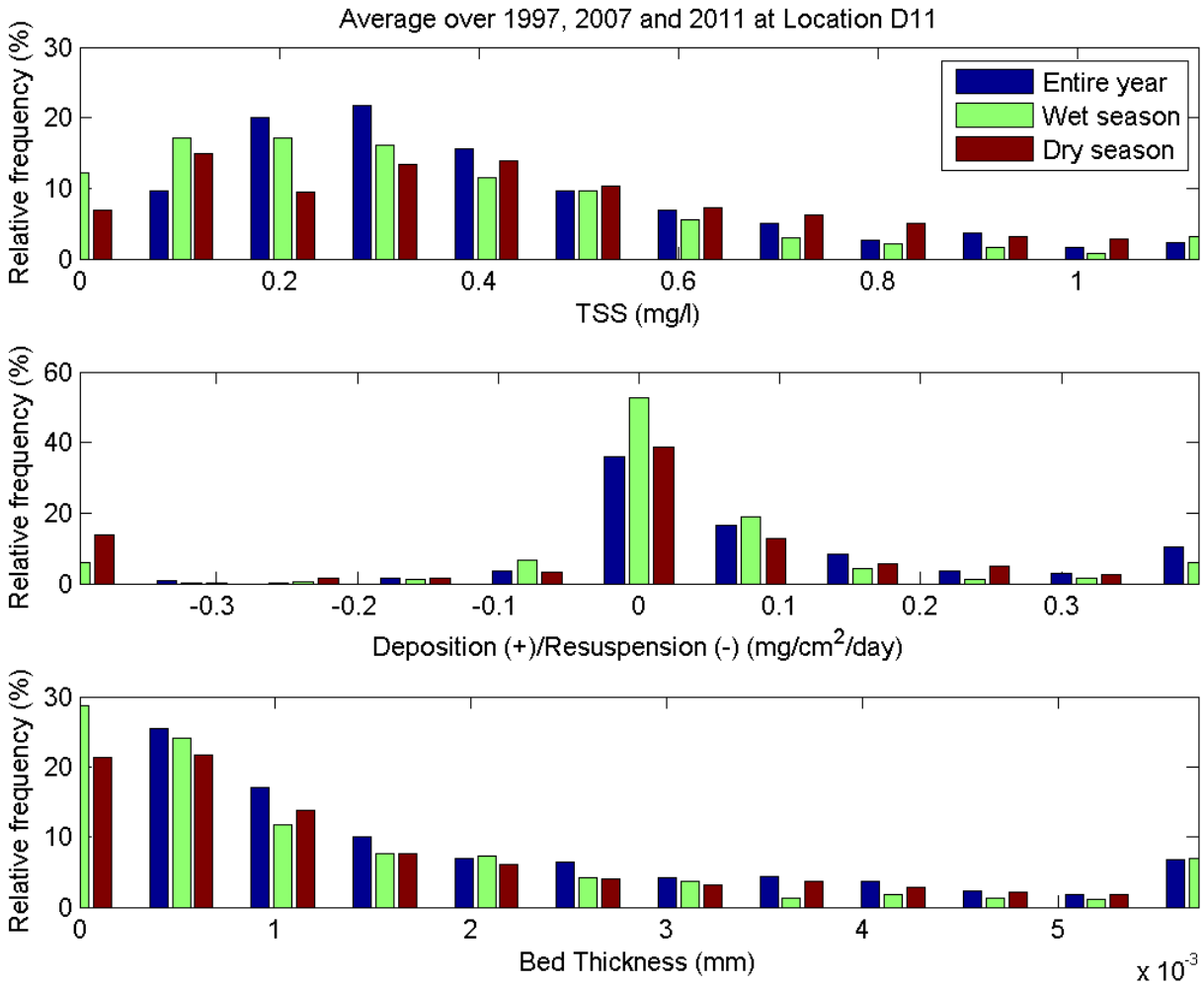

Figure 26 Histogram of TSS, deposition/resuspension and bed thickness for all simulations at site D11.

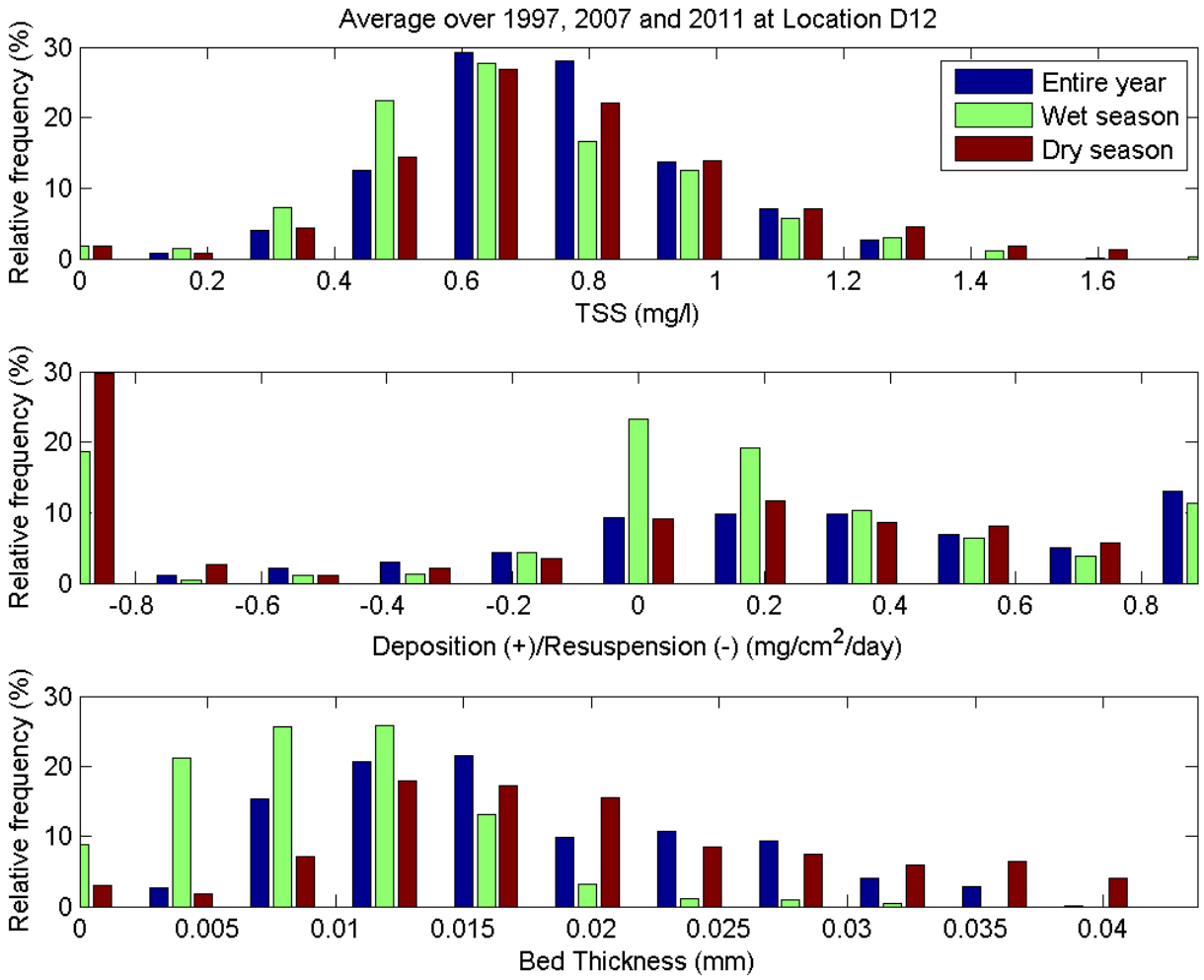

Figure 27 Histogram of TSS, deposition/resuspension and bed thickness for all simulations at site D12.

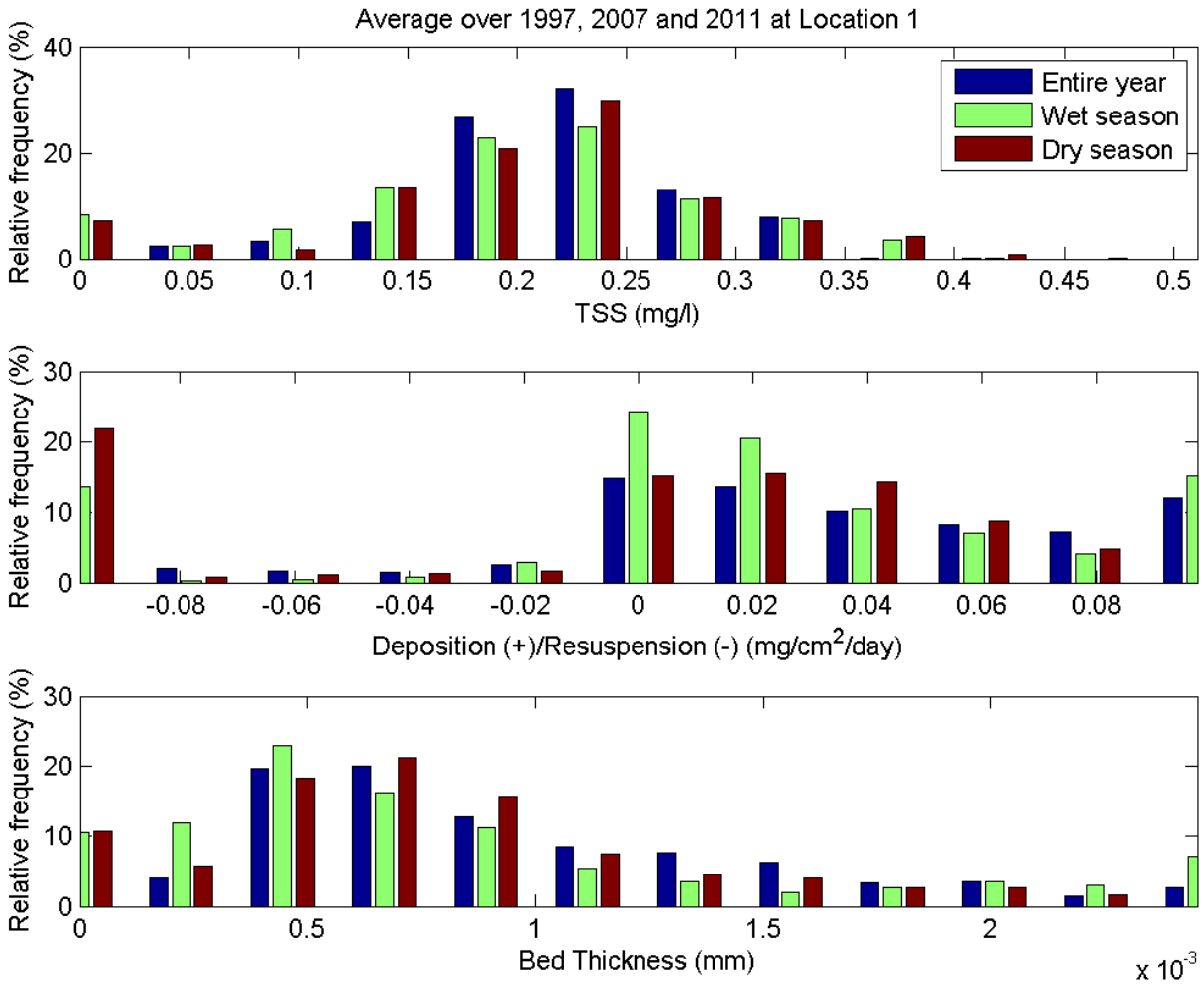

Figure 28 Histogram of TSS, deposition/resuspension and bed thickness for all simulations at site 1.

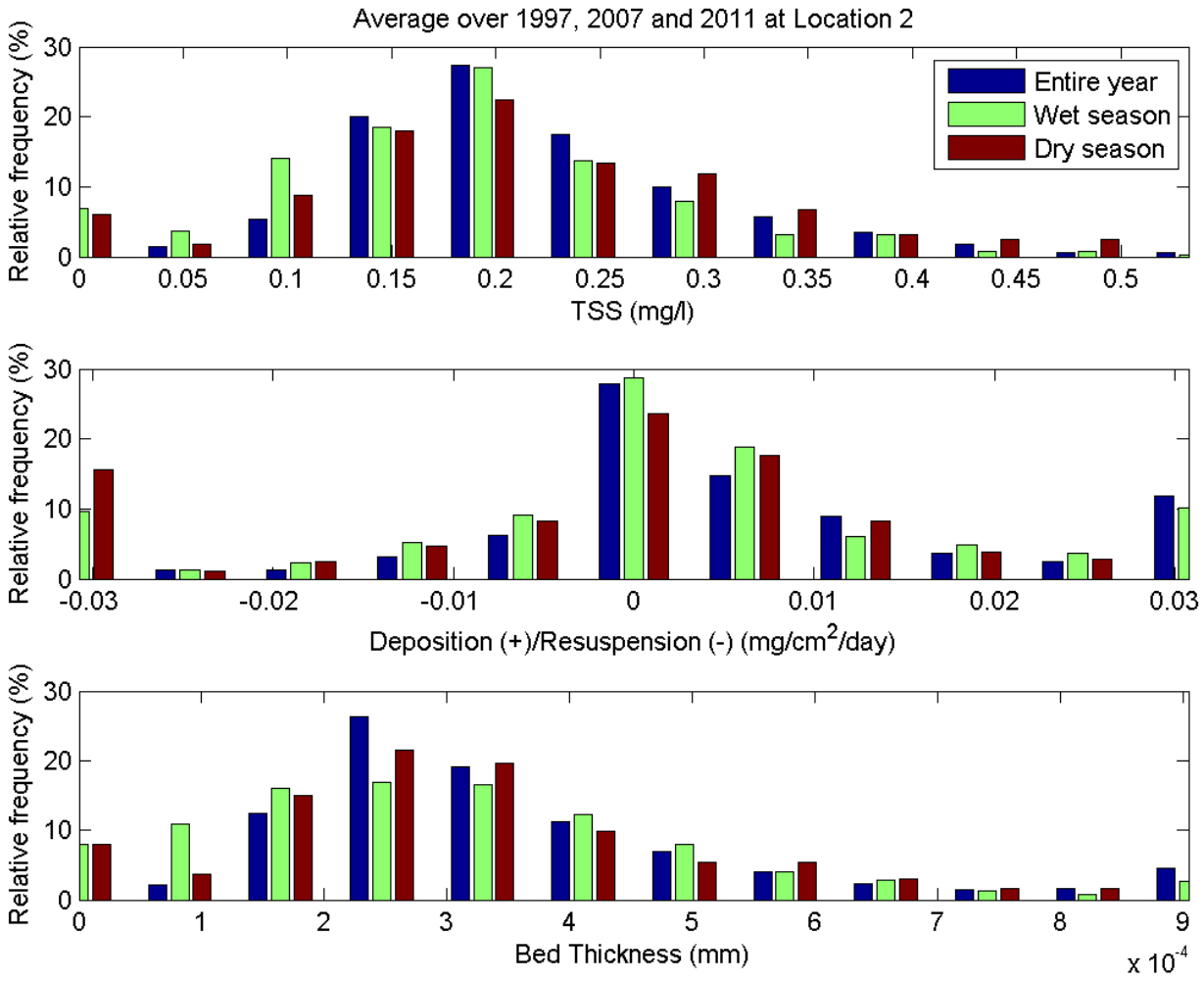

Figure 29 Histogram of TSS, deposition/resuspension and bed thickness for all simulations at site 2.

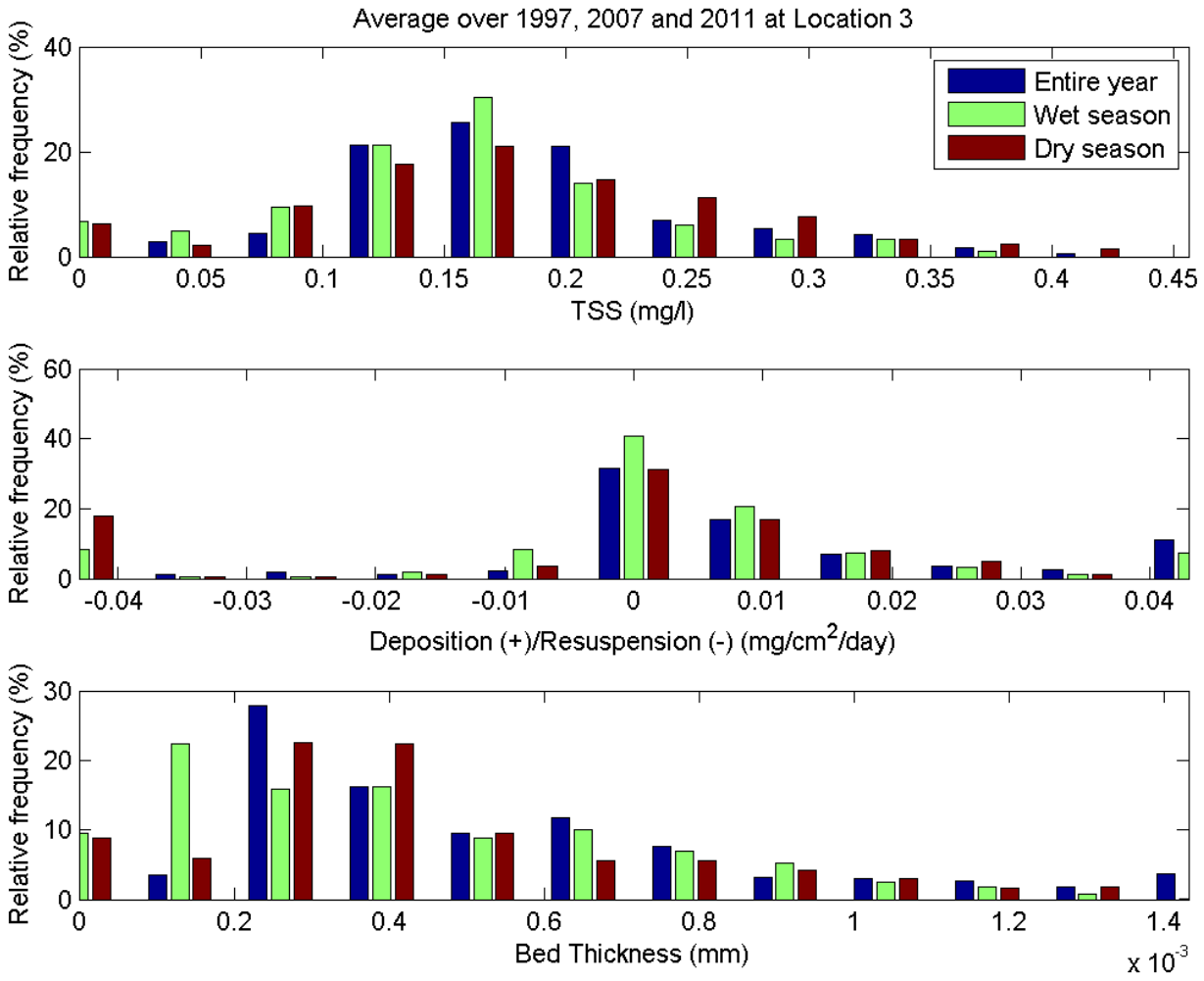

Figure 30 Histogram of TSS, deposition/resuspension and bed thickness for all simulations at site 3.

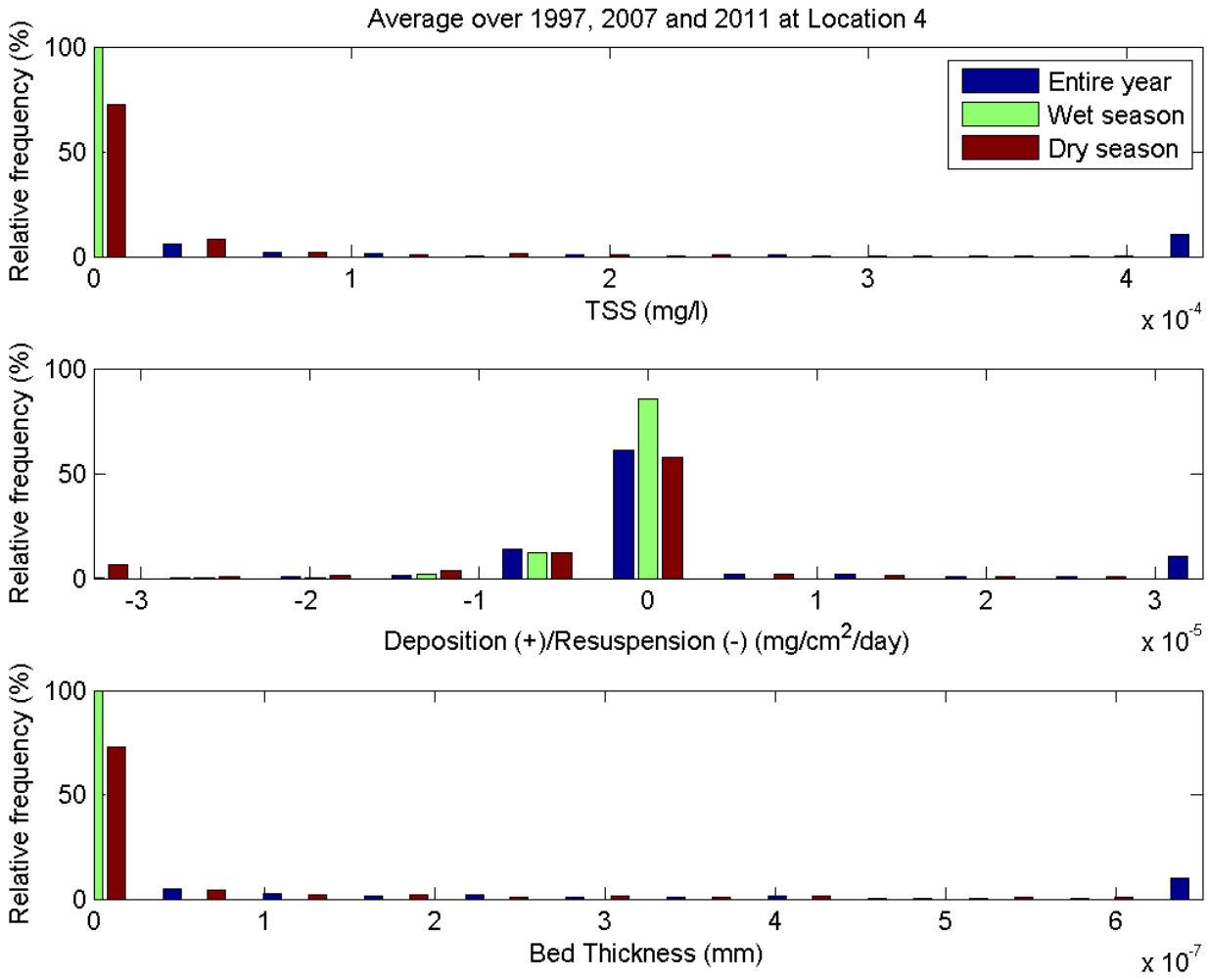

Figure 31 Histogram of TSS, deposition/resuspension and bed thickness for all simulations at site 4.

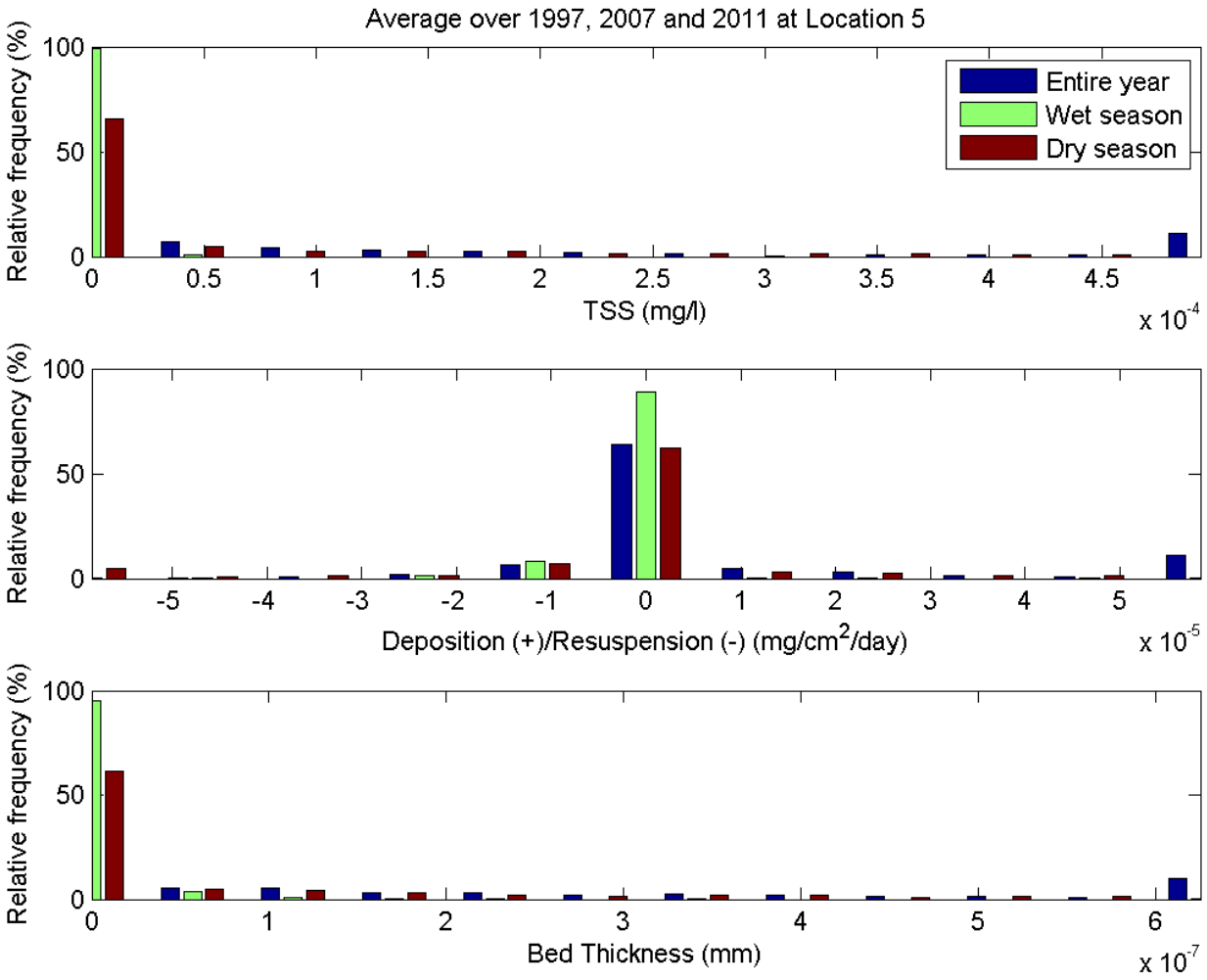

Figure 32 Histogram of TSS, deposition/resuspension and bed thickness for all simulations at site 5.

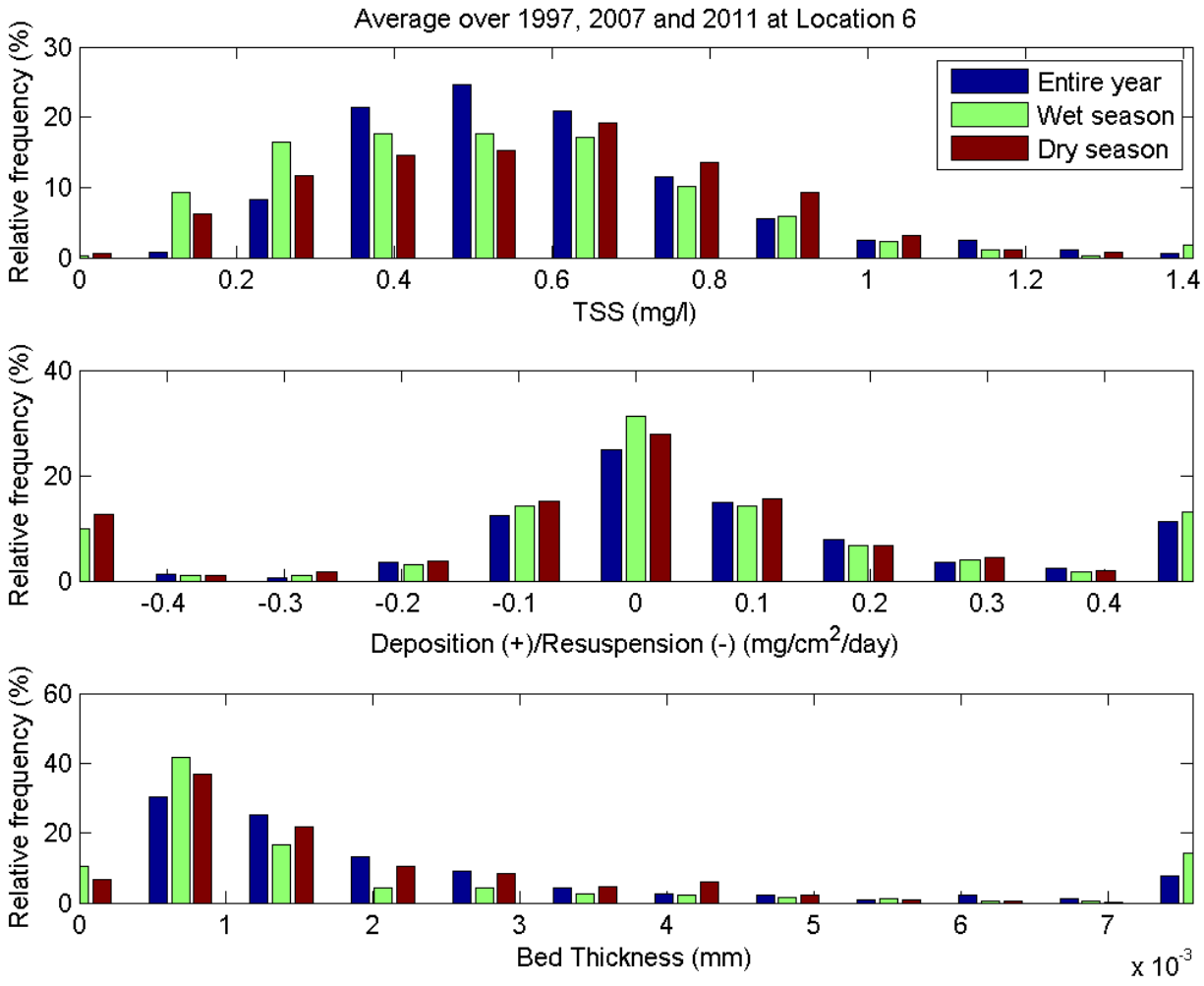

Figure 33 Histogram of TSS, deposition/resuspension and bed thickness for all simulations at site 6.

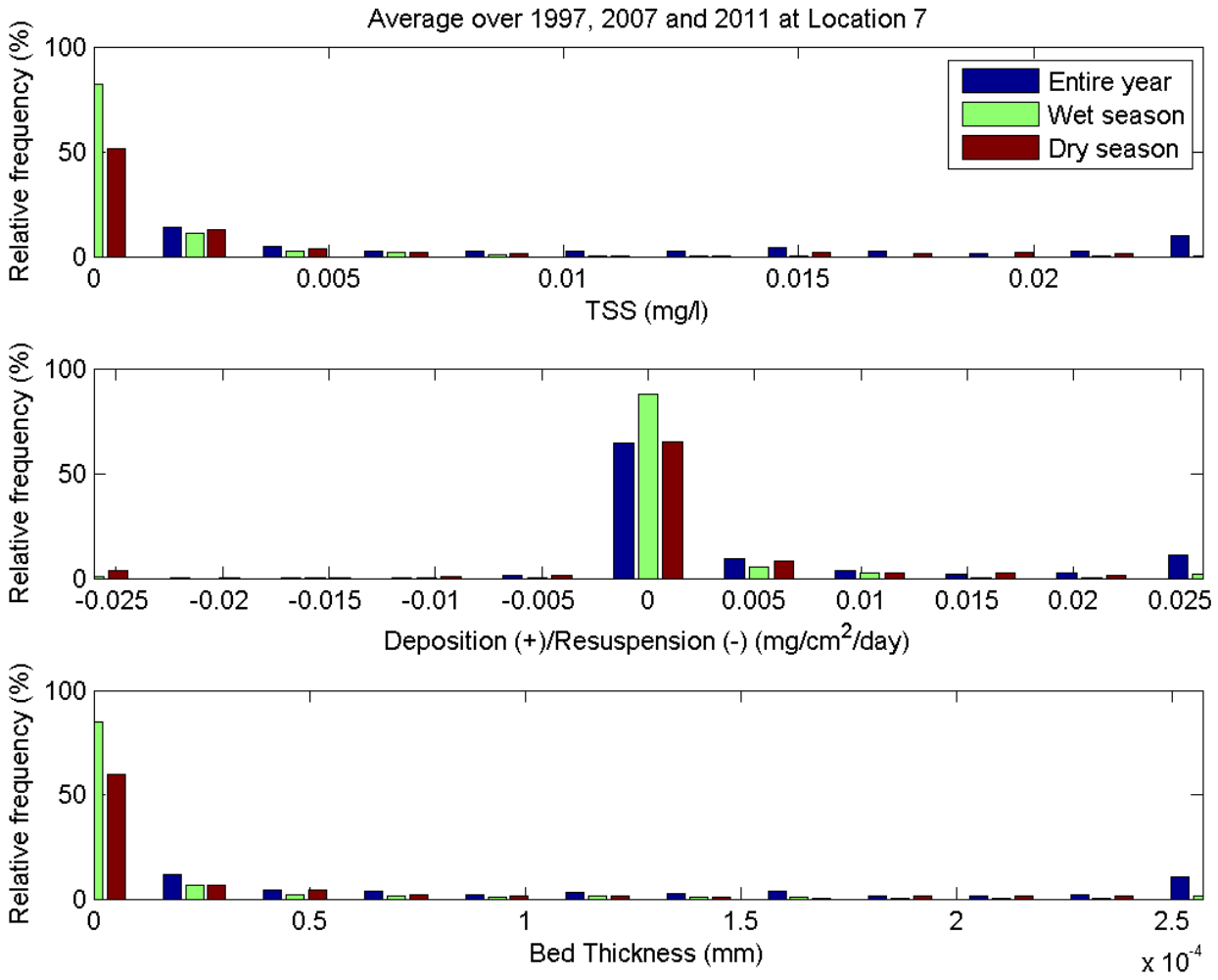

Figure 34 Histogram of TSS, deposition/resuspension and bed thickness for all simulations at site 7.